

PRODUCTION OF THERMOPLASTIC CASSAVA STARCH REINFORCED BY NATURAL
FIBER: PERFORMANCE, BIODEGRADABILITY, AND ENVIRONMENTAL IMPACTS

By

Tanatorn Tongsumrith

A DISSERTATION

Submitted to
Michigan State University
in partial fulfillment of the requirements
for the degree of

Packaging – Doctor of Philosophy

2015

ABSTRACT

PRODUCTION OF THERMOPLASTIC CASSAVA STARCH REINFORCED BY NATURAL FIBER: PERFORMANCE, BIODEGRADABILITY, AND ENVIRONMENTAL IMPACTS

By

Tanatorn Tongsumrith

A biopolymer composite, thermoplastic cassava starch (TPCS) was reinforced with natural fibers and glycerol as a plasticizer. Paper fiber and vetiver fiber were used as a reinforcing material in this study. The mixture experimental design approach was applied in order to develop mathematical models that can be used to determine the formulation of TPCS biocomposites correlated to output properties. Statistical methods were used to obtain models used to estimate or predict the required properties of the biocomposites.

The thermoplastic cassava starch reinforced by paper fiber was studied as a preliminary experiment, which provide the suggested proportions of the components to be used with the thermoplastic cassava starch based on vetiver fiber. The formulations of thermoplastic cassava starch reinforced by paper fiber were statistically analyzed by maximizing performance of the biocomposites.

In this study, mechanical properties of thermoplastic composites were improved compared to pure TPCS (without natural fibers) at the weight fractions of 65 wt.% cassava starch and 35 wt.% glycerol. The tensile strength of pure TPCS was increased from 0.7 MPa to 11.6 MPa or increased by 16.5 times at a weight fraction of 66 wt.% cassava starch, 21 wt.% glycerol and 13 wt.% vetiver fiber, while the elongation was reduced from 65.8 % to 14.5 %. The elongation decreased when the cassava starch load increased, associated with the decrease of glycerol. SEM micrographs showed good adhesion between starch and fibers but dispersion was not uniform. The

thermal stability of TPCS reinforced by natural fibers was improved compared to the unreinforced material.

Biodegradation of thermoplastic cassava starch biocomposites was examined in a simulated aerobic composting environment using a direct measurement respirometric (DMR) system in accordance with the ASTM D5338 and ISO 14855 standards. The thermoplastic cassava starch reinforced by vetiver fiber was easily biodegraded and almost all samples reached above 70 % mineralization in MSU compost. Differences in biodegradation rates were attributed to the intrinsic properties of the compost such as moisture content, pH, and nutrients for the microbes. In addition, a mathematical model for biodegradability correlated to the component proportions of inputs was obtained. The ANOVA test showed that the model was sufficiently reliable to be useful in design of the composites.

A preliminary life cycle assessment (LCA) was conducted according to the ISO 14040 series framework. Comparison of the environmental impacts for two formulations of 1 kg of pellets of thermoplastic cassava starch reinforced by vetiver fiber and a conventional biopolymer, granulated polylactide, showed that the environmental performance of the two formulations were not dramatically different. The major energy consumption was from the electricity for the laboratory scale manufacturing. When compared with the granulated polylactide, the abiotic depletion, eutrophication and global warming (GWP100) of the TPCSV resin were slightly lower than that of the granulated polylactide. Acidification and ozone layer depletion (ODP) were slightly higher than for the granulated polylactide. This study indicated there is no clear winner between two types of materials especially considering the variability of the data and their extraction from different biomass sources.

To my mom, dad, brothers, Achariya and Michaya for their love and support

ACKNOWLEDGEMENTS

I would like to express my gratitude to my major advisor, Dr. Susan Selke for her supporting, patience, encouragement and guidance through my Ph.D. life during my study at Michigan State University. I could not have done this without her precious inputs.

I would also like to thank Dr. Laurent Matuana, Dr. Rafael Auras and Dr. Satish Joshi for their suggestions, comments and guidance during the experiment and research. Also, I am thankful to Dr. Laurent Matuana for his kindness to allow me not only to use his facilities but also his assistance when I have a problem with the machine. Also, I would like to thank Rich Michael, Drown Ed, Askeland Per from the Composite Materials and Structures Center (CMSC) and Aaron Walworth from School of Packaging for their assistance with the instruments.

I am very grateful to School of Packaging at Michigan State University for the financial assistance that I received through my tuition fee. Also my study could not be happened without financial support from the Royal Thai Government Scholarship, Ministry of Science and Technology, and Department of Printing and Packaging Technology, King Mongkut's University of Technology, Thailand.

I am very thankful to my friends: Dr.Sukeewan, Dr.Turk, Dr.Oh, Dr.Kojo, Hayati, Edgar, Rijosh, Woranit, Jin, Marcelo for their friendship, help, motivation and support. In addition, I am thankful to friends who I have unintentionally left out.

Most of all, I would like to thank my parents and brothers for their love and support and never give up on me. In particular, I would like to thank my wife Achariya, who devoted her life and love during my long journey and gave me my wonderful daughter named Michaya.

TABLE OF CONTENTS

LIST OF TABLES.....	xi
LIST OF FIGURES	xvi
Chapter 1.....	1
Introduction.....	1
1.1 Introduction and motivation.....	1
1.2 Research objectives.....	4
Chapter 2.....	6
Literature Review.....	6
2.1 Starch.....	6
2.1.1 Chemical composition of starch.....	7
2.1.2 Starch gelatinization and retrogradation.....	12
2.1.3 Glass transition temperature.....	13
2.2 Thermoplastic starch (TPS).....	14
2.3 Natural fiber biopolymer composites.....	15
2.3.1 Structure, composition and properties of natural fiber.....	16
2.3.1.1 Cellulose.....	18
2.3.1.2 Hemicellulose.....	19
2.3.1.3 Lignin.....	20
2.3.1.4 Extractives.....	22
2.3.1.5 Natural fiber properties.....	23
2.3.1.5.1 Mechanical properties.....	23
2.3.2 Vetiver grass: challenge in fiber reinforcement.....	24
2.3.2.1 Vetiver species.....	25
2.3.2.2 Characteristics of Vetiver grass.....	25
2.3.2.2.1 Morphological characteristics.....	25
2.3.2.2.2 Physiological characteristics.....	26
2.3.3 Natural fiber reinforced biopolymer composites.....	27
2.3.3.1 The processing and mechanical properties of biopolymer composites reinforced by natural fibers.....	27
2.4 Mixture design of experiments and optimization.....	29
2.5 Degradation of Plastics.....	35
2.5.1 Mechanical degradation.....	35
2.5.2 Photodegradation.....	35
2.5.3 Thermal degradation.....	36
2.5.4 Chemical degradation.....	36
2.5.5 Hydrolysis degradation.....	37

2.5.6 Biodegradation.....	37
2.6 Biodegradation of thermoplastic starch blends	38
2.7 Life cycle analysis.....	40
2.7.1 Life cycle assessment methodology	40
2.7.1.1 Goal and scope.....	41
2.7.1.2 Life cycle inventory analysis (LCI).....	41
2.7.1.3 Life cycle impact assessment (LCIA).....	41
2.7.1.4 Interpretation.....	44
2.7.2 Current research on LCA of biopolymers	44
Chapter 3.....	48
The optimum formulation composition of thermoplastic cassava starch reinforced by natural fibers.....	48
3.1 Introduction	48
3.2 Research objectives	48
3.3 Materials and methods	49
3.3.1 Materials	49
3.3.2 Methods	49
3.3.2.1 Fiber preparation.....	49
3.3.2.1.1 Chemical pulp preparation	49
3.3.2.1.2 Vetiver fiber preparation	49
3.3.2.2 Design of experiments with mixture design	50
3.3.2.2.1 Preparation of composites of thermoplastic cassava starch reinforced by paper fiber	51
3.3.2.2.2 Preparation of thermoplastic cassava starch reinforced by vetiver fiber composites.....	53
3.3.2.3 Composite preparation.....	56
3.3.2.3.1 Compounding and processing of composites.....	56
3.3.2.3.2 Compression molding of composites	57
3.4 Characterization	57
3.4.1 Processability characterization	57
3.4.2 Thermal properties.....	58
3.4.3 Composite characterization	58
3.4.3.1 Tensile properties.....	58
3.4.3.2 Flexural properties	59
3.4.3.3 Morphological properties.....	60
3.5 Results and discussion.....	60
3.5.1 Processability of TPCS reinforced by paper fiber	60
3.5.2 Processability of TPCS reinforced by vetiver fiber.....	65
3.5.3 Mechanical properties of thermoplastic cassava starch composites with paper fiber ..	69
3.5.4 Mechanical properties of thermoplastic cassava starch composites with vetiver fiber	70

3.5.5 The relationship between composition of the thermoplastic cassava starch (TPCS) reinforced by paper fiber and mechanical properties.	72
3.5.5.1 The relationship between composition and tensile strength	73
3.5.5.2 The relationship between composition and tensile modulus	78
3.5.5.3 The relationship between composition and flexural strength	82
3.5.5.4 The relationship between composition and flexural modulus	86
3.5.6 The relationship between composition of the thermoplastic cassava starch (TPCS) reinforced by vetiver fiber and mechanical properties.	90
3.5.6.1 The relationship between composition and tensile strength	90
3.5.6.2 The relationship between composition and tensile modulus	95
3.5.6.3 The relationship between composition and flexural strength	99
3.5.6.4 The relationship between composition and flexural modulus	103
3.5.7 Mixture optimization of TPCS and vetiver fiber.....	107
3.5.8 Characteristics of selected thermoplastic starch vetiver fiber composites	110
3.5.8.1 FTIR.....	110
3.5.8.2 Thermal properties.....	112
3.5.8.3 SEM	118
3.6 Conclusions	122
Chapter 4.....	124
Determination of the biodegradability of thermoplastic cassava starch reinforced by natural fibers.....	124
4.1 Introduction	124
4.2 Research objectives	125
4.3 Experimental (Materials and Methods).....	125
4.3.1 Materials	125
4.3.2 Biodegradation.....	125
4.3.2.1 Test system.....	125
4.3.2.2 Compost preparation.....	127
4.3.2.3 Test materials	128
4.4 Calculation of biodegradation testing [81, 121].....	133
4.5 Statistical analysis	134
4.6 Results and discussion.....	135
4.6.1 The biodegradation of cellulose powder in compost.....	135
4.6.2 The biodegradation of raw materials in compost	137
4.6.3 The biodegradation of thermoplastic cassava starch reinforced by paper fiber in compost.....	140
4.6.4 The biodegradation of thermoplastic cassava starch reinforced by vetiver fiber in compost.....	147
4.6.5 The relationship between composition of the thermoplastic cassava starch (TPCS) reinforced by vetiver fiber and biodegradability.	151
4.7 Conclusions	159

Chapter 5.....	160
A preliminary life cycle assessment of thermoplastic cassava starch reinforced by vetiver fiber.....	160
5.1 Introduction.....	160
5.2 Methodology.....	161
5.2.1 Goal and scope definition.....	161
5.2.2 Scope of the study.....	162
5.2.2.1 Product system.....	162
5.2.2.2 Functional unit.....	162
5.2.2.3 System boundary and definitions.....	163
5.2.2.4 Allocation.....	166
5.2.2.5 Data requirement and quality.....	166
5.3 Inventory analysis and assessment.....	167
5.4 Impact assessment and methodology.....	168
5.5 Assumptions and limitations.....	169
5.6 Cut-off criteria.....	170
5.7 Interpretation.....	170
5.8 Results and interpretation.....	171
5.8.1 Life cycle inventory analysis.....	171
5.8.1.1 LCI of the production of thermoplastic cassava starch reinforced vetiver fiber resin.....	171
5.9 Life cycle impact assessment (LCIA).....	174
5.9.1 Characterization.....	175
5.9.1.1 Formulation 1.....	175
5.9.1.2 Formulation 2.....	176
5.9.1.3 Comparative LCIA of the two biocomposite formulations.....	178
5.9.2 Normalization.....	180
5.9.3 Comparative LCIA of the two biocomposite formulations against granulated polylactide (PLA).....	181
5.10 Sensitivity analysis.....	183
5.11 Uncertainty analysis of LCIA.....	185
5.12 Conclusions.....	187
Chapter 6.....	189
Conclusion and Future Study.....	189
6.1 Conclusions.....	189
6.2 Future study.....	191
APPENDICES.....	193
Appendix A THE FOLLOWING FIGURES DEAL WITH CHAPTER 3.....	194
Appendix B THE FOLLOWING TABLES DEAL WITH CHAPTER 5.....	207

REFERENCES.....218

LIST OF TABLES

Table 1.1 The municipal solid waste (MSW) total generated (in millions of tons) and % recovered in the US, 1960 -2012.	2
Table 2.1 Important crop sources of starch in the world [10].....	6
Table 2.2 Characteristics of amylose and amylopectin [9].....	11
Table 2.3 The composition of amylose and amylopectin in different starches [9,18].....	12
Table 2.4 Chemical composition of several natural fibers (adapted from [16, 46, 47, 51]).....	18
Table 2.5 The mechanical properties and spiral angle of plant fibers (adapted from [5, 46, 47])	24
Table 2.6 Comparison of two vetiver species [62]	25
Table 2.7 The adaptability range of vetiver grass (adapted from [63])	26
Table 2.8 Descriptions of impact assessment methods.....	43
Table 3.1 The three-variables mixture design as composed by Design Expert with design point types and leverage values.....	53
Table 3.2 The three-variables mixture design as composed by Design Expert with design point types and leverage values.....	55
Table 3.3 Measured processing values at point “X” of TPCS with paper fiber	63
Table 3.4 Measured processing values at end point (E) of TPCS with paper fiber.....	64
Table 3.5 Measured processing values at Point “X” of TPCS with vetiver fiber.....	65
Table 3.6 Measured polymer processing at end point (E) of TPCS with vetiver fiber.....	68
Table 3.7 Measured tensile and flexural properties of TPCS reinforced by paper fiber	69
Table 3.8 Measured tensile and flexural properties of TPCS reinforced by vetiver fiber	71
Table 3.9 Tensile strength model summary statistics	73

Table 3.10 The ANOVA-test summary statistics of tensile strength model.....	75
Table 3.11 The diagnostic case statistics for tensile strength model	76
Table 3.12 Tensile modulus model summary statistics	79
Table 3.13 The ANOVA-test summary statistics of tensile modulus model.....	79
Table 3.14 The diagnostic case statistics for tensile modulus model	80
Table 3.15 Flexural strength model summary statistics.....	82
Table 3.16 The ANOVA-test summary statistics of flexural strength model.....	83
Table 3.17 The diagnostic case statistics for the flexural strength model	84
Table 3.18 Flexural modulus model summary statistics.....	86
Table 3.19 The ANOVA-test summary statistics of flexural modulus model.....	87
Table 3.20 The diagnostic case statistics for flexural modulus model	88
Table 3.21 Summary of the models and coefficients of determination paper fiber.....	90
Table 3.22 Tensile strength model summary statistics	91
Table 3.23 The ANOVA-test summary statistics of tensile strength model.....	92
Table 3.24 The diagnostic case statistics for tensile strength model	93
Table 3.25 Tensile modulus model summary statistics	95
Table 3.26 The ANOVA-test summary statistics of tensile modulus model.....	96
Table 3.27 The diagnostic case statistics for tensile modulus model	97
Table 3.28 The ANOVA-test summary statistics of flexural strength model.....	100
Table 3.29 The diagnostic case statistics for the flexural strength model	101
Table 3.30 The ANOVA-test summary statistics of flexural modulus model.....	104

Table 3.31 The diagnostic case statistics for the flexural modulus model	105
Table 3.32 Summary of the models and coefficients of determination vetiver fiber	107
Table 3.33 The criteria for each response used of TPCS and vetiver fiber optimization.....	108
Table 3.34 TPCS and vetiver fiber optimization	108
Table 3.35 FTIR spectra of cassava starch, glycerol and TPCSV composites.....	111
Table 4.1 Chemical properties of the composts [128].....	128
Table 4.2 The theoretical carbon content of tested materials	129
Table 4.3 Composition and carbon content of each test material for the first test to the third test	131
Table 4.4 Composition and carbon content of each test materials of the fourth test run.....	132
Table 4.5 Test materials and carbon content for the fifth test	132
Table 4.6 Summary of set-up parameters for the DMR system [128].....	134
Table 4.7 The percent mineralization and average rate of degradation of cellulose powder	137
Table 4.8 The weight and amount of theoretical carbon dioxide evolution of cassava starch, vetiver fiber, paper fiber, glycerol, and cellulose powder	138
Table 4.9 The percent mineralization and average rate of degradation of raw materials (test 5).....	140
Table 4.10 The amount of theoretical carbon dioxide evolution of each bioreactor in test 1 to 3	141
Table 4.11 The percent mineralization and average rate of degradation of test 1	146
Table 4.12 The percent mineralization and average rate of degradation of test 2	147
Table 4.13 The percent mineralization and average rate of degradation of test 3	147
Table 4.14 The amount of theoretical carbon dioxide evolution of each bioreactor of thermoplastic cassava starch reinforced by vetiver fiber	148

Table 4.15 The percent mineralization of thermoplastic cassava starch reinforced by vetiver fiber (test 4)	151
Table 4.16 Measured % mineralization of TPCS reinforced by vetiver fiber	152
Table 4.17 Biodegradability Model Summary Statistics	153
Table 4.18 The ANOVA-test summary statistics of % mineralization model	154
Table 4.19 The diagnostic case statistics for % mineralization model	157
Table 5.1 Global consumption of biodegradable polymers in 2000, 2005 and forecast for 2010 (tons) [138].....	160
Table 5.2 Formulations of TPCSV biocomposite (%w/w).....	162
Table 5.3 The summary of data quality and requirements.....	167
Table 5.4 Life cycle inventory of 1 kg of TPCSV biocomposite pellet	172
Table 5.5 Considered environmental impact categories on this study.....	174
Table 5.6 Summary of LCIA for formulation 1 of TPCSV biocomposite pellet production	175
Table 5.7 Summary of LCIA for formulation 2 of TPCSV biocomposite pellet production	177
Table 5.8 Normalized LCIA profiles for formulation 1 and formulation 2 of TPCS biocomposite pellets	180
Table 5.9 Environmental impacts of the two formulations and PLA (production value per functional unit).....	182
Table 5.10 Quantity and average price of allocation for the production of cassava starch	184
Table 5.11 Uncertainty analysis for TPCSV bioconposite	187
Table B.1 Classification and Characterization factors.....	208
Table B.2 Life cycle inventory of cassava cultivation for 1 ton of cassava starch production [145–149], [158–160].....	211

Table B.3 Life cycle inventory for the production of 1 ton cassava starch [148, 160–162].....	212
Table B.4 Life cycle inventory of vetiver cultivation for 1 ton of vetiver fiber production [151]	213
Table B.5 Life cycle inventory for the production of 1 ton vetiver fiber.....	213
Table B.6 Pedigree matrix.....	214

LIST OF FIGURES

Figure 2.1 Open-chain and pyranose ring structure with α linkages	8
Figure 2.2 α -1,4 and α -1,6 glycosidic bonds of starch.....	9
Figure 2.3 α -1,4 linkages of amylose [9].....	10
Figure 2.4 The structure of amylopectin [11].....	11
Figure 2.5 Demonstration of possible processing pathways for plant fiber [46].....	16
Figure 2.6 The classification of fibers (adapted from [44, 45]).....	17
Figure 2.7 The molecular structure of cellulose [53].....	19
Figure 2.8 Major constituents of hemicelluloses [58]	20
Figure 2.9 Lignin precursors for plants.....	21
Figure 2.10 A structural depiction of part of a softwood lignin molecule.....	22
Figure 2.11 Three-component simplex coordinate system (adapted from [75])	31
Figure 2.12 Example of hydrolysable bonds	37
Figure 3.1 The constrained L-pseudo simplex design region of paper fiber-glycerol-cassava starch mixture.....	52
Figure 3.2 The constrained L-pseudo simplex design region of vetiver fiber-glycerol-cassava starch mixture.....	54
Figure 3.3 The Brabender Plastogram of all TPCS with paper fiber samples.....	61
Figure 3.4 The Brabender Plastogram of all TPCS with vetiver fiber samples.....	66
Figure 3.5 Contour plot of tensile strength.....	77
Figure 3.6 Response surface plot of tensile strength	77

Figure 3.7 Contour plot of tensile modulus	81
Figure 3.8 Response surface graph of tensile modulus.....	81
Figure 3.9 Contour plot of flexural strength	85
Figure 3.10 Response surface graph of flexural strength	85
Figure 3.11 Contour plot of flexural modulus	89
Figure 3.12 Response surface graph of flexural modulus.....	89
Figure 3.13 Contour plot of tensile strength	94
Figure 3.14 Response surface graph of tensile strength	94
Figure 3.15 Contour plot of tensile modulus	98
Figure 3.16 Response surface graph of tensile modulus.....	98
Figure 3.17 Contour plot of flexural strength	102
Figure 3.18 Response surface graph of flexural strength	102
Figure 3.19 Contour plot of flexural modulus	106
Figure 3.20 Response surface graph of flexural modulus.....	106
Figure 3.21 Contour plot of model simulation with constraints at desirability score “0.86”	109
Figure 3.22 Contour plot of model simulation with constraints at desirability score “0.85”	109
Figure 3.23 Contour plot of model simulation with constraints at desirability score “0.82”	110
Figure 3.24 IR spectra of cassava starch, glycerol and selected TPCSV composites. Data are offset for clarity.....	111
Figure 3.25 TGA and DTG curves of cassava starch (black), glycerol (red), vetiver fiber (green); a) TGA curve, b) DTG curve.....	114

Figure 3.26 TGA and DTG curves of selected TPCSV composites; S65G35VF0 (black), S66G21VF13 (red), S60G20VF20 (green) and S60G35VF5 (blue); a) TGA curve, b) DTG curve	115
Figure 3.27 DSC curves of thermoplastic cassava starch composites. Data were offset for clear observation; a) The first heating, b) The second heating.....	117
Figure 3.28 500x Surface view of S66G21VF13.....	118
Figure 3.29 100x Cross section view of S66G21VF13	119
Figure 3.30 500x Surface view of S60G20VF20.....	119
Figure 3.31 100x Cross section view of S60G20VF20	120
Figure 3.32 500x Surface view of S60G35VF5.....	120
Figure 3.33 100x Cross section view of S60G35VF5	121
Figure 3.34 500x Surface view of S80G15VF5.....	121
Figure 3.35 100x Cross section view of S80G15VF5	122
Figure 4.1 Schematic of the direct measurement respirometric system (DMR) adapted from Kijchavengkul et al. [88] and Aguirre [128].....	127
Figure 4.2 Evolution of CO ₂ of cellulose powder under stimulated composting conditions in tests 1 to 5	135
Figure 4.3 Mineralization of cellulose powder under stimulated composting condition in tests 1 to 5	136
Figure 4.4 Evolution of carbon dioxide (a) and mineralization curve (b) of the raw materials .	139
Figure 4.5 Biodegradation of thermoplastic cassava starch reinforced by natural fiber in DMR system	142
Figure 4.6 Evolution of carbon dioxide (a) and mineralization curve (b) of the first test	143
Figure 4.7 Evolution of carbon dioxide (a) and mineralization curve (b) of the second test	144

Figure 4.8 Evolution of carbon dioxide (a) and mineralization curve (b) of the third test.....	145
Figure 4.9 Evolution of carbon dioxide (a) and mineralization curve (b) of the fourth test.....	149
Figure 4.10 Residual vs predicted value.....	156
Figure 4.11 Contour plot of biodegradability	158
Figure 4.12 Response surface plot of biodegradability	158
Figure 5.1 Thermoplastic cassava starch composite pellet system boundary.....	164
Figure 5.2 The process of the production of thermoplastic cassava starch reinforced vetiver fiber resin for formulation 1	173
Figure 5.3 The process of the production of thermoplastic cassava starch reinforced vetiver fiber resin for formulation 2	173
Figure 5.4 Characterization of LCIA profile for formulation 1 (unit 1 kg pellet of TPCSV)	176
Figure 5.5 Characterization of LCIA profile for formulation 2 (unit 1 kg pellet of TPCSV)	177
Figure 5.6 Comparing LCIA of Formulation 1 and Formulation 2	178
Figure 5.7 Normalized LCIA profiles for formulation 1 and formulation 2 of TPCS biocomposite pellets	181
Figure 5.8 Environmental impacts of the two formulations and PLA based on normalization..	182
Figure 5.9 Environmental impact comparison per kg of formulation 1 of TPCSV biocomposite pellet for economic and mass allocation.....	185
Figure 5.10 Probability distribution of characterization of GWP100 for TPCSV biocomposite pellet.....	186
Figure 5.11 Uncertainty of characterization of TPCSV biocomposite	186
Figure A.1 The investigation of significance difference of measured tensile strength (a) and tensile modulus (b) of thermoplastic cassava starch composites reinforced by paper fiber.....	195

Figure A.2 The investigation of significance difference of measured flexural strength (a) and flexural modulus (b) of thermoplastic cassava starch composites reinforced by paper fiber.....196

Figure A.3 The investigation of significance difference of measured tensile strength (a) and tensile modulus (b) of thermoplastic cassava starch composites reinforced by vetiver fiber.....197

Figure A.4 The investigation of significance difference of measured flexural strength (a) and flexural modulus (b) of thermoplastic cassava starch composites reinforced by vetiver fiber...198

Figure A.5 The plots of diagnostic case statistics for tensile strength model of TPCS with vetiver fiber.....199

Figure A.6 The plots of diagnostic case statistics for flexural strength model of TPCS with vetiver fiber.....203

Chapter 1

Introduction

1.1 Introduction and motivation

It has been more than a decade that the usage of synthetic polymers has been increasing not only in terms of the quantity but also in terms of quality, and has become a widely used material for many applications in daily life such as household items, automotive parts and packaging products. Their light weight, good barrier and insulator properties, low cost, transparency, reusability and recyclability are some of the advantages for which synthetic polymers can be tailored.

However, synthetic polymers are derived from petroleum and natural gas, which are non-renewable resources for which prices tend to increase. Besides, they are very stable, durable, and difficult to dispose or degrade in the general environment. Then the polymeric wastes will lead the world to have serious environmental problems [1].

Recently, the municipal solid waste caused by plastic materials which are generated by industries and householders has been increasing, leading to many pollution issues such as air pollution, water pollution and soil pollution since most plastic wastes were disposed by landfilling and incineration which could have harmful effects not only on the environment but also on people's health [2].

The statistics published by the United States Environmental Protection Agency in 2012 reported that the United States generated about 251 million tons of municipal solid waste (MSW), which is 8 million tons more than that generated in 2009. The plastics category is growing rapidly due to the container and packaging segment, In addition, the total materials recovery as a percent

of total generation increased from 33.80% in 2009 to 34.51% in 2012 and the percent of material recovery of plastics generation increased from 7.1% in 2009 to 9.2% in 2012. Trends are shown in Table 1.1. These quantities of MSW will be difficult to dispose by landfilling and incineration since the capacity for landfilling is decreasing and the emissions from incineration may be toxic to the environment [3].

Table 1.1 The municipal solid waste (MSW) total generated (in millions of tons) and % recovered in the US, 1960 -2012.

Year	Generation (in thousands of tons)	Plastics (in thousands of tons)	Percent of materials recovery	
			of total generation	of plastics generation
1960	88,120	390	6.40%	<0.05%
1970	121,060	2,900	6.60%	<0.05%
1980	151,640	6,830	9.60%	0.30%
1990	208,270	17,130	16%	2.20%
2000	243,450	25,550	28.60%	5.80%
2005	253,730	29,380	31.60%	6.10%
2009	244,600	30,070	33.80%	7.10%
2010	250,540	31,970	34.02%	8.30%
2011	251,040	31,940	34.70%	8.80%
2012	254,110	32,520	34.51%	9.20%

As the EPA's results show, about 12% by weight of 251 million tons of total MSW discarded in 2012, which is about 29 million tons, has been used with energy recovery by combustion and the rest or about 53% was landfilled. Therefore, to minimize the environmental problems caused by waste disposal, efforts to use more eco-friendly materials shall be the most promising sustainable solution.

Nowadays, natural polymers have gained a lot of attention to be used as alternative materials. There are two especially important types of natural polymers, which are cellulose and starch. Both of them are polysaccharides that have the same monomer, glucose, but have different

linkages. Starch has α -1,4-glycosidic bonds and α -1,6-glycosidic bonds, while cellulose has β -1,4-glycosidic bonds. Hence, they have a different molecular structure, which affects their properties. Cellulose, a mostly linear structure, has strong bonding, which makes it difficult to transform, so one of the most interesting natural polymers to be used as a plastic is starch, which is abundant and easily found in many plants. Generally, starch is a constituent of many types of plants, for example, corn, potato, wheat and cassava. In addition, starch can be classified by the origin of plants such as seeds, tubers, and roots. Among these starches, cassava starch is of much interest because it is not only inexpensive and renewable but also abundant. It can be grown in most regions.

While the advantages of natural polymers from starch are desirable, they still have some disadvantages, such as being a strongly hydrophilic material, which can make this polymer highly susceptible to moisture and resulting low mechanical properties [4].

To overcome these drawbacks, some modifications need to be applied. Fibers can be used as a reinforcement material to increase the strength or rigidity of the natural polymers. There are two types of fibers that can be used, natural fibers and synthetic fibers. Synthetic fibers such as glass fiber, aramid fiber and carbon fiber all have high strength, high abrasion resistance and high flexibility, but they are generally expensive and may cause environmental problems when compared to natural fibers. At present, the concern about environmental problems is a main driving force for the use of natural fibers instead of synthetic fibers.

Generally, natural fibers from plants are used as a reinforcing material for composite materials. The chemical composition of natural fibers differs depending on the source of the fibers such as stem, leaf or seed fibers. The major components of plant fibers are cellulose, hemicellulose, and lignin, which all contribute to the overall properties of the fiber [5]. The natural fibers such as flax, ramie, jute, and eucalyptus fiber are used since they are all inexpensive, renewable, and

biodegradable [6]. Among these natural fibers, vetiver grass is an interesting source of natural fiber to be used as a reinforcing material in polymer composites.

Vetiver grass, also named *Vetiveria zizanioides*, is a tropical plant, which grows naturally in countries such as China, Australia, Vietnam, Philippines, Bangladesh and Thailand. It can be found in a wide range of areas and in various soil conditions. It belongs to the same grass family as sugarcane, maize, sorghum and lemongrass. In Thailand, vetiver grass is well known as a useful plant because it has been used as a natural barrier against soil erosion as well as pollution or can be applied for preservation and conservation of natural resources such as along the banks of a river or reservoir, or along road shoulders [7]. Owing to a deep thick root system, it expands like an underground curtain to store water and moisture.

In this study, a composite material made of vetiver fiber and thermoplastic cassava starch has been developed in order to enhance performance while maintaining the proper biodegradation and environmental impacts of the composite materials.

1.2 Research objectives

The main objective of this research is to reinforce biobased polymers from thermoplastic cassava starch material by using natural fiber to obtain a fully natural fiber biocomposite. Specific objectives are the following:

1. To produce and determine the optimum formulation composition of thermoplastic cassava starch (TPCS), natural fibers, and glycerol on the mechanical properties and processing characteristics of the composite.
2. To evaluate the biodegradability of the thermoplastic cassava starch reinforced by the vetiver fiber by using an in-house direct measurement respirometric system under simulated environmental conditions.

3. To study the environmental impacts by Life Cycle Assessment of the obtained thermoplastic cassava starch reinforced by the vetiver fiber.

Chapter 2

Literature Review

2.1 Starch

Starch is the source of stored energy in the plants, produced from carbon dioxide and water by photosynthesis [8], and it is reserved in many types of storage organs of the plants such as seeds, stems, roots, and tubers. In general, the amount of starch contained in grain plants is between 60-75 % of the weight of grains [9]. Starch is a polysaccharide, which is a natural and renewable material. It is found in a wide variety of plants and agricultural crops. Table 2.1 lists the important crop sources of starch around the world. From Table 2.1 [10], the major crops used for starch production include grains such as corn, rice, and wheat; and tubers such as potato, cassava and tapioca. In all of these plants, starches exist in the form of fine white granules. In general, the size of the granules ranges from 2-100 μm [11]. Moreover, starch granules can occur in all shapes and sizes such as spheres, ellipsoids, polygons, platelets, and irregular tubules [12]. The properties of the starch depend on the botanical sources, which vary in morphology.

Table 2.1 Important crop sources of starch in the world [10]

Plant Sources of Starch	Regions of the World Where Produced
Corn/maize	North America, South America, Europe, Asia
Potato	United States, Europe, Asia (sweet potato)
Rice	Europe, United States, Asia
Wheat	Europe, United States, South America, Asia
Tapioca	Asia, Africa, Europe
Sorghum	Asia, Africa, North America, South America, Europe
Banana	Africa, South America, Asia, Caribbean
Sago palm	Mostly Southeast Asia

The combination of techniques such as x-ray diffraction, atomic force microscopy (AFM), scanning electron microscopy (SEM) and transmission electron microscopy (TEM) to examine the

starch granules show a unique starch structure. In native starch, granules have a highly structured order, especially at the area of the central hilum, which is surrounded by growth rings composed of amorphous layers and alternating semicrystalline layers. The semicrystalline layers are comprised of ordered crystalline structures known as crystalline lamellae formed by short amylopectin branches and amorphous regions comprised of amylose and nonordered amylopectin branches [10].

The crystal structure of amylose and amylopectin in native starch can be divided into three groups by x-ray diffraction pattern: A-, B-, and C-types (a mixture of A- and B-type). The A-type pattern can be found in cereal starches. The B-type pattern can be found in tuber starches and legumes contain the C-type pattern [10, 13].

2.1.1 Chemical composition of starch

Starch is made up of carbon, hydrogen and oxygen with an empirical formula of $C_6H_{10}O_5$. Starch is a condensation polymer of the six-carbon sugar D-glucose. The structure of D-glucose is shown in Figure 2.1. It can be either an open-chain or a ring configuration which is referred to as a pyranose, such as D-glucopyranose. [9].

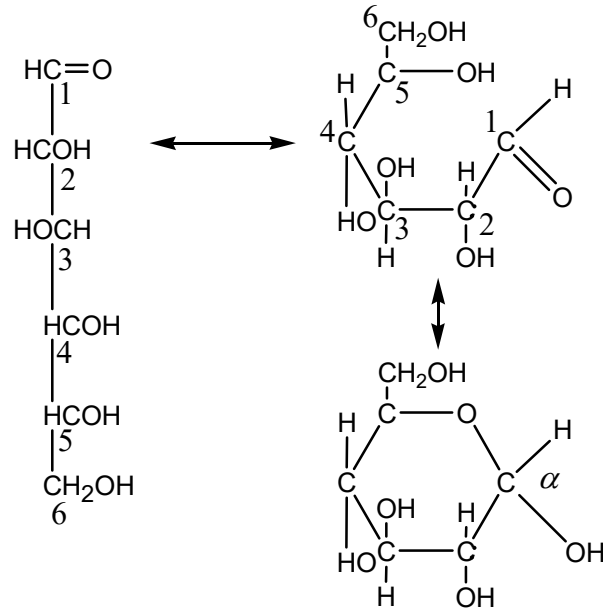


Figure 2.1 Open-chain and pyranose ring structure with α linkages

The D-glucopyranose polymers are linked together by α -1,4 and α -1,6 glycosidic bonds (Figure 2.2), which are formed by reaction between carbon number 1 and carbon number 4 or carbon number 6. The configuration of the glycosidic linkages in the starch is in the alpha (α) form, which is determined by the hydroxyl (-OH) group on carbon number 1 of the pyranose ring. It is very thermodynamically stable [9].

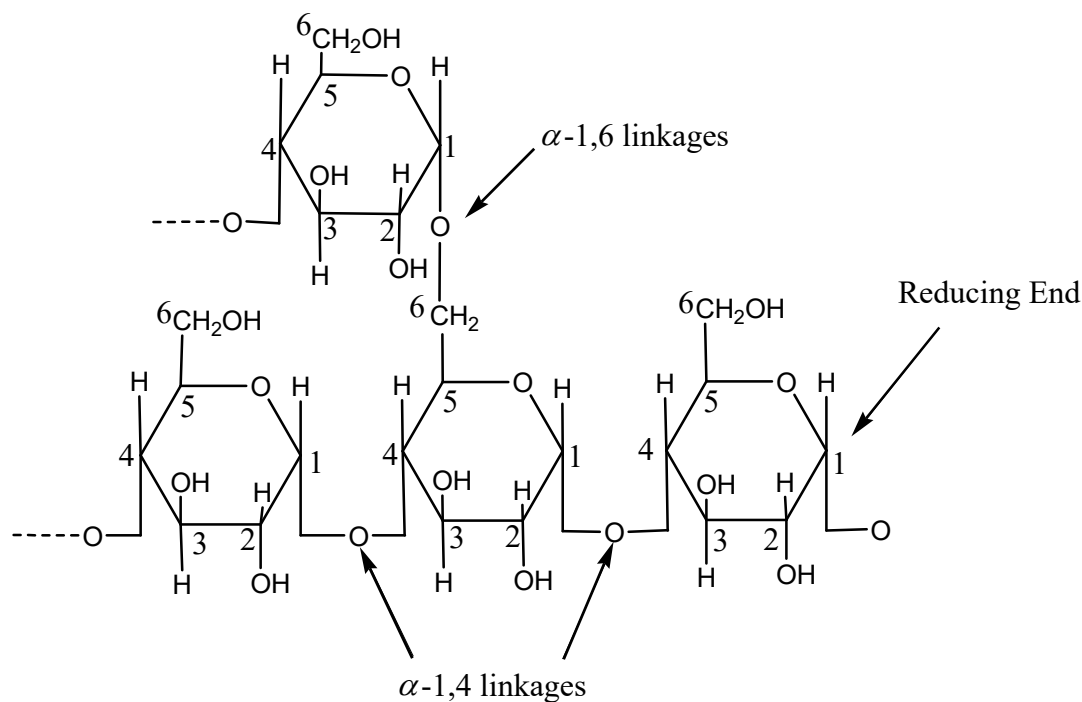


Figure 2.2 α -1,4 and α -1,6 glycosidic bonds of starch

Starch has hydroxyl groups, which are hydrophilic. Starch is also a heterogeneous material, which is influenced by the nature of the glucose-repeating units. These monomers are called the anhydroglucose units (AGU). Starch is generally composed of two structurally different polysaccharides, which are amylose and amylopectin. The different amounts and structures of these two types of polymer contribute to the differences in starch properties and functionalities [11].

Amylose is a mostly linear polymer, produced by α -1,4 linked D-glucose units (Figure 2.3). It has an average molecular weight of 1×10^5 to 2×10^6 , depending on the plant source, and it usually forms a helical structure. Moreover, the linear amylose is a minor component containing in starches, ranging approximately 20- 30% and it is responsible for the crystalline regions in the polymer matrix and makes starch have behavior closer to that of synthetic polymers. For cassava

starch, the amylose content ranges from 16 to 17% and the molecular weight of amylose in cassava starch ranges from 232 to 1250 kDa [14–16].

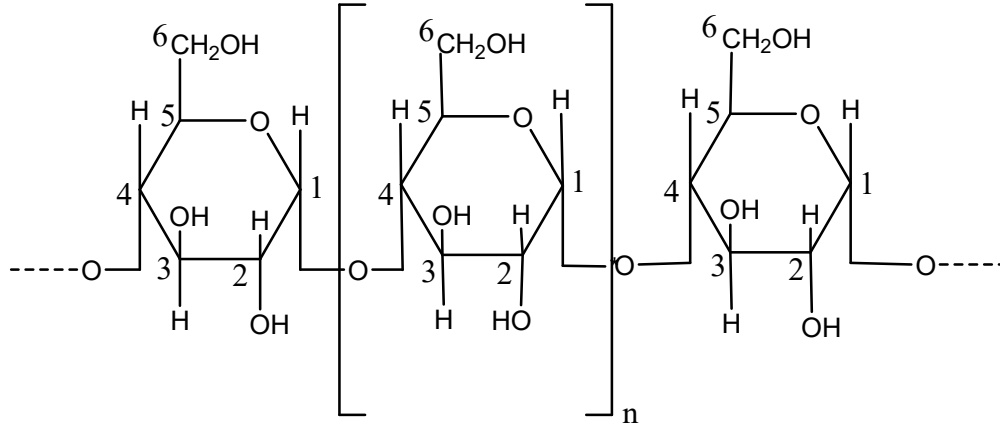


Figure 2.3 α -1,4 linkages of amylose [9]

Amylopectin is a branched polymer with both α -1, 4-linked D-glucose units and α -1,6 - linked D-glucose branches. The linkage branching points occur every 25-30 glucose units (Figure 2.4). Amylopectin has an average molecular weight of 4×10^7 to 4×10^8 and forms a helix crystalline structure [16]. Because of the highly branched amylopectin, the amorphous region is dependent on the amylopectin content. For cassava starch, the amylopectin content ranges from 83 to 84% and the molecular weight of amylopectine in cassava starch is ranging from 1880 to 4500 kDa [14–16]. Some important characteristics of amylose and amylopectin are listed in Table 2.2 [9].

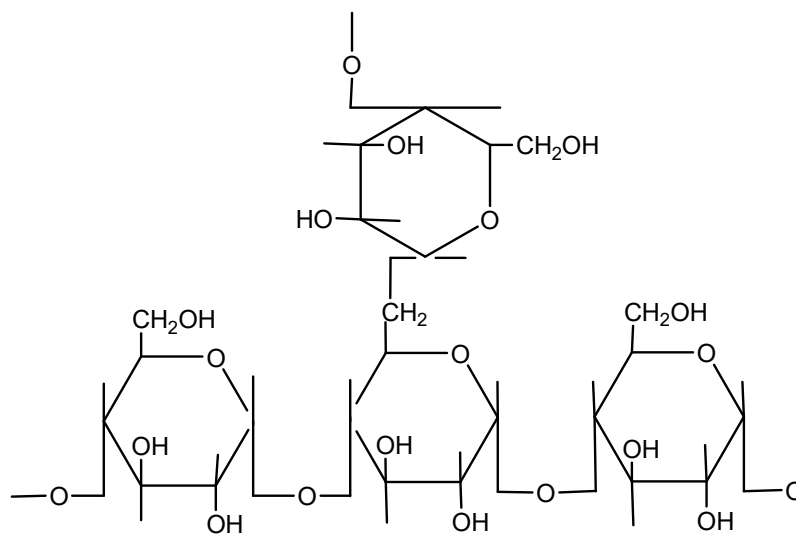


Figure 2.4 The structure of amylopectin [11]

Table 2.2 Characteristics of amylose and amylopectin [9]

Characteristic	Amylose	Amylopectin
Shape	Essentially linear	Branched
Linkage	α -1,4 (some α -1,6)	α -1,4 and α -1,6
Molecular weight	Typically <0.5 million	50-500 million
Films	Strong	Weak
Gel formation	Firm	Non-gelling to soft
Color with iodine	Blue	Reddish brown

For both amylose and amylopectin, the average degree of polymerization (DP) differs depending on the botanical source. In general, amylose has an average degree of polymerization about 1,500 to 6,000 and amylopectin, which is much larger, has a degree of polymerization about 300,000 to 3,000,000 [17]. The molecular weight of amylose can vary from about 213,000 to 972,000 but is typically less than 500,000. For amylopectin, the molecular weight can range from about 10,000,000 to 500,000,000. The approximate amylose and amylopectin contents of several starches are shown in Table 2.3 [9].

Table 2.3 The composition of amylose and amylopectin in different starches [9,18]

Source of starch	Amylose content (%)	Amylopectin content (%)
Dent corn	25	75
Waxy corn	<1	>99
Tapioca or Cassava	16-17	83-84
Potato	20	80
High-amylose corn	55-70 (or higher)	45-30 (or lower)
Wheat	30	70
Rice	20-30	70-80

2.1.2 Starch gelatinization and retrogradation

Starch is generally present in semi-crystalline granular form with a density about 1.5 g/cm³. Starch is insoluble in cold water but can be swelled and dissolved when it absorbs hot water through hydrogen bonding with free hydroxyl groups. Without any moisture or heat, it can be kept for periods of time. Most starches need to be processed before consuming. Therefore, understanding thermal transitions of starch is important for control of the starch functions. When they are heated and suspended in water, starch granules begin to swell and the starch molecules collapse due to the disruption of hydrogen bonding between adjacent glucose units resulting in irreversible changes such as crystallite melting, low viscosity, and solubilization. This phenomenon is called gelatinization, which generally takes place at 55 to 75 °C depending on the type of starch. Gelatinization of potato starch occurs at 58.2±0.1 °C, wheat starch at 57.1±0.3 °C, normal maize starch at 64.1±0.2 °C, and rice starch at 70.3±0.2 °C. Additional heating results in total disruption of all the granules, which occurs at about 60 to 90 °C. The result is called a starch paste, when the starch is heated and stirred to apparent solubilization. Paste temperatures are 63.5, 88.6, 82.0 and 79.9 °C for potato, wheat, maize and rice starch, respectively. After cooling, the cooked starch begins to undergo retrogradation, which means that starch molecules begin to recombine in an ordered structure. This is revealed by the formation of a precipitate or a gel [19]. For example, as 1.5% amylose solutions are cooled, the amylose precipitates out, forming a gel of increasing

modulus with increasing concentration [20]. The concentration of amylose affects the properties of the gels. Amylose-rich gels have good mechanical and thermal resistance and these properties are less susceptible to both chemical and enzymatic degradation than amylopectin-rich gels [21]. To study starch retrogradation, common techniques used include rheological methods, x-ray diffraction, thermal analysis and spectroscopy [22].

2.1.3 Glass transition temperature

The glass transition temperature (T_g) has a great influence in determining the processing and mechanical properties of amorphous polymers and controlling the kinetic amorphous glassy/rubbery systems or the so-called “mobilities” [23–26]. In starch polymers, brittleness is one of the major drawbacks of the material and is related to its high glass transition temperature [27] (approximately 230°C)[28], which is above the thermal degradation temperature. Common methods to determine T_g include differential scanning calorimetry (DSC), nuclear magnetic resonance (NMR) and dynamic mechanical thermal analysis (DMTA).

In amorphous and semi-crystalline polymers, at below their T_g , the mobility is limited due to the restriction of molecular chain motion. Adding plasticizer will change the molecular motion and lower the T_g . In general, plasticization involves lowering the rigidity at room temperature and increasing the elongation to break at room temperature. In studies on the effect of starch plasticizers, water was a popular plasticizer to be used. Starch plasticization with water has been shown by decreasing the T_g . T_g for dry amylose and amylopectin has been estimated as about 277 °C, and the T_g decreases to 56 °C in the presence of 13% water [23]. The highly branched amylopectin has a lower T_g than the amylose. However, the T_g values obtained by researchers differ, due to changes occurring in the starch and the different methods and conditions for measurement. According to Zeleznak and Hoseney [29] the T_g of wheat starch with 13-18.7% moisture content varies between 30 and 90 °C. If the moisture content in starch is above 20%, T_g

will likely be lower than room temperature. Shogren found that the T_g for starch with 7 – 18% moisture content varied from 140 to 150 °C [27]. Lourdin et al. studied the effect of glycerol and other plasticizers concentration at a constant relative humidity of 57% on the T_g of potato starch. They reported the T_g was 89.8 °C without plasticizer and was reduced to the level of ambient temperature with the addition of about 16% of plasticizer [30].

2.2 Thermoplastic starch (TPS)

Thermoplastic starch can be obtained through the destruction of pure starch granules during processing by the presence of plasticizers and under the condition of heating at relatively high temperature about 90 to 180 °C with shearing [31]. This phenomenon is called gelatinization [32]. The conventional polymer processing techniques such as compression, extrusion and injection molding can be used to melt the granular structure of starch with plasticizer, which is known as thermoplastic or plasticized starch. There are several substances that can be used as plasticizers, such as water, glycerol, sorbitol, etc. [33].

Plasticizers are necessary because the melting temperature of pure starch is higher than its decomposition temperature. However, the use of water as a plasticizer is not preferable because the outcome product will be very brittle at room temperature. Plasticizers with high boiling point and low molecular weight will act not only as lubricants to increase the movement in the matrix, but also the T_g and T_m of the polymeric material will decrease [34]. Moreover, to accomplish the purpose of the plasticizer, the chemical structure of the plasticizer should be comparable to that of the polymeric material. For example, glycerol is the most popularly used plasticizer with starch because this hydrophilic plasticizer has hydroxyl groups [35, 36]. Teixeira et al. (2007) showed that a small amount of sugars (glucose, fructose and sucrose) and glycerol in the starch polymer are able to reduce the glass transition temperature [37]. Investigating the optimum usage level of glycerol, the study from Carvalho et al. (2003) showed that with a small amount of glycerol, starch

will be difficult to process and its chain degradation increases; on the other hand, with a large amount of glycerol the starch degradation decreases and the ease of processing increases [38]. Averous et al. found that wheat starch with 10% glycerol was stiff and brittle, and was more flexible if the amount of glycerol was increased up to 35%. Likewise, Vilpoux and Averous (2004) reported a study from Lourdin et al. showing that the optimum amount of plasticizers such as glycerol, sorbitol etc., ranged from 20% to 40% of the starch weight [31]. The amount of plasticizer can directly affect the mechanical properties and glass transition temperature of the material [39, 40].

2.3 Natural fiber biopolymer composites

The use of natural fibers in biocomposite materials dates back to thousands of years ago, since ancient people used natural fibers to build structures such as walls and shelters with clay reinforced with natural fibers. These natural fibers are of many types and have been found in numerous products varying in origin around the world. These natural fibers can provide benefits to our environment, as they are renewable, cheap, non-toxic, and biodegradable [41]. As natural fibers are ecofriendly and economical compared to synthetic fiber based composites with acceptable specific mechanical properties, the use of natural fiber reinforced composites has gained attention in many application areas such as automobiles, housing, packaging, and electronic products [42–44].

The conventional polymer composites from natural fibers, which are flax, hemp, sisal, banana, kenaf, and jute, have been extensively studied. However, the composites from vetiver fiber and biopolymer to develop the green biodegradable plastics are of particular interest in Thailand. Vetiver grass is generally grown in most areas in the country (details on vetiver grass will be covered in section 2.3.2). To optimize the utility of using vetiver fiber, converting this fiber will increase not only the useful applications but also its economic value.

At present, there are many successful attempts to use natural fibers as reinforcement materials in the plastics industry due to the increasing cost of plastics, and because of the environmental aspects of using renewable and biodegradable materials. One study of natural fibers in the automotive industry showed benefits of net energy saving of 50,000 MJ per ton of composite when replacing 30 % by weight of glass fibers with 65 % of hemp fibers [45].

To utilize plants for composites, Rowell and co-workers described the possible processing pathways from plants to composite products as shown in Figure 2.5 (Rowell, 1995). For example, the whole plant (leaves, stock, pith, and roots) can be used directly to fabricate structural and non-structural composites.

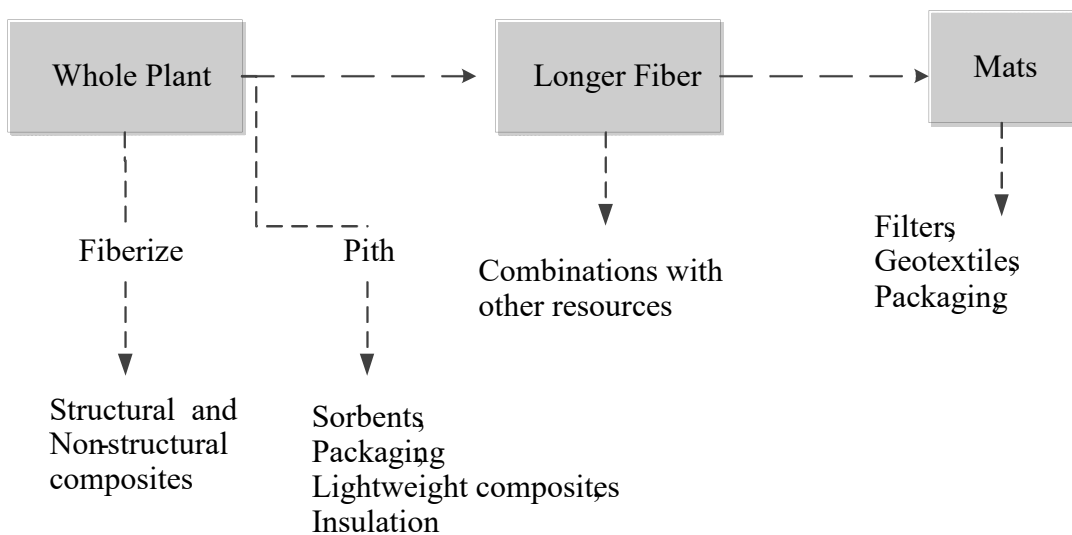


Figure 2.5 Demonstration of possible processing pathways for plant fiber [46]

2.3.1 Structure, composition and properties of natural fiber

In general, the many kinds of natural fibers can be divided into three major categories according to their origin: plants or vegetables, animals and minerals. Many of them can be used to reinforce polymers. Figure 2.6 shows the classification of fibers [47].

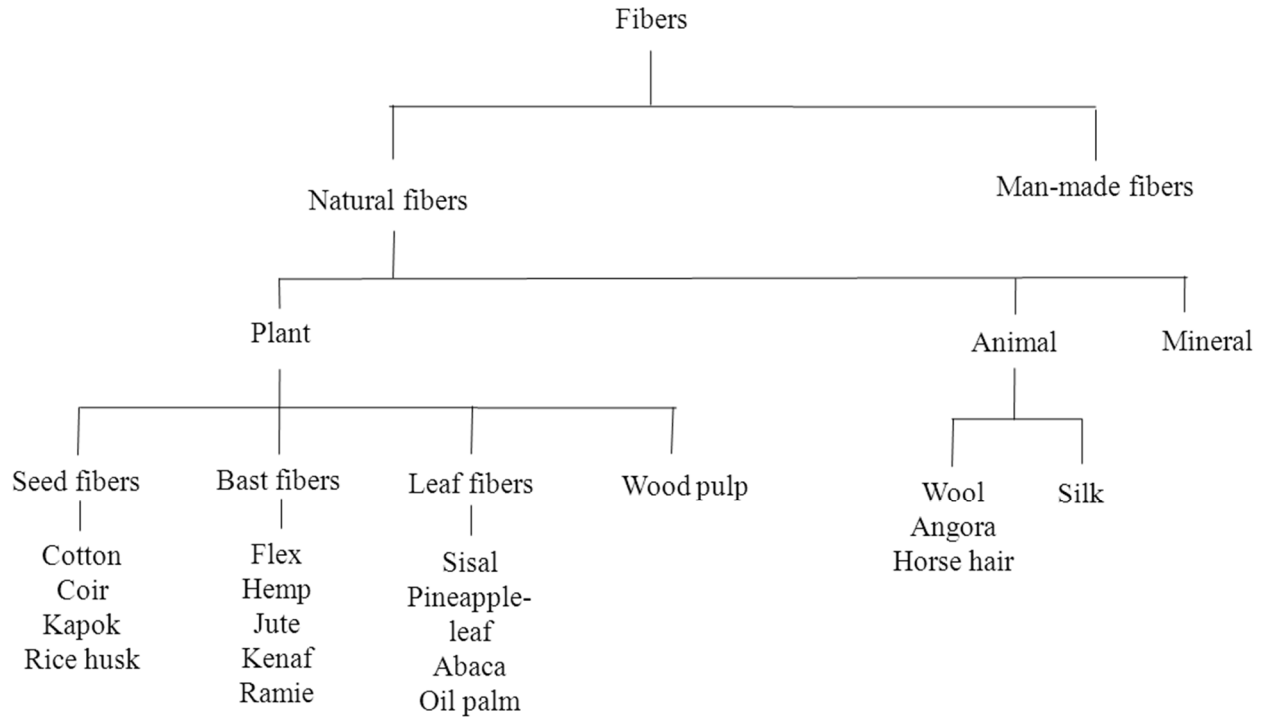


Figure 2.6 The classification of fibers (adapted from [44, 45])

Nowadays, plant or vegetable fibers are popular for use as the reinforcing material in a polymer matrix and can be classified as seed fibers, bast fibers, and leaf fibers [34];

Seed fibers include cotton, coir, kapok, and rice husk, etc. Among this group of fibers, cotton is commonly used in the textile industry.

Bast fibers or stem fibers are obtained from the stems of plants such as flax, hemp, jute, kenaf, and ramie etc. These fibers generally consist of long fibers providing the strength to plants.

Leaf fibers as the name implies, usually come from the leaves of plants such as sisal, abaca and pineapple leaf (PALF). These fibers are rougher than bast fibers. Important applications include rope and coarse textiles.

Natural fibers are originally obtained from plants or vegetables, which are three-dimensional biopolymers and can be considered as composites of chemical substances. In general, the chemical

composition of plant fibers consists of cellulose, hemicellulose, lignin, pectin, waxes, and extractives. The chemical substances of plant fibers vary between species, as shown in Table 2.4.

Table 2.4 Chemical composition of several natural fibers (adapted from [16, 46, 47, 51])

Type of Fiber	Chemical Composition (wt%)						
	Cellulose	Lignin	Hemicellulose	Pectin	Wax	Pentosan	Ash
Jute	61–71.5	12–13	13.6–20.4	0.4	0.5	18-21	0.5-2
Hemp	70.2–74.4	3.7–5.7	17.9–22.4	0.9	0.8	14-17	0.8
Kenaf	31–39	15–19	21.5	–	–	22-23	2-5
Flax	71	2.2	18.6–20.6	2.3	1.7	24-26	5
Ramie	68.6–76.2	0.6–0.7	13.1–16.7	1.9	0.3	5-8	–
Sunn	67.8	3.5	16.6	0.3	0.4	–	–
Sisal	67–78	8–11	10.0–14.2	10	2	21-24	0.6-1
Henquen	77.6	13.1	4–8	–	–	–	–
Cotton	82.7	–	5.7	–	0.6	1-3	0.8-2
Kapok	64	13	23	23	–	–	–
Coir	36–43	41–45	10–20	3–4	–	–	–
Banana	63–67.6	5	19	–	–	–	–
PALF	70–82	5–12	–	–	–	–	–
Bagasse	55.2	25.3	16.8	–	–	27-32	1.5-5
Bamboo	26-43	21-31	30	–	–	15-26	1.7-5
Abaca	56-63	7-9	20-25	–	3	15-17	1-3
Oil palm	65	29	–	–	–	–	–
Wheat straw	38-45	12-20	15-31	–	–	26-32	4.5-9
Rice straw	41-57	8-19	33	–	8-38	23-28	15-20
Vetiver grass	70.2	16.3	–	–	–	30.2	7.2

2.3.1.1 Cellulose

Cellulose is a natural polymer, and is the most abundant and important component of all plants. It is generally known that cellulose molecule is a linear condensation polymer consisting of three elements, which are carbon, hydrogen and oxygen. They are organized into D-anhydroglucose units (often abbreviated as anhydroglucose units or glucose units) joined by β -1,4-glycosidic bonds to form long linear chains. The average size of cellulose molecules (degree of polymerization, DP) in secondary walls of plants varies in the range of 7,000 to 14,000 glucose

units per molecule and in primary walls may be as low as 500 glucose units per molecule [52].

Figure 2.7 shows the chemical structure of cellulose.

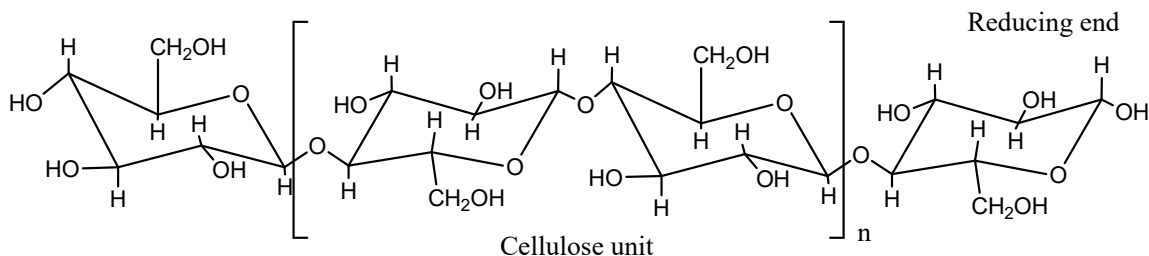


Figure 2.7 The molecular structure of cellulose [53]

The molecular structure of cellulose is responsible for determining its chemical and physical properties. When the molecule is fully extended, it will allow the molecular chain of cellulose to form a flat and ribbon-like long straight chain. This linearity of the molecular makes cellulose highly anisotropic [54–56].

Cellulose molecular is randomly ordered by intra- and intermolecular hydrogen bonds, which make some regions highly ordered. The high packing density proportion of cellulose is the highly crystalline regions and the lower packing density regions are amorphous. The highly crystalline regions may be as much as 80 percent crystalline regions [47].

The degree of crystallinity of the cellulose will be different depending on the source of the plant fibers such as 60 to 70% for wood fibers and 40 to 45% for cotton fibers etc. Moreover, the physical and chemical treatments of the fiber have an influence in changing the degree of crystallinity [55].

2.3.1.2 Hemicellulose

Hemicellulose is a heterogeneous group of polysaccharides composed of 5 or 6-carbon ring sugars in chains that vary depending on the types of plant fibers, including a range of carbohydrates

such as glucose, galactose, mannose, xylose and arabinose (Figure 2.8). They are mostly branched and their chains are relatively short (DP around 50 to 300), which makes them easily soluble in alkali and easily hydrolyzed in acids [57].

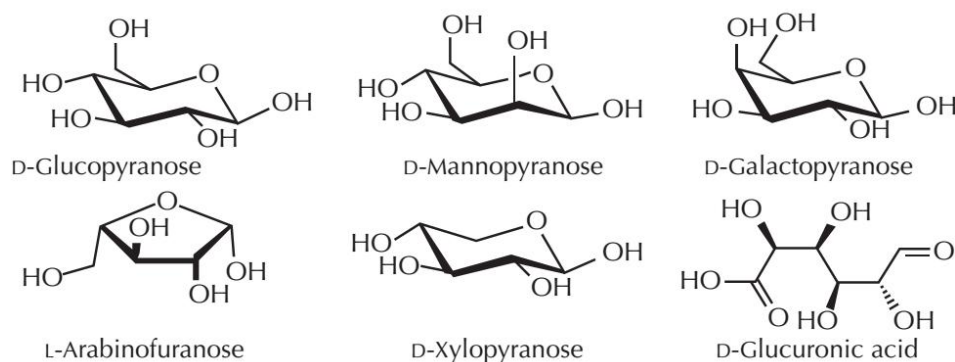


Figure 2.8 Major constituents of hemicelluloses [58]

2.3.1.3 Lignin

Lignin is a highly branched polymer composed of phenylpropane units, which are linked together. It acts as an adhesive or binder in wood that hold cellulose fibers together providing rigidity to the plants. It is mostly concentrated in the middle lamella. The function of lignin is to cover the cellulose/hemicellulose matrix [47]. Lignin is organized in a very complex three-dimensional structure with both aliphatic and aromatic constituents. It has very high molecular weight with unclear chemistry, as only the functional groups and building units can be identified. It is characterized by high carbon but low hydrogen content. Hydroxyl, methoxyl, and carbonyl groups have been identified. Lignin has been found to average five hydroxyl and five methoxyl groups per building unit. The structure detail will be different from one source to another [59].

Three basic monomers can be found in lignin as shown in Figure 2.9. Grass and straw plants contain all three lignin monomers whereas hardwoods contain only coniferyl alcohol (50-

75%) and sinapyl alcohol (25-50%), and softwoods contain only coniferyl alcohol. A representative lignin molecule is shown in Figure 2.10. [53]

The nature of lignin is amorphous and hydrophobic. It is classified as a thermoplastic polymer, having a glass transition temperature around 130 to 150 °C, and the polymer starts to flow at around 170 °C. It is soluble in hot alkali, oxidized, and easily condensable with phenol [53, 57].

In a chemical sense, lignin is rather reactive and therefore any method applied to extract lignin from plant fibers affects its molecular composition and structure [53].

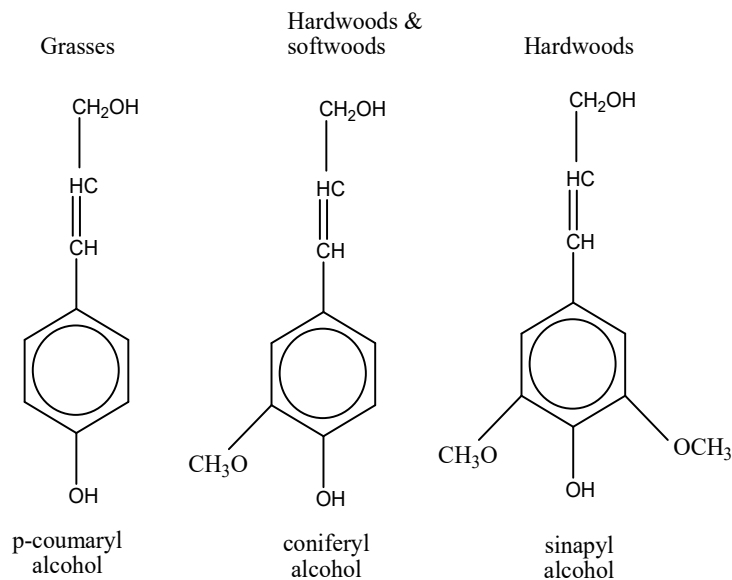


Figure 2.9 Lignin precursors for plants

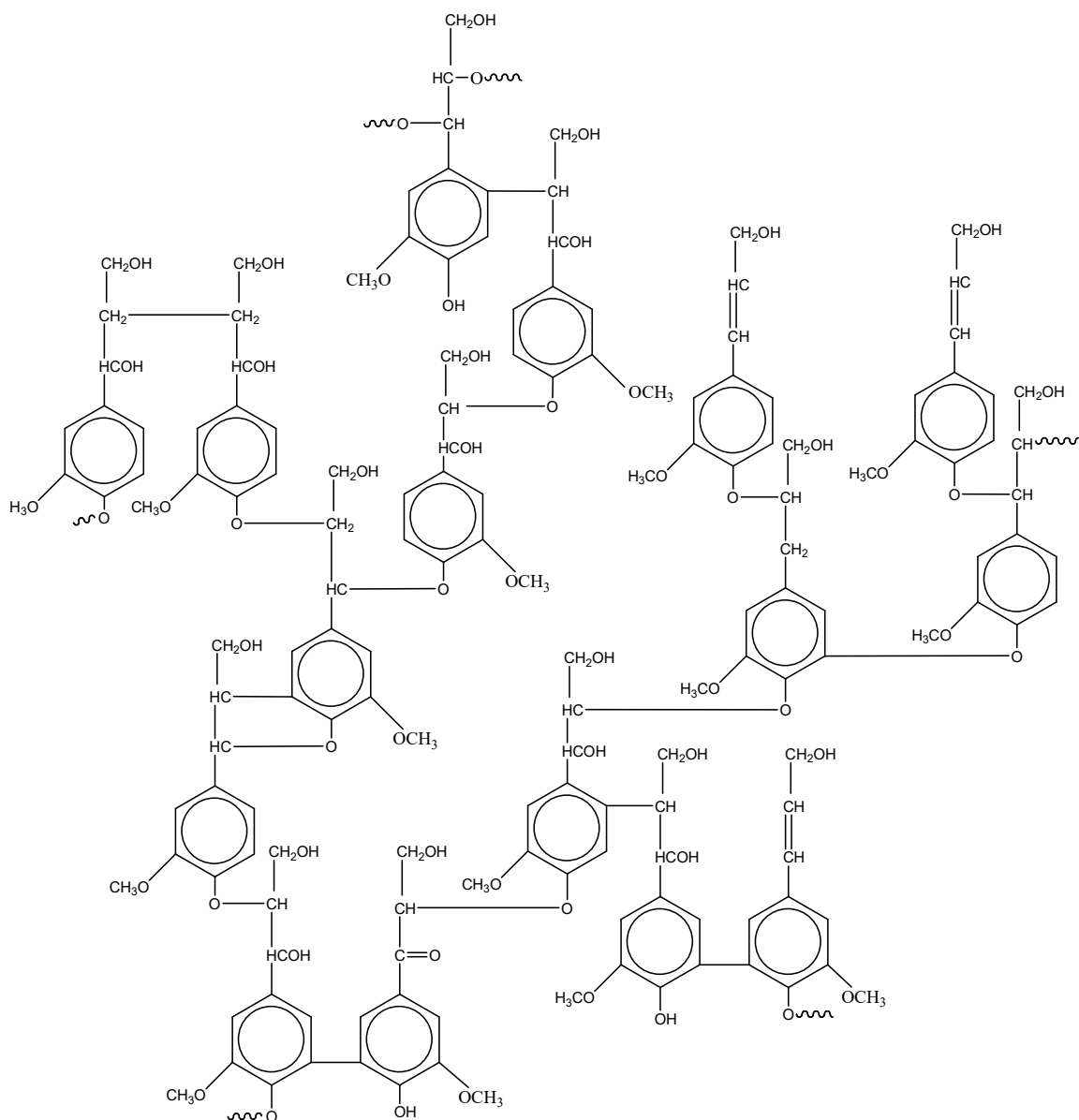


Figure 2.10 A structural depiction of part of a softwood lignin molecule

2.3.1.4 Extractives

Extractives are organic compounds with low to high molecular weights such as waxes, oils, fats, tannins, carbohydrates, acids, gums and resins. They can be removed or extracted by organic solvents or water [53].

2.3.1.5 Natural fiber properties

Natural fibers are a three dimensional biopolymer composite, which is mainly composed of cellulose, hemicellulose, lignin and extractives. These compositions provide the different performance of different sources of plant fibers, depending on their chemical composition, physical properties, mechanical properties and the interaction between fibers and matrix. To utilize natural fibers for polymer composites, it is important to have information about the fiber characteristics, which can affect performance in particular applications.

2.3.1.5.1 Mechanical properties

The molecular interactions and polymer organization in the cell wall affect the mechanical properties of individual plant fibers [59, 60]. Eder et al. [61] reported that, the density of the fiber and the fiber orientation in the cell wall layers are important parameters. The higher density fiber is stronger than the lower density fiber. Moreover, the smaller spiral angle has a higher modulus of elasticity than the larger spiral angle and the stiffness is decreased with a higher spiral angle. Table 2.5 presents the mechanical and physical properties of some plant fibers.

Table 2.5 The mechanical properties and spiral angle of plant fibers (adapted from [5, 46, 47])

Type of Fiber	Mechanical properties of natural fibers					
	Density (g/cm ³)	Diameter (μm)	Tensile strength (MPa)	Young's modulus (GPa)	Elongation at break (%)	Spiral angle (deg)
Jute	1.3–1.45	25–200	393–773	13–26.5	1.16–1.5	8
Hemp	–	–	690	–	1.6	2-6.2
Kenaf	–	–	–	–	2.7	
Flax	1.5	–	345–1100	27.6	2.7–3.2	5-10
Ramie	1	–	400–938	61.4–128	1.2–3.8	7.5
Sunn	–	–	1.17–1.9	–	5.5	
Sisal	1.45	50–200	468–640	9.4–22.0	3-7	10-22
Cotton	1.5–1.6	–	287–800	5.5–12.6	7-8	
Kapok	–	–	–	–	1.2	
Coir	1.15	100–450	131–175	4–6	15–40	30-49
Banana	–	–	1.7–7.9	–	1.5–9.0	
PALF	–	20–80	413–1627	34.5–82.5	1.6	14

The chemical constituents and chemical structure of natural fibers can influence the properties of the fibers. In addition, the strength of natural fibers can be affected by the angle between the axis and the fibril or microfibril of the fibers. The less the degree of the angle between the axis and the fibril, the higher the mechanical properties will be. For example, coir fiber shows the least tensile strength in Table 2.5 due to the high spiral angle 30°-49°. Angles are 10°-22° for sisal, and 14° for pineapple leaf fiber (PALF), while jute, ramie, and hemp fibers have <10° respectively. Moreover the lignin content of the natural fibers affects the structure and morphology of the fibers, and wax affects the wettability and adhesion characteristics [49].

2.3.2 Vetiver grass: challenge in fiber reinforcement

Vetiver is a useful grass. It generally has massive long roots, which can penetrate and anchor deeply and vertically into soils. Therefore, it has been used to help in reducing soil erosion and to protect against nutrient loss in topsoil. Vetiver grass has also been widely used in

applications such as decreasing the rate of water flow, increasing soil humidity, protecting the banks of reservoirs and rivers, and protecting roadside slopes. However, there has been little research on reinforcing biopolymers using vetiver grass.

2.3.2.1 Vetiver species

Vetiver grass has many species. The two common species in Thailand are *Chrysopogon nemoralis* (Balan.) Holtt. Camus and *C. zizanioides* (L.) Roberty. Vetiver grass belongs to the same family as maize, sorghum, sugarcane and lemon grass. Table 2.6 provides a comparison of the two species.

Table 2.6 Comparison of two vetiver species [62]

Variable	<i>C. nemoralis</i>	<i>C. zizanioides</i>
Leaf	<ul style="list-style-type: none"> - Tufted with leaves bending down like lemongrass - 0.35–0.80 m long and 0.04–0.08 m width - Pale green - Coarse texture with non-waxy appearance 	<ul style="list-style-type: none"> - Clumpy with long, erect leaves - 0.45–1.0 m long and 0.06–0.12 m width - Dark green - Smooth texture with waxy appearance
Height (above ground)	- 1.0-1.5 m high	- 1.5-2.0 m high
Root	<ul style="list-style-type: none"> - Has no fragrance - Can penetrate into soil as deep as 0.8-1.0 m 	<ul style="list-style-type: none"> - Has mild fragrance - Can penetrate into soil as deep as 1.0-3.0 m
Uses	- Leaves are used for roof thatching	- Perfume from root extract volatile oils and leaves can use for products like handbags, fans, clothes-hangers, and also used as herbal medicine and closet insect repellents

2.3.2.2 Characteristics of Vetiver grass

2.3.2.2.1 Morphological characteristics

Vetiver grass has a massive root system and is able to grow very fast. In some vetiver species, the roots can reach 3-4 m in the first year. This makes the vetiver plant highly drought

resistant and difficult to dislocate even by strong currents. The stem of the plant is stiff so it can keep standing in deep water flow. Therefore when it has been grown close together it will act as an effective sediment filter and water spreader or can form terraces to trap sediments [63].

2.3.2.2.2 Physiological characteristics

It has an ability to tolerate climatic variations such as extreme droughts or floods, and extreme temperature from -14 °C to +55 °C and can re-grow quickly. The pH of soils can be varied from 3.3 to 12.5 without soil amendment and it is highly resistant to herbicides and pesticides. Besides, it has a very useful ability in absorbing dissolved nutrients such as N and P and heavy metals in polluted water. In Table 2.7, the adaptability range of vetiver is presented [63].

Table 2.7 The adaptability range of vetiver grass (adapted from [63])

Condition characteristic	Australia	Other Countries
Adverse Soil Conditions		
Acidity (pH)	3.3-9.5	4.2-12.5 (high level soluble Al)
Salinity (50% yield reduction)	17.5 mScm ⁻¹	
Salinity (survived)	47.5 mScm ⁻¹	
Aluminium level (Al Sat. %)	Between 68% - 87%	
Manganese level	> 578 mgkg ⁻¹	
Fertilizer		
Vetiver can be established on very infertile soil.	N and P (300 kg/ha)	N and P, farm manure

Table 2.7 (cont'd)

Condition characteristic	Australia	Other Countries
Heavy Metals		
Arsenic (As)	100 - 250 mgkg ⁻¹	
Cadmium (Cd)	20 mgkg ⁻¹	
Copper (Cu)	35 - 50 mgkg ⁻¹	
Chromium (Cr)	200 - 600 mgkg ⁻¹	
Nickel (Ni)	50 - 100 mgkg ⁻¹	
Mercury (Hg)	> 6 mgkg ⁻¹	
Lead (Pb)	> 1500 mgkg ⁻¹	
Selenium (Se)	> 74 mgkg ⁻¹	
Zinc (Zn)	>750 mgkg ⁻¹	
Climate		
Annual Rainfall (mm)	450 - 4000	250 - 5000
Frost (ground temp.)	-11°C	-22 °C
Heat wave	45°C	55 °C
Drought (no effective rain)	15 months	
Location	15°S to 37°S	41°N to 38°S

2.3.3 Natural fiber reinforced biopolymer composites

2.3.3.1 The processing and mechanical properties of biopolymer composites reinforced by natural fibers

Torres et al. (2007) studied the mechanical properties of natural fiber reinforced thermoplastic starch biocomposites by using potato, sweet potato, and corn starch as matrices. Three types of natural fibers, sisal, jute, and cabuya, were used as reinforcing materials varying from 2.5 to 12.5 % w/w in the composites. Water and glycerol were used as plasticizers. It was observed that the tensile and impact strength of biocomposites improved at increasing fiber content. Especially tensile strength appeared to be clearly improved with the addition of 10% by

weight of sisal fibers, and the highest impact strength was obtained for cabuya fibers [64]. Ma et al. (2005) also studied the properties of natural fiber-reinforced thermoplastic corn starch composites. Urea and formamide were used as a plasticizer. The SEM micrographs showed good dispersion of the fiber in the thermoplastic starch (TPS) matrix because the fiber's surface was covered by TPS due to a strong interaction between the fiber and TPS. Tensile strength reached a maximum at a fiber content of 20%, while the elongation was reduced [65]. It was confirmed by Norshahida et al. (2012) that the fiber loading affected the tensile strength and Young's modulus [66].

To study the influence of the type of fibers, Girones et al. (2012) studied the influence of sisal and hemp fiber reinforced thermoplastic starch from corn on physical and chemical properties. The use of sisal and hemp fiber increased the glass transition temperature (T_g) of the composites and also increased the stiffness, storage modulus and Young's modulus. The composites from hemp fiber provided better mechanical properties than sisal due to the fibrillation during mixing that enhanced the mechanical anchoring of the fiber to the matrix [67]. Dias et al. (2011) observed that eucalyptus cellulose fiber reinforced on starch film is not only increases the mechanical properties but also increase the barrier properties. The starch films with fibers had lower water vapor permeability and higher tensile strength when compared to the films without fibers [68].

Curvelo et al. (2001) investigated the amount of plasticizer and nature fibers used are in limited range. Glycerol content of 30% w/w to starch and fiber loading up to 20% wt. showed an increase in tensile strength and modulus of more than 100% and 50%, respectively, compared to non-reinforced thermoplastic starch. SEM of the fractured surfaces showed good incorporation of the fibers in the matrix. However, higher amounts of pulp fibers tended to attach together or self-agglomerate, making the fibers difficult to disperse in the matrix [69]. However, Ibrahim et al.

(2014) studied the characteristics of fully biodegradable starch-based composites containing date palm fibers varying from 20 to 80 wt%, and mixed date palm with flax fiber at 25 wt% each. The samples were fabricated by hot pressing at 5 MPa and 160°C for 30 min. SEM showed strong adhesion between the fibers and matrix. The measurement of density revealed a small void fraction for composites containing up to 50 wt% fiber content. Increasing the fiber weight fraction up to 50 wt% increased the tensile and flexural mechanical properties. Also thermal stability, water uptake and biodegradation increased with increasing fiber content. The authors' work shows the possibility of using starch-based composites of flax and date palm fibers as a competitive eco-friendly candidate for various applications [70].

2.4 Mixture design of experiments and optimization

Experimental designs and optimization are commonly used as standard tools to achieve quality and excellence of products. It is very useful for research, development and improvement in many areas of studies. This tool helps operators to understand how process and product parameters affect response variables such as processability, physical and mechanical properties and product performance. To determine which factors or variables and interactions are significant or insignificant in their contribution to the product or process condition, statistical mathematical methods are used to develop the design of experiments [65, 66].

A mixture experiment is a special type of response surface methodology or RSM. RSM is a collection of statistical and mathematical techniques that is useful for modeling and analysis of the problem in order to obtain the optimal response of interest [73]. In general, the optimal response can be found by fitting a regression model to the collected data, which are received from experiments called response surface design. Examples of response surface design are factorial design, fractional factorial design and mixture design.

A full-factorial experimental design is used to investigate the response at all factor-level combinations of the independent variables. It is applied when the number of factors is very low and when the complete interactions between factors are needed. A fractional factorial design is used when many factors are considered and some key factors need to be determined. This technique is not used to optimize formulations, but it is used as a screening technique to select from a large number of factors (e.g., ingredients and processing factors) affecting a response.

In mixture design, the response from the mixture of components is a function of the proportions of each ingredients or components [73]. The measured response depends on the relative proportion of the components, not on the amount of the mixture [74]. The proportions of ingredients or components are measured by volume, by weight, or by mole fraction. Therefore, if we let q represent the number of ingredients, the sum of all of q component proportions of a mixture experiment must equal to unity or one; meaning that all independent variable x_i correlate to each other and x_i represent variables of fractional proportion of the i th component, then

$$0 \leq x_i \leq 1, \quad i = 1, 2, \dots, q \quad \text{eq. 2.1}$$

and

$$\sum_{i=1}^q x_i = x_1 + x_2 + \dots + x_q = 1.0 \quad \text{eq. 2.2}$$

A coordinate system for mixture proportions with q components is called a simplex coordinate system, which is a regular q -sided figure with q vertices in $q-1$ dimensions. For example, with $q = 3$ components, the experimental region for the simplex coordinate system of three-component mixture is presented in Figure. 2.11 [75].

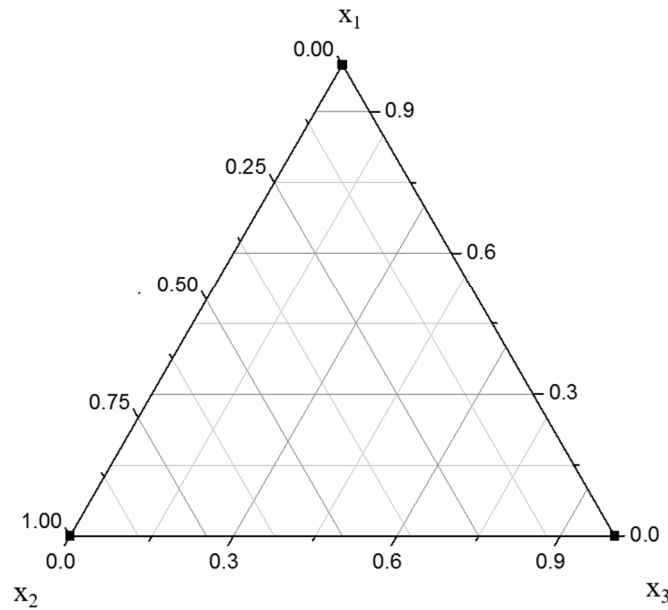


Figure 2.11 Three-component simplex coordinate system (adapted from [75])

With three components, with each component varying from 0 to 1, as factors, the coordinate system defines a triangular experimental space with vertices corresponding to formulations of 100 percent of a single component and each of the three edges of triangle are the binary blends. Moreover, the interior points in the triangle are composed of three components and the centroid of the triangle represents the mixture with equal proportions of the three components. In general, the experimental space for the mixture experimental design covering the entire triangular area consisting of evenly distributed points is called a lattice.

The most common experimental designs developed using the simplex coordinate system technique are simplex-lattice designs, simplex-centroid designs, and augmented simplex-centroid designs [74].

In a simplex-lattice design, the experimental points are spread uniformly in the spaced set of points on a simplex. The lattice may correspond to a form of the mixture polynomial, which is slightly different from the standard polynomial. A polynomial model of degree m in q components can be referred to a $\{q, m\}$ simplex-lattice. The proportions assumed by each component are the $m+1$ equally spaced values from 0 to 1 as follows:

$$x_i = 0, \frac{1}{m}, \frac{2}{m}, \dots, 1 \quad i = 1, 2, \dots, q \quad \text{eq. 2.3}$$

For example, let $q = 3$ and $m = 2$, then all possible combinations of the proportions from equation 2.3 is shown.

$$x_i = 0, \frac{1}{2}, 1 \quad i = 1, 2, 3 \quad \text{eq. 2.4}$$

and the $\{3, 2\}$ simplex-lattice will have six points on the boundary of the triangle.

$$(x_1, x_2, x_3) = (1, 0, 0), (0, 1, 0), (0, 0, 1), \left(\frac{1}{2}, \frac{1}{2}, 0\right), \left(\frac{1}{2}, 0, \frac{1}{2}\right), \left(0, \frac{1}{2}, \frac{1}{2}\right)$$

Because the independent variables x are not unique, the general form of polynomial model that can be fitted to the data at the point of a $\{q, m\}$ simplex-lattice has been modified to use in response surfaces becoming the canonical or Scheffe forms of the mixture polynomial models which are shown as follows:

Linear;

$$E(y) = \sum_{i=1}^q \beta_i x_i \quad \text{eq. 2.5}$$

Quadratic;

$$E(y) = \sum_{i=1}^q \beta_i x_i + \sum_{i<j=2}^q \beta_{ij} x_i x_j \quad \text{eq. 2.6}$$

Full Cubic;

$$E(y) = \sum_{i=1}^q \beta_i x_i + \sum_{i<j=2}^q \beta_{ij} x_i x_j + \sum_{i<j=2}^q \delta_{ij} x_i x_j (x_i - x_j) + \sum_{i<j<k=3}^q \beta_{ijk} x_i x_j x_k \quad 2.7$$

Special Cubic;

$$E(y) = \sum_{i=1}^q \beta_i x_i + \sum_{i<j=2}^q \beta_{ij} x_i x_j + \sum_{i<j<k=2}^q \beta_{ijk} x_i x_j x_k \quad \text{eq. 2.8}$$

In simplex-centroid designs, the experimental points are the same as in simplex-lattice designs but include a centroid point. A q -component simplex-centroid design has 2^q-1 design points. The data from the response will be collected and fitted by the polynomial model:

$$E(y) = \sum_{i=1}^q \beta_i x_i + \sum_{i<j=2}^q \beta_{ij} x_i x_j + \sum_{i<j<k=2}^q \beta_{ijk} x_i x_j x_k + \dots + \beta_{12\dots q} x_1 x_2 \dots x_q \quad 2.9$$

In this q th-order mixture polynomial, from equation 2.9 for $q=3$ components, the model will be :

$$E(y) = \beta_1 x_1 + \beta_2 x_2 + \beta_3 x_3 + \beta_{12} x_1 x_2 + \beta_{13} x_1 x_3 + \beta_{23} x_2 x_3 + \beta_{123} x_1 x_2 x_3 \quad \text{eq. 2.10}$$

In this q th-order mixture polynomial, which is special cubic polynomial from equation 2.9.

For $q=4$ components the model will be as follows:

$$E(y) = \sum_{i=1}^4 \beta_i x_i + \sum_{i<j=2}^4 \beta_{ij} x_i x_j + \sum_{i<j<k=2}^4 \beta_{ijk} x_i x_j x_k + \beta_{1234} x_1 x_2 x_3 x_4 \quad \text{eq. 2.11}$$

This equation will have an additional term. It is a relatively efficient design for fitting the special cubic model.

Cornell (1986) suggests the augmented simplex-centroid design. It has the ability to improve fitting responses. Especially, if the area of the interested is in the complete mixture region, then having more runs in the interior of the simplex is desirable. The augmented simplex-centroid design will have the simplex design plus axial runs with centroid. To define an axial design [76], states that “the axis of component i is the imaginary line extending from the base point $x_i = 0, x_j = 1/(q-1)$ for all $j \neq i$, to the vertex where $x_i = 1, x_j = 0$ all $j \neq i$.

The canonical or Scheffe mixture polynomial models that were obtained from the responses will be used to construct a response surface and a contour plot [73].

In many mixture experiments, one of the most common problems in designing the experiment is the restriction or constraint of the component proportions that prevent researchers from exploring the entire simplex region. The constraint can be upper or lower bounds of the components. To simplify this situation, the constrained mixture design and pseudo-simplex design are examples of design techniques to resolve the inability to explore the entire simplex region.

The mixture design experiment is very popular for use in the area of formulation development, especially in product development such as in most food industries, where constraints or ingredients have to be placed in the allowable range between minimum and maximum proportions of the components. Generally, a mixture design, which includes vertices, faces, edges, and overall centroids, will be used to accomplish the final experimental design.

Using pseudocomponents to fit the mixture model is recommended because a mixture model with pseudocomponents will have fewer effects on the estimators of regression coefficients than using actual components. The various types of mixture design analysis, and model buildings were discussed by Cornell (2002).

2.5 Degradation of Plastics

The change in physical and chemical characteristics of polymer which occur as a consequence of environmental factors, are generally induced by light, heat, moisture, chemical conditions and biological activity. These will affect the polymer properties, resulting in bond scission, chemical transformation and formation of new functional groups. ASTM and the International Organization for Standardization (ISO) describe degradation as “an irreversible process leading to a significant change of the structure of a material, typically characterized by a loss of properties (e.g. integrity, molecular weight, structure or mechanical strength) and/or fragmentation”. In general, polymer degradation can be happen by either abiotic factors (light, temperature) or biotic factors (enzymes, microorganisms) [77].

2.5.1 Mechanical degradation

Mechanical degradation occurs in the presence of various factors such as stress, strain, aging, load, and water or air pressure. The mechanical damage which always occurs is cracking due to physical forces from freezing/thawing, heating/cooling or drying/wetting [77]. Booth et al. [78], investigated the mechanical degradation of polyisoprene. A narrow molecular weight distribution of polyisoprene was used to study the changes in molecular weight after mechanical degradation. The author found that the chain scissions occur at a point far from the ends but , do not necessarily occur near the center of the molecules [79].

2.5.2 Photodegradation

Photodegradation or photo-oxidation is the degradation that takes place under exposure to light, generally ultraviolet light (UV) in the presence of oxygen (air) [80]. The mechanism is that the electrons from the ground state will be brought to an excited state due to the photon molecules having high energy. Therefore, it will bring about the oxidation and cleavage of the polymer. These will result in degradation [77]. The addition of catalysts, usually metal salts (Co, Fe, Mg, Zn, Ce

etc.) of unsaturated fatty acids and pro-oxidant additives, can increase the photodegradability. A major difficulty is to make conventional plastics in a way that they can predictably degrade if the exposure time to light is known. It will be useful to mention that toxic photometabolites from some polymers have been observed. Several photodegradable plastic materials are commercially available. [80].

2.5.3 Thermal degradation

Thermal degradation of polymers is molecular deterioration as a result of overheating [81]. It can occur as a result of depolymerisation and chain scission at high temperature when the rigid polymer form is changed to its liquid form, which is related to the melting temperature and the glass transition temperature [77]. This will make the long chain backbone of the polymer begin to separate (chain scission) and will react with one another to change the properties of the polymer [81]. Thermal degradation also leads to changes in physical and optical properties. Thermal degradation generally involves changing the molecular weight (and molecular weight distribution) of the polymer and typical property changes included reduced ductility and embrittlement, chalking, color changes, cracking and general reduction in most other desirable physical properties [81].

2.5.4 Chemical degradation

Chemical degradation or chemodegradation includes reactions with oxygen (oxidation) and water (hydrolysis). Oxygen (O_2) and ozone (O_3) are important chemicals for the oxidation of polymers. This reaction will bring about cleavage of the covalent bonds in the polymer, releasing free radicals that can lead to cross-linking/chain scission. Unsaturated bonds and branched polymers are more sensitive to oxidation than others [77].

2.5.5 Hydrolysis degradation

Polymers that contain hydrolysable bonds such as esters, anhydrides, ethers, etc., can go through hydrolytic degradation as shown in Figure 2.12 [77]. They can be degraded by hydrolysis into low molecular weight oligomers as the primary degradation and then undergo microbial assimilation in the biodegradation process [82]. The result of hydrolysis is mainly depolymerization which normally occurs in the amorphous regions of the polymer [83].

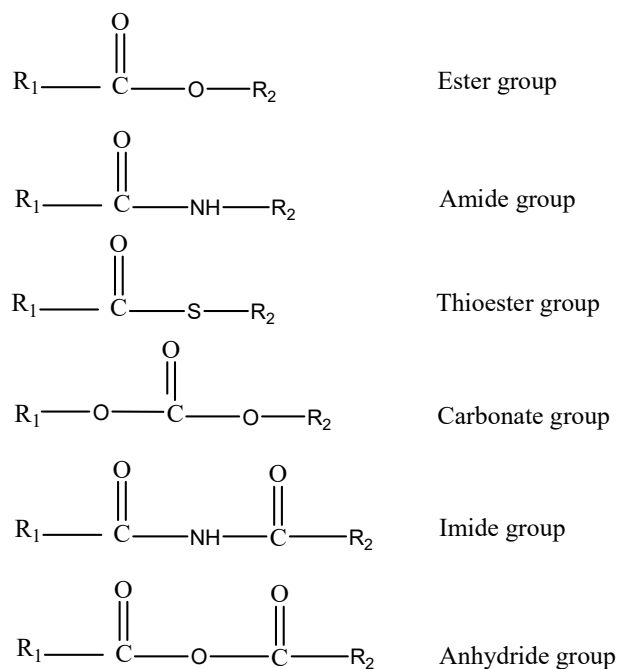


Figure 2.12 Example of hydrolysable bonds

2.5.6 Biodegradation

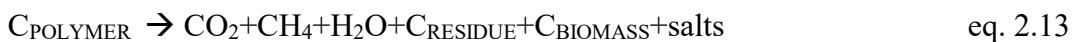
The biodegradation of polymers involves not only the chemistry of the polymer but also the biological processes [84]. Microorganisms that can stimulate the degradation of both natural and synthetic plastics are bacteria, fungi, and algae [81, 85]. To investigate the biodegradability of a material, the factors of concern are: the presence of microorganisms, oxygen, water, temperature and the chemical environment (pH, electrolytes, etc.) [84]. The biodegradation process can be separated in considering of producing carbon dioxide (CO₂) and/or methane (CH₄) and water

(H₂O). If oxygen is present, the biodegradation is aerobic degradation, or if oxygen is not present, the biodegradation is anaerobic [85]. The degradation process can be represented as shown in equation 2.12 and 2.13 [86];

Aerobic biodegradation:



Anaerobic biodegradation:



The conversion process of biodegradable materials or biomass to gases, carbon dioxide, methane, nitrogen compounds, water, salts, and residuals is called mineralization. Complete mineralization occurs when all the biodegradable material, the original substrate, is consumed and all the carbon is completely converted to carbon dioxide or methane [80, 81].

2.6 Biodegradation of thermoplastic starch blends

The presence of starch in mixtures with conventional polymers such as polyethylene (PE), polystyrene (PS) and polypropylene (PP) can accelerate the degradation rate of these polymers due to the porosity in the matrix, which microorganisms create by digesting the starch. It increases the surface area that makes it easy to interact with oxygen [89].

Kijchavengkul et al. [88] determined polymer biodegradation under simulated environmental conditions by building an automatic direct measurement respirometric system. The amount of carbon dioxide produced from poly(lactide) bottles, corn starch powder and poly(ethylene terephthalate) bottles was converted to percentage of mineralization which was used as an indicator of polymer biodegradation. The authors reported that the automatic direct measurement respirometric system ran smoothly and efficiently for more than 63 days at 58±2°C

with 55 ± 5 %RH. The % mineralization of PLA, corn starch, and PET were $64.2 \pm 0.5\%$, $72.4 \pm 0.7\%$, and 2.7 ± 0.2 respectively. Therefore, a PLA bottle is qualified as a biodegradable polymer according to ASTM D6400 and ISO 14855.

Vikman et al.[90] measured the suitability of an in vitro enzymatic method for determining the biodegradation of starch-based materials. Commercial starch-based materials and thermoplastic starch films prepared by extrusion from glycerol and native potato starch, native barley starch, and crosslinked amylo maize starch were studied. To perform enzymatic hydrolysis, *Bacillus licheniformis* α -amylase and *Aspergillus niger* glucoamylase at 37°C and 80°C were used. Biodegradation was determined by weight loss and incubating the samples in a compost environment. It was found that this testing provided a rapid means to get information about the biodegradability of starch-based materials.

Gattin et al.[91] studied the degradation of a co-extruded starch and poly (lactic acid) film in liquid, inert solid and composting media. The experiments were performed according to ASTM D-5338 and ISO/CEN 14855 standards and used two different physical forms of the tested material, film and powder forms. The study showed that the mineralization percentage of starch-based material was always greater than 60%, regardless of the different media. In addition, this study concluded that starch facilitated biodegradation of the polylactic acid component.

Biodegradation of thermoplastic starch and blends with poly(lactic acid) and polyethylene was studied by Li et al. [92] The investigation of mineralization of these polymers was performed under room temperature degradation conditions. The results showed that the morphology and continuity behavior of the blends are correlated. They also found that thermoplastic starch degrades faster than native starch. The amount of glycerol content in the thermoplastic starch has no significant effect on the biodegradation behavior but the amount of thermoplastic starch itself contributed to biodegradation due to a significant increase in TPS surface area.

Pang et al. [93] studied the degradation of blends of thermoplastic starch from agricultural waste with polypropylene using aerobic biodegradation and soil burial. The starch from agricultural waste was obtained from seeds and tubers with low starch contents of approximately 50%. The biodegradation was evaluated based on the extent of carbon conversion. The rate of biodegradation was dependent on the water absorption behavior and molecular structure of the starch component. In soil burial conditions, outdoors showed greater weight loss and deterioration in tensile properties compared to indoor soil burial.

Du et al. [94] studied the biodegradation behaviors of thermoplastic starch (TPS) and thermoplastic dialdehyde starch (TPDAS) under controlled composting conditions. The experiment was built according to the ISO 14855 standard. The TPS degraded quicker than TPDAS under controlled composting conditions due to the chemical modification of starch. The degradation rate and final biodegradation percentage of TPDAS were not significantly different related to the degree of oxidation of dialdehyde starch (DAS). The authors observed that in the biodegradation process of TPS and TPDAS, there were three phases with different degradation rates. In the first phase, the biodegradation speed was slow, then faster in the second phase and leveling off in the third phase. From the compost, three kinds of actinomycete were isolated and identified as micromonospora, nocardia and streptomycete, which were degrading microorganisms of the tested starch.

2.7 Life cycle analysis

2.7.1 Life cycle assessment methodology

Life cycle assessment (LCA) is a methodological framework for estimating and assessing the environmental aspects and potential impacts during the life cycle of a product such as from raw material acquisition through production, use, and disposal or the cradle-to-grave [79, 89, 90, 97]. The general categories of environmental impacts attributed to a product's life cycle include

climate change, stratospheric ozone depletion, tropospheric ozone (smog) creation, eutrophication, acidification, toxicological stress on human health and ecosystems, the depletion of resources, water use, land use, noise, and others [90, 92].

LCA has been standardized according to the International Standard ISO 14040 [99]. It consists of four phases including goal and scope definition, life cycle inventory analysis (LCI), life cycle impact assessment (LCIA) and interpretation of results [100].

According to the framework of LCA, it can be described as follows:

2.7.1.1 Goal and scope

Goal and scope definition is the first part of LCA study. It has to state clearly and unambiguously the intended application, the reason for the study, and the intended audience. In this step, the functional unit, the product system, the system boundaries, the environmental impact categories and the methodology of impact assessment and the sources of the data will be declared.

2.7.1.2 Life cycle inventory analysis (LCI)

Life cycle inventory analysis involves the collection of data and calculation procedures to quantify all the relevant inputs and outputs to each stage of a product life cycle. It will be used for estimating the inputs including consumption of resources such as raw material and energy consumed and outputs including the quantities of waste flows and emissions to air and water, and solid waste produced associated with the product system. These processes can be modeled to represent the product system including its total inputs and outputs [101].

2.7.1.3 Life cycle impact assessment (LCIA)

The life cycle impact assessment (LCIA) aims to describe and evaluate the significant environmental consequences of the environmental impacts quantified in the inventory analysis. This is achieved by using the results of the life cycle inventory analysis. The results from LCIA

are used for an evaluation of a product life cycle, which is based on the functional unit. In the impact assessment phase, several environmental impact categories are included such as climate change, toxicological stress, noise, land use, etc. [102]. In some cases, it will be shown in an aggregated way such as years of human life lost due to climate change, carcinogenic effects, noise, etc. According to International Standard ISO 14044 [99], LCIA consists of two mandatory elements, classification and characterization, and three optional elements, normalization, grouping, and weighting. Moreover, it has an additional LCIA data quality analysis that consists of gravity, uncertainty, and sensitivity analysis to fulfill the goal and scope of the LCA [101].

There are a variety of impact assessment methods, which have been incorporated into available LCA software (SimaPro, Gabi, etc.) including CML 2 baseline 2000, Eco-indicator 99, EDIP 2003, Impact 2002+, and TRACI 2.0, etc. Some of impact assessment methods are described in Table 2.8.

Table 2.8 Descriptions of impact assessment methods

Method	Descriptions	Origin
CML 2 baseline 2000 [100, 103]	This approach has been offered as a baseline method for characterization and normalization. There are nine impact categories considered: abiotic depletion, global warming potential, ozone layer depletion, acidification, eutrophication, human toxicity, aquatic eco-toxicity, terrestrial eco-toxicity and photochemical potential.	Center for Environmental Studies (CML), University of Leiden
Eco-Indicator 99 [100, 103]	This approach is one of the most widely used impact assessment method in LCA study. There are three different types of environmental damage: ecosystem quality, human health and resources. There are nine impact categories considered, which are minerals, fossil fuels, ozone layer, climate change, acidification/ eutrophication, carcinogens, eco-toxicity, respiratory organic and inorganic, radiation and land use.	Developed under the cooperated by companies, research institutes and Dutch government
EDIP 2003 [104, 105]	This approach is a Danish LCA methodology. The major improvements from EDIP 1997 method is in the possibility of exposure in the characterization modelling of non-global impact categories.	Developed by the Institute for Product Development (IPU) at the Technical University of Denmark in Lyngby
IMPACT 2002+ [105]	This method provides a feasible implementation of a combined midpoint and damage approach, which are linking all types of LCI results with 14 midpoint categories to four damage categories	Developed at the Swiss Federal Institute of Technology - Lausanne (EPFL)
ReCiPe[104, 106]	This method integrate the "problem oriented approach" of CML and the "damage oriented approach" of Eco-indicator 99. This approach has implemented on midpoint and endpoint impact categories.	Developed at RIVM and Radboud University, CML, and PRé Consultants

Table 2.8 (cont'd)

Method	Descriptions	Origin
TRACI 2.0 [104, 105]	The Tool for the Reduction and Assessment of Chemical and other environmental Impacts has been used to assist in impact assessment for Sustainability Metrics, industrial ecology, process design and pollution prevention with U.S. locations.	Developed by the Environmental Protection Agency of the United States

2.7.1.4 Interpretation

The interpretation in LCA occurs at every stage in the study [96]. In order to evaluate the study of a product life cycle, the inventory analysis and the impact assessment are combined to derive conclusions and recommendations. This stage is to find the information that can be used for improving or redesigning the production process or optimizing the cost and materials [101].

2.7.2 Current research on LCA of biopolymers

Shen et al. [95] reviewed life cycle assessment (LCA) of the use of polysaccharide materials, such as food, clothing, paper packaging and construction, polysaccharide products in order to gain the insight into the environmental profiles of polysaccharide products such as natural fiber polymer composites in comparison with conventional products such as cotton or petrochemical polymers. It is found that for each stage of the life cycle including production, use phase and waste management, polysaccharide-based products show better environmental profiles than conventional products in the categories of non-renewable energy use (NREU) and greenhouse gas (GHG) emissions. However, cotton has high environmental impact due to the use of fertilizers, herbicides, pesticides and high water consumption.

Hottle et al. [107] reviewed the published life cycle assessments (LCAs) and LCA databases that quantify the environmental sustainability of bio-based polymers. This study compares three bio-based polymers, polylactic acid (PLA), polyhydroxyalkanoate (PHA), and

thermoplastic starch (TPS) with five common petroleum derived polymers from a standard database. The literature showed that biopolymers, coming out of a relatively new industry, reveal similar impacts compared to petroleum-based plastics in term of global warming potential (GWP) and fossil resource depletion due to the technology improvements and productivity. That makes biopolymers currently on par compared to traditional plastics. The lack of LCA on the impacts of different disposal methods will be critical for future sustainability assessments of biopolymers to include accurate end of life impacts.

Qiang et al. [108] studied the life cycle assessment of polylactide-based wood plastic composites (WPC). The environmental impacts of wood flour (WF) reinforced PLA-based composite was evaluated based on input-output substances such as the energy demand, environmental impacts, and water requirements during cradle-to-gate stages. The attribute hierarchy model (AHM) was used to determine the weighting factors of the different environmental impact categories for the environmental impact load (EIL). The resulted showed that the energy demand for 1000 kg of the unmodified PLA-based WPC is a bit higher than with polyhydroxyalkanoates (PHAs). This is also the same with water requirements. Photochemical oxidation potential produced the highest impact among global warming potential, acidification potential, photochemical oxidation potential, eutrophication potential, smog potential and ecotoxicity potential, but the eutrophication potential was the least for the wood plastic composites with and without polyhydroxyalkanoates (PHAs). The cradle-to-gate LCA will contribute to optimize the design, to reduce the energy consumption and pollutant emissions during the production of the PLA-based WPC.

Madival et al.[109] assessed the environmental impacts of PLA, PET and PS clamshell containers using Life Cycle Assessment (LCA). The calculation of environmental impacts depends on the system boundary during the study. This study is a cradle-to-cradle LCA of thermoformed

clamshell containers made from polylactic acid (PLA) in comparison with polyethylene terephthalate (PET) and polystyrene (PS), which are used for packaging of strawberries with different end-of-life scenarios. All inputs such as fertilizers, pesticides, herbicides and seed corn for growing and harvesting of corn are considered for PLA manufacture. The extraction of crude oil and cracking process from crude oil through styrene and ethylene glycol and terephthalic acid are considered for PET and PS. The midpoint impact indicators, which consist of global warming, aquatic acidification, aquatic eutrophication, aquatic ecotoxicity, ozone depletion, non-renewable energy and respiratory organics, land occupation and respiratory inorganics, were selected. The geographical scope was Europe, North America and the Middle East. The results showed that PET had the highest values for all impact categories due to the higher weight of the containers, and the main impacts were associated with the resin production and transportation phases.

Bohlmann [110] compared a biodegradable polymer with a conventional commodity polymer in packaging applications using life cycle assessment (LCA) methodology. The study provided a cradle-to-grave LCA of two polymers, polylactide (PLA) and polypropylene (PP), which were derived from corn and natural gas in the United States, respectively. The impact assessment focused on global warming. The data source was the Process Economics Program (PEP) that provided the energy inventories and greenhouse gas emissions. The results showed that PLA was more energy efficient than PP for thermoformed yogurt cups as food packaging. The difference between PLA and PP systems became noticeable when uncertainty was taken into consideration. The greenhouse emissions of PLA and PP were equivalent if the carbon in PLA was fully sequestered in landfills.

Joshi et al. [111] reviewed and compared the life cycle assessment of natural fiber reinforced (NFR) and glass fiber reinforced (GFR) composites. They reported that the natural fiber reinforced composites were environmentally superior in many cases to glass fiber reinforced

composites. The reasons were that natural fiber production results in lower environmental impacts compared to glass fiber production and NFR composites had higher fiber content for equivalent performance, which reduced the amount of more polluting base polymers. Moreover, the lower weight of the NFR composites improved fuel efficiency and reduced emissions during the use phase of the component and the end of life incineration of NFR composites resulted in energy and carbon credits.

Chapter 3

The optimum formulation composition of thermoplastic cassava starch reinforced by natural fibers

3.1 Introduction

Nowadays, starch bio-composites are gaining more attention as alternative materials to fossil-based composites. Moreover, natural fibers are mainly used as fillers to reduce cost or to improve mechanical properties of the matrix. The primary advantages are that they are economical and environmentally friendly. Many researchers have studied the use of various natural fibers with different polymer matrices but there has not been research on vetiver grass. In this study, mixture design of experiments was used to study in order to create response surface models that can be applied to correlate the input formulation and the final properties of the output sample. The obtained models can be used to predict and to optimize the final properties based on the inputs, which are cassava starch, glycerol, and paper fiber or vetiver fiber. The properties examined, which can be predicted from the obtained models, are tensile strength, tensile modulus, flexural strength, and flexural modulus.

3.2 Research objectives

The objective of this study is to produce and determine the optimum formulation composition of thermoplastic cassava starch (TPCS), natural fibers, and glycerol on the mechanical properties and processing characteristics of the composite.

3.3 Materials and methods

3.3.1 Materials

Cassava (tapioca) starch was obtained from Erawan Marking LTD., Bangkok Thailand. It contained 10.5 to 11.5% moisture content, measured by moisture analyzer, and it contained $25 \pm 6\%$ amylose content. Two types of natural fibers were employed in this study, chemical pulp for printing and writing paper was used as received. (Georgia-Pacific[®] Atlanta, GA) and Vetiver grass was cultivated by the Royal Development Projects in Phetchaburi, Thailand with an age of 6-8 months, which were used as the reinforced material. Glycerol 99+%, food grade was obtained from Aldrich Chemical Company, Inc, Milwaukee, WI.

3.3.2 Methods

3.3.2.1 Fiber preparation

3.3.2.1.1 Chemical pulp preparation

To obtain the chemical pulp, the commercial printing and writing paper was immersed in water at least 24 hours before dispersion using a high-speed blender (Papenmeier, Type TGAHK20) for 10 minutes until no big clumps of pulp were seen. Then it was dried in an oven at 80 °C for 24 hours. These paper fibers were used to prepare the thermoplastic starch composites reinforced by paper fiber throughout this study.

3.3.2.1.2 Vetiver fiber preparation

To obtain vetiver fiber or vetiver pulp, vetiver grass was washed with water to get rid of dirt and dried under sunlight, and then cut into small pieces. Next, the vetiver fiber was produced by a chemical pulping process using 1 M of sodium hydroxide (NaOH) at 10% (oven dry weight) boiling at 150°C in a closed chamber for 4 hours. The alkali-vetiver fiber was then washed thoroughly with running water several times until the pH of the water was neutral. The vetiver fiber was refined to get rid of large particles using a flat screen machine and dried in an oven at

80°C for 24 hours. These vetiver fibers were used to prepare the thermoplastic starch composites reinforced by vetiver fiber throughout this study.

3.3.2.2 Design of experiments with mixture design

Design of experiments (DOE) is a systematic approach to determine cause and effect relationships. DOE is commonly used to guide production lines. It helps operators to understand how process and product parameters affect response variables such as processability, physical, and mechanical properties and product performances. Also it can be used to determine which factors or variables and interactions are significant or insignificant in contribution to the product or process conditions. Statistical mathematical methods are used to develop the design of experiments [64, 65].

In this study, a constrained three-component mixture of experimental design was performed to develop promising statistical models for the correlation between the natural fibers (vetiver fiber and paper fiber), glycerol and cassava starch. The statistical models were used to determine the process operating range. The proportions of the three variable inputs are in weight percentage of cassava starch, glycerol, and natural fiber. The response variables of mechanical properties of this study are impact strength, tensile strength, tensile modulus, flexural strength, and flexural modulus.

Design-Expert Software version V7.0 (Stat-Ease Corp. Minnesota) was used to generate a constrained L-pseudo simplex design of a three-component mixture and to evaluate the properties of the designed points by considering the leverage values and the D-optimality. The D-optimality was selected to find the optimal design.

3.3.2.2.1 Preparation of composites of thermoplastic cassava starch reinforced by paper fiber

In order to know the proper range of composition for each component, a tentative range based on preliminary experiments was used to set up the constrained L-pseudo simplex design of the three-component mixture design as follows:

$$0.60 \leq x_1 \leq 0.80$$

$$0.15 \leq x_2 \leq 0.35$$

$$0.00 \leq x_3 \leq 0.15$$

where x_1 , x_2 , and x_3 are the weight fractions of cassava starch, glycerol, and paper fiber, respectively.

The set of design points was created using the Design-Expert Software. Since the main objective of this experiment was to find the optimum point of the components, the D-optimality criterion was chosen. The constrained L-pseudo simplex design region, 16 design points was constructed as shown in Figure 3.1. The design points were evaluated by considering the leverage values and the D-optimality.

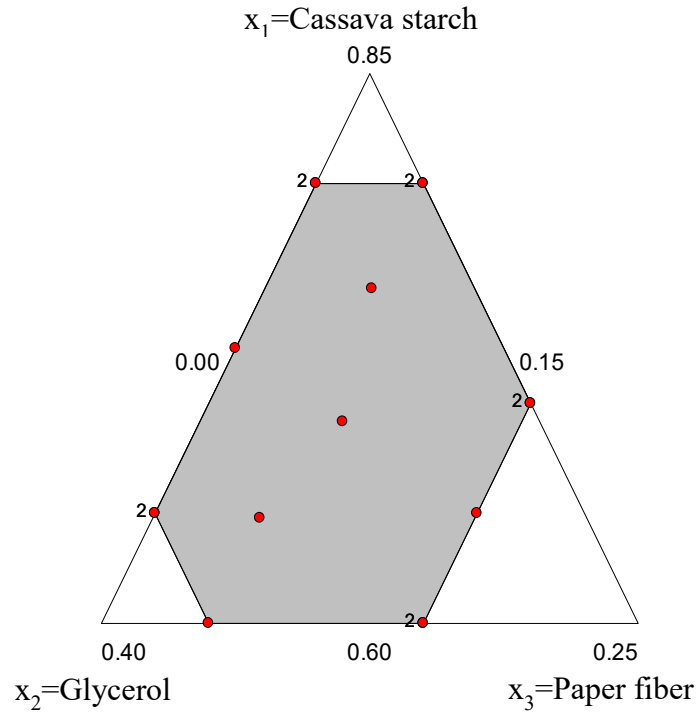


Figure 3.1 The constrained L-pseudo simplex design region of paper fiber-glycerol-cassava starch mixture

The proportions are in real values, the dots are the design points, and “2” indicates the points are replicated twice. The constrained L-pseudo simplex design consists of: 1) one centroid; 2) six vertices, which are replicated twice providing lack-of-test, 3) two center-edge points, and 4) two axial-check-blend points. These coordinated points and leverage numbers of the design are shown in Table 3.1.

To fit the coordinated points in the parameter of Scheffe’s canonical model, the L-pseudo component, x_i' is defined using a linear transformation as

$$x_i' = \frac{x_i - L_i}{1 - L} \quad \text{eq. 3.1}$$

where $L = 0.60 + 0.15 + 0 = 0.75$, so that the L-pseudo components are:

$$x_1' = \frac{x_1 - 0.60}{0.25}, \quad x_2' = \frac{x_2 - 0.15}{0.25}, \quad x_3' = \frac{x_3 - 0.00}{0.25}$$

The evaluation of design shows the average value of leverage is 0.375. This means that the low value of leverage is highly recommended for the experimental design and can show the uniformity which the influence of design point will distribute evenly in the design space. The data points with high leverage are likely to have the potential of shifting the regression line up or down which makes the estimation of coefficient incorrect.

Table 3.1 The three-variables mixture design as composed by Design Expert with design point types and leverage values

Standard order	L-Pseudo simplex coordinates			Original Composition, wt. fraction			Type	Leverage
	X ₁	X ₂	X ₃	X ₁	X ₂	X ₃		
ws1	0.20	0.80	0.00	0.65	0.35	0.00	Vertex	0.3828
2	0.80	0.20	0.00	0.80	0.20	0.00	Vertex	0.3674
3	0.00	0.80	0.20	0.60	0.35	0.05	Vertex	0.5466
4	0.00	0.40	0.60	0.60	0.25	0.15	Vertex	0.4099
5	0.40	0.00	0.60	0.70	0.15	0.15	Vertex	0.4047
6	0.37	0.37	0.26	0.69	0.24	0.07	Center	0.4462
7	0.50	0.50	0.00	0.73	0.27	0.00	CentEdge	0.3663
8	0.59	0.18	0.23	0.75	0.20	0.05	AxialCB	0.2636
9	0.18	0.59	0.23	0.65	0.30	0.05	AxialCB	0.2845
10	0.20	0.20	0.60	0.65	0.20	0.15	CentEdge	0.2276
11	0.80	0.00	0.20	0.80	0.15	0.05	Vertex	0.3678
12	0.80	0.20	0.00	0.80	0.20	0.00	Vertex	0.3674
13	0.80	0.00	0.20	0.80	0.15	0.05	Vertex	0.3678
14	0.00	0.40	0.60	0.60	0.25	0.15	Vertex	0.4099
15	0.40	0.00	0.60	0.70	0.15	0.15	Vertex	0.4047
16	0.20	0.80	0.00	0.65	0.35	0.00	Vertex	0.3828

3.3.2.2.2 Preparation of thermoplastic cassava starch reinforced by vetiver fiber composites

The selected properties from section 3.3.2.2.1 were used to set up the range of compositions in this study. The constrained L-pseudo simplex design of the three-component mixture design was:

$$0.60 \leq x_1 \leq 0.80$$

$$0.15 \leq x_2 \leq 0.35$$

$$0.05 \leq x_3 \leq 0.20$$

where x_1 , x_2 , and x_3 are the weight fraction of cassava starch (denoted as A), glycerol (denoted as B), and vetiver fiber (denoted as C), respectively.

The set of design points was created by using Design-Expert Software (the same as previous study). The constrained L-pseudo simplex design region, 16 design points, was constructed as shown in Figure 3.2. The design points were evaluated by considering the leverage values and the D-optimality.

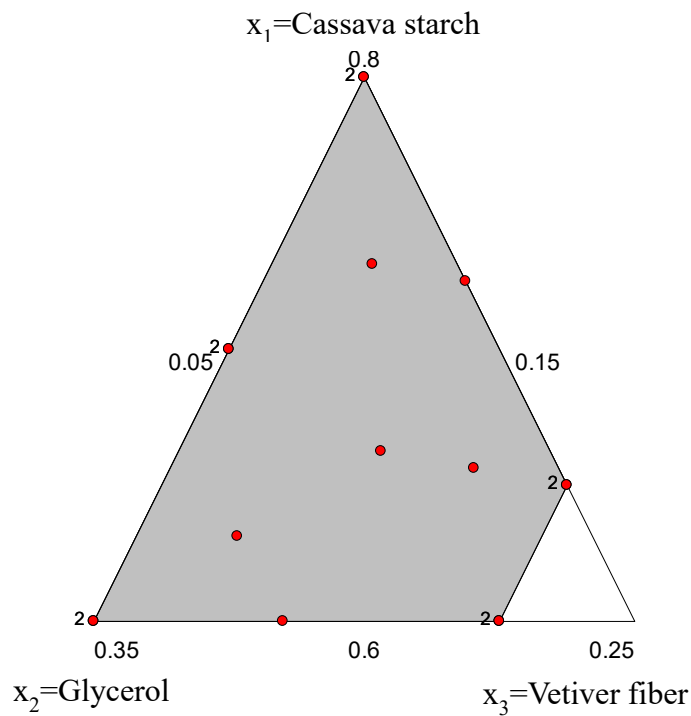


Figure 3.2 The constrained L-pseudo simplex design region of vetiver fiber-glycerol-cassava starch mixture

The proportions are in real values, the dots are the design points, and “2” indicates the points are replicated twice. The constrained L-pseudo simplex design consists of; 1) one centroid; 2) four vertices, which are replicated twice providing lack-of-test, 3) three center-edge points (one of them replicated twice), and 4) three axial-check-blend points. These coordinated points and leverage numbers for the design are shown in Table 3.2.

According to equation 3.1, it can be used to fit the coordinated points in the parameter of scheffe’s canonical model or the L-pseudo component, x_i' . where $L = 0.60+0.15+0.05 = 0.75$, so that the L-pseudo components are:

$$x_1' = \frac{x_1 - 0.60}{0.20}, \quad x_2' = \frac{x_2 - 0.15}{0.20}, \quad x_3' = \frac{x_3 - 0.05}{0.20}$$

The evaluation of design shows the average value of leverage is 0.375. The low value of leverage is the highly recommended for the experimental design and can show the uniformity which the influence of each design point will distribute evenly in the design space.

Table 3.2 The three-variables mixture design as composed by Design Expert with design point types and leverage values

Standard order	L-Pseudo simplex coordinates			Original Composition, wt. fraction			Type	Leverage
	X'1	X'2	X'3	X1	X2	X3		
1	0.63	0.00	0.37	0.72	0.15	0.13	CentEdge	0.432
2	0.00	0.25	0.75	0.60	0.20	0.20	Vertex	0.383
3	0.50	0.50	0.00	0.70	0.25	0.05	CentEdge	0.446
4	0.00	1.00	0.00	0.60	0.35	0.05	Vertex	0.474
5	1.00	0.00	0.00	0.80	0.15	0.05	Vertex	0.473
6	0.00	0.62	0.38	0.60	0.28	0.12	CentEdge	0.468
7	0.31	0.31	0.38	0.66	0.21	0.13	Center	0.238
8	0.25	0.00	0.75	0.65	0.15	0.20	Vertex	0.366
9	0.65	0.16	0.19	0.73	0.18	0.09	AxialCB	0.198
10	0.16	0.65	0.19	0.63	0.28	0.09	AxialCB	0.207
11	0.28	0.16	0.56	0.66	0.18	0.16	AxialCB	0.172
12	0.00	1.00	0.00	0.60	0.35	0.05	Vertex	0.474

Table 3.2 (cont'd)

Standard Order	L-Pseudo simplex coordinates			Original Composition, wt. fraction			Type	Leverage
	X ₁	X ₂	X ₃	X ₁	X ₂	X ₃		
13	1.00	0.00	0.00	0.80	0.15	0.05	Vertex	0.473
14	0.50	0.50	0.00	0.70	0.25	0.05	CentEdge	0.446
15	0.00	0.25	0.75	0.60	0.20	0.20	Vertex	0.383
16	0.25	0.00	0.75	0.65	0.15	0.20	Vertex	0.366

3.3.2.3 Composite preparation

For composites of thermoplastic cassava starch reinforced by natural fibers, the specimens were prepared by two steps: compounding and compression molding. The materials consist of natural fiber, cassava starch and glycerol as the reinforcing material, polymer matrix and plasticizer, respectively.

3.3.2.3.1 Compounding and processing of composites

Compounding is the process in which the polymer is melted by heat and mixed with fibers and additives to form a homogeneous compound. Compounding is commonly carried out by extrusion or using an internal mixer. In this study, the materials were compounded using a three-piece internal mixer (3:2 gear ratio) with mixing roller style from C.W. Brabender® Instruments, Inc. As described by Matuana [112] the three-piece mixer was powered by a 5.6 kilowatt (7.5 hp) Intelli-Torque Plasti-Corder Torque Rheometer® drive (C.W. Brabender® Instruments South Hackensack, NJ).

Cassava starch, natural fiber and glycerol were used to prepare the starch-natural fiber polymer composites. Starch and natural fiber were kept in an oven at 50°C for at least 24 hours prior to processing. Cassava starch, natural fiber and glycerol were premixed in a plastic bag about 3-5 minutes in 25 gram lots in the proportions in Table 3.1 for paper fiber and Table 3.2 for vetiver

fiber. (The amount of fiber was calculated as a percentage of the total dry weight of starch and glycerol.) Then it was loaded into the heated chamber at 130°C, which was maintained at this temperature throughout the compounding process. After loading the materials, a 5 kg dead load was applied directly above the inlet port of the chamber of the internal mixer, the speed of rotors operated at 40 rpm throughout the experiment, and it was discharged after four minutes for paper fiber, and three minutes for vetiver fiber. The gelation and melt characteristics such as time, temperature, torque, and energy were recorded and analyzed by the Brabender® Mixer program (WINMIX, version 3.2.11). Each sample was run at least in triplicate in order to obtain average values for the gelation characteristics

3.3.2.3.2 Compression molding of composites

These compounded mixtures were compression-molded into two shapes: a tensile dogbone-shaped mold (3.0 millimeters in thickness and 2.5 inches in length) following the Type V tensile specimens of ASTM D638 [113], and flexural bar shaped mold (2.5 inches in length , 0.5 inch in width, and 3.0 millimeters in thickness) following the flexural testing specimens of ASTM D790 [114]. The composite mixtures were placed in a Carver Hydraulic Laboratory Press, Menomonee Falls, Wisconsin, USA (Model 12-10HC) at 350°F about 3 minutes using 5,000 psi of pressure for the preheating step and 5 minutes using 20,000 psi of pressure for the heating step. Then the mold was cooled down to room temperature under pressure.

3.4 Characterization

3.4.1 Processability characterization

The processability characterization used the data that was obtained from the compounding step by recording and analyzing the gelation and melt characteristics such as time, temperature, torque, and energy using the Brabender® Mixer program (WINMIX, version 3.2.11).

3.4.2 Thermal properties

Thermogravimetric analysis (TGA) and derivative thermogravimetry (DTG) have been used to investigate and characterize the effects of temperature on weight loss for a variety of materials. It was carried out using a TGA Q50 (TA instruments, New Castle, DE, USA). The samples were weighed in an aluminum pan in accordance with ASTM D3418 [115]. The samples were heated from 30°C to 700°C or as indicated with a constant heating rate of 10°C/min under a controlled environment of nitrogen atmosphere to investigate the weight change of samples as a function of temperature. The data from TGA and DTG provide information about the thermal degradation temperature and weight loss of the materials.

The thermal transitions such as T_g , T_m , enthalpies of cold crystallization (ΔH_c) and melting (ΔH_m) were identified using a DSC Q100 (TA instruments, New Castle, DE, USA) equipped with a refrigerated cooling system unit. The samples were weighed in a hermetic aluminum pan in accordance with ASTM D3418 [115]. The samples were heated from -60°C to 250°C or as indicated with a heating rate of 10°C/min, under nitrogen atmosphere.

3.4.3 Composite characterization

3.4.3.1 Tensile properties

The tensile properties are an important indicator for the material under loading of tension. Tensile properties evaluated in this study were tensile strength, tensile modulus (Young's modulus), and elongation at break. The tensile strength (σ) is given by

$$\sigma = \frac{F}{bh} \quad \text{eq. 3.2}$$

where; F: load

b: width of the sample

h: thickness of the sample

Strain is defined as:

$$\varepsilon = \frac{\Delta l}{l_0} \quad \text{eq. 3.3}$$

where: Δl : the extension

l_0 : the initial gauge length

The tensile testing was performed using a United Testing Systems (UTS) model SFM-20 load frame equipped with a non-contact laser extensometer which was used for determining the distance within the gage length as the test specimen was stretched, following ASTM D638-10 [113]. All TPCS with natural fiber samples were measured, using crosshead speed of testing at 0.05 in/min and distance between grips at 1 inch.

3.4.3.2 Flexural properties

Flexural properties of the composite samples were tested using a United Testing Systems (UTS) model SFM-20 load frame according to ASTM D790-10 [114]. For this three-point bending test, the dimensions of the specimens were $63.5 \times 12.7 \times 3$ mm. The load was applied and the deflection of the specimen was measured. The flexural strength (σ_f) was determined using equation 3.4 and the modulus of elasticity (E_b) was calculated using equation 3.5:

$$\text{Flexural strength} = \frac{3PL}{2bd^2} \quad \text{eq. 3.4}$$

$$\text{Modulus of elasticity} = \frac{L^3 m}{4bd^3} \quad \text{eq. 3.5}$$

Where: P: Applied load

L: Support span

b: Sample width

d: Sample depth

m: initial slope of the load vs. deflection curve

All TPCS with natural fiber samples were measured, using a crosshead speed of testing at 0.05 in/min.

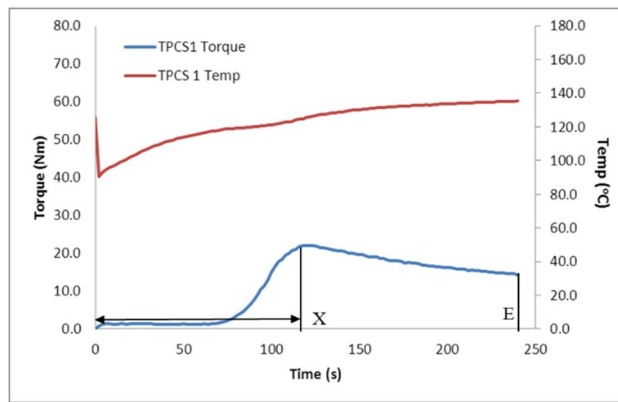
3.4.3.3 Morphological properties

Surface and cross section morphologies of the composites were examined using a model EVO LS 25 (Carl Zeiss Microscopy Ltd., Cambridge, UK) scanning electron microscope at 10 keV.

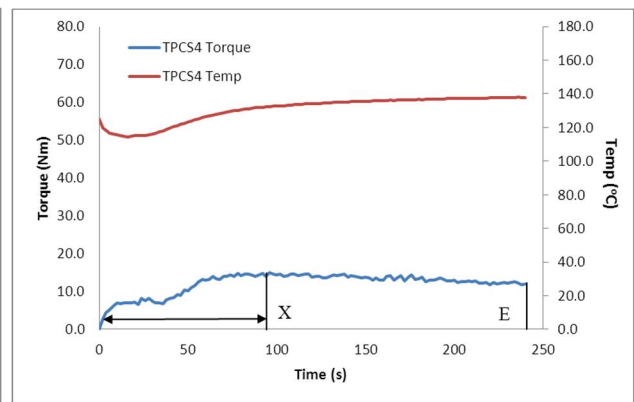
3.5 Results and discussion

3.5.1 Processability of TPCS reinforced by paper fiber

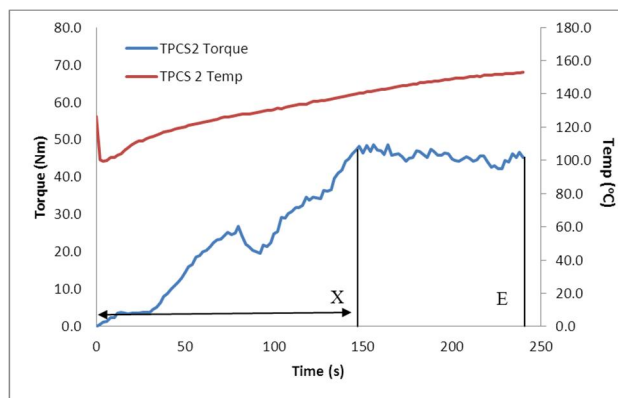
Processing conditions for compounding thermoplastic cassava starch (S) in the presence of glycerol (G) and paper fiber (PF) were studied in a 60-ml electrically heated three-piece internal mixer (3:2 gear ratio) with roller mixing blade (C.W. Brabender® Instruments Inc., South Hackensack, NJ). The Data Processing Plastic-Corder was used to analyze the processing data [112]. The composition of cassava starch, glycerol and paper fiber by weight % is shown in Table 3.3. Typical graphs of Brabender Plastograms show specific points: maximum point (denoted as X), end point (denoted as E), and the area under the curve between the time zero (starting point) to the maximum point, and the time zero to the end point. The graph, at the point “X”, shows the compaction and the onset of gelation, at which the material reached a void-free state and melted between the material and the hot surface metal. Consequently, the portion between the starting point to the gelation point “X” is referred to as gelation temperature, gelation torque and gelation energy, respectively. Similarly, the portion between the starting point to the point “E” is the gelation temperature, gelation torque and gelation energy at the end of processability as reported by Matuana et al. and Collins [106, 111]. The material should be completely melted and the Brabender Rheometer will stop rotating. The results for processing of the thermoplastic cassava starch reinforced by paper fiber samples at point “X” are presented in Figure 3.3 (a to k).



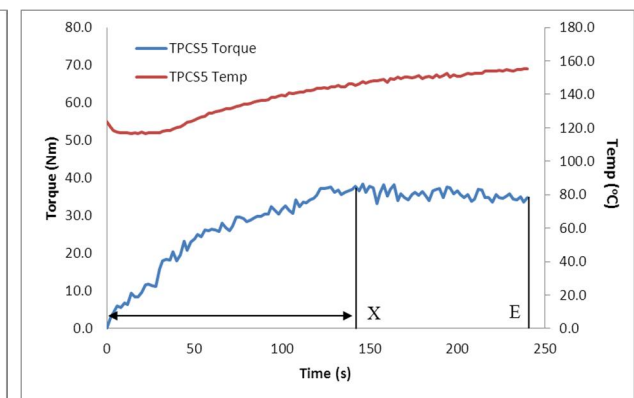
a.



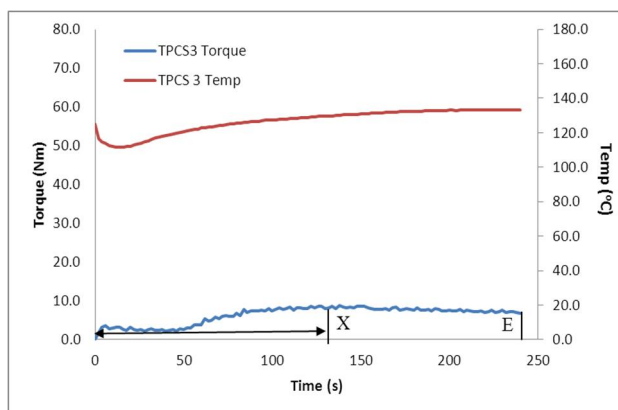
d.



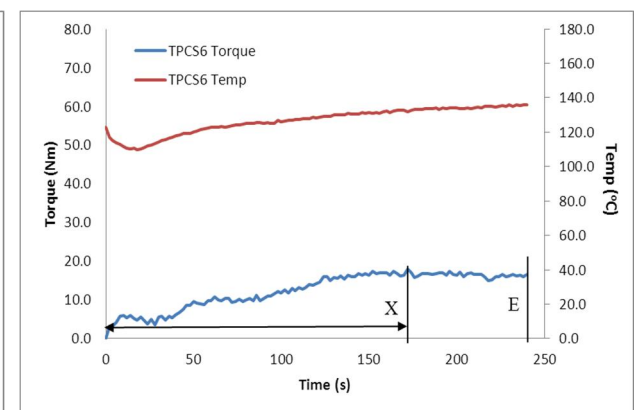
b.



e.



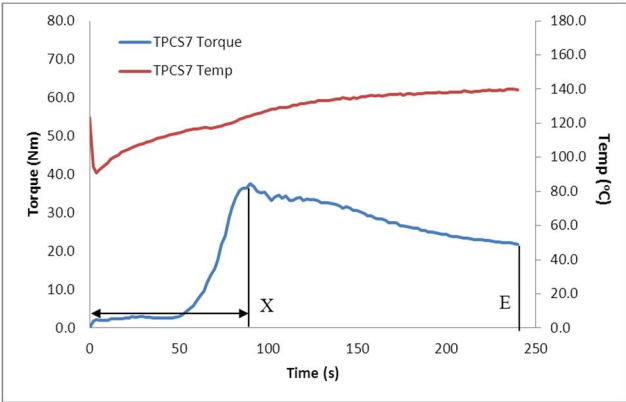
c.



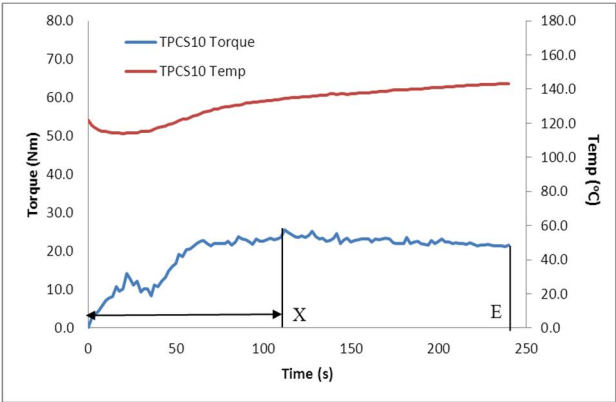
f.

Figure 3.3 The Brabender Plastogram of all TPCS with paper fiber samples

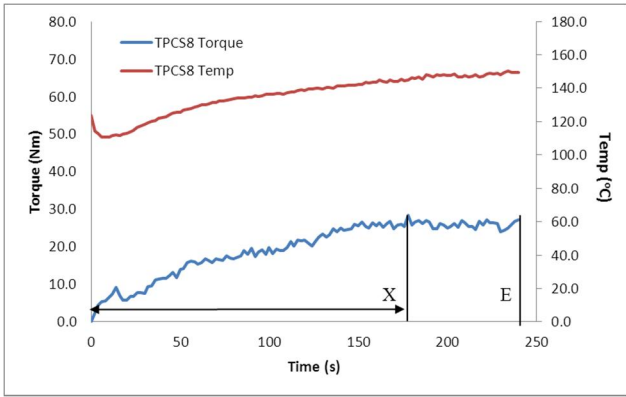
Figure 3.3 (cont'd)



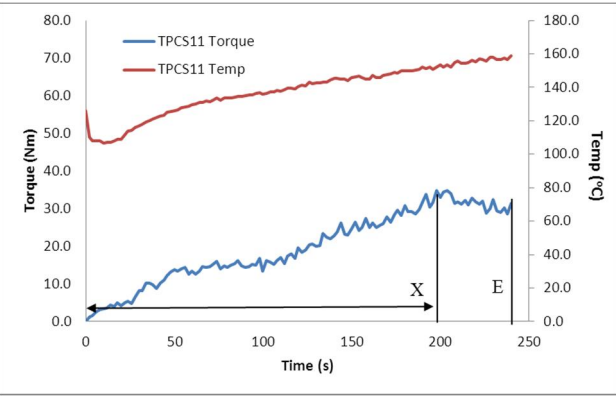
g.



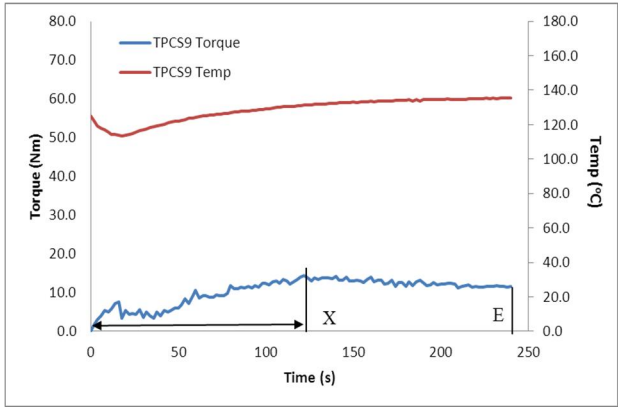
j.



h.



k.



i.

Table 3.3 Measured processing values at point “X” of TPCS with paper fiber

Composi- tion #	Original Composition, wt. fraction			Time (s) at point X	Torque (Nm)	Temp (°C)	Energy at Loading Peak to point X (kJ)
	S*	G*	PF*				
1	0.65	0.35	0	114±8.7	21±1.1	124.2±1.5	2.2±0.3
2	0.8	0.2	0	144±18.3	46.3±7.6	139.6±10.0	10.5±1.5
3	0.6	0.35	0.05	138±13.8	8.8±1.1	130.2±3.8	2.6±0.8
4	0.6	0.25	0.15	96±11.0	15.1±3.1	132.4±4.3	3.6±1.9
5	0.7	0.15	0.15	146±15.4	38.4±3.9	147.7±7.5	12.9±6.5
6	0.69	0.24	0.07	172±20.4	17.9±2.6	131.9±4.3	6.7±2.1
7	0.73	0.27	0	90±2.3	37.6±1.4	124.4±3.0	2.6±0.2
8	0.75	0.2	0.05	178±15.6	28.5±1.6	145±8.2	11.7±3.1
9	0.65	0.3	0.05	120±13.7	13.9±0.8	131.1±4.5	4.1±1.0
10	0.65	0.2	0.15	112±12.1	25.6±1.0	134.4±5.3	6.6±3.2
11	0.8	0.15	0.05	198±15.1	34.8±2.3	152.3±8.1	14.5±5.9

*The acronyms S, G and PF refer to cassava starch, glycerol and paper fiber, respectively.

The processibility for TPCS with paper fiber in the Brabender Plastogram presents the filling material, which is premixed cassava starch, glycerol, and paper fiber put into the chamber of the internal mixer. After loading the material, the temperature dropped and then increased when the material started melting at the interface between the material and the hot metal. Point “X” represents the maximum compaction and the onset of gelation of the material as the material changed into the melting state. The duration between the starting point and the maximum point “X” is denoted as the gelation time. In the same way, the torque, temperature and energy at point “X” are denoted as the gelation torque, gelation temperature, and gelation energy, respectively [107, 111]. As shown in Figure 3.3 and Table 3.3, the gelation time ranged between 90.0 seconds and 198.0 seconds (Composition#4 and #11), while the gelation torque varied from 8.8 Nm to 46.3 Nm (composition#2 and #3). The gelation temperature ranged from 124.2 °C to 152.3 °C (composition#1 and #11) and the gelation energy from loading peak to point “X” varied from 2.2

kJ to 14.5 kJ (composition#1 and #11). In this stage, the processability depended on the glycerol content, as a high amount of glycerol decreased the gelation torque, which made it easier to process comparing Figure 3.3(c) and (d). However, high amounts of cassava starch in the composition increased the torque and also resulted in high values for the gelation torque and gelation temperature, comparing Figure 3.3(b) and (j), which means it was difficult to process and may cause thermal degradation of the starch when the temperature is above 150°C.

The results for the processing of thermoplastic cassava starch reinforced by paper fiber samples at point “E” are presented in Table 3.4 and Figure 3.3.

Table 3.4 Measured processing values at end point (E) of TPCS with paper fiber

Composition #	Original Composition, wt. fraction			End Torque (Nm)	End Temp (°C)	Energy at Loading Peak to point E (kJ)
	S*	G*	PF*			
1	0.65	0.35	0	14.3±0.8	135.3±2.1	11.5±0.3
2	0.8	0.2	0	45.2±7.3	152.8±9.0	28.7±1.2
3	0.6	0.35	0.05	6.9±0.4	133.4±2.7	6±0.4
4	0.6	0.25	0.15	12.1±0.9	138±1.6	10.6±1.7
5	0.7	0.15	0.15	34.9±3.2	155.3±8.3	25.4±3.0
6	0.69	0.24	0.07	16.6±1.3	135.7±6.2	11.3±0.6
7	0.73	0.27	0	21.9±0.6	139.7±4.5	20.5±0.8
8	0.75	0.2	0.05	27.1±3.6	149.5±10.5	17.7±0.7
9	0.65	0.3	0.05	11.5±0.9	135.5±2.4	20.9±0.6
10	0.65	0.2	0.15	21.6±1.9	143.2±4.8	17.2±0.5
11	0.8	0.15	0.05	31.3±1.1	158.8±4.0	19.2±3.5

*The acronyms S, G and PF refer to cassava starch, glycerol and paper fiber, respectively.

As shown in Figure 3.4 and Table 3.4, at point “E” the processing time was stopped at 240 seconds, and the gelation torque varied from 6.9 Nm to 45.2 Nm (composition #3 and #2). Also the gelation temperature ranged from between 133.4 °C and 158.8 °C (composition #3 and #11) and the gelation energy from the starting point to point “E” varied from 6.0 kJ to 28.7 kJ (composition #3 and #2). This study showed that composition “2” which consisted of 80% cassava

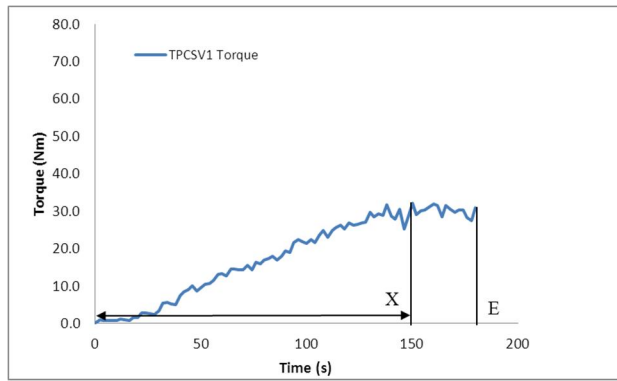
starch and 20% glycerol consumed the highest energy of 28.7 kJ and was difficult to process due to the high value of torque of 45.2 Nm (Figure 3.3b). In contrast, composition “3” which was comprised of 60% cassava starch, 35% glycerol, and 5% paper fiber had the lowest torque and consumed the lowest energy (Figure 3.3c).

3.5.2 Processability of TPCS reinforced by vetiver fiber

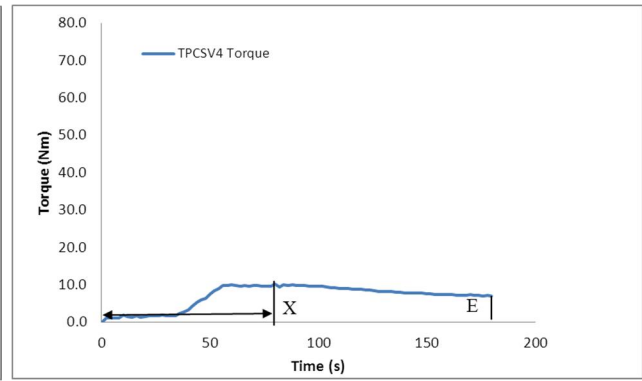
The second natural fiber being studied is vetiver fiber. The same technique of processing data analysis was applied to the samples of thermoplastic cassava starch reinforced by vetiver fiber samples. The composition of cassava starch (S), glycerol (G) and vetiver fiber (VF) by weight % is shown in Table 3.5. In addition, Figure 3.4 (a to k) provides the processing results.

Table 3.5 Measured processing values at Point “X” of TPCS with vetiver fiber

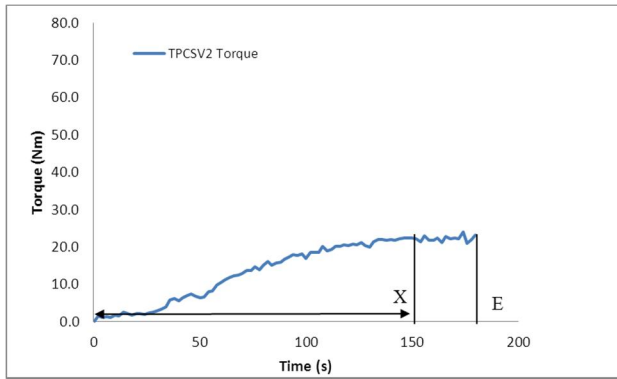
Composition #	Original Composition, wt. fraction			Time (s) at point X	Torque (Nm)	Energy at Loading Peak to point X (kJ)
	Starch	Glycerol	Vetiver fiber			
1	0.72	0.15	0.13	150±10.3	32±6.7	11±1.5
2	0.6	0.2	0.2	156±10.1	23±3.4	10±2.7
3	0.7	0.25	0.05	144±17.0	23.9±2.4	10.1±2.3
4	0.6	0.35	0.05	80±4.2	10.2±1.0	1.5±0.1
5	0.8	0.15	0.05	146±7.1	46.8±6.5	14.8±2.5
6	0.6	0.28	0.12	148±12.1	13.1±1.4	4.7±0.9
7	0.66	0.21	0.13	126±17.4	21.9±0.9	7±1.1
8	0.65	0.15	0.2	138±18.9	24.2±2.3	9.4±3.9
9	0.73	0.18	0.09	158.7±6.6	21.2±3.2	8.1±0.8
10	0.63	0.28	0.09	118±16.3	14.5±3.6	4.5±1.9
11	0.66	0.18	0.16	148±15.1	26.4±1.4	10±2.3



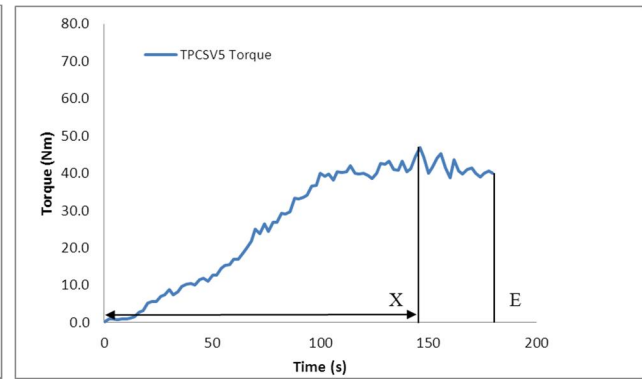
a.



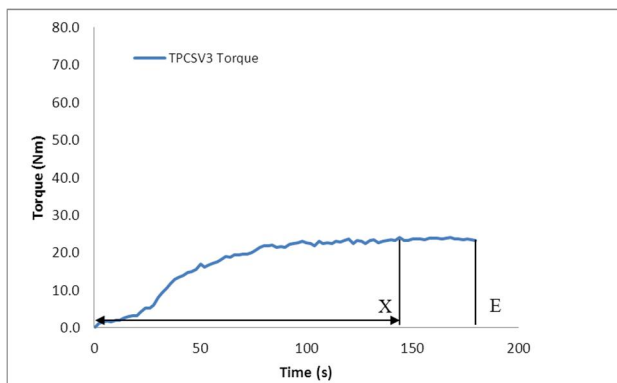
d.



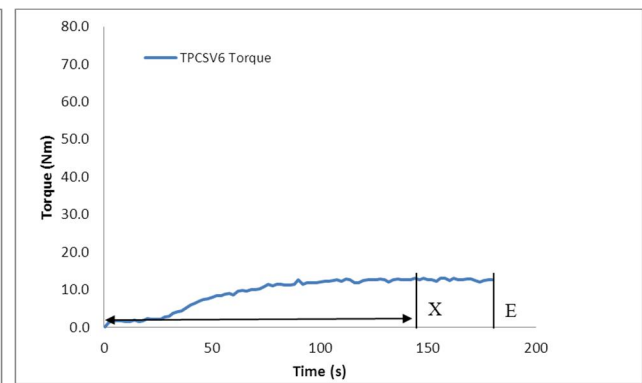
b.



e.



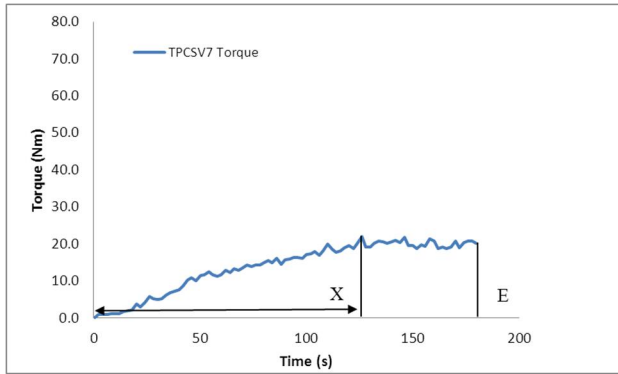
c.



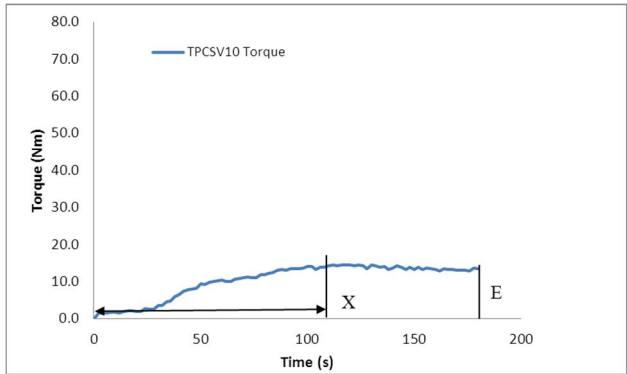
f.

Figure 3.4 The Brabender Plastogram of all TPCS with vetiver fiber samples

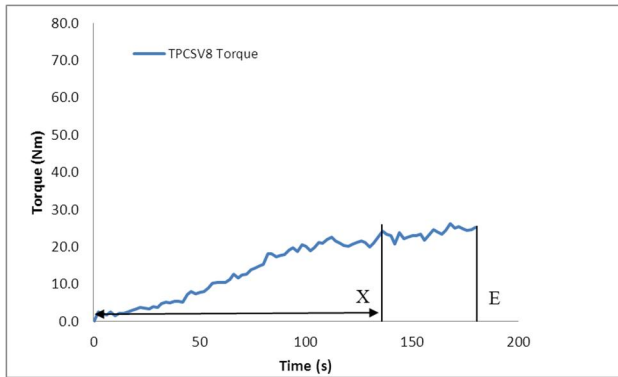
Figure 3.4 (cont'd)



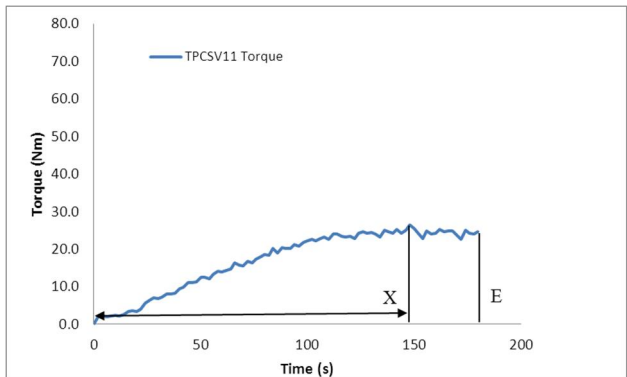
g.



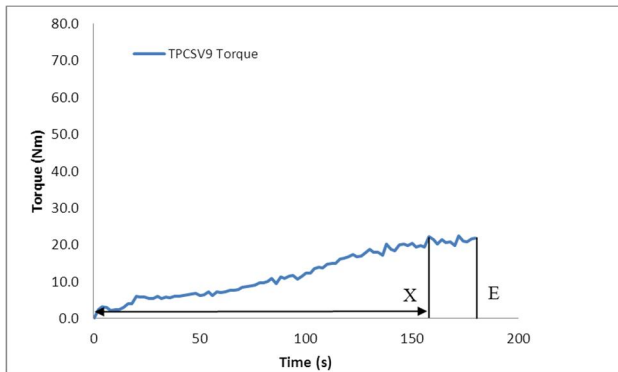
j.



h.



k.



i.

The processibility from time zero to point “X” for TPCS with vetiver fiber showed the gelation time ranged between 80.0 seconds and 158.7 seconds (composition #2 and #9), while the gelation torque varied from 10.2 Nm to 46.8 Nm (composition #4 and #5). The gelation temperature could not be measured because the temperature sensor was not available during the experiment. However, the gelation energy at point “X” varied from 1.5 kJ to 14.8 kJ (composition #4 and #5). The effect of glycerol and starch content on processibility was similar to the previous study. A high amount of glycerol content decreased the gelation energy and made it easier to process as seen in Figure 3.4(b) and (d). Meanwhile a high amount of cassava starch increased the torque and gelation energy as seen in Figure 3.4(e) and (h), which means it was difficult to process and may cause thermal degradation of starch when the temperature rose above 150°C.

The experimental results for TPCS reinforced by vetiver fiber samples at point “E” are presented in Table 3.6 and Figure 3.4.

Table 3.6 Measured polymer processing at end point (E) of TPCS with vetiver fiber

Composition #	Original Composition, wt. fraction			End Torque (Nm)	Energy at Loading Peak to point E (kJ)
	Starch	Glycerol	Vetiver fiber		
1	0.72	0.15	0.13	30.8±6.3	13.4±2.2
2	0.6	0.2	0.2	23.2±3.1	14.7±3.5
3	0.7	0.25	0.05	23.3±1.9	15.1±2.0
4	0.6	0.35	0.05	7±0.9	5.7±0.9
5	0.8	0.15	0.05	39.9±4.6	24.2±5.1
6	0.6	0.28	0.12	12.7±1.7	8.1±0.6
7	0.66	0.21	0.13	20.2±4.0	12±3.1
8	0.65	0.15	0.2	25.3±2.5	11.5±5.9
9	0.73	0.18	0.09	21.8±2.6	10.6±2.2
10	0.63	0.28	0.09	13.4±3.0	8.7±2.8
11	0.66	0.18	0.16	24.6±6.1	14.6±0.8

At point “E” the gelation time was ended at 180 second. The gelation torque varied from 7 Nm to 39.9 Nm (composition #4 and #5). Also the gelation energy from starting point to end was

varied from 5.7 kJ to 24.2 kJ (composition #4 and #5). This study showed that composition “5” which consisted of 80% of cassava starch, 15% glycerol and 5% vetiver fiber consumed the highest energy of 24.2 kJ and was difficult to process due to the high torque value of 39.9 Nm. In contrast, composition “4” which was comprised of 60% cassava starch, 35% glycerol, and 5% vetiver fiber consumed the lowest torque and energy of 7.0 and 5.7 kJ, respectively, which is similar to the previous study.

3.5.3 Mechanical properties of thermoplastic cassava starch composites with paper fiber

The results for mechanical properties of the samples of thermoplastic cassava starch (TPCS) reinforced by paper fiber are presented in Table 3.7.

Table 3.7 Measured tensile and flexural properties of TPCS reinforced by paper fiber

Standard Order	Composition, (weight %)			Tensile Strength (MPa)		Tensile Modulus (MPa)		Flexural Strength (MPa)		Flexural Modulus (MPa)	
	S*	G*	PF*	Mean	SD	Mean	SD	Mean	SD	Mean	SD
1	0.65	0.35	0.00	0.8	0.0	3.8	0.2	1.7	0.1	65.1	9.3
2	0.80	0.20	0.00	4.2	0.8	134.2	10.4	1.1	0.3	43.4	16.0
3	0.60	0.35	0.05	1.5	0.1	9.0	0.3	2.0	0.3	51.4	11.0
4	0.60	0.25	0.15	1.9	0.2	11.2	1.5	2.6	0.4	52.8	5.0
5	0.70	0.15	0.15	8.5	0.2	357.9	11.5	9.3	3.1	765.3	143.9
6	0.69	0.24	0.07	1.7	0.1	12.2	0.9	1.8	0.3	23.0	45.9
7	0.73	0.27	0.00	0.6	0.0	2.2	0.2	1.3	0.1	23.7	2.1
8	0.75	0.20	0.05	8.6	0.9	249.0	13.0	3.8	1.2	135.1	54.7
9	0.65	0.30	0.05	0.9	0.1	4.0	1.0	2.9	0.2	63.2	14.1
10	0.65	0.20	0.15	7.3	1.3	192.1	26.4	1.0	0.1	21.9	2.1
11	0.80	0.15	0.05	2.4	0.2	251.1	6.6	14.0	5.5	1392.6	163.7
12	0.80	0.20	0.00	3.3	0.2	129.8	12.1	1.6	0.7	52.2	16.7

*The acronyms S, G and PF refer to cassava starch, glycerol and paper fiber, respectively.

Table 3.7 (cont'd)

Stand- ard Order	Composition, (weight %)			Tensile Strength (MPa)		Tensile Modulus (MPa)		Flexural Strength (MPa)		Flexural Modulus (MPa)	
	S*	G*	PF*	Mean	SD	Mean	SD	Mean	SD	Mean	SD
13	0.80	0.15	0.05	2.1	0.2	242.0	5.3	14.5	4.2	1303.0	150.1
14	0.60	0.25	0.15	1.3	0.1	10.8	2.3	2.4	0.3	64.2	7.5
15	0.70	0.15	0.15	6.7	0.3	365.4	17.0	13.0	2.4	888.2	82.6
16	0.65	0.35	0.00	0.6	0.0	1.8	0.1	1.6	0.1	49.9	9.2

*The acronyms S, G and PF refer to cassava starch, glycerol and paper fiber, respectively.

The tensile properties of the thermoplastic cassava starch reinforced by paper fiber are shown in Table 3.7. The samples were made of 60-80% cassava starch, 15-35% glycerol and 0-15% paper fiber using the mixture design method. The range of tensile strength varied between 0.6 MPa and 8.6 MPa and tensile modulus varied between 1.8 MPa and 365.4 MPa. Tukey's test method was used to investigate significance differences of measured tensile strength and tensile modulus, which can be seen in Figure A.1.

The flexural properties of the thermoplastic cassava starch reinforced by paper fiber are also shown in Table 3.7. The samples were made as in the previous study using the mixture design method. The flexural strength ranged between 1.0 MPa to 14.5 MPa and the flexural modulus varied between 21.9 MPa and 1392.6 MPa. Tukey's test method was used to investigate significance differences in measured flexural strength and flexural modulus, which can be seen in Figure A.2.

3.5.4 Mechanical properties of thermoplastic cassava starch composites with vetiver fiber

The results for mechanical properties of the samples of thermoplastic cassava starch (TPCS) reinforced by vetiver fiber samples are presented in Table 3.8

Table 3.8 Measured tensile and flexural properties of TPCS reinforced by vetiver fiber

Stand- ard Order	Composition, (weight %)			Tensile Strength (MPa)		Tensile Modulus (MPa)		Flexural Strength (MPa)		Flexural Modulus (MPa)	
	S*	G*	VF*	Mean	SD	Mean	SD	Mean	SD	Mean	SD
1	0.72	0.15	0.13	6.9	0.6	232.9	15.5	23.7	8.6	1758.3	126.1
2	0.60	0.20	0.20	10.3	1.3	226.3	39.7	17.2	5.4	1167.4	153.2
3	0.70	0.25	0.05	10.7	3.4	235.1	20.1	19.9	2.8	1050.0	130.5
4	0.60	0.35	0.05	8.5	1.1	113.9	8.2	1.6	0.2	63.5	9.9
5	0.80	0.15	0.05	3.1	0.3	168.6	9.9	4.0	0.6	83.1	15.8
6	0.60	0.28	0.12	10.8	2.7	232.7	23.2	4.2	0.6	118.6	24.2
7	0.66	0.21	0.13	4.8	1.0	240.6	18.3	15.5	3.3	1332.2	207.0
8	0.65	0.15	0.20	7.7	1.6	207.6	9.4	33.7	2.8	1912.2	112.3
9	0.73	0.18	0.09	8.5	0.9	218.1	27.2	18.7	6.3	1261.8	219.8
10	0.63	0.28	0.09	8.3	2.4	183.5	13.2	24.0	7.0	1582.1	115.5
11	0.66	0.18	0.16	11.0	2.3	227.6	27.0	22.3	3.9	1370.8	69.5
12	0.60	0.35	0.05	9.9	1.5	116.0	2.6	2.0	0.1	72.8	9.1
13	0.80	0.15	0.05	4.9	0.9	205.5	13.9	2.3	0.7	77.8	12.6
14	0.70	0.25	0.05	10.3	2.0	203.9	14.9	15.7	1.9	861.1	51.9
15	0.60	0.20	0.20	12.9	2.1	218.9	22.8	19.1	3.8	1352.4	98.9
16	0.65	0.15	0.20	8.5	1.4	221.1	43.0	30.6	3.0	1642.6	109.9

*The acronyms S, G and VF refer to cassava starch, glycerol and vetiver fiber, respectively.

The tensile properties of the thermoplastic cassava starch reinforced by vetiver fiber are represented in Table 3.8. The samples were made of 60-80% cassava starch, 15-35% glycerol and 5-20% vetiver fiber using the mixture design method. The fiber content was changed from the previous study due to the paper fiber, which results showed that almost samples with high fiber content were stronger than those with lower content. Therefore, the range of fiber content was increased by 5% to discover the maximum strength. The results revealed that tensile strength varied between 3.1MPa and 12.9 MPa and the tensile modulus varied between 113.9 MPa and 240.6 MPa. Tukey's test method was used to investigate significance differences in measured tensile strength and tensile modulus, which can be seen in Figure A.3.

The flexural properties of the thermoplastic cassava starch reinforced by vetiver fiber are also presented in Table 3.8. The samples were made of 60-80% cassava starch, 15-35% glycerol and 5-20% vetiver fiber using the mixture design method. The flexural strength varied between 1.6 MPa and 33.7 MPa and flexural modulus varied between 63.5 MPa and 1912.2 MPa. . Tukey's test method was used to investigate significance differences in measured flexural strength and flexural modulus, which can be seen in Figure A.4.

3.5.5 The relationship between composition of the thermoplastic cassava starch (TPCS) reinforced by paper fiber and mechanical properties.

In this study, the obtained results from Table 3.7 were analyzed using Design Expert software (version 7.0.0, Stat-Ease, Inc., Minneapolis, MN, USA). The following steps: transformation of the response; model fitting; analysis of variance (ANOVA) test; model diagnostics; and response surface graphs, were performed for each response variable. To choose the best fit model, first a transformation of the response was considered. Possible transformations included square root, natural log and base 10 log etc. will be applied in order to improve the statistical properties of the analysis. Then comparing various coefficients of R^2 values between linear, quadratic, special cubic and cubic canonical polynomial model were selected, then the determination of Adjusted- R^2 and Predicted- R^2 values were chosen based on the maximum value. After that, the number of model terms may be reduced based on the F-value by applying backward elimination technique in order to get the model terms, which provide maximum R^2 values. Backward elimination is the method for sequentially adding or removing variables. To examine the influence of each design points or the model, model diagnostics was carried out. Finally, the graph of the response surface of the selected model is presented [117].

3.5.5.1 The relationship between composition and tensile strength

Table 3.9 represents the summary statistics for the tensile strength model of TPCS reinforced by paper fiber. The ratio of max to min is greater than 10, indicating that a transformation is required. In this case, base 10 log is applied to this response prior to selecting the model. The tensile strength model summary shows the results for sequentially fitting the linear, quadratic, special cubic, and cubic models to the data. The cubic canonical polynomial model is better than the other models, because it has higher adjusted- R^2 value and Predicted- R^2 value which means that the model is able to describe the response variations for all design points better than the other models. Moreover, the prediction error sum of squares (PRESS), called the PRESS residual, provides a residual scaling. The regression models with small values of PRESS are usually good for prediction equations. The cubic canonical polynomial model has the smallest value of PRESS. Therefore, it was chosen to construct the model.

Table 3.9 Tensile strength model summary statistics

Source	Std.Dev.	R^2	Adjusted- R^2	Predicted- R^2	PRESS	remark
Linear	0.260	0.6305	0.5737	0.4585	1.3	
Quadratic	0.290	0.6416	0.4623	0.0802	2.22	
Special Cubic	0.260	0.7416	0.5694	0.2152	1.89	
Cubic	0.120	0.9600	0.9143	0.5917	0.98	Suggested

After backward elimination was applied to the cubic canonical polynomial model, the final or best fit model in terms of the pseudo components was obtained as follows:

Log₁₀ (Tensile Strength)

$$\begin{aligned}
 &= -0.1 x_1' + 1.8 x_2' + 4.5 x_3' - 4.3 x_1'x_2' - 6.3 x_1'x_3' - 13.4 x_2'x_3' + 27.8 x_1'x_2'x_3' + 9.6 x_1'x_2'(x_1' - x_2') \\
 &\quad (0.4) \quad (0.4) \quad (1.0) \quad (1.2) \quad (2.1) \quad (3.0) \quad (6.1) \quad (1.9) \\
 &+ 5.6 x_1'x_3'(x_1' - x_3') \quad \text{eq. 3.6} \\
 &\quad (2.5)
 \end{aligned}$$

where x_1' , x_2' and x_3' are weight fractions of cassava starch, glycerol, and paper fiber, respectively. The standard errors of the parameter coefficients are shown in parentheses. The model is presented as a model for L-pseudo component coding with transformation formula as previously described. After transforming the formula for the actual component model, the equation using of the real values in term of weight fractions of the components became:

Log₁₀ (Tensile Strength)

$$\begin{aligned}
 &= -17.4 x_1 + 497.6 x_2 + 582.5 x_3 - 901.6 x_1x_2 - 920.1 x_1x_3 - 1866.4 x_2x_3 + 1777.7 x_1x_2x_3 + \\
 &\quad 617 x_1x_2(x_1 - x_2) + 358.1 x_1x_3(x_1 - x_3) \quad \text{eq. 3.7}
 \end{aligned}$$

The proposed model gives a prediction of the tensile strength with $R^2 = 0.9600$, Adjusted- $R^2 = 0.9143$ and Predicted- $R^2 = 0.5917$ associated with the small P-value less than 0.05. The Adjusted- R^2 value of 0.9143 is higher than the suggested minimum Adjusted- R^2 value for response surface model, which is 0.7, which is recommended by the Design Expert program. The summary of the ANOVA-test for the response surface model is indicated in Table 3.10. The p-value of the model and parameters, in this case linear mixture components, x_1' , x_2' , x_3' , $x_1'x_2'$, $x_1'x_3'$, $x_2'x_3'$,

$x_1'x_2'x_3'$, and $x_1'x_2' (x_1'-x_2')$ terms are less than 0.05, but $x_1'x_3' (x_1'-x_3')$ term is higher than 0.05, indicating that the model and parameter terms are significant. However the term $x_1'x_3' (x_1'-x_3')$ needs to be in the equation in order for the “Lack of fit F-value” to be insignificant. The lack of fit measures the error due to deficiencies in the model. If the lack of fit is significant (p-value is less than 0.05), the model is not adequate. The p-value of lack of fit of 0.0966 shows that the selected model is statistically significant, so it can be used as a tensile strength model.

Table 3.10 The ANOVA-test summary statistics of tensile strength model

Source	Sum of Squares	df	Mean Square	F-Value	p-value Prob > F	remark
Model	2.31	8	0.29	21	0.0003	significant
Linear Mixture	1.52	2	0.76	55.16	< 0.0001	
AB	0.18	1	0.18	13.02	0.0086	
AC	0.12	1	0.12	9.06	0.0196	
BC	0.28	1	0.28	20.55	0.0027	
ABC	0.29	1	0.29	20.9	0.0026	
AB(A-B)	0.37	1	0.37	26.7	0.0013	
AC(A-C)	0.07	1	0.07	5.07	0.0591	
Residual	0.096	7	0.014			
Lack of Fit	0.059	2	0.029	3.87	0.0966	not significant
Pure Error	0.038	5	0.01			
Cor Total	2.41	15				

The summary of the diagnostic case statistics for the tensile strength model is presented in Table 3.11. The residuals between the predicted values and actual values show good dispersion throughout the data points within the range of -0.144 to 0.136. The residuals should be randomly around zero. This can be seen by plotting the studentized residuals that lie approximately along a straight line. However, the internally studentized residual values are within the range of -3 to +3 and the externally studentized residual values are within the range of -3.5 to + 3.5 indicating no outliers in the dataset. The leverage values range from 0.474 to 0.916. In general, lower leverage

values are preferred. Data points that have high leverage values could have the potential to result in inaccurate estimation of coefficients. The difference between the fitted value or DFFITS and Cook's distance was used for detecting influential data points. The values with asterisks exceeded the suggested ranges of values, indicating that not all data points constitute the model evenly.

Table 3.11 The diagnostic case statistics for tensile strength model

Standard Order	Actual Value	Predicted Value	Residual	Leverage	Internally Studentized Residual	Externally Studentized Residual	Influence on Fitted Value DFFITS	Cook's Distance
1	-0.075	-0.157	0.082	0.479	0.963	0.957	0.917	0.095
2	0.621	0.562	0.059	0.482	0.699	0.671	0.648	0.051
3	0.168	0.212	-0.044	0.916	-1.297	-1.378	* -4.54	* 2.03
4	0.280	0.192	0.089	0.476	1.046	1.055	1.006	0.111
5	0.931	0.868	0.063	0.479	0.742	0.716	0.686	0.056
6	0.241	0.385	-0.144	0.474	-1.688	-2.030	-1.927	0.285
7	-0.232	-0.184	-0.048	0.739	-0.807	-0.784	-1.321	0.205
8	0.933	0.820	0.113	0.782	2.059	3.034	* 5.74	* 1.68
9	-0.065	-0.201	0.136	0.681	2.056	3.026	* 4.42	1.004
10	0.863	0.890	-0.027	0.618	-0.374	-0.350	-0.445	0.025
11	0.379	0.373	0.006	0.479	0.071	0.066	0.063	0.001
12	0.520	0.562	-0.042	0.482	-0.500	-0.471	-0.455	0.026
13	0.322	0.373	-0.051	0.479	-0.606	-0.576	-0.553	0.037
14	0.117	0.192	-0.074	0.476	-0.876	-0.860	-0.820	0.078
15	0.829	0.868	-0.040	0.479	-0.467	-0.439	-0.421	0.022
16	-0.233	-0.157	-0.077	0.479	-0.904	-0.891	-0.854	0.083

* Exceeds limits

The contour plot and response surface plot based on the model for tensile strength are shown in Figure 3.5 and Figure 3.6, respectively.

Design-Expert® Software
 Transformed Scale
 Log10(Tensile Strength)
 ● Design Points
 0.932975
 -0.233461

X1 = A: Cassava Starch
 X2 = B: Glycerol
 X3 = C: Paper fiber

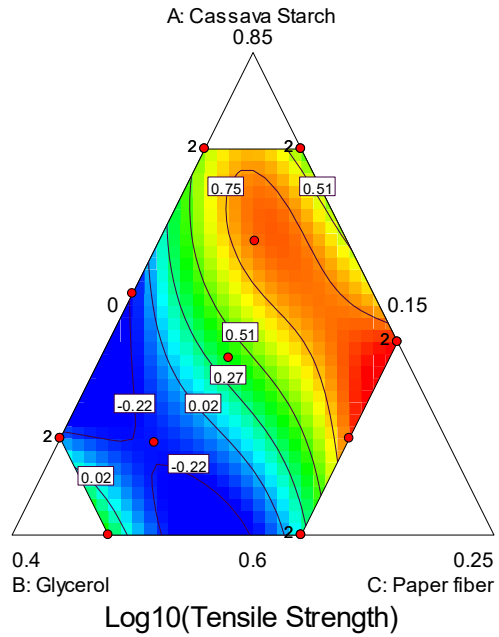


Figure 3.5 Contour plot of tensile strength

Design-Expert® Software
 Transformed Scale
 Log10(Tensile Strength)
 ● Design Points
 0.932975
 -0.233461

X1 = A: Cassava Starch
 X2 = B: Glycerol
 X3 = C: Paper fiber

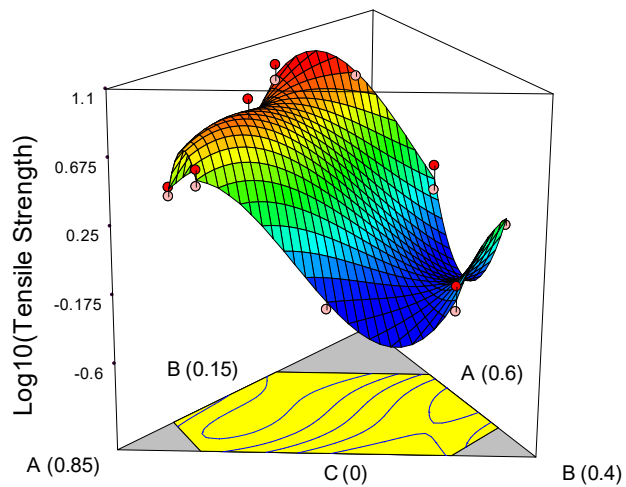


Figure 3.6 Response surface plot of tensile strength

3.5.5.2 The relationship between composition and tensile modulus

A similar technique of data analysis was applied to the tensile modulus of the TPCS with paper fiber composite. Similarly to the tensile strength, base 10 log transformation was applied to this response prior to selecting the model. The tensile modulus model summary shows that the cubic canonical polynomial model gave the best coefficient of determination values of 0.995 and 0.9876 for R^2 and Adjusted- R^2 respectively as presented in Table 3.12. The models for both L-pseudo component coding and the actual component model in term of weight fractions are as follows:

Log₁₀ (Tensile Modulus)

$$\begin{aligned}
 &= 2.5 x_1' + 3.1 x_2' + 31.9 x_3' - 9.7 x_1'x_2' - 64.3 x_1'x_3' - 72.9 x_2'x_3' + 123.1 x_1'x_2'x_3' + 10.9 x_1'x_2'(x_1' - x_2') + \\
 &\quad (0.3) \quad (0.3) \quad (7.1) \quad (1.0) \quad (15.6) \quad (15.6) \quad (23.9) \quad (1.6) \\
 &\quad 45.0 x_1'x_3'(x_1' - x_3') + 39.2 x_2'x_3'(x_2' - x_3') \quad \text{eq. 3.8} \\
 &\quad (11.3) \quad (11.3)
 \end{aligned}$$

Log₁₀ (Tensile Modulus)

$$\begin{aligned}
 &= -11.5 x_1 + 597.4 x_2 + 4779.7 x_3 - 1092.8 x_1x_2 - 7672.5 x_1x_3 - 9168.0 x_2x_3 + 7877.3 x_1x_2x_3 + \\
 &\quad 694.9 x_1x_2(x_1 - x_2) + 2883.1 x_1x_3(x_1 - x_3) + 2507.5 x_2x_3(x_2 - x_3) \quad \text{eq. 3.9}
 \end{aligned}$$

Table 3.12 Tensile modulus model summary statistics

Source	Std.Dev.	R ²	Adjusted-R ²	Predicted-R ²	PRESS	remark
Linear	0.39	0.8283	0.8019	0.7474	2.88	
Quadratic	0.39	0.8684	0.8025	0.6742	3.72	
Special Cubic	0.31	0.9217	0.8696	0.7661	2.67	
Cubic	0.097	0.995	0.9876			Suggested

The summary of ANOVA-test, the model significance and model terms are presented in Table 3.13. All of p-values of the component in the model are significant due to less than 0.05 and the p-value of lack-of-fit is insignificant, so it can be used as the proposed model.

Table 3.13 The ANOVA-test summary statistics of tensile modulus model

Source	Sum of Squares	df	Mean Square	F-Value	p-value Prob > F	remark
Model	11.35	9	1.26	133.34	< 0.0001	significant
Linear Mixture	9.45	2	4.72	499.51	< 0.0001	
AB	0.88	1	0.88	93.12	< 0.0001	
AC	0.16	1	0.16	17.09	0.0061	
BC	0.21	1	0.21	21.95	0.0034	
ABC	0.25	1	0.25	26.48	0.0021	
AB(A-B)	0.46	1	0.46	49.02	0.0004	
AC(A-C)	0.15	1	0.15	15.86	0.0073	
BC(B-C)	0.11	1	0.11	12	0.0134	
Residual	0.057	6	0.01			
Lack of Fit	0.01	1	0.01	0.78	0.4163	not significant
Pure Error	0.049	5	0.01			
Cor Total	11.41	15				

The summary of the diagnostic case statistics for the tensile modulus model is presented in Table 3.14. The residuals between predicted value and actual value show good dispersion throughout the data point within the range of -0.150 to 0.170, which assumed the variance of the statistic model, was constant which made the model reliable. However, in this case, the standard

order of point #6 has a leverage of 1.00 which can be considered as an outlier. Moreover, some data points in the calculated values of DFFITS and Cook's distance values exceeded the suggested ranges of values as shown by asterisks, indicating that not all data points constitute the model evenly. The contour plot and response surface plot based on the model for tensile modulus are shown in Figure 3.7 and Figure 3.8 respectively.

Table 3.14 The diagnostic case statistics for tensile modulus model

Standard Order	Actual Value	Predicted Value	Residual	Leverage	Internally Studentized Residual	Externally Studentized Residual	Influence on Fitted Value DFFITS	Cook's Distance
1	0.570	0.410	0.170	0.484	2.390	** 10.00	* 9.69	0.537
2	2.130	2.110	0.018	0.484	0.259	0.238	0.231	0.006
3	0.960	0.980	-0.025	0.916	-0.902	-0.886	* -2.93	0.889
4	1.050	1.030	0.020	0.480	0.288	0.265	0.255	0.008
5	2.550	2.550	0.008	0.480	0.111	0.101	0.097	0.001
6	1.090	1.090	0.000	1.00 *				
7	0.340	0.390	-0.044	0.751	-0.902	-0.886	-1.536	0.245
8	2.400	2.370	0.025	0.916	0.902	0.886	* 2.93	0.889
9	0.600	0.570	0.025	0.916	0.902	0.886	* 2.93	0.889
10	2.280	2.330	-0.049	0.684	-0.902	-0.886	-1.304	0.176
11	2.400	2.400	-0.005	0.479	-0.067	-0.061	-0.059	0.000
12	2.110	2.110	0.004	0.484	0.054	0.050	0.048	0.000
13	2.380	2.400	-0.021	0.479	-0.295	-0.271	-0.260	0.008
14	1.030	1.030	0.004	0.480	0.064	0.058	0.056	0.000
15	2.560	2.550	0.017	0.480	0.241	0.221	0.212	0.005
16	0.260	0.410	-0.150	0.484	-2.077	-3.575	* -3.47	0.405

* Case(s) with leverage of 1.0000: Student Residuals, Cooks Distance & External Stud. Residuals undefined.

** Case(s) with |External Stud. Residuals| > 4.76. * Exceeds limits

Design-Expert® Software
 Transformed Scale
 Log10(Tensile Modulus)
 ● Design Points
 2.5628
 0.262938

X1 = A: Cassava Starch
 X2 = B: Glycerol
 X3 = C: Paper fiber

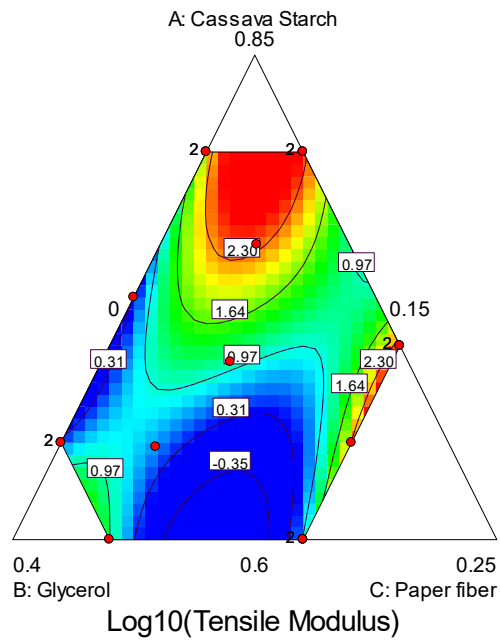


Figure 3.7 Contour plot of tensile modulus

Design-Expert® Software
 Transformed Scale
 Log10(Tensile Modulus)
 ● Design Points
 2.5628
 0.262938

X1 = A: Cassava Starch
 X2 = B: Glycerol
 X3 = C: Paper fiber

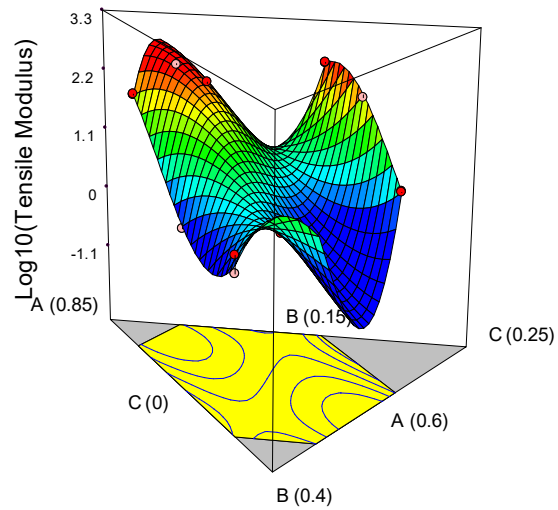


Figure 3.8 Response surface graph of tensile modulus

3.5.5.3 The relationship between composition and flexural strength

The results for flexural properties of the TPCS composite samples are presented in Table 3.7. The analysis of the results was conducted by using the same technique as the previous studies. The reduced cubic canonical polynomial model was chosen because of giving the best coefficient of determination values of 0.9773 and 0.9575 for R² and Adjusted-R² respectively as shown in Table 3.15. The models for both L-pseudo component coding and actual component model in term of weight fractions are as follows:

Flexural Strength

$$= 7.3 x_1' - 5.2 x_2' - 15.9 x_3' + 2.3 x_1' x_2' + 73.4 x_1' x_3' + 59 x_2' x_3' - 226.9 x_1' x_2' x_3' - 42.3 x_1' x_2' (x_1' - x_2')$$

(2.2) (2.4) (5.0) (10.4) (15.8) (15.6) (47.8) (9.4) eq. 3.10

Flexural Strength

$$= 101.9 x_1 - 2058 x_2 - 2117.8 x_3 + 3695.9 x_1 x_2 + 2945.6 x_1 x_3 - 11283 x_2 x_3 - 14521.7 x_1 x_2 x_3 - 2709.9 x_1 x_2 (x_1 - x_2)$$

eq. 3.11

Table 3.15 Flexural strength model summary statistics

Source	Std.Dev.	R ²	Adjusted-R ²	Predicted-R ²	PRESS	remark
Linear	3.93	0.456	0.3724	0.1595	309.73	
Quadratic	2.34	0.8519	0.7779	0.6122	142.9	
Special Cubic	1.81	0.9198	0.8664	0.734	98.03	
Cubic	1.1	0.9803	0.9508			Suggested

The summary of ANOVA-test on the model significance and model terms are presented in Table 3.16. After backward elimination regression, p-values of the components in the model are significant except the term of x_1x_2 , but it needs to be in the equation in order to make the model hierarchical and the p-value of lack-of-fit is insignificant, so it can be used as the proposed model.

Table 3.16 The ANOVA-test summary statistics of flexural strength model

Source	Sum of Squares	df	Mean Square	F-Value	p-value Prob > F	remark
Model	360.16	7	51.45	49.29	< 0.0001	significant
Linear Mixture	168.06	2	84.03	80.5	< 0.0001	
AB	0.054	1	0.054	0.051	0.8263	
AC	22.51	1	22.51	21.56	0.0017	
BC	15.02	1	15.02	14.39	0.0053	
ABC	23.52	1	23.52	22.53	0.0015	
AB(A-B)	21.19	1	21.19	20.3	0.002	
Residual	8.35	8	1.04			
Lack of Fit	1.43	3	0.48	0.34	0.7958	not significant
Pure Error	6.92	5	1.38			
Cor Total	368.51	15				

Table 3.17 provides a summary of the diagnostic case statistics for the flexural strength model. The obtained model has good dispersion within the range of -1.60 to 2.04 and the variance of the observations is constant for all response values, which indicates the model is reliable. The contour plot and response surface plot based on the model for flexural strength are shown in Figure 3.9 and Figure 3.10, respectively.

Table 3.17 The diagnostic case statistics for the flexural strength model

Std Order	Actual Value	Predicted Value	Residual	Leverage	Internally Studentized Residual	Externally Studentized Residual	Influence on Fitted Value DFFITS	Cook's Distance
1	1.720	1.770	-0.045	0.454	-0.059	-0.056	-0.051	0.000
2	1.090	1.080	0.009	0.454	0.012	0.012	0.011	0.000
3	2.000	2.130	-0.130	0.915	-0.436	-0.413	-1.353	0.255
4	2.640	2.540	0.100	0.463	0.134	0.125	0.116	0.002
5	9.340	10.940	-1.600	0.463	-2.142	-3.067	* -2.85	0.493
6	1.780	1.640	0.130	0.469	0.181	0.170	0.160	0.004
7	1.330	1.640	-0.310	0.739	-0.587	-0.562	-0.945	0.122
8	3.780	4.360	-0.580	0.319	-0.688	-0.663	-0.454	0.028
9	2.850	2.100	0.750	0.316	0.892	0.879	0.597	0.046
10	1.020	1.390	-0.370	0.617	-0.586	-0.561	-0.712	0.069
11	14.000	14.350	-0.350	0.479	-0.481	-0.457	-0.437	0.027
12	1.580	1.080	0.490	0.454	0.654	0.629	0.574	0.044
13	14.510	14.350	0.160	0.479	0.218	0.205	0.196	0.005
14	2.360	2.540	-0.170	0.463	-0.231	-0.217	-0.201	0.006
15	12.980	10.940	2.040	0.463	2.720	** 9.30	* 8.63	0.796
16	1.640	1.770	-0.130	0.454	-0.168	-0.158	-0.144	0.003

** Case(s) with |External Stud. Residuals| > 4.17

* Exceeds limits

Design-Expert® Software

Flexural Strength

● Design Points

14.5126

1.01876

X1 = A: Cassava Starch

X2 = B: Glycerol

X3 = C: Paper fiber

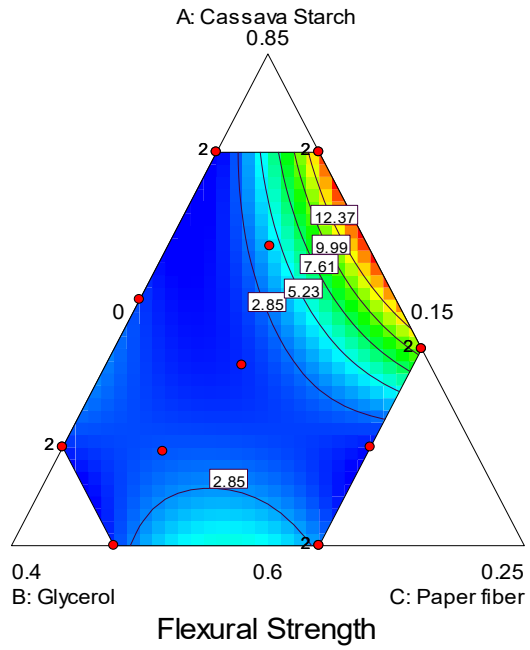


Figure 3.9 Contour plot of flexural strength

Design-Expert® Software

Flexural Strength

14.5126

1.01876

X1 = A: Cassava Starch

X2 = B: Glycerol

X3 = C: Paper fiber

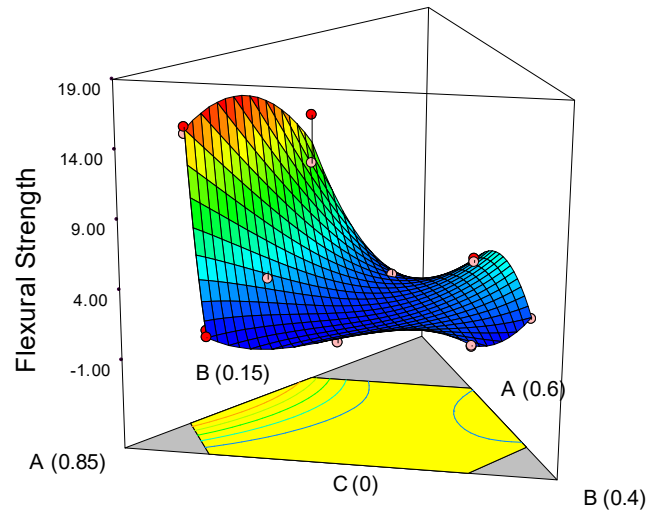


Figure 3.10 Response surface graph of flexural strength

3.5.5.4 The relationship between composition and flexural modulus

A similar technique of data analysis was applied to the flexural modulus of the TPCS composite. The response values show that transformation is needed due to the high ratio of max to min values. The transformation that was used is square root of the response values. Then, the reduced cubic canonical polynomial model presents the best coefficient of determination values of 0.9952 and 0.9910 for R^2 and Adjusted- R^2 respectively as shown in Table 3.18. The models for both L-pseudo component coding and the actual component model in term of weight fractions are as follows:

Sqrt (Flexural Modulus)

$$= 24 x_1' - 5.3 x_2' - 26.8 x_3' - 14.5 x_1'x_2' + 144.9 x_1'x_3' + 107.4 x_2'x_3' - 489.3 x_1'x_2'x_3' - 97.5 x_1'x_2'(x_1' - x_2')$$

(2.4) (2.6) (5.4) (11.3) (17.2) (16.9) (52.0) (10.2) eq. 3.12

Sqrt (Flexural Modulus)

$$= 261.4 x_1 - 4573.4 x_2 - 4396.1 x_3 + 8195.5 x_1 x_2 + 6078.5 x_1 x_3 - 24251 x_2 x_3 - 31312.3 x_1 x_2 x_3 - 6242.7 x_1 x_2 (x_1 - x_2)$$

eq. 3.13

Table 3.18 Flexural modulus model summary statistics

Source	Std.Dev.	R ²	Adjusted-R ²	Predicted-R ²	PRESS	remark
Linear	9.27	0.4612	0.3783	0.172	1717.16	
Quadratic	4.89	0.8847	0.827	0.6927	637.19	
Special Cubic	3.69	0.941	0.9017	0.7937	427.78	
Cubic	1.08	0.9966	0.9915			Suggested

The summary of ANOVA-test, the model significance and model terms are presented in Table 3.19. After backward elimination regression, p-values of the model and component in the model are significant and the p-value of lack-of-fit is insignificant, so it can be used as the proposed model.

Table 3.19 The ANOVA-test summary statistics of flexural modulus model

Source	Sum of Squares	df	Mean Square	F-Value	p-value Prob > F	remark
Model	2064.0	7	294.85	239.15	< 0.0001	significant
Linear Mixture	956.4	2	478.21	387.87	< 0.0001	
AB	2.1	1	2.05	1.66	0.2332	
AC	87.8	1	87.78	71.2	< 0.0001	
BC	49.7	1	49.74	40.34	0.0002	
ABC	109.3	1	109.34	88.68	< 0.0001	
AB(A-B)	112.5	1	112.46	91.21	< 0.0001	
Residual	9.9	8	1.23			
Lack of Fit	5.9	3	1.95	2.43	0.1808	not significant
Pure Error	4.0	5	0.80			
Cor Total	2073.8	15				

The summary of the diagnostic case statistics for the flexural modulus model is presented in Table 3.20. The residuals between predicted values and actual values have good dispersion throughout the data points within the range of -0.940 to 1.650. Since the values of internally studentized residual and externally studentized residual do not fall out of the range, the assumption of constant variance of each data points is not rejected, so the model is reliable. The contour plot and response surface plot based on the model for tensile modulus are shown in Figure 3.11 and Figure 3.12, respectively.

Table 3.20 The diagnostic case statistics for flexural modulus model

Standard Order	Actual Value	Predicted Value	Residual	Leverage	Internally Studentized Residual	Externally Studentized Residual	Influence on Fitted Value DFFITS	Cook's Distance
1	8.070	7.630	0.440	0.454	0.534	0.508	0.464	0.030
2	6.590	6.420	0.170	0.454	0.203	0.190	0.174	0.004
3	7.170	7.630	-0.460	0.915	-1.408	-1.519	* -4.98	* 2.66
4	7.270	7.610	-0.340	0.463	-0.418	-0.395	-0.367	0.019
5	27.660	28.290	-0.630	0.463	-0.768	-0.747	-0.693	0.063
6	4.790	4.890	-0.100	0.469	-0.124	-0.117	-0.110	0.002
7	4.870	5.720	-0.860	0.739	-1.510	-1.671	* -2.81	0.808
8	11.620	12.140	-0.520	0.319	-0.565	-0.540	-0.370	0.019
9	7.950	6.300	1.650	0.316	1.792	2.167	1.471	0.185
10	4.680	5.630	-0.940	0.617	-1.375	-1.472	-1.870	0.382
11	37.320	36.990	0.330	0.479	0.412	0.389	0.373	0.019
12	7.220	6.420	0.800	0.454	0.975	0.972	0.886	0.099
13	36.100	36.990	-0.890	0.479	-1.110	-1.129	-1.082	0.141
14	8.010	7.610	0.410	0.463	0.498	0.473	0.439	0.027
15	29.800	28.290	1.510	0.463	1.858	2.305	* 2.14	0.371
16	7.070	7.630	-0.570	0.454	-0.691	-0.666	-0.608	0.050

* Exceeds limits

Design-Expert® Software
 Transformed Scale
 Sqrt(Flexural Modulus)
 ● Design Points
 37.3176
 4.68244

X1 = A: Cassava Starch
 X2 = B: Glycerol
 X3 = C: Paper fiber

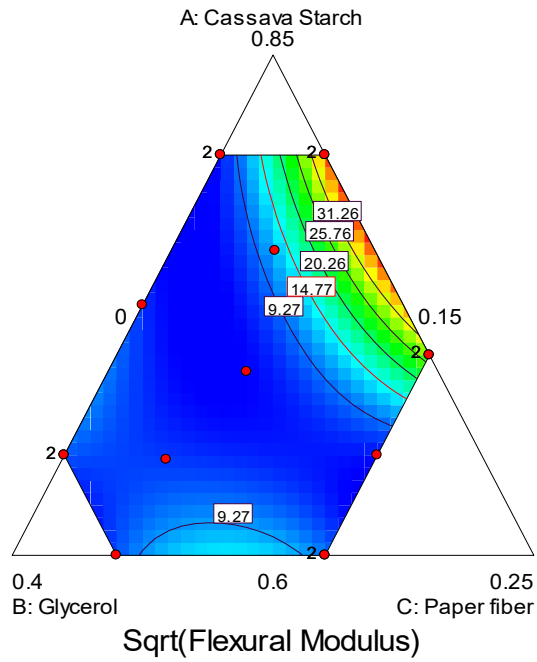


Figure 3.11 Contour plot of flexural modulus

Design-Expert® Software
 Transformed Scale
 Sqrt(Flexural Modulus)
 ● Design Points
 37.3176
 4.68244

X1 = A: Cassava Starch
 X2 = B: Glycerol
 X3 = C: Paper fiber

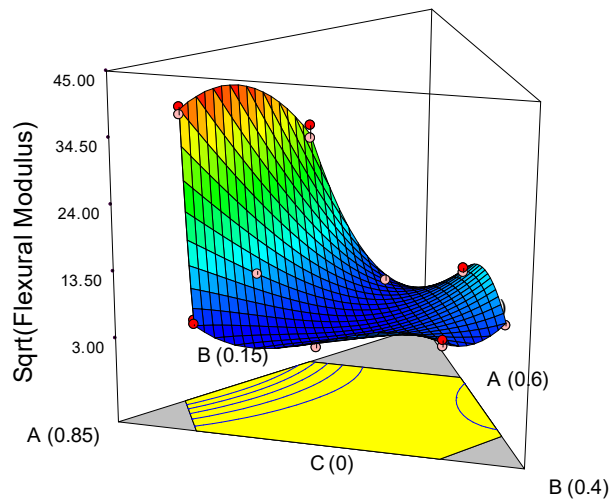


Figure 3.12 Response surface graph of flexural modulus

Table 3.21 provides a summary of the proposed mechanical property models for thermoplastic cassava starch reinforced by paper fiber in term of L-pseudo component coding.

Table 3.21 Summary of the models and coefficients of determination paper fiber

Properties	Models	R ²	Adjusted R ²
Log ₁₀ (TS)	$= -0.1 x_1' + 1.8 x_2' + 4.5 x_3' - 4.3 x_1'x_2' - 6.3 x_1'x_3' - 13.4 x_2'x_3' + 27.8 x_1'x_2'x_3' + 9.6 x_1'x_2'(x_1' - x_2') + 5.6 x_1'x_3'(x_1' - x_3')$	0.9600	0.9143
Log ₁₀ (TM)	$= 2.5 x_1' + 3.1 x_2' + 31.9 x_3' - 9.7 x_1'x_2' - 64.3 x_1'x_3' - 72.9 x_2'x_3' + 123.1 x_1'x_2'x_3' + 10.9 x_1'x_2'(x_1' - x_2') + 45.0 x_1'x_3'(x_1' - x_3') + 39.2 x_2'x_3'(x_2' - x_3')$	0.9950	0.9876
FS	$= 7.3 x_1' - 5.2 x_2' - 15.9 x_3' + 2.3 x_1'x_2' + 73.4 x_1'x_3' + 59 x_2'x_3' - 226.9 x_1'x_2'x_3' - 42.3 x_1'x_2'(x_1' - x_2')$	0.9773	0.9575
Sqrt(FM)	$= 24 x_1' - 5.3 x_2' - 26.8 x_3' - 14.5 x_1'x_2' + 144.9 x_1'x_3' + 107.4 x_2'x_3' - 489.3 x_1'x_2'x_3' - 97.5 x_1'x_2'(x_1' - x_2')$	0.9952	0.9901

3.5.6 The relationship between composition of the thermoplastic cassava starch (TPCS) reinforced by vetiver fiber and mechanical properties.

3.5.6.1 The relationship between composition and tensile strength

The results for tensile strength of the thermoplastic cassava starch (TPCS) reinforced by vetiver fiber samples are presented in Table 3.8 (see page 71). Table 3.22 presents the summary of statistics for the tensile strength model of TPCS reinforced by vetiver fiber. It shows that the quadratic canonical model is better for describing the response variations of the design points than the other models. The model provides coefficient of determination values of 0.6238 and 0.4920 for R² and Adjusted-R² respectively. The low R-square value is due to high variability in the data. However, the ANOVA test summary in Table 3.23 showed the model is significant, so it can be used to describe the response variable better than the other models.

Table 3.22 Tensile strength model summary statistics

Source	Std.Dev.	R ²	Adjusted-R ²	Predicted-R ²	PRESS	remark
Linear	2.06	0.4639	0.3815	0.2442	77.76	
Quadratic	1.97	0.6238	0.4357	0.2121	81.06	Suggested
Special Cubic	1.84	0.703	0.505	0.1954	82.78	
Cubic	1.89	0.7919	0.4797	-54.2873	5688.05	

After backward elimination was performed, the model for the L-pseudo component coding in terms of weight fractions was as follows:

$$\text{Tensile Strength} = 4.1 x_1' + 9.3 x_2' + 10.8 x_3' + 11.9 x_1' x_2' \quad \text{eq. 3.14}$$

(1.2) (1.2) (1.2) (6.1)

where x_1' , x_2' and x_3' are weight fractions of cassava starch, glycerol, and vetiver fiber, respectively. The standard errors of the parameter coefficients are shown in the parenthesis. The model is presented as a model for L-pseudo component coding with transformation formula as previously described. After transforming the formula for the actual component model, the model for the real values in term of weight fractions in the component proportion became:

$$\text{Tensile Strength} = -19.4 x_1 - 127.8 x_2 + 59.0 x_3 + 298.5 x_1 x_2 \quad \text{eq. 3.15}$$

The ANOVA-test, the model significance and model terms summarized in Table 3.23. The p-values of the component in the model are significant except for the x_1x_2 parameter that needs to be kept to make the p-value of lack-of-fit is insignificant, so it can be used as the proposed model.

Table 3.23 The ANOVA-test summary statistics of tensile strength model

Source	Sum of Squares	df	Mean Square	F-Value	p-value Prob > F	remark
Model	61.07	3	20.36	5.84	0.0107	significant
Linear Mixture	47.73	2	23.87	6.85	0.0104	
AB	13.34	1	13.34	3.83	0.0741	
Residual	41.81	12	3.48			
Lack of Fit	35.52	7	5.07	4.03	0.0721	not significant
Pure Error	6.3	5	1.26			
Cor Total	102.88	15				

Table 3.24 presents the diagnostic case statistics for the tensile strength model. The residuals between the predicted value and actual value show good dispersion throughout the data points within the range of -4.53 to 2.48 and the leverage values range from 0.094 to 0.408. The contour plot and response surface plot based on the model for tensile modulus are shown in Figure 3.13 and Figure 3.14, respectively. The residual plots can be seen in Figure A.5.

Table 3.24 The diagnostic case statistics for tensile strength model

Standard Order	Actual Value	Predicted Value	Residual	Leverage	Internally Studentized Residual	Externally Studentized Residual	Influence on Fitted Value DFFITS	Cook's Distance
1	6.940	6.590	0.350	0.156	0.204	0.196	0.084	0.002
2	10.290	10.410	-0.120	0.206	-0.075	-0.072	-0.037	0.000
3	10.700	9.650	1.050	0.408	0.730	0.715	0.593	0.092
4	8.540	9.260	-0.720	0.392	-0.494	-0.478	-0.383	0.039
5	3.120	4.070	-0.950	0.398	-0.655	-0.639	-0.519	0.071
6	10.850	9.800	1.050	0.166	0.615	0.599	0.267	0.019
7	4.850	9.380	-4.530	0.094	-2.550	-3.608	-1.159	0.168
8	7.730	9.120	-1.390	0.202	-0.833	-0.821	-0.414	0.044
9	8.480	7.370	1.120	0.131	0.643	0.626	0.243	0.016
10	8.270	9.960	-1.690	0.132	-0.973	-0.971	-0.379	0.036
11	11.050	9.190	1.860	0.111	1.055	1.060	0.374	0.035
12	9.930	9.260	0.670	0.392	0.461	0.445	0.357	0.034
13	4.880	4.070	0.810	0.398	0.563	0.546	0.444	0.052
14	10.280	9.650	0.630	0.408	0.439	0.424	0.351	0.033
15	12.890	10.410	2.480	0.206	1.489	1.579	0.804	0.144
16	8.500	9.120	-0.610	0.202	-0.367	-0.353	-0.178	0.009

Design-Expert® Software

Tensile strength

● Design Points

12.8915

3.1201

X1 = A: Cassava Starch

X2 = B: Glycerol

X3 = C: Vetiver Fiber

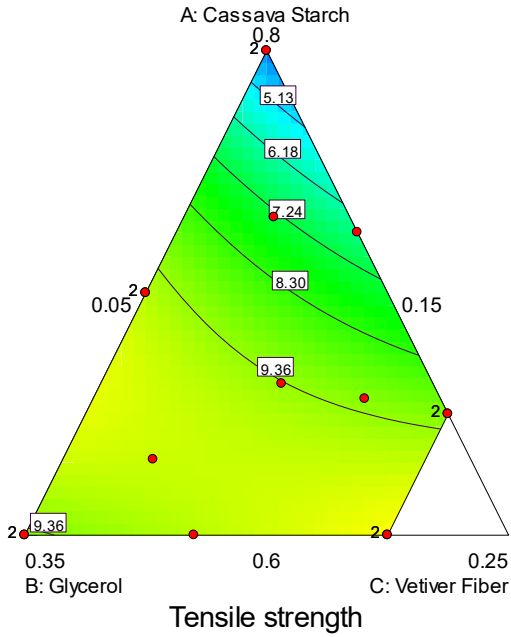


Figure 3.13 Contour plot of tensile strength

Design-Expert® Software

Tensile strength

12.8915

3.1201

X1 = A: Cassava Starch

X2 = B: Glycerol

X3 = C: Vetiver Fiber

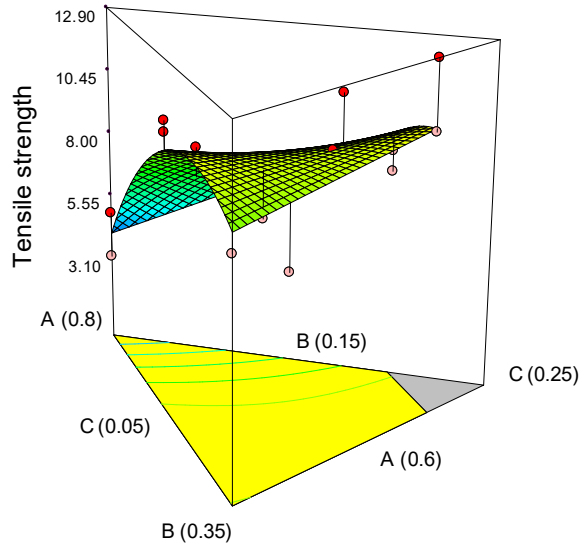


Figure 3.14 Response surface graph of tensile strength

3.5.6.2 The relationship between composition and tensile modulus

The same technique of data analysis was performed for the tensile modulus of the TPCS with vetiver composite. Similar to the tensile strength, the quadratic canonical polynomial model gave the best coefficient of determination values of 0.8809 and 0.8213 for R^2 and Adjusted- R^2 respectively as shown in Table 3.25. The models for both L-pseudo component coding and actual component model in term of weight fractions are as follows:

Table 3.25 Tensile modulus model summary statistics

Source	Std.Dev.	R^2	Adjusted- R^2	Predicted- R^2	PRESS	remark
Linear	31.4	0.4496	0.365	0.0969	21027.28	
Quadratic	16.65	0.8809	0.8213	0.6564	7999.23	Suggested
Special Cubic	14.99	0.9132	0.8553	0.6951	7099.96	
Cubic	16.34	0.9312	0.828	-4.2828	123000.00	

$$\text{Tensile modulus} = 188.5 x_1' + 115.9 x_2' + 182.2 x_3' + 237.6 x_1'x_2' + 152.0 x_1'x_3' + 316.0 x_2'x_3' \quad \text{eq 3.16}$$

(11.5) (11.4) (23.6) (54.5) (77.0) (79.4)

Tensile modulus

$$= -128.7 x_1 - 3369.2 x_2 - 2544.7 x_3 + 5939.5 x_1 x_2 + 3801.1 x_1 x_3 + 7900.4 x_2 x_3 \quad \text{eq. 3.17}$$

The summary of ANOVA-test, the model significance and model terms are presented in Table 3.26. The p-values of the components in the model are significant. While the $x_1'x_2'$ parameter is not significant after backward elimination regression, it needs to be in the equation in order to make the p-value of lack-of-fit insignificant, so it can be used as the proposed model.

Table 3.26 The ANOVA-test summary statistics of tensile modulus model

Source	Sum of Squares	df	Mean Square	F-Value	p-value Prob > F	remark
Model	20509.36	5	4101.87	14.79	0.0002	significant
Linear Mixture	10468.63	2	5234.32	18.87	0.0004	
AB	5269.72	1	5269.72	19	0.0014	
AC	1081.42	1	1081.42	3.9	0.0766	
BC	4393.6	1	4393.6	15.84	0.0026	
Residual	2773.66	10	277.37			
Lack of Fit	1486.43	5	297.29	1.15	0.4392	not significant
Pure Error	1287.23	5	257.45			
Cor Total	23283.03	15				

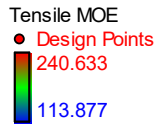
The summary of the diagnostic case statistics for the tensile modulus model is presented in Table 3.27. The residuals between predicted values and actual values show good dispersion throughout the data points within the range of -23.86 to 23.50. This means that the variance of the observations is constant for all response values, so the model is reliable. The data points also constituted the model evenly. The contour plot and response surface plot based on the model for tensile modulus are shown in Figure 3.15 and Figure 3.16, respectively.

Table 3.27 The diagnostic case statistics for tensile modulus model

Standard Order	Actual Value	Predicted Value	Residual	Leverage	Internally Studentized Residual	Externally Studentized Residual	Influence on Fitted Value DFFITS	Cook's Distance
1	232.900	221.770	11.140	0.431	0.887	0.876	0.763	0.099
2	226.350	224.900	1.440	0.387	0.111	0.105	0.084	0.001
3	235.080	211.590	23.500	0.446	1.896	2.247	* 2.02	0.483
4	113.880	115.910	-2.040	0.472	-0.168	-0.160	-0.151	0.004
5	168.630	188.470	-19.850	0.473	-1.642	-1.822	-1.727	0.404
6	232.670	211.020	21.650	0.463	1.774	2.033	1.888	0.45 2
7	240.630	241.510	-0.880	0.239	-0.060	-0.057	-0.032	0.000
8	207.620	212.300	-4.680	0.366	-0.353	-0.337	-0.256	0.012
9	218.050	228.290	-10.240	0.198	-0.686	-0.667	-0.331	0.019
10	183.530	207.380	-23.860	0.206	-1.608	-1.772	-0.904	0.112
11	227.560	235.890	-8.330	0.173	-0.550	-0.530	-0.242	0.011
12	115.950	115.910	0.038	0.472	0.003	0.003	0.003	0.000
13	205.500	188.470	17.030	0.473	1.409	1.493	1.415	0.297
14	203.880	211.590	-7.710	0.446	-0.622	-0.602	-0.540	0.052
15	218.900	224.900	-6.010	0.387	-0.461	-0.442	-0.352	0.022
16	221.080	212.300	8.780	0.366	0.662	0.642	0.488	0.042

* Exceeds limits

Design-Expert® Software



X1 = A: Cassava Starch
X2 = B: Glycerol
X3 = C: Vetiver Fiber

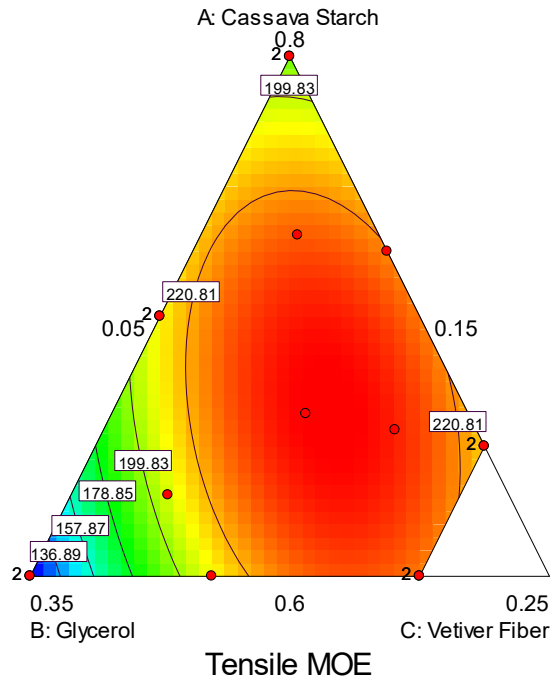
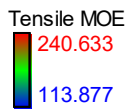


Figure 3.15 Contour plot of tensile modulus

Design-Expert® Software



X1 = A: Cassava Starch
X2 = B: Glycerol
X3 = C: Vetiver Fiber

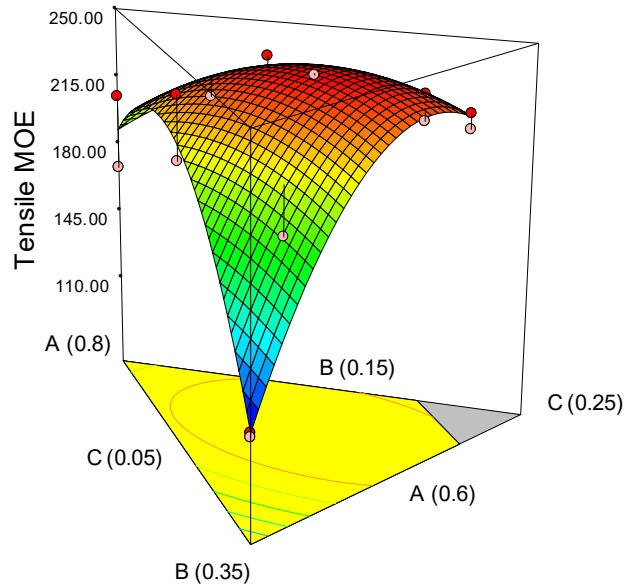


Figure 3.16 Response surface graph of tensile modulus

3.5.6.3 The relationship between composition and flexural strength

The results of flexural properties on the TPCS composite samples are presented in Table 3.8 (see page 71). The analysis of the results was conducted by using the same technique as for the previous studies. Transformation of the data was needed, so the base 10 log was applied before selecting the model. The reduced cubic canonical polynomial model was chosen because it gave the best coefficient of determination values of 0.9733 and 0.9333 for R^2 and Adjusted- R^2 respectively. The models for both L-pseudo component coding and the actual component model in term of weight fractions are as follows:

$\text{Log}_{10}(\text{Flex strength})$

$$\begin{aligned}
 &= 0.5 x_1' + 0.3 x_2' + 2.1 x_3' + 3.7 x_1'x_2' + 0.7 x_1'x_3' - 1.3 x_2'x_3' - 5.1 x_1'x_2'(x_1' - x_2') + 3.6 x_1'x_3'(x_1' - x_3') + \\
 &\quad (0.1) \quad (0.1) \quad (0.4) \quad (0.4) \quad (0.9) \quad (1.0) \quad (2.1) \quad (1.5) \\
 &\quad 1.6 x_2'x_3'(x_2' - x_3') \qquad \qquad \qquad \qquad \qquad \qquad \qquad \qquad \qquad \text{eq. 3.18} \\
 &\quad (1.5)
 \end{aligned}$$

$\text{Log}_{10}(\text{Flex strength})$

$$\begin{aligned}
 &= 11.0 x_1 - 534.6 x_2 + 464.6 x_3 + 989.2 x_1 x_2 - 847.9 x_1 x_3 + 22.1 x_2 x_3 - 639.9 x_1 x_2 (x_1 - x_2) + \\
 &\quad 448.2 x_1 x_3 (x_1 - x_3) + 198.6 x_2 x_3 (x_2 - x_3) \qquad \qquad \qquad \qquad \qquad \qquad \qquad \qquad \qquad \text{eq. 3.19}
 \end{aligned}$$

The summary of ANOVA-test on the model significance and model terms are presented in Table 3.28. All of p-values of the component in the model are significance and the p-value of lack-of-fit is insignificant, which can be used as the proposed model.

Table 3.28 The ANOVA-test summary statistics of flexural strength model

Source	Sum of Squares	df	Mean Square	F-Value	p-value Prob > F	remark
Model	2.97	8	0.37	21.66	0.0003	significant
Linear Mixture	1.4	2	0.7	40.89	0.0001	
AB	1.25	1	1.25	72.88	< 0.0001	
AC	0.009	1	0.009	0.51	0.4988	
BC	0.028	1	0.028	1.66	0.239	
AB(A-B)	0.099	1	0.099	5.8	0.0468	
AC(A-C)	0.089	1	0.089	5.19	0.0568	
BC(B-C)	0.018	1	0.018	1.07	0.3344	
Residual	0.12	7	0.017			
Lack of Fit	0.08	2	0.04	4.97	0.0647	not significant
Pure Error	0.04	5	0.008			
Cor Total	3.09	15				

Table 3.29 provides a summary of the diagnostic case statistics for the flexural strength model. The obtained model has got the good dispersion within the range of -0.17 to 0.23 and the variance of the observations is constant for all response values so the model is reliable. The contour plot and response surface plot based on the model for flexural strength are shown in Figure 3.17 and Figure 3.18, respectively. The plots for the residuals can be seen in Figure A.6.

Table 3.29 The diagnostic case statistics for the flexural strength model

Standrad Order	Actual Value	Predicted Value	Residual	Leverage	Internally Studentized Residual	Externally Studentized Residual	Influence on Fitted Value DFFITS	Cook's Distance
1	1.374	1.473	-0.099	0.834	-1.856	-2.411	* -5.41	* 1.93
2	1.236	1.254	-0.018	0.499	-0.196	-0.182	-0.182	0.004
3	1.298	1.297	0.001	0.449	0.009	0.008	0.007	0.000
4	0.207	0.252	-0.045	0.499	-0.484	-0.456	-0.454	0.026
5	0.607	0.487	0.121	0.500	1.302	1.385	1.383	0.188
6	0.621	0.711	-0.090	0.837	-1.702	-2.057	* -4.66	* 1.65
7	1.189	1.276	-0.087	0.444	-0.889	-0.874	-0.780	0.070
8	1.528	1.507	0.021	0.491	0.229	0.212	0.208	0.006
9	1.272	1.127	0.146	0.705	2.051	3.008	* 4.65	* 1.12
10	1.380	1.227	0.153	0.695	2.117	3.270	* 4.93	* 1.13
11	1.349	1.281	0.068	0.611	0.833	0.813	1.018	0.121
12	0.296	0.252	0.045	0.499	0.483	0.455	0.454	0.026
13	0.367	0.487	-0.120	0.500	-1.299	-1.380	-1.379	0.187
14	1.196	1.297	-0.101	0.449	-1.045	-1.053	-0.950	0.099
15	1.280	1.254	0.026	0.499	0.285	0.265	0.265	0.009
16	1.486	1.507	-0.020	0.491	-0.219	-0.204	-0.200	0.005

* Exceeds limits

Design-Expert® Software
 Transformed Scale
 Log10(Flexural strength)
 ● Design Points
 1.52807
 0.206723

X1 = A: Cassava Starch
 X2 = B: Glycerol
 X3 = C: Vetiver Fiber

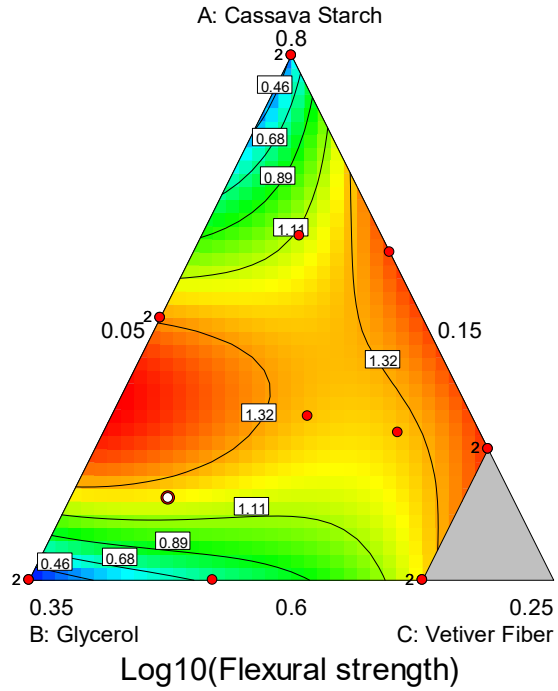


Figure 3.17 Contour plot of flexural strength

Design-Expert® Software
 Transformed Scale
 Log10(Flexural strength)
 1.52807
 0.206723

X1 = A: Cassava Starch
 X2 = B: Glycerol
 X3 = C: Vetiver Fiber

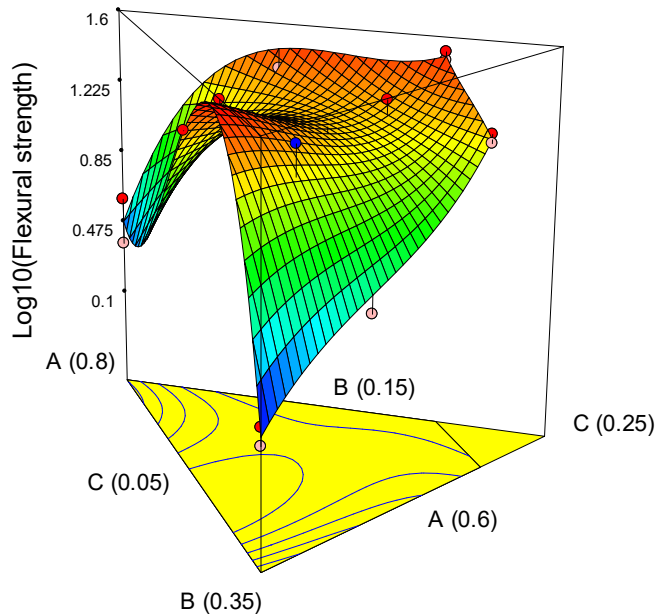


Figure 3.18 Response surface graph of flexural strength

3.5.6.4 The relationship between composition and flexural modulus

A similar technique of data analysis was applied to the flexural modulus of the composite. Due to the response values requiring transformation, the square root method was used. The cubic canonical polynomial model gave the best coefficient of determination values of 0.9902 and 0.9756 for R^2 and Adjusted- R^2 respectively. The models for both L-pseudo component coding and actual component model in term of weight fractions are as follows:

Sqrt (Flexural Modulus)

$$\begin{aligned}
 &= 9 x_1' + 8.3 x_2' + 99 x_3' - 61.8 x_1' x_2' - 161.2 x_1' x_3' + 453.1 x_2' x_3' + 453 x_1' x_2' x_3' - 206.1 x_1' x_2' (x_1' - x_2') \\
 &\quad (2.4) \quad (2.6) \quad (5.4) \quad (11.3) \quad (17.2) \quad (16.9) \quad (52.0) \quad (10.2) \\
 &+ 240.4 x_1' x_3' (x_1' - x_3') + 113.2 x_2' x_3' (x_2' - x_3') \quad \text{eq.} \quad 3.20 \\
 &\quad (11.3) \quad (17.2)
 \end{aligned}$$

Sqrt (Flexural Modulus)

$$\begin{aligned}
 &= 592.7 x_1 - 19670.6 x_2 + 36743.8 x_3 + 36383.3 x_1 x_2 - 65605.8 x_1 x_3 - 44834.2 x_2 x_3 + 56642.8 x_1 x_2 x_3 - \\
 &\quad 25757.8 x_1 x_2 (x_1 - x_2) + 30047.5 x_1 x_3 (x_1 - x_3) + 14151.0 x_2 x_3 (x_2 - x_3) \quad \text{eq. 3.21}
 \end{aligned}$$

The summary of ANOVA-test, the model significance and model terms are presented in Table 3.30. All of p-values of the component in the model are significant and the p-value of lack-of-fit is insignificant, so it can be used as the proposed model.

Table 3.30 The ANOVA-test summary statistics of flexural modulus model

Source	Sum of Squares	df	Mean Square	F-Value	p-value Prob > F	remark
Model	2851.32	9	316.81	67.64	< 0.0001	significant
Linear Mixture	1297.76	2	648.88	138.53	< 0.0001	
AB	664.76	1	664.76	141.92	< 0.0001	
AC	19.31	1	19.31	4.12	0.0886	
BC	121.81	1	121.81	26.01	0.0022	
ABC	98.86	1	98.86	21.11	0.0037	
AB(A-B)	160.97	1	160.97	34.37	0.0011	
AC(A-C)	204.22	1	204.22	43.6	0.0006	
BC(B-C)	47.41	1	47.41	10.12	0.019	
Residual	28.10	6.00	4.68			
Lack of Fit	14.70	1.00	14.70	5.48	0.0662	not significant
Pure Error	13.40	5.00	2.68			
Cor Total	2879.43	15				

The summary of the diagnostic case statistics for the flexural modulus model is presented in Table 3.31. The residuals between the predicted value and actual value shown good dispersion throughout the data points within the range of -2.644 to 2.186. This means that the variance of the observations is constant for all response values, and the model is reliable. The data points also constituted the model evenly. The contour plot and response surface plot based on the model for tensile modulus are shown in Figure 3.19 and Figure 3.20, respectively.

Table 3.31 The diagnostic case statistics for the flexural modulus model

Standard Order	Actual Value	Predicted Value	Residual	Leverage	Internally Studentized Residual	Externally Studentized Residual	Influence on Fitted Value DFFITS	Cook's Distance
1	41.933	42.364	-0.431	0.987	-1.772	-2.342	* -20.71	* 24.54
2	34.167	35.495	-1.329	0.500	-0.868	-0.848	-0.847	0.075
3	32.404	31.006	1.398	0.499	0.912	0.897	0.895	0.083
4	7.967	8.340	-0.373	0.499	-0.244	-0.224	-0.224	0.006
5	9.118	9.023	0.095	0.500	0.062	0.057	0.057	0.000
6	10.892	11.127	-0.235	0.996	-1.772	-2.342	* -38.10	* 83.09
7	36.500	39.144	-2.644	0.524	-1.772	-2.342	* -2.46	0.346
8	43.728	42.378	1.350	0.496	0.878	0.859	0.852	0.076
9	35.522	34.525	0.996	0.932	1.772	2.342	* 8.70	* 4.33
10	39.776	38.545	1.231	0.897	1.772	2.342	* 6.91	* 2.73
11	37.024	34.838	2.186	0.675	1.772	2.342	* 3.38	0.652
12	8.533	8.340	0.193	0.499	0.126	0.115	0.115	0.002
13	8.819	9.023	-0.204	0.500	-0.133	-0.122	-0.122	0.002
14	29.344	31.006	-1.662	0.499	-1.085	-1.105	-1.102	0.117
15	36.774	35.495	1.279	0.500	0.836	0.812	0.812	0.070
16	40.529	42.378	-1.849	0.496	-1.203	-1.261	-1.250	0.142

* Exceeds limits

Design-Expert® Software
 Transformed Scale
 Sqrt(Flex MOE)
 ● Design Points
 43.7282
 7.96704

X1 = A: Cassava Starch
 X2 = B: Glycerol
 X3 = C: Vetiver Fiber

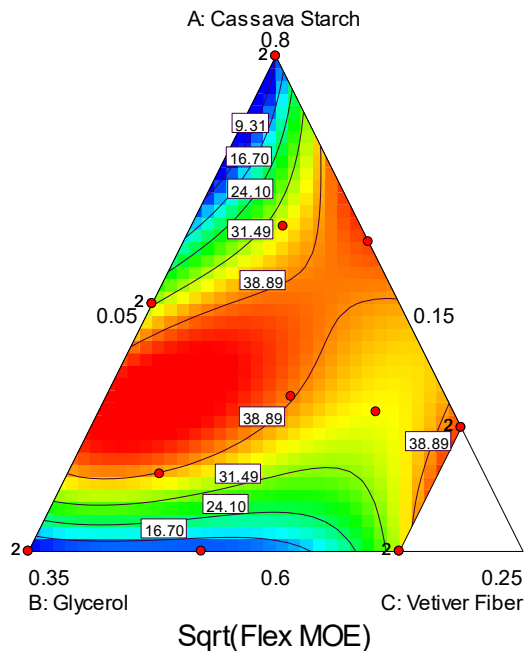


Figure 3.19 Contour plot of flexural modulus

Design-Expert® Software
 Transformed Scale
 Sqrt(Flex MOE)
 43.7282
 7.96704

X1 = A: Cassava Starch
 X2 = B: Glycerol
 X3 = C: Vetiver Fiber

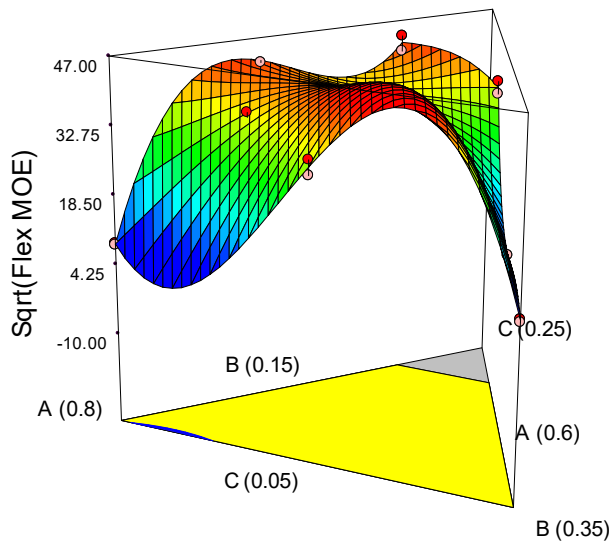


Figure 3.20 Response surface graph of flexural modulus

Table 3.32 presents a summary of proposed mechanical property models for thermoplastic cassava starch reinforced by vetiver fiber in term of L-pseudo component coding.

Table 3.32 Summary of the models and coefficients of determination vetiver fiber

Properties	Models	R ²	Adjusted R ²
TS	$= 4.1 x_1' + 9.3 x_2' + 10.8 x_3' + 11.9 x_1'x_2'$	0.6238	0.4920
TM	$= 188.5 x_1' + 115.9 x_2' + 182.2 x_3' + 237.6 x_1'x_2' + 152.0 x_1'x_3' + 316.0 x_2'x_3'$	0.8809	0.8213
Log ₁₀ (FS)	$= 0.5 x_1' + 0.3 x_2' + 2.1 x_3' + 3.7 x_1'x_2' + 0.7 x_1'x_3' - 1.3 x_2'x_3' - 5.1 x_1'x_2' (x_1' - x_2') + 3.6 x_1'x_3' (x_1' - x_3') + 1.6 x_2'x_3' (x_2' - x_3')$	0.9733	0.9333
Sqrt(FM)	$= 9 x_1' + 8.3 x_2' + 99 x_3' - 61.8 x_1'x_2' - 161.2 x_1'x_3' + 453.1 x_2'x_3' + 453 x_1'x_2'x_3' - 206.1 x_1'x_2' (x_1' - x_2') + 240.4 x_1'x_3' (x_1' - x_3') + 113.2 x_2'x_3' (x_2' - x_3')$	0.9902	0.9756

3.5.7 Mixture optimization of TPCS and vetiver fiber

The optimization of TPCS and vetiver fiber used regression models to be performed with the Design-Expert software. The constraints or targets were set at the maximum values for all response properties in order to construct a desirability score that can optimize all of the fitted models. A desirability score of one represents the ideal case and a zero represents one or more responses falling outside the limits. Table 3.33 presents the goals or criteria for each response in order to obtain the optimal condition.

Table 3.33 The criteria for each response used of TPCS and vetiver fiber optimization

Properties	Goal
Tensile strength, MPa	maximize
Tensile Modulus, MPa	maximize
Flexural strength, MPa	maximize
Flexural Modulus, MPa	maximize

The results of optimization are presented in Table 3.34. Three solutions were generated to meet all criteria with varying degrees of desirability. Additionally the graphical information can be generated as contour plots based on degrees of desirability. The flag area in the contour plots shows that the TPCS with vetiver fiber was able to meet all the target properties with desirability scores of 0.86, 0.85, and 0.82 as shown in Figure 3.21, Figure 3.22, and Figure 3.23 respectively.

Table 3.34 TPCS and vetiver fiber optimization

Solution No.	Starch	Glycerol	Vetiver Fiber	Tensile strength	Tensile Modulus	Flexural strength	Flexural Modulus	Desirability
1	0.66	0.24	0.10	9.65	233.61	22.31	1912.16	0.86
2	0.63	0.17	0.20	9.83	221.06	28.93	1755.14	0.85
3	0.63	0.18	0.19	9.8	228.92	26.21	1326.85	0.82

Design-Expert® Software

Desirability
● Design Points
1
0

X1 = A: Cassava Starch
X2 = B: Glycerol
X3 = C: Vetiver Fiber

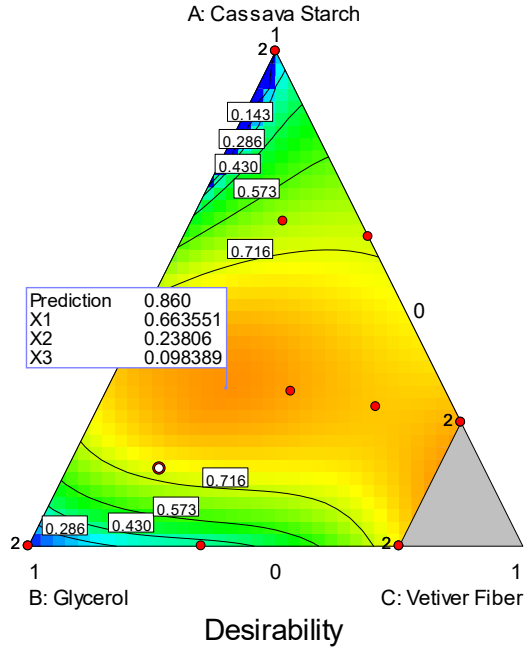


Figure 3.21 Contour plot of model simulation with constraints at desirability score “0.86”

Design-Expert® Software

Desirability
● Design Points
1
0

X1 = A: Cassava Starch
X2 = B: Glycerol
X3 = C: Vetiver Fiber

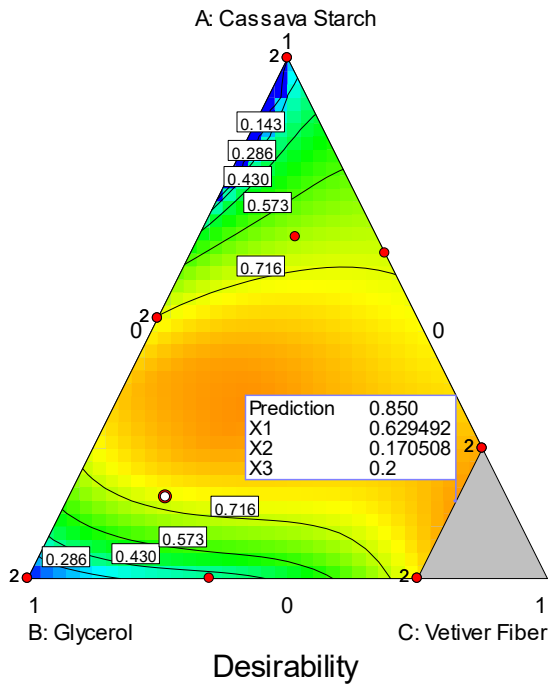


Figure 3.22 Contour plot of model simulation with constraints at desirability score “0.85”

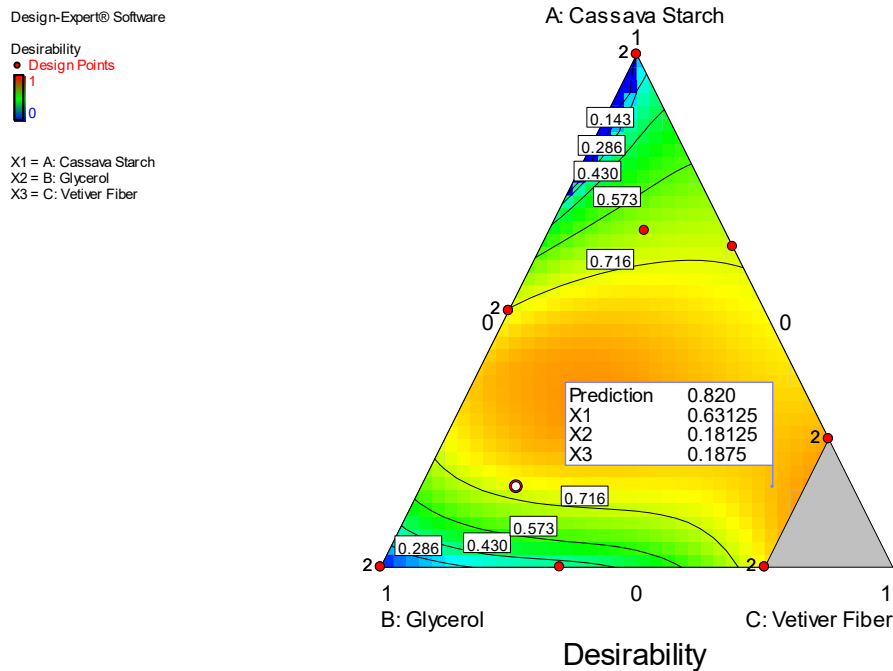


Figure 3.23 Contour plot of model simulation with constraints at desirability score “0.82”

3.5.8 Characteristics of selected thermoplastic starch vetiver fiber composites

3.5.8.1 FTIR

The FTIR spectra of selected thermoplastic cassava starch composites are shown in Figure 3.24, which are: cassava starch, glycerol, S66G21VF13, S60G20VF20, S60G35VF5 and S65G35VF0. Their characteristic chemical bonds and the observed signal peaks are listed in Table 3.35. The cassava starch and glycerol spectra were similar owing to the hydroxyl groups in their structures [118]. The common signals for polysaccharides in starch and glycerol are ascribed to O-H stretching at $3500\text{-}3200\text{ cm}^{-1}$ and C-H stretching of aliphatic groups at $3100\text{-}2900\text{ cm}^{-1}$ as mentioned by Mano et al., [119]. Moreover, the obtained FTIR spectra of cassava starch, glycerol and composites showed high similarity but were different in intensity, which can be seen in Figure 3.24. Peaks at 1637 and 1147 cm^{-1} indicating H_2O absorbed and C-O stretching present in cassava starch and the composites but not in glycerol.

Table 3.35 FTIR spectra of cassava starch, glycerol and TPCSV composites

Infrared signal mode	Signal wave length (cm ⁻¹)					
	Cassava starch	Glycerol	S66G21VF13	S60G20VF20	S65G35VF0	S60G35VF5
O-H stretching	3277	3296	3304	3301	3315	3311
C-H stretching	2924	2920	2916	2922	2918	2924
H ₂ O absorbed	1637	na	1637	1641	1643	1641
C-O stretching	1147	na	1148	1151	1149	1149
C-C stretching	1076	1105	1079	1076	1076	1076
C-H bending	1334	1382	1357	1354	1334	1334
C-OH bending	1246	1203	1238	1238	1238	1238

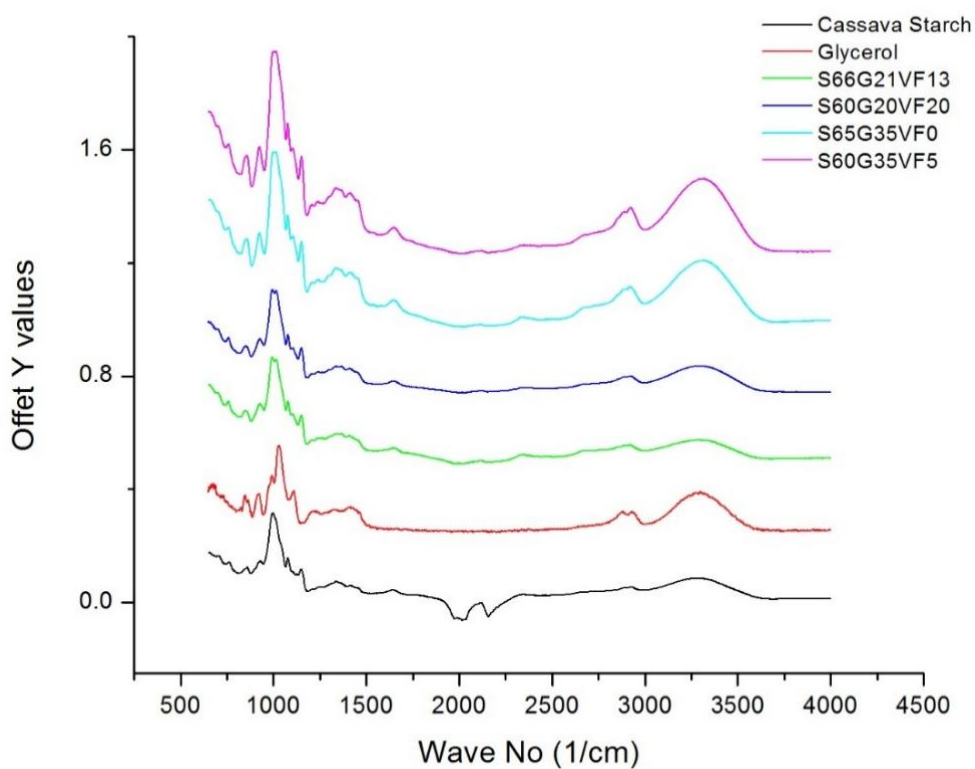


Figure 3.24 IR spectra of cassava starch, glycerol and selected TPCSV composites. Data are offset for clarity

3.5.8.2 Thermal properties

In the thermogravimetric analysis (TGA and DTG), pure cassava starch, glycerol, vetiver fiber and selected TPCSV samples were used as follows: S65G35VF0, S66G21VF13, S60G20VF20 and S60G35VF5 composites. These samples were evaluated for thermal stability and degradation temperature. The main area of interest of thermogravimetric analysis curves (TGA and DTG) such as onset, maximum, end decomposition temperature and non-volatile residuals are presented in Figure 3.25 to Figure 3.26, respectively.

The TGA curve for glycerol is presented in Figure 3.25. The graph shows a single step of degradation from 59 °C to 212 °C. This step corresponded to removal of moisture and volatiles and was followed by pyrolysis with a total weight loss of about 99.5%. The maximum decomposition temperature was observed at 206 °C. The weight of the sample remained almost constant after 212 °C with total degradation of 99.9% to 237 °C. The residual ash was 0.005% of the original sample weight.

In TGA of cassava starch, as shown in Figure 3.25, the first weight loss was observed between 25 °C and 125 °C and the sample gradually reached a constant weight plateau after losing 12.4% of the original weight. This weight loss corresponds to desorption of moisture and light volatiles from the cassava starch. The DTG curve of cassava starch shows maximum weight loss at 300 °C. The second weight loss was observed between 206 °C and 375 °C with degradation of 71.4%. This step of decomposition was attributed to thermal degradation of starch. The third weight loss was observed between 400°C and 489 °C, which shows pyrolysis with total degradation of 97.4% and leading to carbonization and ash as a residual of 0.3% at 550°C of the original sample weight. The DTG curve indicates the second change of weight at 478 °C.

In the case of vetiver fiber as shown in Figure 3.25, the weight loss was observed between 28 °C and 200 °C corresponding to moisture content and light volatiles from vetiver fiber with a

loss of 6.5%, and the sample reached a constant weight plateau at 215 °C. The DTG curve of vetiver fiber shows the maximum weight loss at 360 °C, which is the thermal degradation of hemicellulose. The second weight loss observed between 475 °C and 570 °C, which shows the degradation of cellulose. The residual ash was less than 1% of the original sample weight at 570°C.

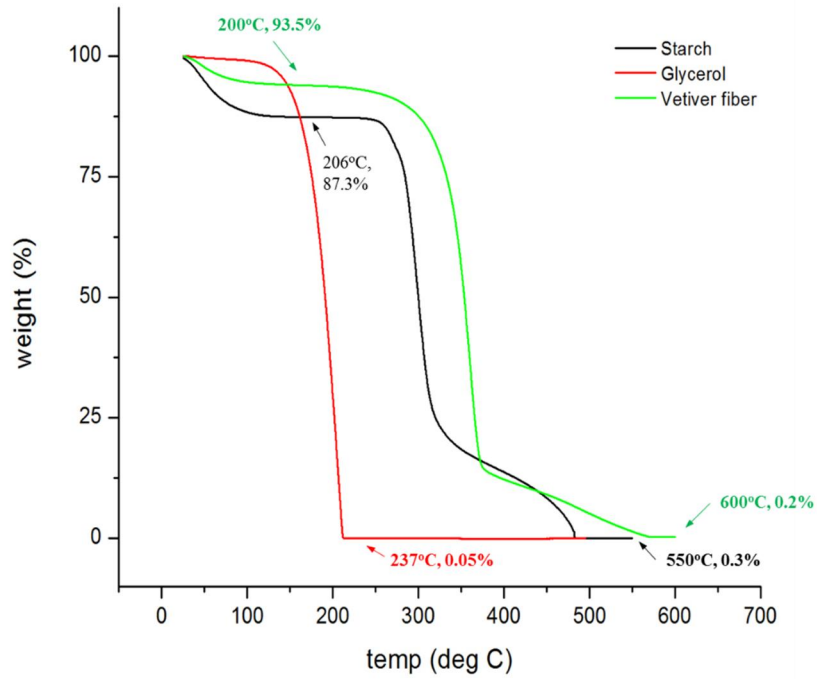
The TGA of the S65G35VF0 composite shows a single step of degradation. The initial weight loss was gradually decreased between 27 °C and 173 °C of about 11% due to the moisture content and light volatile materials. The weight loss between 173 °C to 386 °C shows pyrolysis with total degradation of 91.1%. The DTG curve shows the maximum weight loss at 297.4 °C. The residual ash was about 6.0% of the original sample weight at 550 °C as shown in Figure 3.26.

Thermal analysis of the S66G21VF13 composite as shown in Figure 3.26, the initial weight loss was gradually decreased between 30 °C and 202 °C of 6.1% due to the moisture content and light volatile materials. The weight loss between 202°C and 459 °C shows pyrolysis with total degradation of 83.9%. The DTG curve presents the maximum weight loss at 324 °C. The residual ash was about 7.9% of the original sample weight at 700 °C.

The TGA of S60G20VF20 composites, the initial weight loss started from 40 °C to 210 °C due to evaporation of moisture from water desorption from plasticizer, cassava starch and vetiver fiber with a total loss of 6.8%. The pyrolysis zone was observed between 210 °C and 469 °C with total degradation of 82.6%. The DTG curve indicates maximum change of weight at 317.3°C and the residual ash was about 8.7% of the original sample weight at 700 °C as shown in Figure 3.26.

In the case of S60G35VF5 composite, degradation occurred from 199°C to 410°C. The initial weight loss was observed from 30 °C to 199 °C due to evaporation of moisture from water desorption from the plasticizer, cassava starch and vetiver fiber with a total loss of 8.9%. The pyrolysis zone was observed between 199 °C and 410 °C with total degradation of 80.8 %. The

DTG curve indicates maximum change of weight at 317.7 °C and the residual was 7.2% of the original sample weight at 700 °C as shown in Figure 3.26.

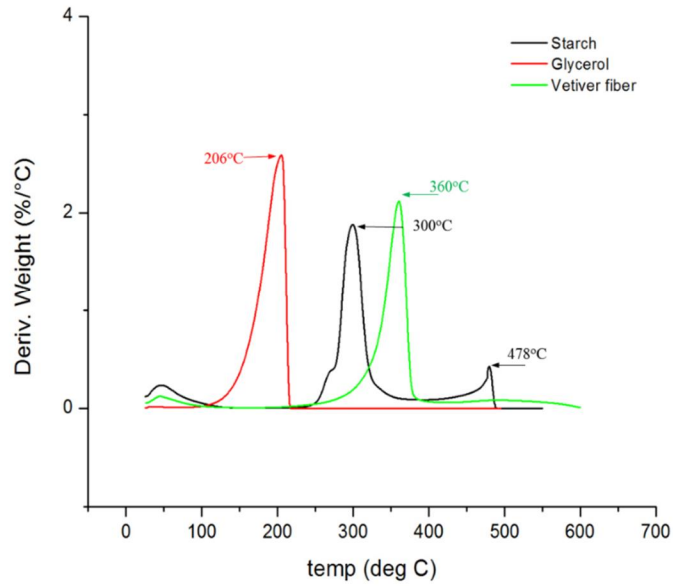


a)

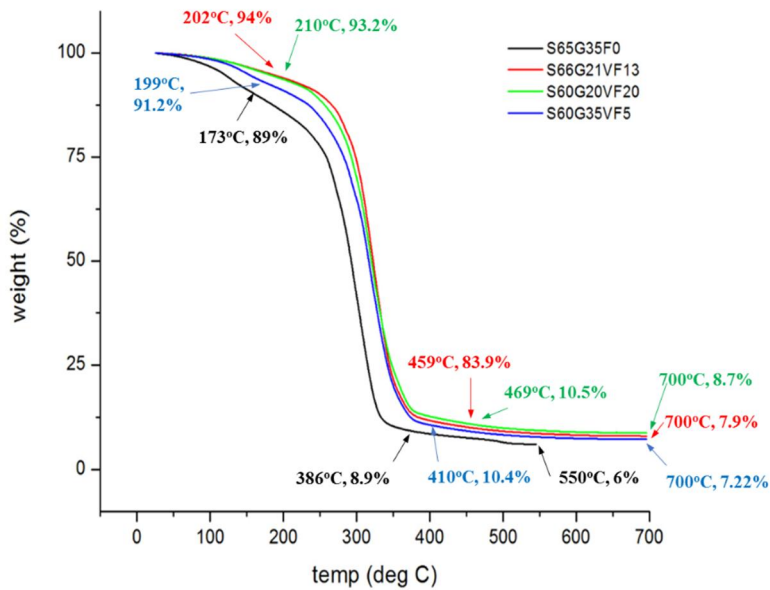
Figure 3.25 TGA and DTG curves of cassava starch (black), glycerol (red), vetiver fiber (green);

a) TGA curve, b) DTG curve

Figure 3.25 (cont'd)



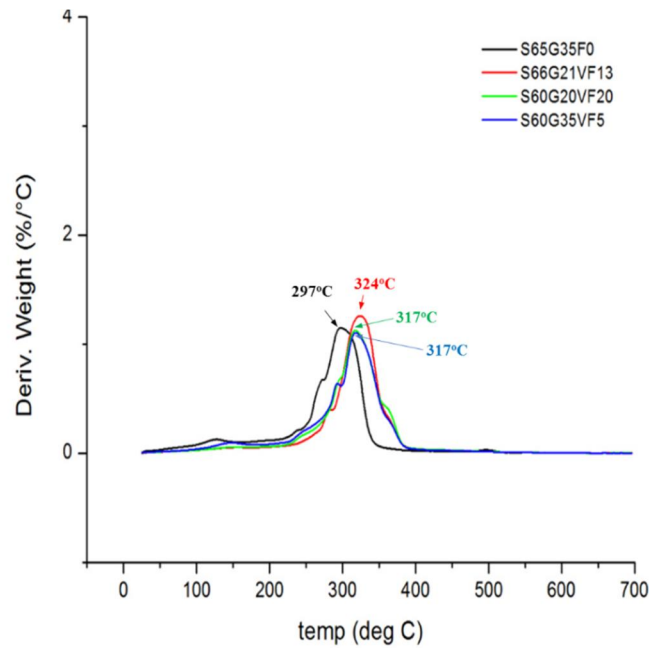
b)



a)

Figure 3.26 TGA and DTG curves of selected TPCSV composites; S65G35VF0 (black), S66G21VF13 (red), S60G20VF20 (green) and S60G35VF5 (blue); a) TGA curve, b) DTG curve

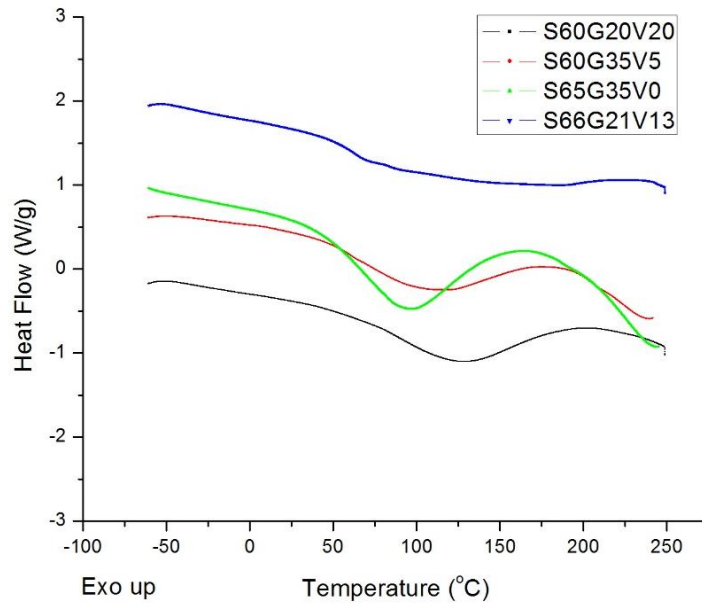
Figure 3.26 (cont'd)



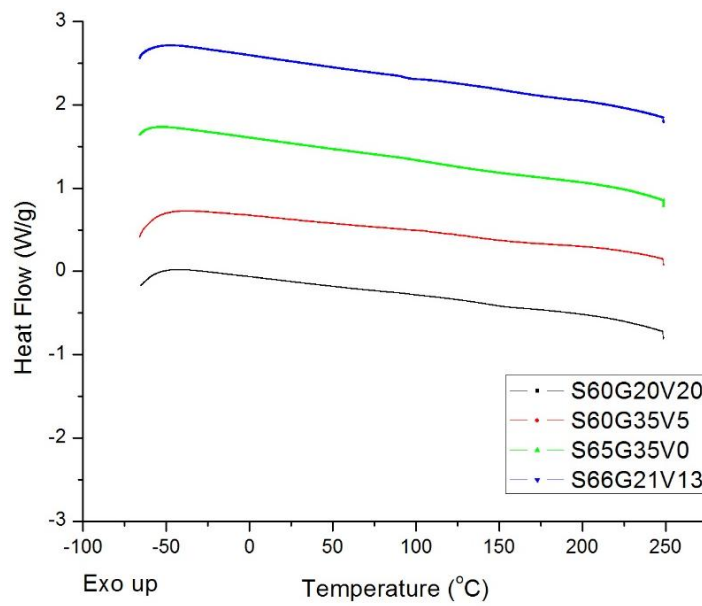
b)

Differential scanning calorimetry (DSC) is one of the tools used to determine the quantity of heat either absorbed or released when materials undergo thermal changes. In this study, the first heating cycle, relating to the melting point of the samples, was performed to remove the thermal history and moisture in the sample [120] as shown in Figure 3.27a. Moisture greatly affected the samples as can be seen from the broad endothermic peaks of thermoplastic cassava starch composites that occurred from the range of room temperature to about 120 °C (onset temperature at about 45-60 °C). This was due to disruption of starch crystallites or their gelatinization, as discussed by Mano *et al.*'s study [119]. The second heating cycle was used to analyze the thermal properties of the composites. As mentioned by Wattanakornsiri *et al.*[121], the glass transition of TPCS composites was difficult to detect by DSC due to the small change in heat capacity at the

T_g. Figure 3.27b presents the change in thermal transitions of the TPCS composites, which were not significantly different from each other.



a)



b)

Figure 3.27 DSC curves of thermoplastic cassava starch composites. Data were offset for clear observation; a) The first heating, b) The second heating

3.5.8.3 SEM

SEM of the optimized thermoplastic cassava starch composites showed uneven surfaces due to the stickiness of the samples when removed from the mold and some showed cracked surfaces due to shrinkage. The fractured surfaces showed that the vetiver fibers were well immersed in the matrix but with bundles. They curled and randomly aligned within the composite as shown in Figures 3.28 to 3.35.

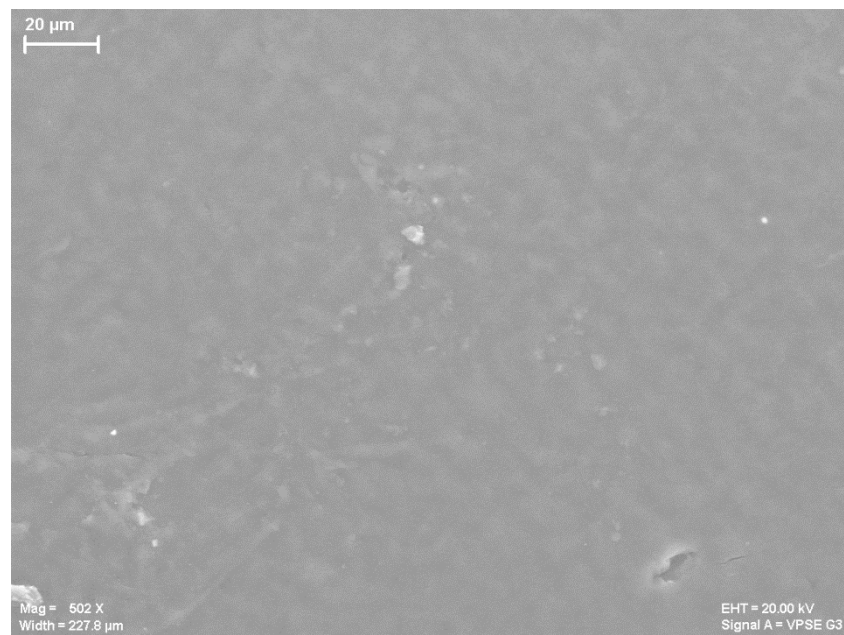


Figure 3.28 500x Surface view of S66G21VF13

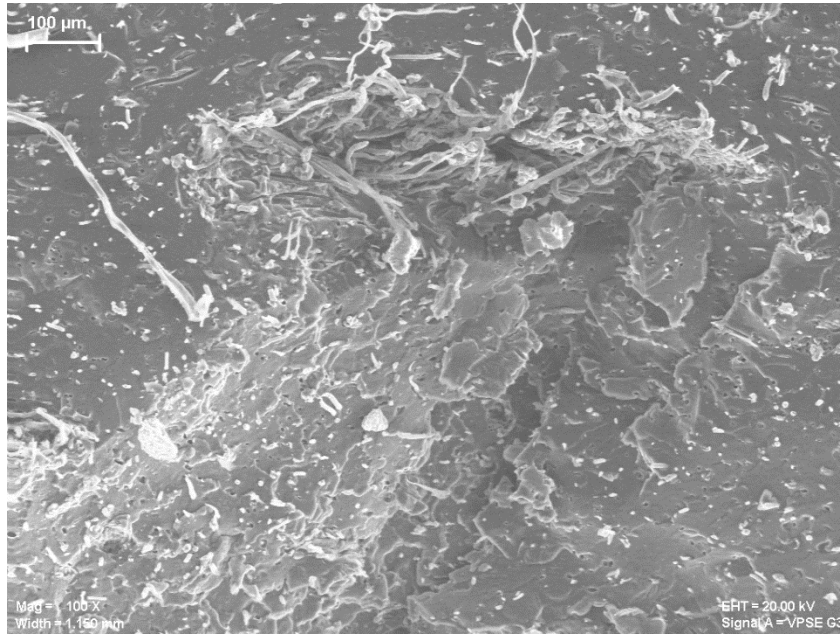


Figure 3.29 100x Cross section view of S66G21VF13

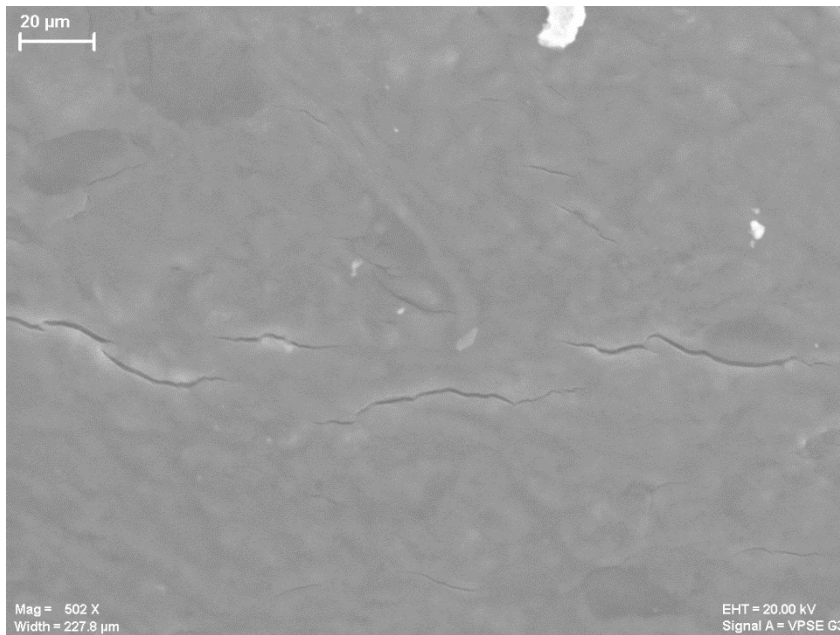


Figure 3.30 500x Surface view of S60G20VF20

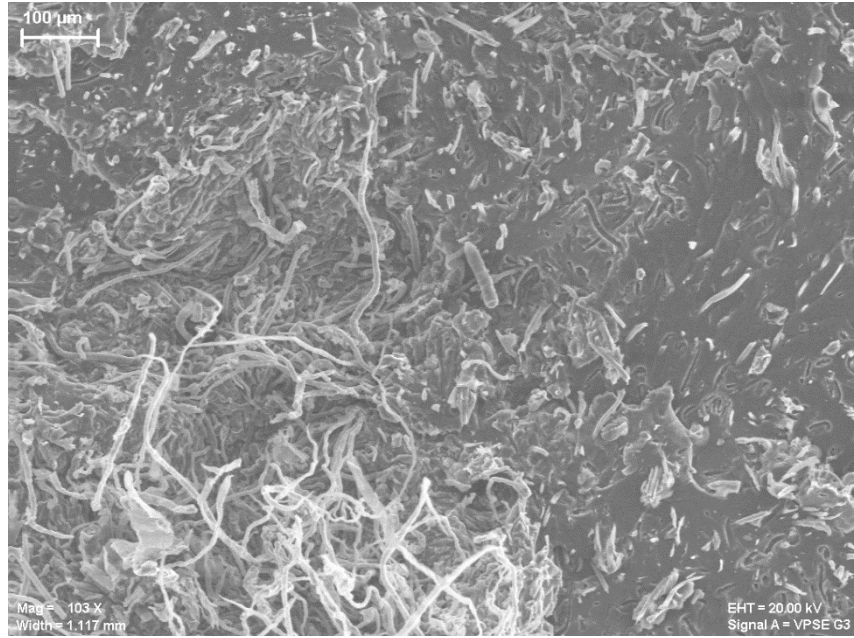


Figure 3.31 100x Cross section view of S60G20VF20

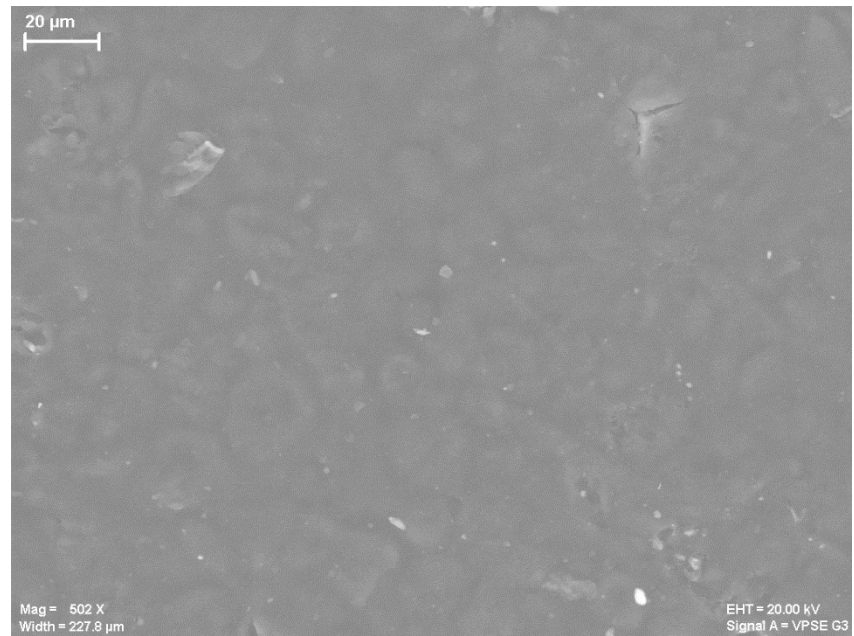


Figure 3.32 500x Surface view of S60G35VF5

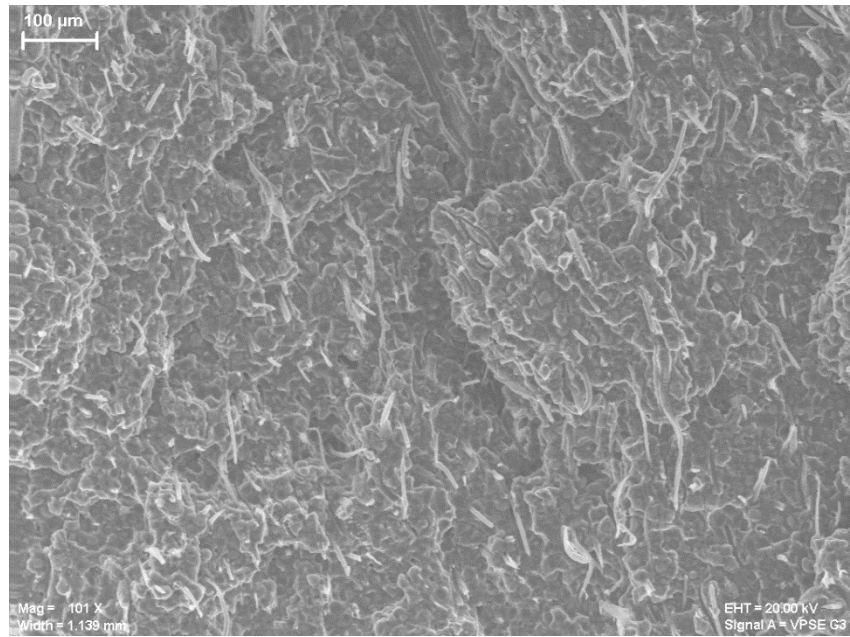


Figure 3.33 100x Cross section view of S60G35VF5

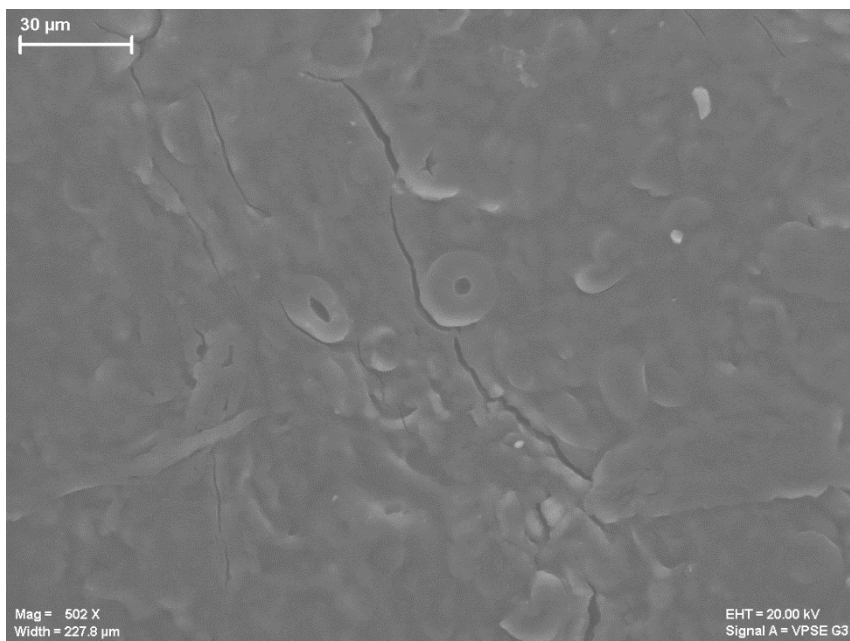


Figure 3.34 500x Surface view of S80G15VF5

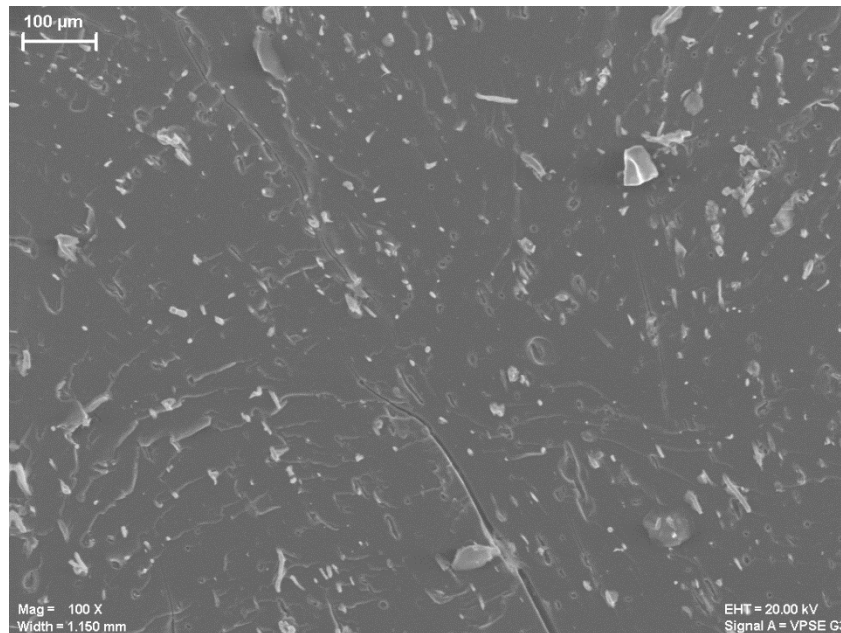


Figure 3.35 100x Cross section view of S80G15VF5

3.6 Conclusions

In this study, the processing behavior of thermoplastic cassava starch reinforced by natural fibers was determined using a Brabender® Torque Rheometer. The processability was mainly influenced by the amount of starch and glycerol. For gelation torque of TPCS with vetiver fiber (Table 3.5), compositions with the same amount of cassava starch but different amounts of glycerol such as #2 vs #4 and #7 vs #11 generated less gelation torque with a higher amount of glycerol. On the other hand, samples with the same amount of glycerol but different amounts of cassava starch such as #1 vs #5 and #6 vs #10 generated higher gelation torque and gelation energy with higher amounts of cassava starch.

Mixture design of experiments was used successfully to propose mechanical property models for thermoplastic cassava starch reinforced by natural fiber. The models correlated the response variables as functions of component proportions in term of L-pseudo component coding.

The summary of ANOVA statistics showed that the models were able to explain the variables as a function of component proportions. Diagnostic case statistics were used to check the appropriateness of the assumptions for the multiple linear regressions.

Using mixture design of experiments, the optimum formulation composition for any proportion of cassava starch, glycerol and vetiver fiber in the design space can be estimated using the response surface methodology. This information can be useful to guide further experiments or to design composite products.

Chapter 4

Determination of the biodegradability of thermoplastic cassava starch reinforced by natural fibers

4.1 Introduction

The production of plastic has increased all around the world over the last few decades due to its properties such as light weight, low cost, good mechanical strength and resistance to degradation. At the end of their useful life, they eventually will end up in the environment as plastic wastes. The US EPA states that in 2013, the US produced about 254 million tons of trash, of which 87.2 million tons or about 34.3% was recycled or composted. Waste generation increased about 1.6 % from 2010 or about 4.25 million tons of trash, and recycling and composting by about 2.34% from 2010 or about 2.04 million tons [1, 2]. In many countries, plastic wastes are disposed not only by dumping in landfills but also by burning in incinerators. These methods are commonly used as waste treatments, but the limitations of these methods include lack of landfill sites or regulated dumping areas and production of a variety of volatile and gaseous emissions [124]. In this situation, efforts to produce a fully biodegradable plastic could help to decrease the negative impacts on the environment compared to non-biodegradable plastics. Nowadays, one of the prominent materials that can be used as a naturally biodegradable material is starch, which can be found in many starchy plants all around the world. Biodegradable plastics from starch were discussed in chapter 2.

4.2 Research objectives

The objective of this study was to evaluate and to estimate the biodegradability of the fabricated thermoplastic cassava starch reinforced by natural fibers using an in-house direct measurement respirometric system (DMR) under simulated composting conditions.

4.3 Experimental (Materials and Methods)

4.3.1 Materials

Thermoplastic cassava starch composites prepared as discussed in chapter 3 were used. Earthgro® organic manure compost from Scotts Miracle-Gro., Marysville, OH, USA and A 12-month-old manure compost from the Michigan State University Composting Facility, East Lansing, MI, USA were used in this test with vermiculite premium grade from Sun Grow Horticulture Distribution Inc., Bellevue, Washington, USA. Cellulose powder 20- μ m grade, Sigma Aldrich, St Louis, Mo., USA was used as the positive control.

The moisture content of the materials and pH were determined by a moisture analyzer (MX-50, A&D Company, Tokyo, Japan) and pH meter (Omega Engineering Inc., CT, USA). The carbon to nitrogen (C/N) ratio was measured by a PerkinElmer 2400 Series II CHNS/O Elemental analyzer (Waltham, Mass., USA).

4.3.2 Biodegradation

4.3.2.1 Test system

A respirometric system is a tool used for measuring the respiration activity of living organisms. It was used to measure the biodegradability of the composite materials under aerobic conditions on a laboratory scale. Generally, the testing system was comprised of three major parts: 1) a pressurized CO₂-free air system used as a carrier gas to control the aeration rate. 2) a set of bioreactors, which were air-tight closed vessels containing a mixture of test materials with compost

and 3) a carbon dioxide detection system used as a measuring device. The test was conducted in accordance with ISO 14855 [4, 5] and ASTM 5338 [127].

In this study, an automated direct measurement respirometric system (DMR) which was built by the School of Packaging at Michigan State University, USA was used to determine the biodegradation in compost of the thermoplastic cassava starch reinforced by natural fibers [121, 81]. The system components included an air supply, a scrubbing unit, a controllable environmental chamber, an air-tight closed container called a bioreactor and devices for controlling the flow and measuring the carbon dioxide (CO₂), as shown in Figure 4.1. To operate the test system, samples are kept in air-tight bioreactors in which the CO₂-free air passes through inlet ports with controlled temperature, air-flow rate and humidity. The evolved CO₂ from the bioreactors was periodically conducted through to a non-dispersive infrared gas analyzer (model Li-820 from LI-COR Inc., Lincoln, NE, USA). This operation was controlled by the combination of DMR control program and DMR data analyzer, which were developed by LabVIEW™ (version 7.1) (National Instruments Corporation, Austin, TX, USA). The run time for samples from each bioreactor was 1020 seconds. It can be divided into two parts, which are 300 seconds of CO₂-free air for purge time in order to clean the detector, and 720 seconds for the measurement time with the last 30 seconds at the steady state used for analysis. The software was run on a personal computer that was used to record and to interpret the data for measurement of CO₂ concentration [6, 7].

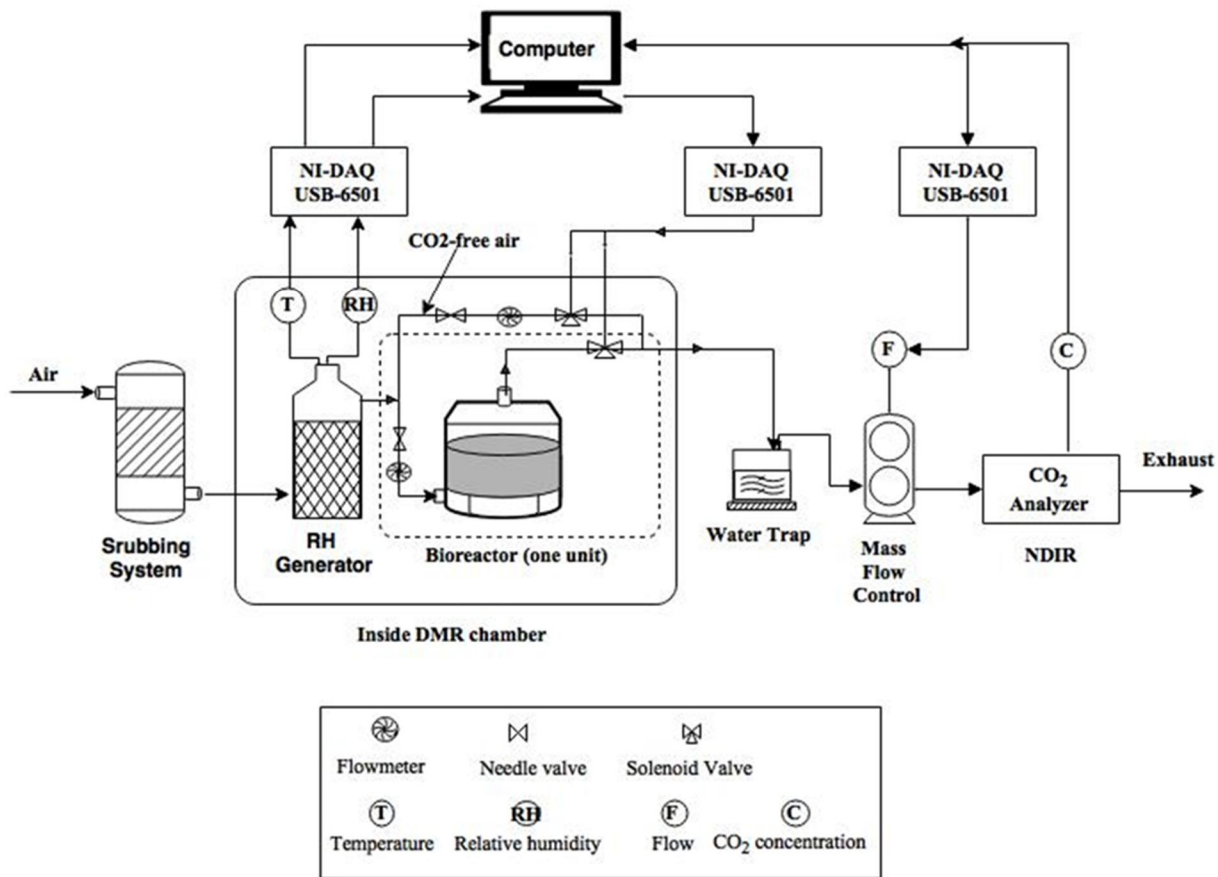


Figure 4.1 Schematic of the direct measurement respirometric system (DMR) adapted from Kijchavengkul et al. [88] and Aguirre [128]

4.3.2.2 Compost preparation

Two types of compost were used in this study: 1) about 6 month old yard compost from Earthgro (commercial compost) purchased from Home Depot, East Lansing, Michigan USA, used for the first test and; 2) about 12 month old manure compost from the composting facility at Michigan State University, East Lansing, Michigan USA, used for tests 2 to 5. After they were received, the composts were sieved on a 10-mm screen to remove big and inert substances and were analyzed for carbon to nitrogen ratio (C/N ratio) using a PerkinElmer CHN analyzer (Waltham, Mass., USA). According to ASTM 5338, the range of C/N ratio of a good quality

compost should be between 10 and 40 [127]. In addition, a thermogravimetric analysis of the compost was performed to determine the ash content and dry solids. The heating rate was set at 10 °C/min from room temperature to 560 °C. The characteristics of the composts are presented in Table 4.1.

Table 4.1 Chemical properties of the composts [128]

Chemical properties	Commercial compost	MSU compost
Moisture (%)	42.62	45.11
Dry solids (%)	57.38	54.89
Ash content (%)	39.68	25.39
pH	7.6	8.3
C/N ratio	12.5	12.5

Before using the compost in the biodegradability experiment, one part of vermiculite was saturated with five parts of distilled water and mixed with the compost at a ratio of 1:4 parts dry weight compost to allow good aeration and to avoid blocking and to retain moisture in the incubator. Then the compost was pre-conditioned by placing the compost inside an environmental chamber at 50±1 °C for 3 days in order to acclimatize to the test conditions. The ability of compost to produce carbon dioxide was evaluated for compliance with ISO 14855 and ASTM 5338 standards: yard and manure compost should produce between 50 and 150 mg of carbon dioxide per gram of volatile solids over the first 10 days of the test.

4.3.2.3 Test materials

Thermoplastic cassava starch composites were used as test materials and cellulose powder was used as a reference or a positive control for the biodegradation experiment as shown in Table 4.3 to Table 4.5. The test and reference materials (cassava starch, paper fiber, vetiver fiber, glycerol and cellulose powder) were analyzed for carbon content using a PerkinElmer 2400 Series II CHNS/O Elemental analyzer (Waltham, Mass., USA). These values were used for calculation of

the % mineralization, which can be interpreted as the percentage of the carbon in the tested materials that was converted to CO₂. The theoretical carbon contents of the materials are presented in Table 4.2. The percentage carbon content of the experimental samples is presented in Table 4.3 to Table 4.5.

Table 4.2 The theoretical carbon content of tested materials

Test material	Carbon content (% by weight)
Vetiver fiber	43.2
Paper fiber	32.8
Glycerol	39.1
Cassava starch	39.7
Cellulose powder	43.5

In this study, the experiments were divided into five test runs for determining the aerobic biodegradation of thermoplastic cassava starch reinforced by natural fiber under composting conditions. These tests were divided due to the limitation of the space in the DMR system. The tests were performed following the requirements and methodology of ASTM 6400, ASTM 5338 and ISO 14855 [6, 9, 118]. To validate the biodegradation study, the percentage of mineralization of the positive control (cellulose) should reach 70% in a test period of 45 days according to ASTM 5338 and the test period should not exceed 180 days according to ISO 14855.

The first test included three types of bioreactor: 1) blanks (550 g, commercial compost wet weight), 2) positive controls (550 g, commercial compost wet weight with 8 g of cellulose powder) and 3) samples (550g, commercial compost wet weight with 8 g of test materials). For the second to fifth tests, the bioreactors contained: 1) 400 g, MSU compost wet weight for blanks, 2) 400 g, of MSU compost wet weight with 8 g of cellulose powder for positive control, and 3) 400 g, MSU compost wet weight with 8 g of sample cut into 1cm × 1cm for test materials. Each sample type was run in at least triplicate.

After the bioreactors were filled, they were placed into an environmental chamber, which maintained the temperature and humidity at 58 ± 2 °C and 50-60 % RH, respectively, with CO₂-free air at a flow rate of 40 scm³/min. The experiment was continued until the carbon dioxide evolution of the samples reached a plateau or for at least 45 days.

The first to third test runs evaluated the biodegradation of thermoplastic cassava starch reinforced by paper fiber (Table 4.3). The fourth test evaluated the biodegradation of thermoplastic cassava starch reinforced by vetiver fiber (Table 4.4) and the fifth run was used to determine the biodegradability of each raw material separately (Table 4.5).

During the tests, temperature, air flow, moisture content and pH were monitored. Injection of deionized water and shaking of all bioreactors were done when the moisture content was lower than a control value or the compost started to clump up, respectively, usually once a week.

Table 4.3 Composition and carbon content of each test material for the first test to the third test

Test material code	Original Composition, wt. fraction			Experiment No.	Carbon Content (%)
	Cassava starch	Glycerol	Paper fiber		
S65G35P0	0.65	0.35	0.00	1	39.5
S80G20P0	0.80	0.20	0.00	N/A	39.6
S60G35P5	0.60	0.35	0.05	2	39.1
S60G25P15	0.60	0.25	0.15	1	38.6
S70G15P15	0.70	0.15	0.15	1	38.6
S69G24P7	0.69	0.24	0.07	2	39.1
S73G27P0	0.73	0.27	0.00	3	39.5
S75G20P5	0.75	0.20	0.05	N/A	39.2
S65G30P5	0.65	0.30	0.05	2	39.0
S65G20P15	0.65	0.20	0.15	3	38.6
S80G15P5	0.80	0.15	0.05	3	39.3
S80G20P0	0.80	0.20	0.00	2	39.6
S80G15P5	0.80	0.15	0.05	1	39.3
S60G25P15	0.60	0.25	0.15	3	38.6
S70G15P15	0.70	0.15	0.15	3	38.6
S65G35P0	0.65	0.35	0.00	3	39.5

N/A = Not Applicable

Table 4.4 Composition and carbon content of each test materials of the fourth test run

Test material code	Original Composition, wt. fraction			Carbon Content (%)
	Cassava starch	Glycerol	Vetiver fiber	
S72G15VF13	0.72	0.15	0.13	40.1
S60G20VF20	0.60	0.20	0.20	40.3
S70G25VF5	0.70	0.25	0.05	39.7
S60G35VF5	0.60	0.35	0.05	39.7
S80G15VF5	0.80	0.15	0.05	39.8
S60G28VF12	0.60	0.28	0.12	40.0
S66G21VF13	0.66	0.21	0.13	40.0
S65G15VF20	0.65	0.15	0.20	40.3
S73G18VF9	0.73	0.18	0.09	39.9
S63G28VF9	0.63	0.28	0.09	39.9
S66G18VF16	0.66	0.18	0.16	40.2
S60G35VF5	0.60	0.35	0.05	39.7
S80G15VF5	0.80	0.15	0.05	39.8
S70G25VF5	0.70	0.25	0.05	39.7
S60G20VF20	0.60	0.20	0.20	40.3
S65G15VF20	0.65	0.15	0.20	40.3

Table 4.5 Test materials and carbon content for the fifth test

No.	Test material	Carbon content (%)
1.	Vetiver fiber	43.2
2.	Paper fiber	32.8
3.	Glycerol	39.1
4.	Cassava starch	39.7
5.	Cellulose	43.5

4.4 Calculation of biodegradation testing [81, 121]

The set-up parameters for the DMR system are shown in Table 4.6. The concentration of CO₂ (ppm) was converted to mass of CO₂ (g) evolved from each bioreactor over each period of time using equation 4-1.

$$gCO_2 = \frac{C \times F \times t \times 44}{22414 \times 10^6} \quad (eq. 4 - 1)$$

where gCO₂ is the cumulative mass of evolved CO₂ (g), F is the flow rate (sccm), t is the time between measurement intervals, C is the concentration of evolved CO₂ during the measurement interval (ppm), 44 is the molecular weight of CO₂ (g/mol), 22414 is the volume of 1 mol of ideal gas in cc at STP and 10⁶ is the ppm conversion factor.

The cumulative amount of CO₂ evolved for each measurement interval was calculated using the summation of the area under the time/concentration curve, measuring at time t_n and t_{n-1} and using the trapezoidal method. To get the cumulative mass of CO₂ of the sample, the cumulative mass of CO₂ of the blanks needed to be subtracted at the same time interval.

This was then used to calculate the percent mineralization of the samples, using eq. 4-2.

$$\%Mineralization = \frac{gCO_{2s} - gCO_{2b}}{W \times \frac{\%C}{100} \times \frac{44}{12}} \times 100 \quad (eq. 4 - 2)$$

where gCO_{2s} is the cumulative amount of CO₂ evolved from the sample or the cellulose bioreactor, gCO_{2b} is the cumulative amount of CO₂ from the compost bioreactor or blank, W is the weight of sample or cellulose, %C is the percent organic carbon in the sample or cellulose obtained from the CHN analyzer, 44 is the molecular weight of carbon dioxide, and 12 is molecular weight of carbon.

In addition, the standard error (Se) of % mineralization of the test materials was calculated using eq. 4-3 (ASTM, 2003).

$$Se = \frac{\sqrt{\frac{S_{test}^2}{n_1} + \frac{S_{blank}^2}{n_2}}}{g_{mat}} \times 100 \quad (eq. 4 - 3)$$

where SE is the standard error (%), s is the standard deviation of total CO₂ evolution of each material, n₁, n₂ are the numbers of replicates of the test material and blank, and g is the mass of the test material (g).

Table 4.6 Summary of set-up parameters for the DMR system [128]

Parameter	Setting
Humidity, (%)	55±5
Air flow rate, (sccm)	40±2
Temperature, (°C)	58±2
Duration/cycle (s)	1020
Purging time/cycle (s)	300
Measuring time/cycle (s)	30

4.5 Statistical analysis

Three replicates were used for each treatment. Analysis of variance (ANOVA) was calculated for the average maximum percentage of mineralization for each sample. Turkey-Kramer HSD analysis was performed for mineralization comparisons of all pairs of samples at a significant difference level of $\alpha = 0.05$. Statistical analysis was performed using the Minitab statistical program version 16 (Minitab Inc., State College, PA, USA).

4.6 Results and discussion

4.6.1 The biodegradation of cellulose powder in compost

The data analysis was performed by the combination of the DMR control program and DMR data analyzer. The amount of CO₂ evolved from cellulose samples in bioreactors from tests 1 to 5 are shown in Figure 4.2. The percentage of mineralization from the cellulose samples in each test were converted using equation 4-2. The results of tests 1 to 5 showed that the degrees of biodegradation of the cellulose powder (reference material) in the compost at day 45 were 52.3%, 86.7%, 95.3%, 87.2%, and 80.9 % respectively, as shown in Figure 4.3.

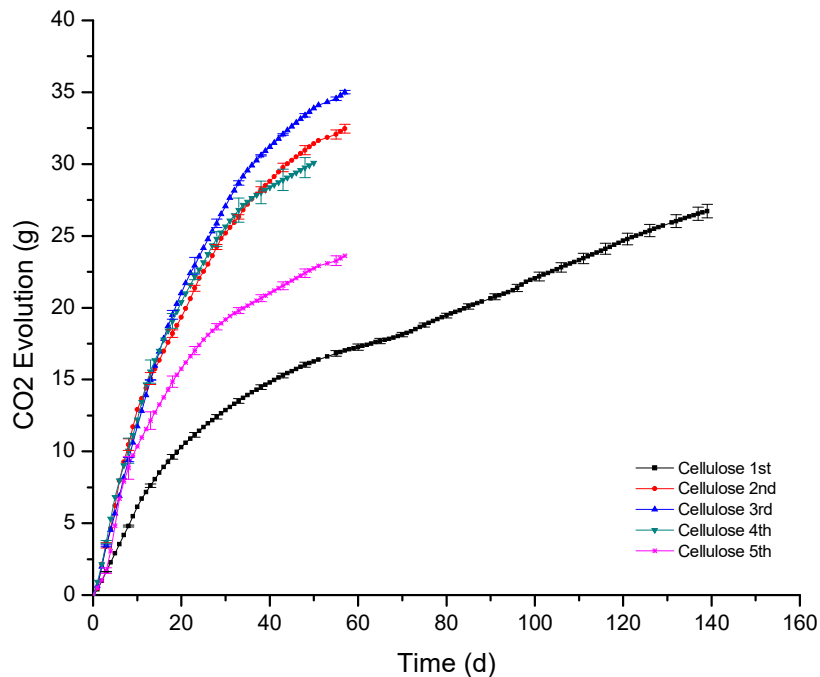


Figure 4.2 Evolution of CO₂ of cellulose powder under stimulated composting conditions in tests 1 to 5

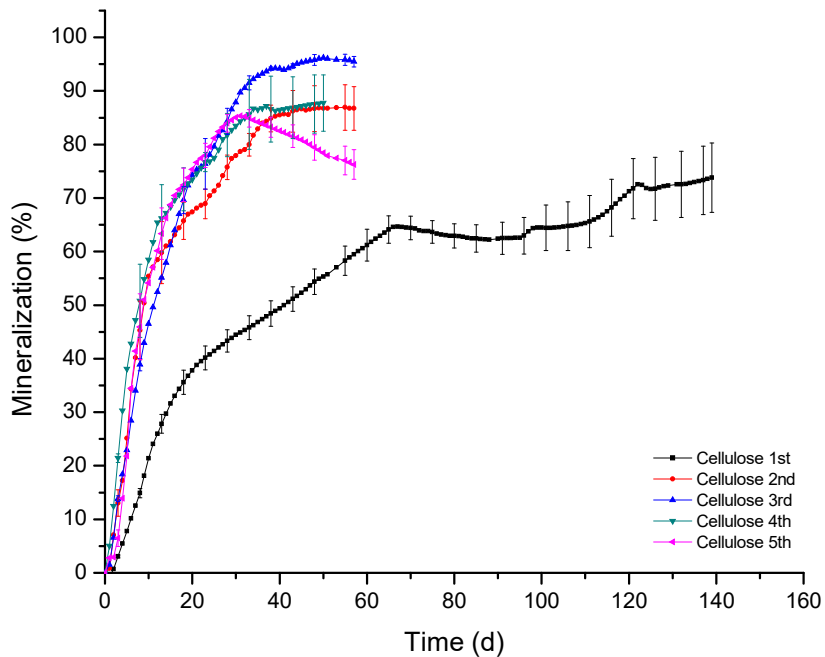


Figure 4.3 Mineralization of cellulose powder under stimulated composting condition in tests 1 to 5

The percent mineralization of cellulose powder in tests 1 to 5 reached 70% at days 119, 24, 18, 17, and 16 respectively. The maximum degrees of mineralization were 73.8%, 86.9%, 96.2%, 87.7%, and 85.3% respectively. The mineralization results in this study showed similar trends of degradation for tests 2 to 5, while test 1 differed. This is most likely due to the different types of composts, as mentioned earlier, with commercial compost used in test 1 and MSU compost used in tests 2 to 5. The commercial compost likely had less activity than the MSU compost, since it was stored in a plastic bag for a long period of time, while the MSU compost was directly taken from the compost pile, which had high microbial activity and population due to high moisture and temperature conditions [130]. Moreover, a decreased rate of evolved CO₂ was observed about day 70 in test 1 and deionized water was added to keep the moisture content of the compost around 50 % RH, after which the CO₂ evolution increased. Similarly, Richard et al., and Aguirre reported that moisture content of the compost affected polymer degradation [7, 11].

Table 4.7 shows that the rate of change for test 1 was much lower than for the other tests. It reached 70% and maximum mineralization at day 119 and 139, respectively. Besides, the Tukey test indicated that the maximum percentage of mineralization of cellulose from test 1 was significantly different from test 3, whereas the differences for tests 2, 4 and 5 were not statistically significantly different.

Table 4.7 The percent mineralization and average rate of degradation of cellulose powder

Cellulose at run	%Mineralization			
	At 70%	day	At Maximum	day
Test 1	70.43 ± 5.52	119	73.81 ± 6.47 ^b	139
Test 2	70.44 ± 3.00	24	86.90 ± 4.23 ^{ab}	53
Test 3	69.62 ± 2.53	18	96.19 ± 1.11 ^a	50
Test 4	70.66 ± 4.28	17	87.74 ± 5.23 ^{ab}	50
Test 5	70.47 ± 4.02	16	85.34 ± 1.59 ^{ab}	31

* Different letter subscripts indicate significant differences (p < 0.05)

* Values: mean ± standard error

4.6.2 The biodegradation of raw materials in compost

In this study (test 5), the aim was to observe the degree of biodegradation of the raw materials that were used as feedstocks to produce the thermoplastic cassava starch composites. The carbon content of cassava starch, vetiver fiber, paper fiber, glycerol, and cellulose powder were 39.7%, 43.2%, 32.8%, 39.1% and 43.5%, respectively, and the theoretical carbon dioxide evolution for each sample is shown in Table 4.8.

Table 4.8 The weight and amount of theoretical carbon dioxide evolution of cassava starch, vetiver fiber, paper fiber, glycerol, and cellulose powder

No.	Materials	Average Weight (g)	Theoretical CO ₂ content (g)
1	Cassava starch	8.1280	3.2268
2	Vetiver fiber	8.0034	3.4559
3	Paper fiber	8.0038	2.6260
4	Glycerol	8.1600	3.1930
5	Cellulose	8.0020	3.4841

The analysis of the data was the same as in the previous study. The amount of CO₂ evolved and the percentage of mineralization of each sample in the bioreactors at day 45 were 94.7%, 94.2%, 98.3%, 151.0%, and 86.9% for starch, vetiver fiber, paper fiber, glycerol, and cellulose powder, respectively, and are shown in Figure 4.4a and Figure 4.4b. In this study, the biodegradation of glycerol showed values higher than 100%. A value 151% was reached at day 45, which can be interpreted as due to the priming effect. Among test samples, glycerol is an easily-decomposable organic substance which increases the decomposition of other organic carbon in the compost resulting in high CO₂ emissions, which was reflected in a high percentage of mineralization [132]. When comparing with the blank, the evolved CO₂ had smoothly increased, different from the evolved CO₂ of glycerol that had highly increased from day 1 to day 30. The result agrees with Kuzyakov et al., who reported that priming effects are short-term changes of releasing the soil-derived carbon as CO₂ or nitrogen leading to an extra mineralization of carbon after the substance addition.

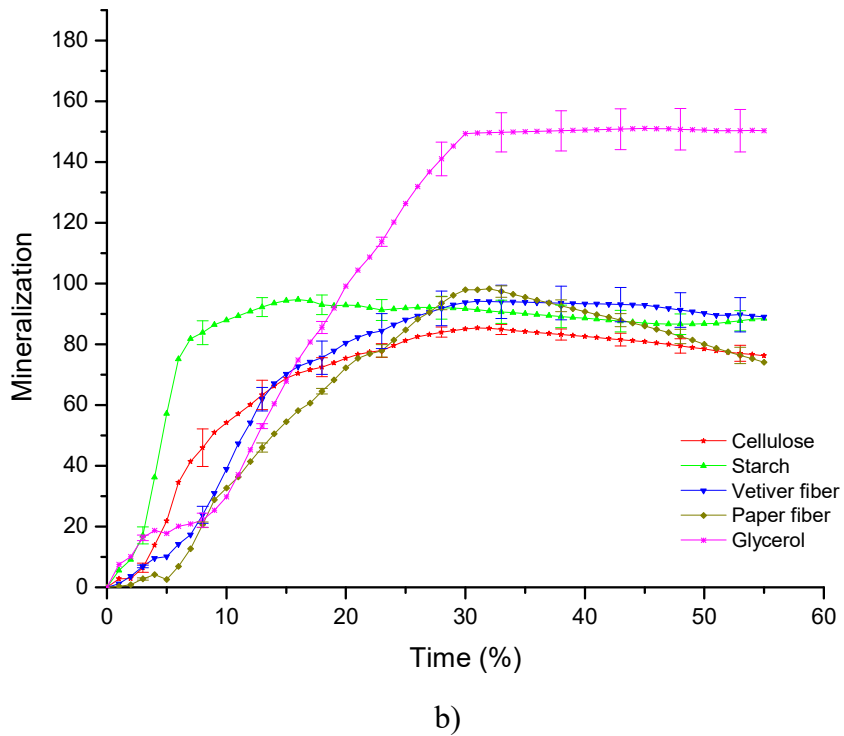
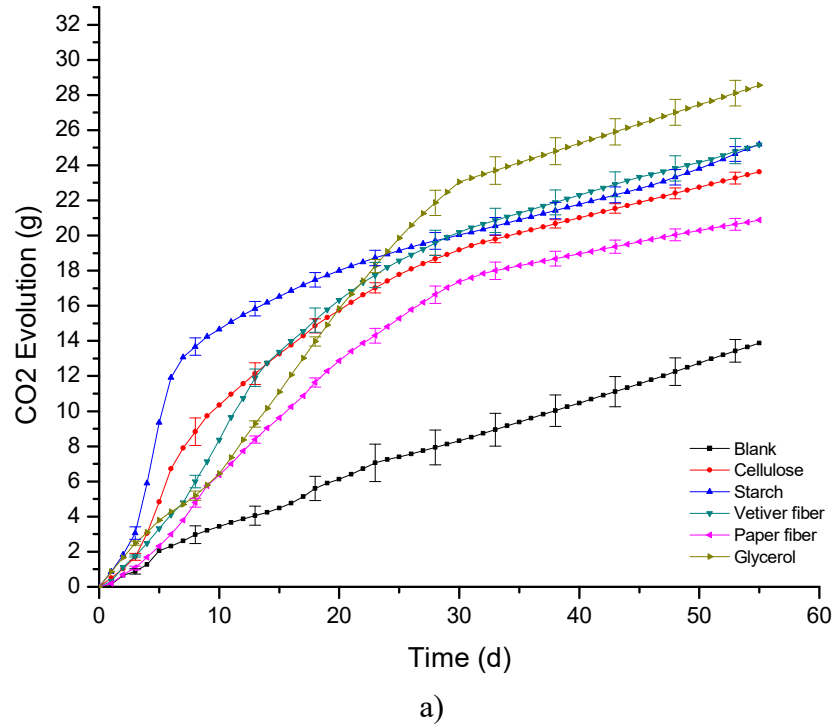


Figure 4.4 Evolution of carbon dioxide (a) and mineralization curve (b) of the raw materials

The degree of mineralization of cellulose, glycerol, paper fiber, starch, and vetiver fiber reached 70% at days 16, 16, 20, 6, and 15, respectively. The maximum degrees of mineralization were 85.3%, 151.0%, 98.3%, 94.7%, and 94.2%, respectively. Based on statistical analysis (Table 4.9), the biodegradation of glycerol was significantly different from cellulose, paper fiber, starch and vetiver fiber. The rate of degradation for starch was the highest among all the samples. It reached 70% and maximum mineralization with 6 days and 16 days, respectively. Results are shown in the Table 4.9.

Table 4.9 The percent mineralization and average rate of degradation of raw materials (test 5)

Sample	%Mineralization			
	At 70%	day	At Maximum	day
Cellulose	70.47 ± 4.02	16	85.34 ± 1.59 ^b	31
Glycerol	74.81 ± 1.51	16	151.02 ± 6.77 ^a	45
Paper fiber	72.23 ± 1.06	20	98.26 ± 1.93 ^b	32
Starch	75.18 ± 2.82	6	94.68 ± 3.21 ^b	16
Vetiver fiber	70.22 ± 5.01	15	94.20 ± 5.45 ^b	31

* Different letter subscripts indicate significant differences ($p < 0.05$)

* Values: mean ± standard error

4.6.3 The biodegradation of thermoplastic cassava starch reinforced by paper fiber in compost

The biodegradation of thermoplastic cassava starch reinforced by paper fiber was investigated in test 1 to test 3. As mentioned earlier, these studies were performed separately due to the limited space in the environmental chamber. The percentage of carbon content (Table 4.3) of thermoplastic cassava starch reinforced by paper fiber was used to calculate the theoretical carbon dioxide evolution. Table 4.10 presents a summary of the percentage of carbon content and the theoretical carbon dioxide evolution of materials that were used in test 1 to test 3.

Table 4.10 The amount of theoretical carbon dioxide evolution of each bioreactor in test 1 to 3

Experiment No.	Materials	Average Weight (g)	Theoretical CO ₂ content (g)
1	S65G35P0	8.0635	3.1851
1	S60G25P15	8.0519	3.1113
1	S70G15P15	8.0301	3.0980
1	S80G15P05	8.0667	3.1710
1	cellulose	8.0150	3.4865
2	S60G35P5	8.1285	3.1742
2	S69G24P7	8.1353	3.1809
2	S65G30P5	8.1732	3.1875
2	S80G20P0	8.1063	3.2085
2	cellulose	8.4238	3.6677
3	S73G27P0	8.0809	3.1944
3	S65G20P15	8.1047	3.1276
3	S80G15P5	8.0955	3.1823
3	S60G25P15	8.1464	3.1478
3	S70G15P15	8.2140	3.1690
3	S65G35P0	8.1658	3.2255
3	S65G35P0/ Ground TPCS	8.0512	3.1802
3	starch	8.1139	3.2212
3	cellulose	7.6578	3.3342

Based on visual inspection, all samples of thermoplastic cassava starch reinforced by natural fiber had dramatic changes during the first week. Changes in color and shape were found and also white particles were clearly observed. Visual examination was discontinued after the first week because the samples merged with the compost due to this fast degradation as shown in Figure 4.5. This result shows that temperature (58°C), relative humidity (50-60 %RH) and polymer characteristics (hydrophilic property) play important roles in affecting polymer biodegradation, which generally happens by surface erosion and bulk erosion through hydrolysis reactions [133].



Figure 4.5 Biodegradation of thermoplastic cassava starch reinforced by natural fiber in DMR system

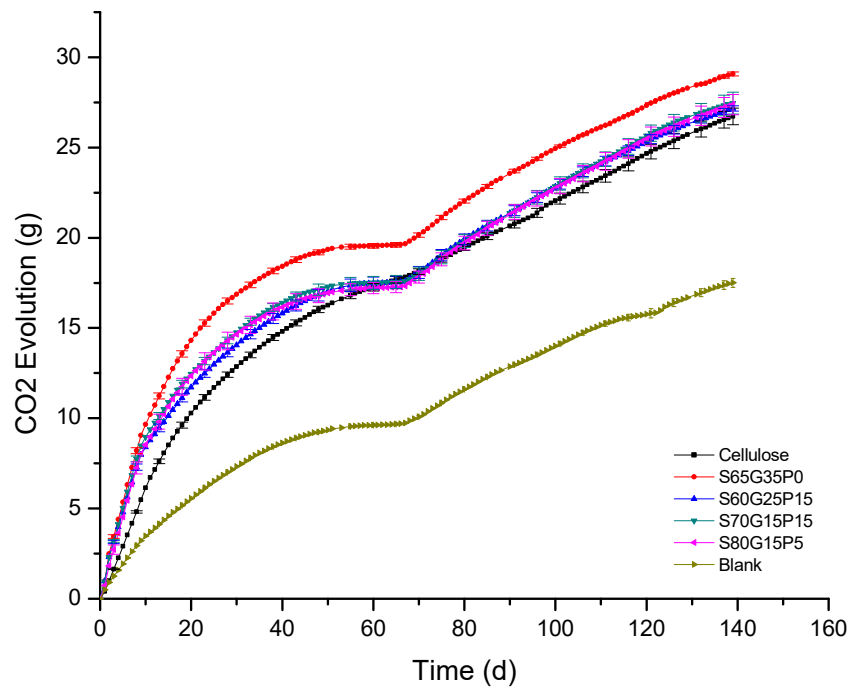
In the first test, the incubation period was extended to 139 days because the cellulose did not reach the plateau stage after 45 days. The second and third tests used an incubation period of 55 days. The major difference in incubation period was due to the type of compost, as mentioned earlier (commercial compost for the first test and MSU manure compost for the second and third test). After 139 days incubation in the first test, the CO₂ evolution from each bioreactor was calculated and is shown in Figure 4.6a. The percentages of mineralization of mixtures of TPCS with different proportions of cassava starch, glycerol and paper fiber, and the reference material in the commercial compost were 100.6%, 85.3%, 88.7%, 85.1% and 73.8% for S65G35P0, S80G15P5, S60G25P15, S70G15P15, and cellulose powder, respectively, as shown in Figure 4.6b.

After 55 days of incubation in the second test, the CO₂ evolution from each bioreactor was calculated and is shown in Figure 4.7a. The percentages of mineralization were 76.9%, 53.8%, 84.9%, 83.1%, and 86.9% for S60G35P5, S69G24P7, S65G30P5, S80G20P0, and cellulose powder, respectively, as shown in Figure 4.7b.

In the third test, the CO₂ evolution and the percentages of mineralization at 55 days were 89.9%, 61.3%, 80.6%, 77.2%, 70.3%, 78.3%, 64.0%, 82.2%, and 96.2% for S65G20P15,

S70G15P15, S80G15P5, S60G25P15, S65G35P0, S73G27P0, starch, ground S65G35P0, and cellulose powder, respectively. The evolution of carbon dioxide and mineralization curves of the third test are shown in Figure 4.8a and Figure 4.8b, respectively.

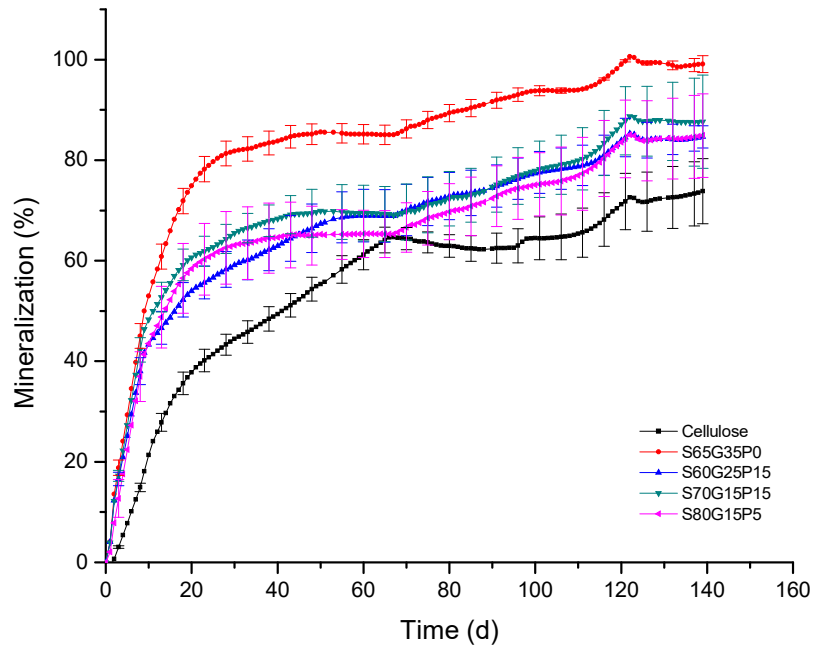
Based on statistical analysis (Table 4.11 to Table 4.13), the differences in biodegradation of the samples in each test when it reached 70% and obtained the maximum degree of mineralization generally were not significantly different, except that the biodegradation of cellulose powder and S65G35P0 were significantly different in test 1.



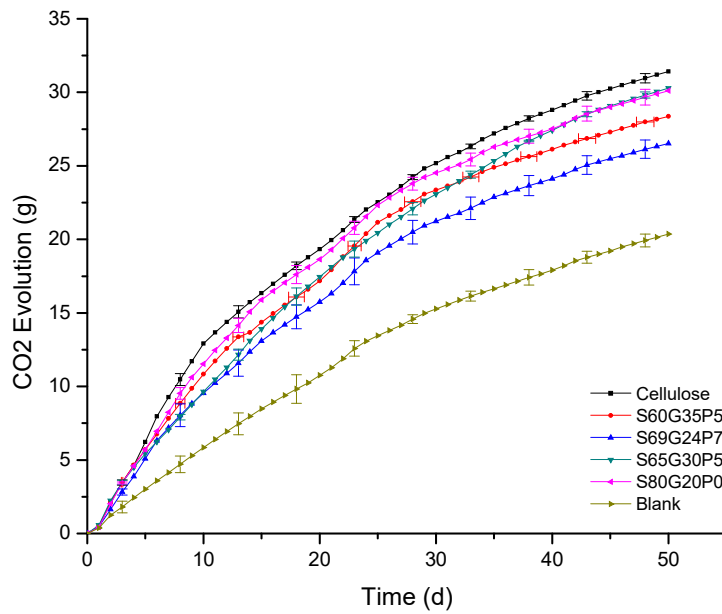
a)

Figure 4.6 Evolution of carbon dioxide (a) and mineralization curve (b) of the first test

Figure 4.6 (cont'd)



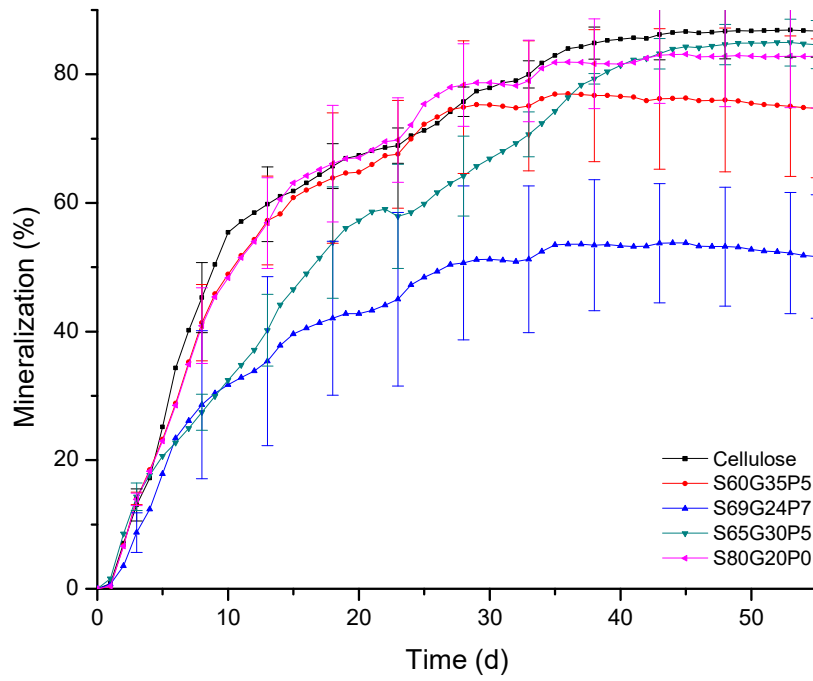
b)



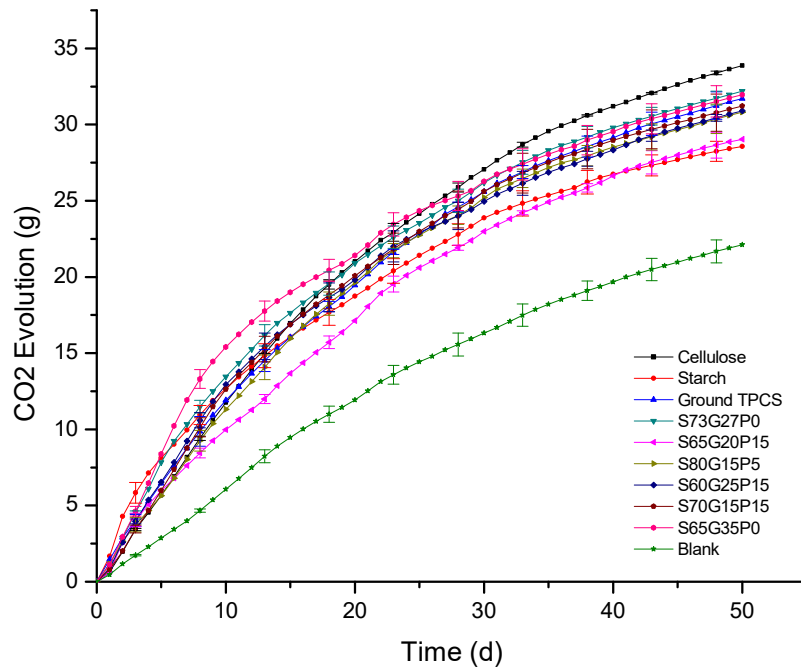
a)

Figure 4.7 Evolution of carbon dioxide (a) and mineralization curve (b) of the second test

Figure 4.7 (cont'd)



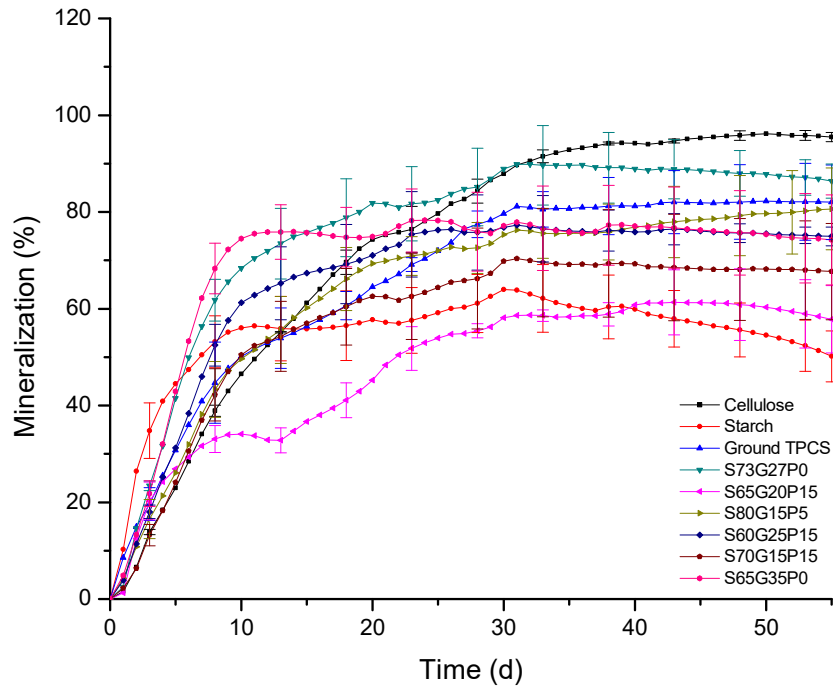
b)



a)

Figure 4.8 Evolution of carbon dioxide (a) and mineralization curve (b) of the third test

Figure 4.8 (cont'd)



b)

Table 4.11 The percent mineralization and average rate of degradation of test 1

Sample	%Mineralization			
	At 70%	day	At Maximum	day
Cellulose 1st	70.43 ± 5.52	119	73.81 ± 6.47 ^b	139
S65G35P0	70.16 ± 2.53	17	100.58 ± 0.25 ^a	122
S80G15P5	70.09 ± 5.65	82	85.06 ± 7.77 ^{ab}	122
S60G25P15	70.08 ± 5.10	70	85.32 ± 3.78 ^{ab}	122
S70G15P15	70.26 ± 5.61	73	88.72 ± 6.79 ^{ab}	122

* Different letter subscripts indicate significant differences ($p < 0.05$)

* Values: mean ± standard error

Table 4.12 The percent mineralization and average rate of degradation of test 2

Sample	%Mineralization			
	At 70%	day	At Maximum	day
Cellulose 2nd	70.44 ± 3.00	24	86.90 ± 4.23 ^a	53
S60G35P5	69.94 ± 8.54	24	76.96 ± 10.05 ^a	36
S80G20P0	69.77 ± 6.57	23	83.13 ± 7.66 ^a	45
S65G30P5	70.65 ± 3.49	33	84.94 ± 3.58 ^a	52
S69G24P7	53.81 ± 9.27	44	53.81 ± 9.27 ^a	44

* Different letter subscripts indicate significant differences ($p < 0.05$)

* Values: mean ± standard error

Table 4.13 The percent mineralization and average rate of degradation of test 3

Sample	%Mineralization			
	At 70%	day	At Maximum	day
Cellulose 3rd	69.62 ± 2.53	18	96.19 ± 1.11 ^a	50
Ground TPCS	70.37 ± 1.95	24	82.21 ± 7.92 ^a	50
Starch	63.98 ± 6.44	30	63.98 ± 6.44 ^a	30
S65G20P15	61.32 ± 6.69	43	61.32 ± 6.69 ^a	43
S70G15P15	70.34 ± 10.96	31	70.34 ± 10.96 ^a	31
S80G15P5	70.49 ± 4.33	22	80.63 ± 8.43 ^a	55
S60G25P15	70.01 ± 8.21	19	77.25 ± 7.58 ^a	31
S65G35P0	68.32 ± 5.18	9	78.29 ± 6.87 ^a	24
S73G27P0	70.41 ± 6.98	11	89.86 ± 8.54 ^a	31

* Different letter subscripts indicate significant differences ($p < 0.05$)

* Values: mean ± standard error

4.6.4 The biodegradation of thermoplastic cassava starch reinforced by vetiver fiber in compost

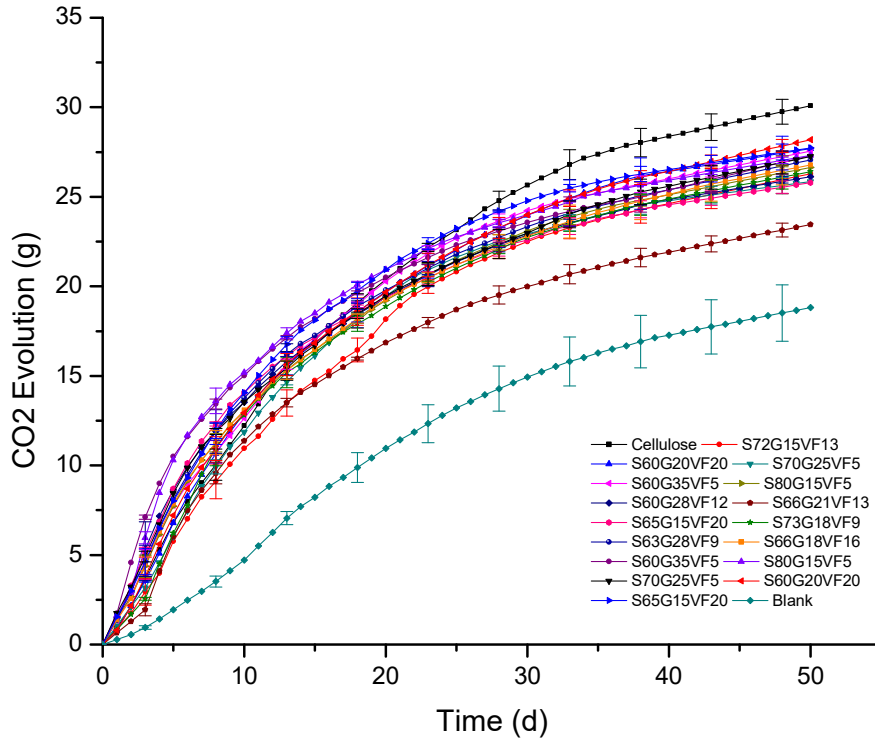
The biodegradation of thermoplastic cassava starch reinforced by vetiver fiber was investigated in test 4. The percentages of carbon content (Table 4.4) of all feedstocks were used to calculate the theoretical carbon dioxide evolution of each sample in the bioreactors. Table 4.14 presents a summary of the theoretical carbon dioxide evolution of the materials that were used in test 4.

Table 4.14 The amount of theoretical carbon dioxide evolution of each bioreactor of thermoplastic cassava starch reinforced by vetiver fiber

No	Materials	Average Weight (g)	Theoretical CO ₂ content (g)
1	S72G15VF13	8.0025	3.2066
2	S60G20VF20	8.0019	3.2232
3	S70G25VF5	8.0039	3.1799
4	S60G35VF5	8.0041	3.1752
5	S80G15VF5	8.0067	3.1859
6	S60G28VF12	8.0032	3.2013
7	S66G21VF13	8.0018	3.2031
8	S65G15VF20	8.0050	3.2268
9	S73G18VF9	8.0076	3.1958
10	S63G28VF9	8.0057	3.1903
11	S66G18VF16	8.0011	3.2124
12	S60G35VF5	8.0020	3.1744
13	S80G15VF5	8.0015	3.1838
14	S70G25VF5	8.0007	3.1787
15	S60G20VF20	8.0043	3.2241
16	S65G15VF20	8.0031	3.2260

The incubation period in this study was 50 days. The CO₂ evolution from each bioreactor is shown in Figure 4.9a. The maximum percentages of mineralization of a mixture of TPCS with different proportions of cassava starch, glycerol and vetiver fiber, and reference material in the manure compost were 65.5%, 78.6%, 70.1%, 86.2%, 71.9%, 75.6%, 56.6%, 80.2%, 70.0%, 80.2%, 70.8%, 88.5%, 87.4%, 75.8%, 79.3%, 83.6,% and 87.7% for S72G15VF13, S60G20VF20, S70G25VF5, S60G35VF5, S80G15VF5, S60G28VF12, S66G21VF13, S65G15VF20, S73G18VF9, S63G28VF9, S66G18VF16, S60G35VF5, S80G15VF5, S70G25VF5, S60G20VF20, S65G15VF20, and cellulose powder, respectively and are shown in Figure 4.9b. The differences of biodegradability of these thermoplastic cassava starch composites were generally not statistically significantly different. However, the biodegradation of S66G21VF13 was statistically significantly different from cellulose (Table 4.15). For the S66G21VF13 sample,

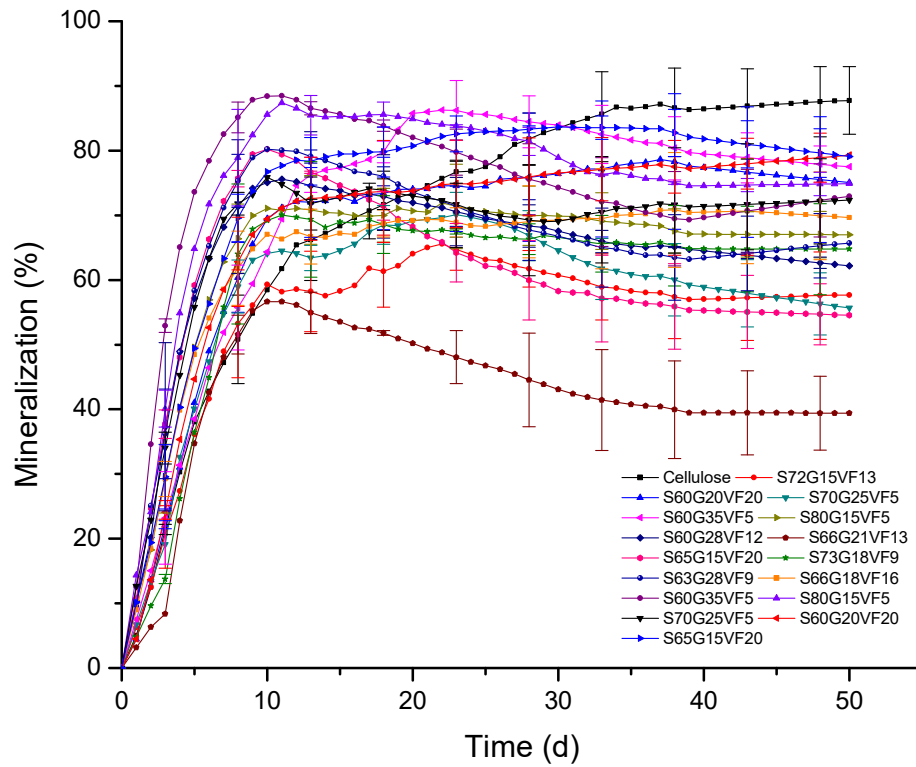
evolved carbon dioxide and % mineralization started decreasing around day 12. This may have occurred due to the dryness of the compost, which can reduce the activity of microbes and reduce the rate of biodegradability [7, 14, 15].



a)

Figure 4.9 Evolution of carbon dioxide (a) and mineralization curve (b) of the fourth test

Figure 4.9 (cont'd)



b)

The percent mineralization of thermoplastic cassava starch reinforced by vetiver fiber when it reached 70% and obtained the maximum degree of mineralization are shown in Table 4.15.

Table 4.15 The percent mineralization of thermoplastic cassava starch reinforced by vetiver fiber (test 4)

Sample	%Mineralization			
	At 70%	day	At Maximum	day
Cellulose 4th	70.66 ± 4.28	17	87.74 ± 5.23 ^a	50
S72G15VF13	65.55 ± 3.88	22	65.55 ± 3.88 ^{ab}	22
S60G20VF20	71.16 ± 6.92	11	78.64 ± 10.12 ^{ab}	37
S70G25VF5	70.07 ± 3.49	23	70.07 ± 3.49 ^{ab}	23
S60G35VF5	69.43 ± 0.22	11	86.25 ± 4.97 ^{ab}	22
S80G15VF5	69.90 ± 5.30	9	71.93 ± 6.71 ^{ab}	22
S60G28VF12	71.34 ± 10.35	8	75.57 ± 8.57 ^{ab}	11
S66G21VF13	56.64 ± 2.10	10	56.64 ± 2.10 ^b	10
S65G15VF20	72.21 ± 1.44	7	80.20 ± 1.14 ^{ab}	10
S73G18VF9	70.04 ± 10.45	11	70.04 ± 10.45 ^{ab}	11
S63G28VF9	71.18 ± 4.88	7	80.24 ± 2.98 ^{ab}	10
S66G18VF16	70.11 ± 8.34	35	70.66 ± 8.12 ^{ab}	43
S60G35VF5	73.63 ± 1.73	5	88.49 ± 1.56 ^a	11
S80G15VF5	71.76 ± 7.08	6	87.39 ± 1.26 ^{ab}	11
S70G25VF5	71.80 ± 1.77	8	75.84 ± 0.77 ^{ab}	10
S60G20VF20	71.14 ± 7.37	11	79.29 ± 3.74 ^{ab}	50
S65G15VF20	69.59 ± 3.66	8	83.64 ± 0.41 ^{ab}	30

* Different letter subscripts indicate significant differences ($p < 0.05$)

* Values: mean ± standard error

4.6.5 The relationship between composition of the thermoplastic cassava starch (TPCS) reinforced by vetiver fiber and biodegradability.

The results for biodegradability of the composite samples is presented in Table 4.16.

Table 4.16 Measured % mineralization of TPCS reinforced by vetiver fiber

Standard. order	Original Composition, wt. fraction			% mineralization	
	S	G	VF	Mean	S.E.
1	0.72	0.15	0.13	65.55	3.88
2	0.60	0.20	0.20	78.64	10.12
3	0.70	0.25	0.05	70.07	3.49
4	0.60	0.35	0.05	86.25	4.97
5	0.80	0.15	0.05	71.93	6.71
6	0.60	0.28	0.12	75.57	8.57
7	0.66	0.21	0.13	56.64	2.10
8	0.65	0.15	0.20	80.20	1.14
9	0.73	0.18	0.09	70.04	10.45
10	0.63	0.28	0.09	80.24	2.98
11	0.66	0.18	0.16	70.66	8.12
12	0.60	0.35	0.05	88.49	1.56
13	0.80	0.15	0.05	87.39	1.26
14	0.70	0.25	0.05	75.84	0.77
15	0.60	0.20	0.20	79.29	3.74
16	0.65	0.15	0.20	83.64	0.41

*The acronyms for S, G and VF refer to cassava starch, glycerol and vetiver fiber, respectively.

The steps of analysis were similar to the previous study in chapter 3. It was analyzed by using Design Expert software. The steps of analysis were: model fitting; analysis of variance (ANOVA) test; model diagnostics; and response surface graphs. To select the best-fit model, the various R^2 values for linear, quadratic, special cubic and cubic canonical polynomial models were compared and the model with the maximum value of Adjusted- R^2 and Predicted- R^2 values was chosen. Next, the number of model terms may be reduced based on the F-value by applying the backwards elimination technique in order to get the model terms, which provide maximum R^2 values. Backward elimination is the method for sequentially adding or removing variables. The advantage of this technique is that provides the opportunity to look at all independent variables in the model before removing variables that are not significant. To examine the influence of each

design points on the model, model diagnostics was carried out. Finally, the graph of the response surface of the selected model is presented.

Table 4.17 represents a summary of the statistics for the biodegradability model of TPCS reinforced by vetiver fiber. It shows that the quadratic canonical model is preferred and can better describe the response variations for design points than the other models. The model provides coefficient of determination values of 0.6867 and 0.5301 for R^2 and Adjusted- R^2 respectively.

Table 4.17 Biodegradability Model Summary Statistics

Source	Std.Dev.	R^2	Adjusted- R^2	Predicted- R^2	PRESS	remark
Linear	8.66	0.1139	-0.0224	-0.3526	1489.69	
Quadratic	5.87	0.6867	0.5301	0.1905	891.54	Suggested
Special Cubic	6.09	0.6971	0.4952	-0.0583	1165.51	
Cubic	6.41	0.7762	0.4405	-34.1155	38673.9	

After backward elimination was applied to the model, the models for both L-pseudo component coding and the actual component model in term of weight fractions were as follows:

$$\% \text{ Mineralization} = 79.5 x_1' + 89.1 x_2' + 100.3 x_3' - 43.4 x_1'x_2' - 83.3 x_1'x_3' - 88.7 x_2'x_3' \quad (\text{eq. 4-4})$$

$$(4.04) \quad (4.04) \quad (8.34) \quad (19.22) \quad (27.16) \quad (28.00)$$

where x_1' , x_2' and x_3' are the weight fractions of cassava starch, glycerol, and vetiver fiber, respectively. The standard errors of the parameter coefficients are shown in parentheses. The model is presented as a model for L-pseudo component coding with transformation formula as previously described in chapter 3. After transforming the formula for the actual component model, the values in terms of weight fractions in the composite became:

$$\begin{aligned} \% \text{ Mineralization} = & 157.1 x_1 - 700.0 x_2 + 1576.2 x_3 - 1084.6 x_1 x_2 - 2082.2 x_1 x_3 \\ & - 2216.8 x_2 x_3 \end{aligned} \quad (\text{eq. 4-5})$$

The ANOVA test results for the model significance and model terms are summarized in Table 4.18. The p-values of the components in the model are significant. The model gives a prediction of %mineralization with $R^2 = 0.6867$, Adjusted- $R^2 = 0.5301$, and Predicted- $R^2 = 0.1905$. The Predicted- R^2 value being much lower than the Adjusted- R^2 may indicate a block effect in the data. However, the adequate precision indicates the model can be used. The value of 6.449 adequate precision is greater than the suggested value of 4. Consequently, the p-value of lack-of-fit is insignificant so it can be concluded that the model can be used as the proposed model.

Table 4.18 The ANOVA-test summary statistics of % mineralization model

Source	Sum of Squares	df	Mean Square	F Value	p-value Prob > F	remark
Model	756.33	5	151.27	4.38	0.0225	significant
Linear Mixture	125.43	2	62.72	1.82	0.2121	
AB	175.72	1	175.72	5.09	0.0476	
AC	324.5	1	324.5	9.41	0.0119	
BC	345.92	1	345.92	10.03	0.01	
Residual	345	10	34.5			
Lack of Fit	200.21	5	40.04	1.38	0.3654	not significant
Pure Error	144.79	5	28.96			
Cor Total	1101.33	15				

A summary of the diagnostic case statistics for the mineralization model is presented in Table 4.19. This information were used to detect the outliers by determining of residual analysis and diagnostic plots. The residuals versus predicted values shows a random scatter throughout the data points. The plot should not show any sign of pattern. This means that the model is reliable and the assumptions for the ANOVA are not violated. This can be seen in Figure 4.10. It is

generally recommended that the internally studentized residual values should lie within the range of -3 to +3 and the externally studentized residual values should lie within the range of -3.5 to +3.5 indicating that there are no outliers in the dataset [75]. The value of the leverage point can have an effect on the estimate of regression coefficients. As a rule of thumb, the maximum leverage value is $2p/n$ where p is the number of model terms including the intercept and n is the number of experiments. In this case the leverage should not exceed $2(4)/16 = 0.5$. The leverage values in this study range from 0.173 to 0.473. In general, lower leverage values are preferred. In this case, leverage levels are not so high to cause a likelihood of inaccurate estimation of coefficients. Moreover, the difference in fits (DFFITS) and Cook's distance are used to detect the influential runs. As a general rule, DFFITS values outside of ± 2 should be a concern and Cook's distances that are greater than $4/n$, where n is the number of experiments, (in this case, $4/16 = .25$) may be problematic. Only the values of DFFITS and Cook's distances with asterisks exceed the suggested ranges of values, indicating that not all data points constitute the model evenly. Therefore, the diagnostic case statistics shows that the obtained model has properly met the criteria for a response surface model [17, 18] .

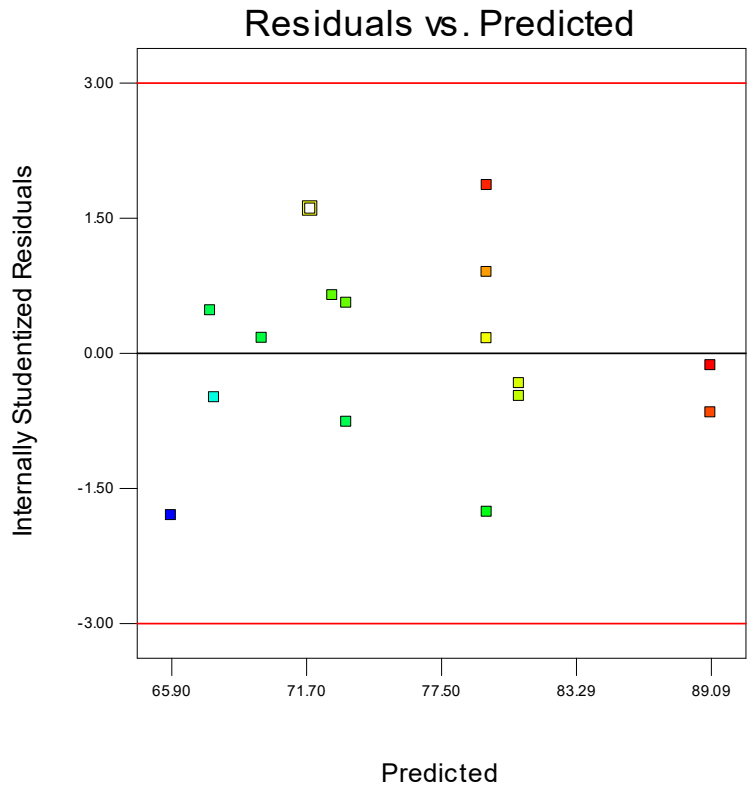


Figure 4.10 Residual vs predicted value

Table 4.19 The diagnostic case statistics for % mineralization model

Standard order	Actual value	Predicted value	Residual	Leverage	Internally studentized residual	Externally studentized residual	Influence on fitted value DFFITS	Cook's distance
1	65.55	67.76	-2.21	0.431	-0.498	-0.479	-0.417	0.031
2	78.64	80.86	-2.22	0.387	-0.483	-0.464	-0.369	0.025
3	70.07	73.44	-3.37	0.446	-0.771	-0.754	-0.677	0.08
4	86.25	89.09	-2.84	0.472	-0.666	-0.647	-0.612	0.066
5	71.93	79.47	-7.54	0.473	-1.77	-2.026	-1.92	0.469*
6	75.57	72.84	2.73	0.463	0.635	0.615	0.571	0.058
7	56.64	65.9	-9.26	0.239	-1.807	-2.089	-1.171	0.171
8	80.2	79.47	0.73	0.366	0.157	0.149	0.113	0.002
9	70.04	67.58	2.46	0.198	0.467	0.448	0.222	0.009
10	80.24	71.89	8.35	0.206	1.596	1.754	0.895	0.11
11	70.66	69.81	0.85	0.173	0.16	0.152	0.069	0.001
12	88.49	89.09	-0.6	0.472	-0.142	-0.134	-0.127	0.003
13	87.39	79.47	7.92	0.473	1.857	2.176	* 2.06	0.516*
14	75.84	73.44	2.4	0.446	0.55	0.529	0.475	0.041
15	79.29	80.86	-1.57	0.387	-0.342	-0.326	-0.259	0.012
16	83.64	79.47	4.17	0.366	0.892	0.882	0.67	0.077

* Exceeds limits

The contour plot and response surface plot based on the model for % mineralization are shown in Figure 4.11 and Figure 4.12, respectively.

Design-Expert® Software

Max % Min
● Design Points
88.49
56.64

X1 = A: Cassava Starch
X2 = B: Glycerol
X3 = C: Vetiver Fiber

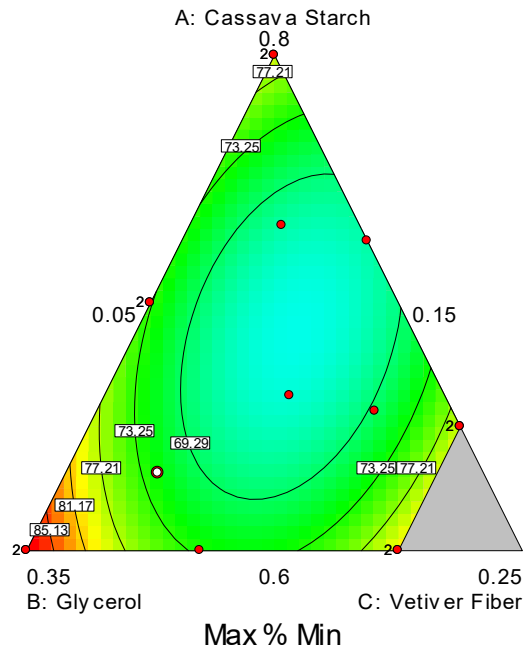


Figure 4.11 Contour plot of biodegradability

Design-Expert® Software

Max % Min
88.49
56.64

X1 = A: Cassava Starch
X2 = B: Glycerol
X3 = C: Vetiver Fiber

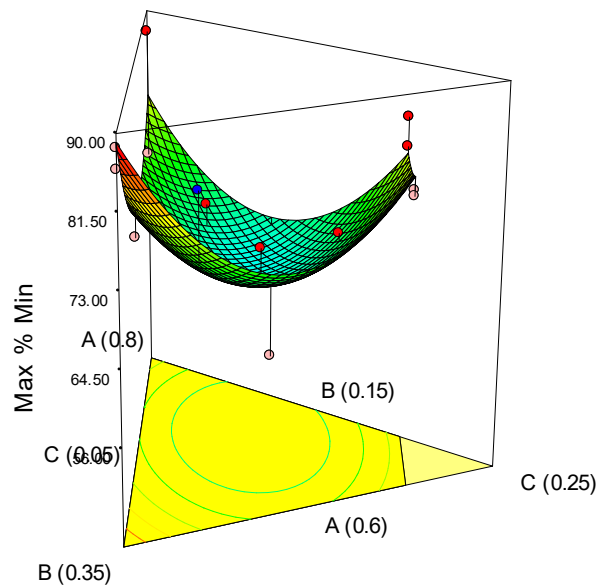


Figure 4.12 Response surface plot of biodegradability

4.7 Conclusions

The biodegradability of thermoplastic cassava starch reinforced by natural fibers was tested in a direct measurement respirometric (DMR) system under aerobic composting conditions related to the ASTM D5338 and IS 14855 standards. The variations of the degradation in the study can be attributed to the intrinsic properties of the compost used such as moisture content, temperature, pH and nutrients. Moreover, the polymer characteristics themselves play an important role in degradation. The assessment of the biodegradability under controlled composting condition showed that all of the thermoplastic cassava starch composite samples evaluated can be considered biodegradable polymers, because the percent mineralization of almost all test samples was greater than 70% in accordance with the ISO 14855 standards. In some cases, although the percent mineralization did not reach 70% (such as S69G24P7 in test 2 and S66G21VF13 in test 4), they were not statistically significantly different from the others in those same tests.

The relationship between composition of the thermoplastic cassava starch (TPCS) reinforced by vetiver fiber and biodegradability was observed using mixture design of experiments. A model was successfully obtained for biodegradability. The ANOVA test summary showed that the model was able to correlate to the biodegradability of component proportions.

Chapter 5

A preliminary life cycle assessment of thermoplastic cassava starch reinforced by vetiver fiber

5.1 Introduction

Biodegradable polymers in the packaging industry are gaining more importance than in the past, in efforts to find alternative materials to replace or reduce the use of petroleum-based polymers [1]. This can be seen in the report of the global consumption of biodegradable polymers by type for 2000 compared to 2005 (Table 5.1). In addition, Plastic Business reported that the trend of consumption of biodegradable polymer would be increasing in North America, Europe and Asia nearly 15 % during the five-year period ending in 2017, due to consumer pressure and legislation. The demand is expected to grow nearly 525,000 tons from the current 269,000 tons during that time frame [137].

Table 5.1 Global consumption of biodegradable polymers in 2000, 2005 and forecast for 2010 (tons) [138]

Materials	2000	2005	2010
Starch	15500	44800	89200
PLA	8700	35800	89500
PHA	0	200	2900
Synthetic	3900	14000	32800
Total	28100	94800	214400

Nowadays, one of the most promising natural materials, which could be improved and used as a biopolymer, is starch, which can be found in many types of starch plants such as corn, potato, wheat, cassava, etc. Among these starches, in tropical countries, the cassava plant is of considerable interest because it is inexpensive, abundant and renewable.

Moreover, a main benefit of using biopolymers is to have lower environmental impacts since it has the potential to reduce environmental pollution by being naturally biodegradable. However, it is not guaranteed that biopolymer will perform be favorable to petroleum-based polymers. Additional tools such as life cycle assessment (LCA) can be used to assess the environmental performance and sustainability of those polymers in order to compare or improve the environmental impacts.

Life Cycle Assessment (LCA) in accordance with ISO 14040/44 (ISO 2006) is used as a tool to quantify the environmental impacts of products. Inputs and outputs of the products are classified and converted to impacts in LCA studies. The environmental impacts can be classified into categories such as global warming potential, land occupation, ozone depletion potential, etc. Therefore, LCA has been used as a tool to evaluate the environmental impacts associated with the thermoplastic cassava starch composites, which are the main focus material of this study.

5.2 Methodology

This Life Cycle Assessment (LCA) study was conducted in accordance with the International Organization for Standardization (ISO) guidelines, which are defined in the ISO 14040 series framework [139]. According to this framework, the four-step LCA methodology involves: goal and scope definition, inventory (input and output analysis), impact assessment and interpretation of the results. The details can be found in Section 2.7.

5.2.1 Goal and scope definition

The goal of performing this Life Cycle Assessment (LCA) study was to quantify the environmental impacts of the two compounding formulations of thermoplastic cassava starch reinforced by vetiver fiber (TPCSV) biocomposite pellets produced using a three-piece mixer on a laboratory scale and to compare the environment impacts to granulated PLA biopolymer. This LCA study was also intended to provide data to support biopolymer product entrepreneurs using

it as an alternative material to increase the market opportunities and intended for LCA practitioners.

The two formulations of TPCSV biocomposite pellets were selected based on Section 3.5.5 in this study as shown in Table 5.2.

Table 5.2 Formulations of TPCSV biocomposite (%w/w)

Formulation No.	Cassava Starch	Glycerol	Vetiver Fiber
1	0.66	0.21	0.13
2	0.60	0.20	0.20

5.2.2 Scope of the study

This study was conducted as cradle-to-factory gate, using the attributional LCA approach and performed in accordance with the four-phase LCA methodology in ISO 14040 [139] and ISO 14044 [99].

5.2.2.1 Product system

The investigation of this product system included agricultural operations from cassava cultivation and vetiver cultivation through cassava starch production, vetiver fiber extraction and production of thermoplastic cassava starch biocomposite pellets. In this study, cassava starch, glycerol and vetiver fiber were used as feedstocks to produce thermoplastic cassava starch reinforced by vetiver fiber. This study only investigated the process of TPCSV biocomposite pellets as mentioned above. Agricultural land occupation, transportation, end-of-life and disposal stages were not taken into account.

5.2.2.2 Functional unit

The functional unit of this study is 1 kg of pellets of thermoplastic cassava starch reinforced by vetiver fiber.

5.2.2.3 System boundary and definitions

The life cycle assessment of biocomposite pellets of thermoplastic cassava starch reinforced by vetiver fiber was investigated as cradle-to-factory gate, following the ISO 14040 standard for LCA. The cradle is determined as the raw materials used for all processes while the factory gate is determined as a finished product or biopolymer pellet or resin. The system boundary of the production of thermoplastic cassava starch biocomposite included materials, energy inputs, and environmental outputs associated with the production of these biocomposites. The system boundary from cradle-to-factory gate for thermoplastic cassava starch biocomposite pellets is shown in Figure 5.1. The inventory data for extraction of glycerol, fertilizer and herbicide processes, the dashed lines, used inventory information from existing data from the ecoinvent database (version 2.0). As mentioned earlier, land occupation, human labor, transportation, end of life scenarios and disposal stages were not considered in this study.

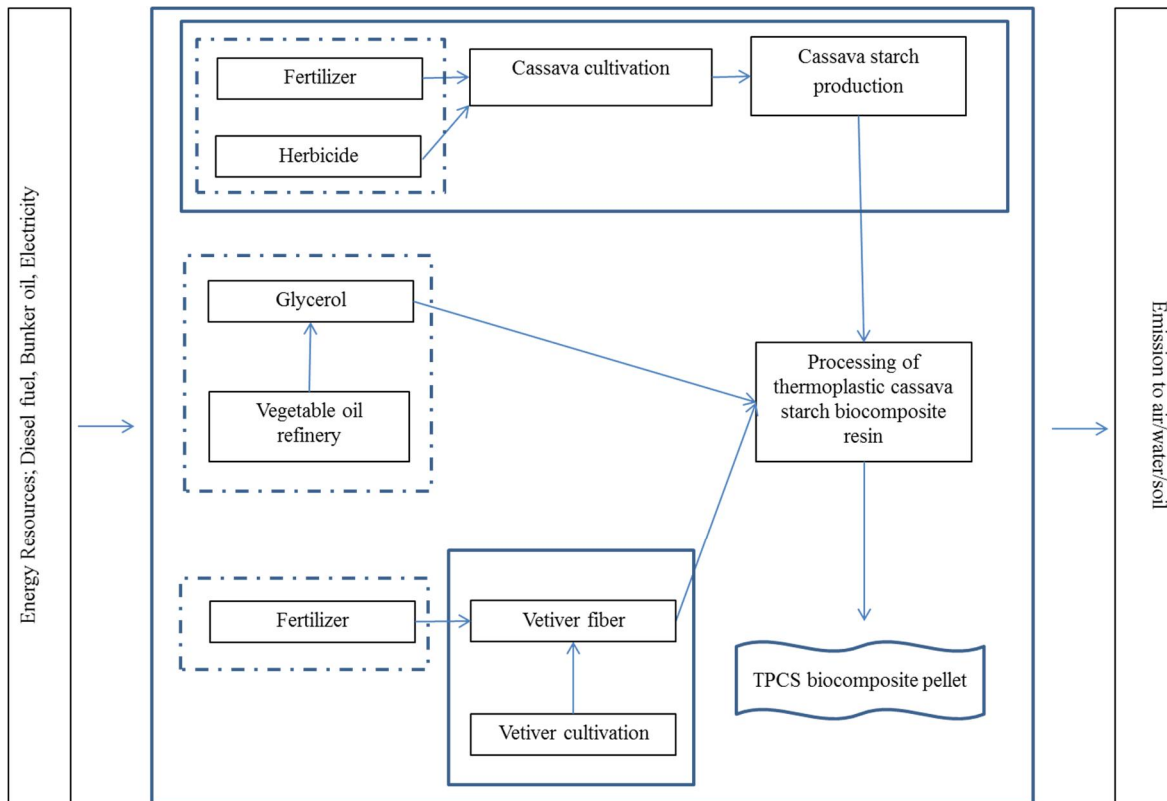


Figure 5.1 Thermoplastic cassava starch composite pellet system boundary

The product definitions for each unit process in the system boundary are as follows;

Cassava cultivation. This step included land preparation, planting, fertilization, and harvesting. Usually cassava responds well to N, P and K fertilization. Cassava is planted using stems. Each stem is at least 20-25 cm long with about 5-8 nodes and is pressed into the soil, one stem for every 1 m². Time to harvest is usually 8-12 months. Background information on this stage was obtained from various sources, which included information on inputs such as fuel, labor, and agrochemical materials.

Cassava starch production. Cassava roots are processed within 24 hours. Roots are washed and screened of dirt and then transferred to a chopper process where they are cut into 1-2 cm. chunks and fed into a saw-tooth rasper to make a pulpy slurry. This slurry is sent to a decanter to separate the water and pumped through a set of coarse and fine extractors to get starch clumps.

The residue pulp is separated as cassava pulp. After separation, the water in the starch clumps is eliminated in a dewatering process and the clumps next are dried to a moisture content of about 13% before packing.

Vetiver grass cultivation [134, 135]. Planting of vetiver grass should start early in the rainy season when the soil has been moistened. Vetiver grass is propagated generally by root division or slips. Usually 2-3 slips are planted in each grouping close together about 8-10 cm. The plants often grow 2 meters in height in a few months. For this process, the data included land preparation, planting, and harvesting. Irrigation and seeds were not included.

Vetiver fiber production. The production of vetiver fiber was carried out on a laboratory scale in a system designed by the Department of Printing and Packaging, King Mongkut's University, Thailand. The conditions were as follows: vetiver grass was cut into small pieces and dried under sunlight. Then the vetiver grass pulp was produced using a chemical pulping process with sodium hydroxide at 15%w/w of sodium hydroxide to vetiver grass (oven dry weight). Pulping was carried out at 150 °C in a closed chamber system for 4 hours. The cooking pulp was washed with water several times to a neutral pH. The pulp was dispersed in a standard pulp disintegrator for 10 minutes, which disintegrated the bundles of pulp into single fibers. The vetiver fibers produced were used as a raw material for the production of thermoplastic cassava starch biocomposite pellets.

Thermoplastic cassava starch compounding. In this unit, cassava starch, glycerol, and vetiver fiber were received as raw materials. They were dry mixed in a plastic bag according to the formulations in Table 5.2. Then, they were put into a three-piece internal mixer equipped roller mixing blades (C.W.Brabender Instruments, Inc., South Hackensack, NJ) and a 5.6 kilowatt (7.5 hp) Intelli-Toque Plasti-Corder Torque Rheometer® (C.W.Brabender Instruments, Inc., South Hackensack, NJ) for 3 minutes at a sample charge weight of 30 grams. After melt blending in the

three-piece mixer, the blended sample was cooled and granulated using a cutting tool to transform the compound to pellets.

5.2.2.4 Allocation

According to ISO 14044, allocation should be avoided if possible through system expansion. However, if this is not possible, allocation should be considered. The ISO standard recommends that allocation should be based on physical characteristics such as mass, energy content, or economic value. In this study, allocation of the environmental impacts between the primary product and byproducts are an important concern. In this attributional life cycle analysis (ALCA), the allocation method for cassava starch production was based on the market value and mass. A sensitivity analysis was conducted to evaluate the effect of differences between allocation methods.

5.2.2.5 Data requirement and quality

The inventory data for thermoplastic cassava starch composite pellets were quantified or derived using values from numerous literature sources to complete the life cycle inventory, such as journal articles, government reports, theses, websites and commercial databases. Data were gathered for cassava cultivation through cassava starch plant production and vetiver cultivation through vetiver fiber production. For the compounding step, firsthand data for energy consumption were gathered using primary data from Section 3.3.2.3 for laboratory scale manufacture of the two TPCS biocomposites. For glycerol and fertilizer production, data were obtained from commercial databases. All transportation was excluded from the system boundary due to the limitations on acquiring the materials to produce the prototype biocomposite pellets for this study. Table 5.3 shows the data in relation to time, geographical and technological coverage and data requirements.

Table 5.3 The summary of data quality and requirements

Life cycle stage	Data required	Data source and Time related coverage	Geographical coverage	Technological coverage
Energy resources	Diesel fuel Natural gas Electricity Coal	2000, US-EI	U.S.	Current
Vegetable oil production	Glycerol	2000, USLCI/US-EI	U.S.	Current
Raw materials	Fertilizer Herbicide	2000, LCA Food DK, Ecoinvent	U.S.	Current
Cassava cultivation	Fuel Fertilizer Herbicide	Literature based, estimation [142–150]	Asia	Current
Vetiver cultivation	Fertilizer	Literature based[151–153]	Asia	Current
Vetiver fiber production	Natural gas water	Literature based, Estimation [154]	Asia	Current
Cassava starch production	Water Cassava root Electricity Fuel Sulfur	Literature based[142, 144, 148, 155, 156]	Asia	Current
TPCS biocomposite production	Electricity	In-house data, estimation	U.S.	Current

5.3 Inventory analysis and assessment

SimaPro 7.3.3 software with CML 2 baseline 2000 method was used as a tool to provide industrial data and determine the environmental impacts of a process or product. This software contains a variety of inventory databases for many materials including energy usage and emissions. The CML 2 baseline 2000 method is embedded into the SimaPro 7.3.3 software that was used for the thermoplastic starch biocomposite pellets. The required data that were not included in the SimaPro 7.3.3 software were obtained from literature sources.

5.4 Impact assessment and methodology

The process of impact assessment in LCA involves classification and characterization, normalization and evaluation. In this study, the CML 2 baseline 2000 method was employed for the impact assessment step. This approach is used for the midpoint impact assessment.

There are five impact categories that are considered in this study: abiotic depletion potential (ADP), acidification potential (AP), eutrophication potential (EP), global warming potential (GWP) and ozone depletion potential (ODP). The classification and characterization factors can be seen in Table B.1. The reasons related to these environmental impacts are as follows.

The use of fertilizers such as N, P and K for cassava and vetiver cultivation can result in mineral run off, which will cause environmental impacts such as abiotic depletion potential, acidification potential and eutrophication potential, Moreover, the emissions from energy or power used in the agricultural equipment and the production of fertilizer and pesticides can generate greenhouse gases causing global warming/climate change effects.

For cassava starch production, vetiev fiber production and thermoplastic cassava starch compounding, there are environmental issues due to energy use and the associated emissions such as CO, NO_x and SO_x etc. These will cause environmental impacts in global warming potential, ozone depletion potential, and human toxicity.

5.5 Assumptions and limitations

In this study, there were various limitations based on available sources of data. Some of limitations have been shown as assumptions as follows:

The processes of cassava cultivation, starch production, vetiver cultivation, and vetiver fiber making were included in this LCA study. Resources such as infrastructure, machinery and labor were not included in the system boundary due to the assumption that the infrastructure, machinery and labor are usually common in the production site.

After cassava plantation and vetiver grass harvesting, the rest of the plants (branches and leaves) are left in the field to prepare the seed bed. Impacts associated with this practice were not included.

In terms of plant cultivation, there was no data on soil quality before and after cassava or vetiver plantation. In addition, irrigation was not included in the study. It was assumed the plants were grown in normal conditions where irrigation is not needed.

This LCA study was not able to specify the geographical location and amount of land used, because the study used data from numerous literature sources involving various locations of cassava and vetiver cultivation. The data used were mainly from Asia countries such as Thailand, Vietnam, and China but also included Europe and elsewhere.

The raw material extraction for the production of glycerol, fertilizer, pesticide and polylactic acid (PLA) was based on secondary LCI data sources as shown in Table 5.4.

In the processing stage of cassava starch production and vetiver fiber making, the waste water is assumed to be released to the environment without further treatment. In addition, the cassava pulp, which is left from the cassava starch production, will be used as animal feed or discarded as organic waste. No associated burdens were included.

The preliminary study of comparative LCA of thermoplastic cassava starch composite pellets were manufactured at the lab scale, and it should be noted that the results of this study might not apply in individual cases, as these may differ from the situation analyzed here.

5.6 Cut-off criteria

In this study, cut-off was applied in case of input and output flows less than 1 % of the cumulative mass and energy of all the inputs and outputs in each unit process. Therefore, some environmental effects were excluded from the study on the assumption that the environmental impacts were minor.

5.7 Interpretation

This is the final phase of a life cycle assessment study, which comes after the impacts are assessed. The conclusion and recommendation are drawn from the results of the impact assessment.

5.8 Results and interpretation

5.8.1 Life cycle inventory analysis

The input and output data for thermoplastic cassava starch reinforced by vetiver fiber are presented in order to quantify raw materials, energy and waste or other releases from the products.

5.8.1.1 LCI of the production of thermoplastic cassava starch reinforced vetiver fiber resin.

The LCI for the production of pellets of thermoplastic cassava starch reinforced by vetiver fibers is composed of five major processes: cassava cultivation, cassava starch production, vetiver cultivation, vetiver fiber production and the polymer compounding process, as shown in Figure 5.1. The inventory analysis for cassava cultivation, cassava starch production, vetiver cultivation and vetiver fiber production is presented in Table B.2-B.5.

Table 5.4 presents the life cycle inventory for the production of the two thermoplastic cassava starch biocomposite formulations at the laboratory site. They are composed of cassava starch, glycerol and vetiver fiber in different proportions. The two formulations were selected based on their performance as described in section 3.5.5. The processes for production of the two formulations of thermoplastic cassava starch reinforced vetiver fiber resin are shown in Figure 5.2 and Figure 5.3.

In the production of thermoplastic cassava starch biocomposite pellets, the two formulations used total energy of about 75.2 MJ for manufacturing on a laboratory scale. Among the processes, compounding is the most energy-consuming step, which is about 74.6% (15.57/20.88) of the total energy demand. Electricity is a major input that is used for drying raw materials and blending of the fibers to obtain uniform mixing and beating to increase separation of the individual fibers. This compounding process generates about 2% of waste product, which could be disposed of or recycled. There are some emission outputs in the processing step such as

CO₂, etc. due to the heat from the internal mixer and compression molding but they were not investigated in the laboratory scale manufacturing operation.

Table 5.4 Life cycle inventory of 1 kg of TPCSV biocomposite pellet

Input	Unit	Quantities per 1 kg	
		Formulation 1	Formulation 2
Materials			
Cassava starch	kg	0.66	0.60
Glycerol	kg	0.21	0.20
Vetiver fiber	kg	0.13	0.20
Electricity			
Raw material processing			
Starch preparation	kWh (MJ)	0.17 (0.62)	0.17 (0.62)
Fiber preparation	kWh (MJ)	0.37 (1.35)	0.37 (1.35)
Total	kWh (MJ)	0.54 (1.97)	0.54 (1.97)
Biocomposite processing			
Drying	kWh (MJ)	4.89 (17.6)	4.89 (17.6)
Blender	kWh (MJ)	0.42 (1.51)	0.42 (1.51)
Compounding	kWh (MJ)	15.57 (56.10)	15.57 (56.10)
Total	kWh (MJ)	20.88 (75.20)	20.88 (75.20)
Total energy	kWh (MJ)	21.42 (77.17)	21.42 (77.17)
Output			
Products			
TPCS composite resin	kg	1.00	1.00
Soild Waste	kg	0.02	0.02

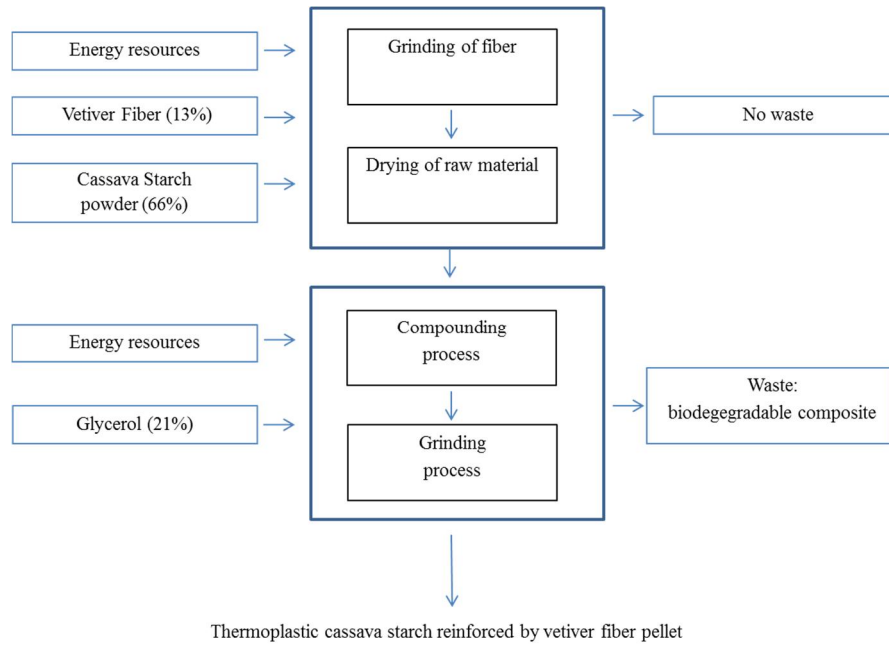


Figure 5.2 The process of the production of thermoplastic cassava starch reinforced vetiver fiber resin for formulation 1

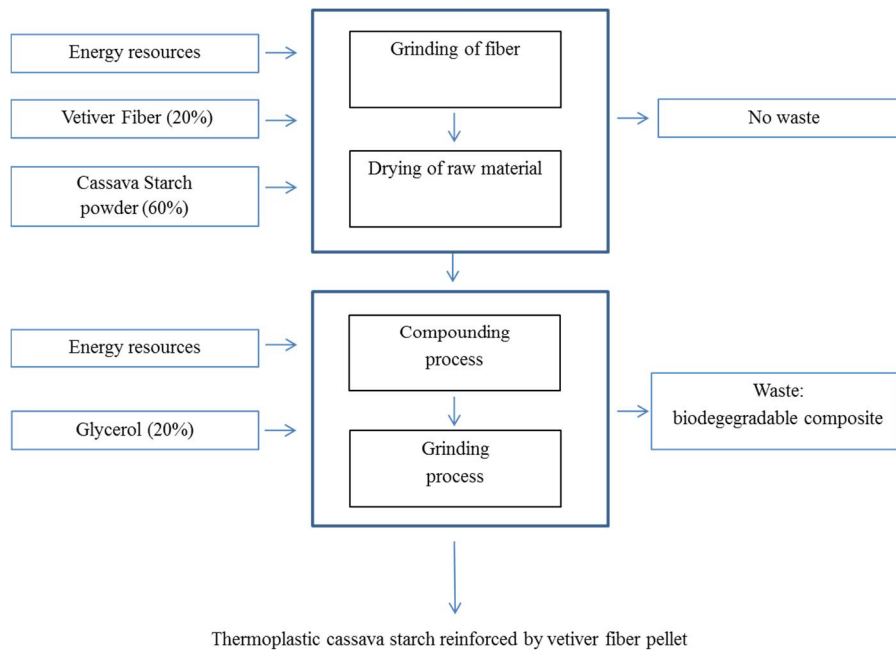


Figure 5.3 The process of the production of thermoplastic cassava starch reinforced vetiver fiber resin for formulation 2

5.9 Life cycle impact assessment (LCIA)

The inventory data were converted to the five potential environmental impacts in the impact assessment to make this data more useable. The potential environmental impacts were considered based on the midpoint method and included classification and characterization steps. The results are based on a functional unit of 1 kg TPCSV biocomposite. The five potential environmental impacts that were chosen as indicators were: abiotic depletion potential (ADP), acidification potential (AP), eutrophication potential (EP), global warming potential (GWP) and ozone depletion potential (ODP). These abbreviations are used to ease the presentation in the graph. Table 5.5 shows the environmental impact categories.

Table 5.5 Considered environmental impact categories on this study

Impact categories	Unit
Abiotic Depletion Potential (ADP)	kg Sb-Equiv.
Acidification Potential (AP)	kg SO ₂ -Equiv.
Eutrophication Potential (EP)	kg Phosphate-Equiv.
Global Warming Potential (GWP)	kg CO ₂ -Equiv.
Ozone Layer Depletion Potential (ODP)	kg CFC-11 Equiv.

5.9.1 Characterization

5.9.1.1 Formulation 1

The results for the LCIA of formulation 1, based on the functional unit of 1 kg TPCSV biocomposite resin, are presented in Table 5.6.

Table 5.6 Summary of LCIA for formulation 1 of TPCSV biocomposite pellet production

TPCSV 1kg	ADP	AP	EP	GWP	ODP
Charaterization / Unit	kg Sb eq	kg SO ₂ eq	kg PO ₄ eq	kg CO ₂ eq	kg CFC-11 eq
Cassava starch production	2.73E-03	3.31E-03	6.08E-03	5.61E-01	1.89E-07
Glycerine	2.54E-03	3.76E-03	3.21E-04	5.86E-01	4.29E-10
Vetiver fiber production	3.30E-03	2.12E-03	4.27E-04	2.57E-01	3.83E-07
Electricity	1.14E-01	1.50E-01	5.38E-03	1.62E+01	1.31E-10
Total	1.22E-01	1.59E-01	1.22E-02	1.76E+01	5.73E-07
Normalization	ADP	AP	EP	GWP	ODP
Cassava starch production	1.84E-13	1.21E-13	4.88E-13	1.17E-13	2.27E-15
Glycerine	1.71E-13	1.38E-13	2.57E-14	1.22E-13	5.15E-18
Vetiver fiber production	2.22E-13	7.76E-14	3.43E-14	5.35E-14	4.59E-15
Electricity	7.67E-12	5.49E-12	4.31E-13	3.37E-12	1.57E-18
Total	8.25E-12	5.83E-12	9.79E-13	3.66E-12	6.87E-15

One of the aims of this study was to identify the processes, materials and stages in the product life cycle that have the largest contribution to the environmental impacts or have the potential to improve that product system. According to Table 5.5, formulation 1, which is composed of 66% cassava starch, 24% glycerol and 10% vetiver fiber, requires about 77.2 MJ of total energy per kilogram of TPCSV biocomposite on a life cycle basis. About 73% of this energy was used in the compounding process, 23% for drying of raw materials and 4% for mixing in the blender. In order to evaluate the environmental loads of TPCSV composite of formulation 1 from cradle-to-gate, the contribution of all unit processes to the overall impacts is presented in Figure 5.4 and Table 5.6. Electricity, more than 80 %, is shown as the most significant factor that affects the impact categories, especially abiotic depletion, acidification and global warming potential. However, for eutrophication and ozone layer depletion, cassava starch production and vetiver fiber

production were found to be the dominant processes that significantly contribute to those impact categories.

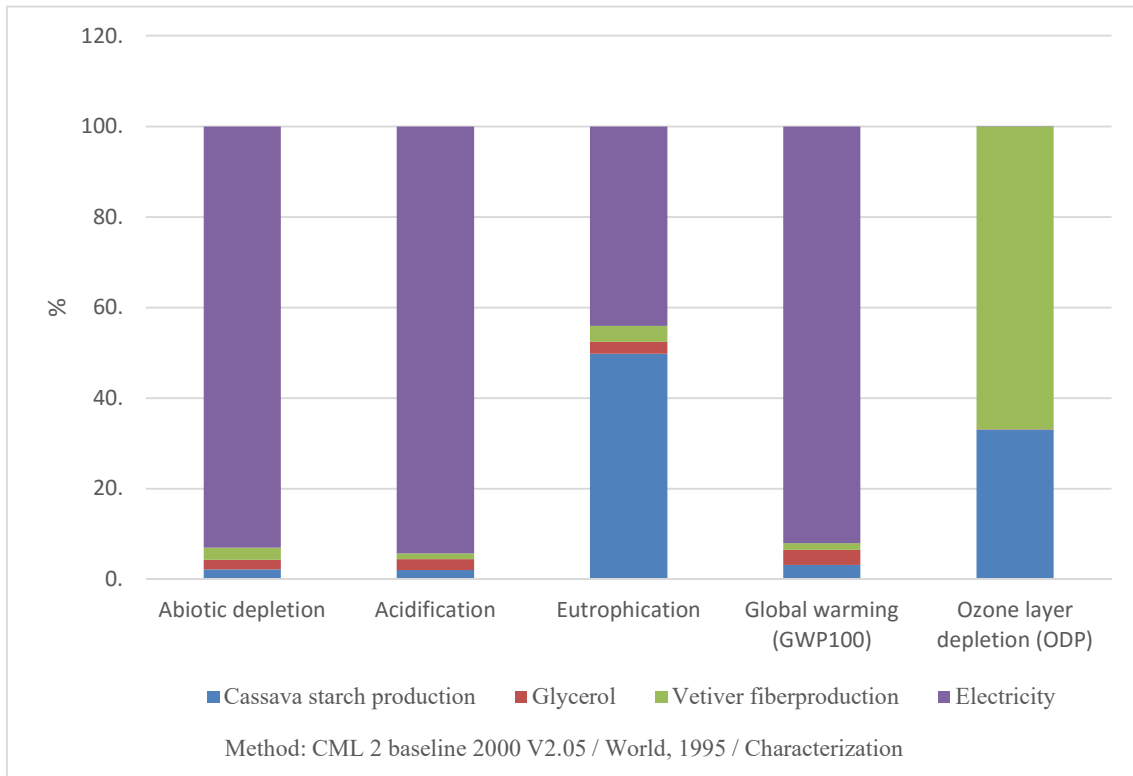


Figure 5.4 Characterization of LCIA profile for formulation 1 (unit 1 kg pellet of TPCSV)

5.9.1.2 Formulation 2

Formulation 2, which is composed of 63% cassava starch, 17% glycerol and 20% vetiver fiber, requires 77.2 MJ of total energy per kilogram of TPCSV biocomposite, which is the same as for Formulation 1. Table 5.7 shows the results of the LCIA of formulation 2, which is based on the functional unit of 1 kg TPCSV biocomposite resin. Electricity was found to be the dominant process that significantly contributed 90% of impacts for abiotic depletion, acidification and global warming. Vetiver fiber production was found to be dominant, contributing 80%, for ozone layer depletion. Cassava starch production was the main process, causing about 47 % of impacts, for eutrophication. Figure 5.5 presents a graphical view of the LCIA profile for formulation 2.

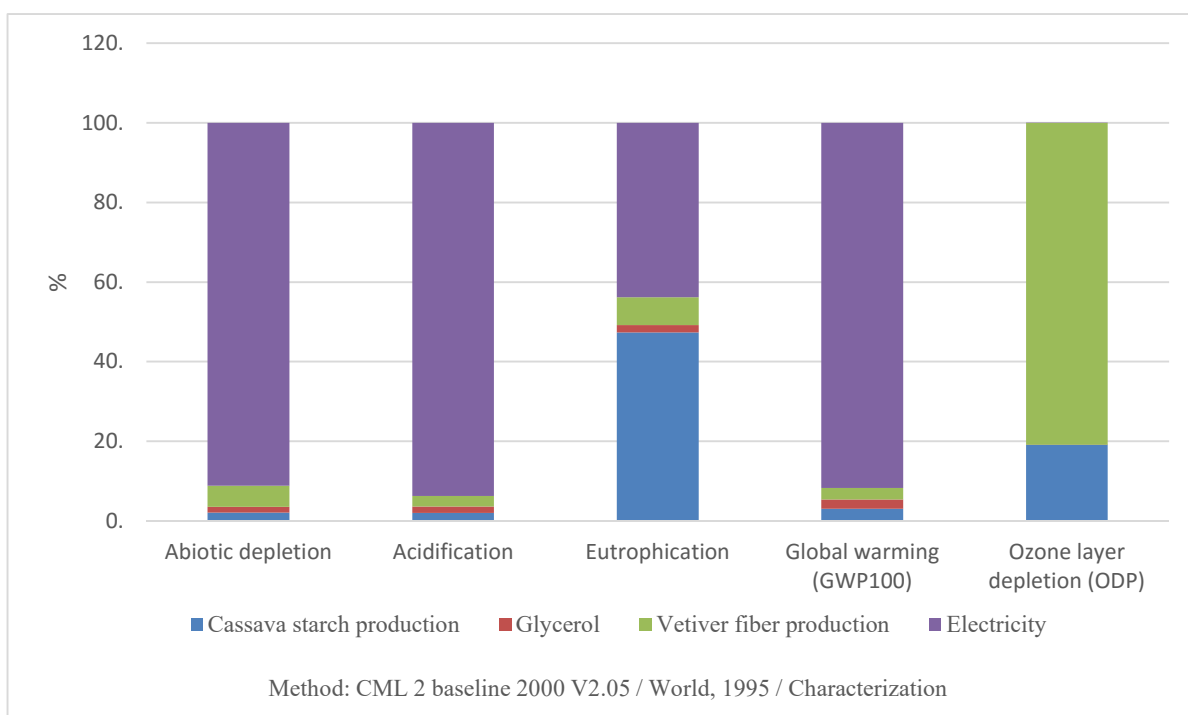


Figure 5.5 Characterization of LCIA profile for formulation 2 (unit 1 kg pellet of TPCSV)

Table 5.7 Summary of LCIA for formulation 2 of TPCSV biocomposite pellet production

TPCSV 1kg	ADP	AP	EP	GWP	ODP
Charaterization / Unit	kg Sb eq	kg SO ₂ eq	kg PO ₄ eq	kg CO ₂ eq	kg CFC-11 eq
Cassava starch production	2.60E-03	3.16E-03	5.81E-03	5.35E-01	1.81E-07
Glycerine	1.80E-03	2.66E-03	2.27E-04	4.15E-01	3.04E-10
Vetiver fiber production	6.60E-03	4.24E-03	8.55E-04	5.14E-01	7.65E-07
Electricity	1.14E-01	1.50E-01	5.38E-03	1.62E+01	1.31E-10
Total	1.25E-01	1.60E-01	1.23E-02	1.77E+01	9.46E-07
Normalization	ADP	AP	EP	GWP	ODP
Cassava starch production	1.75E-13	1.16E-13	4.66E-13	1.11E-13	2.17E-15
Glycerine	1.21E-13	9.75E-14	1.82E-14	8.63E-14	3.65E-18
Vetiver fiber production	4.45E-13	1.55E-13	6.86E-14	1.07E-13	9.18E-15
Electricity	7.67E-12	5.49E-12	4.31E-13	3.37E-12	1.57E-18
Total	8.41E-12	5.86E-12	9.84E-13	3.67E-12	1.14E-14

5.9.1.3 Comparative LCIA of the two biocomposite formulations

The characterization results of the impact assessment for cradle-to-factory gate of the two formulations of TPCSV biocomposite pellets are presented in Figure 5.6. Formulation 1 gives similar environmental performance in most impact categories to formulation 2 except ozone layer depletion (ODP) impact due to less vetiver fiber in formulation 1.

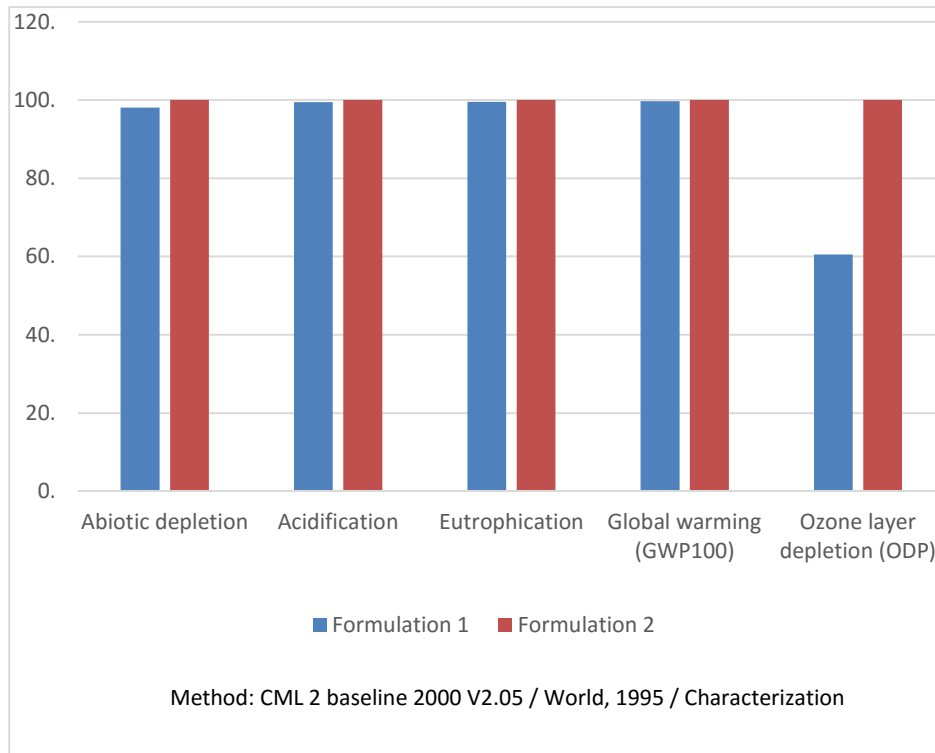


Figure 5.6 Comparing LCIA of Formulation 1 and Formulation 2

The Global Warming Potential (GWP) comparison of TPCSV biocomposite pellets of formulation 1 and formulation 2 is shown in Figure 5.6. The primary gases that contribute to the global warming potential are carbon dioxide (CO₂), methane (CH₄), nitrous oxide (N_xO) and volatile organic compounds (VOCs). The total GWP of formulation 1 (1.76E+01 kg CO₂ eq.) is essentially the same as formulation 2 (1.77E+01 kg CO₂ eq.). The process that contributed most to global warming potential was the electricity unit process, followed by glycerol and cassava starch production. The vetiver fiber production process contributed less.

The total abiotic depletion potential (ADP) comparison of TPCSV biocomposite pellets of formulation 1 and formulation 2 is shown in Figure 5.6. Abiotic depletion is the term that is used for resource depletion due to the consumption of resources. Usually, this impact category refers to the depletion of non-renewable resources such as fossil fuels, minerals and metals, etc. The reference unit for abiotic depletion is antimony (Sb) or kg Sb equivalent. The results for ADP show that formulation 1 (1.22E-01 kg Sb eq.) is slightly lower than formulation 2 (1.25E-01 kg Sb eq.). The most important process contributing to the abiotic depletion potential was electricity; next were vetiver fiber production and cassava starch production. Glycerol production had the least impact.

For the total acidification potential (AP), the main contributions to acidification potential were nitrogen oxide (NO_x), sulfur dioxide (SO₂) and ammonia (NH₃). The results of AP are from fuel consumption and sulfur consumption in cassava starch production. Comparison of total acidification potential between formulations 1 and formulation 2 showed that the AP of formulation 1 (1.59E-01 kg SO₂ eq.) was about the same as formulation 2 (1.60E-01 kg SO₂ eq.). The main process that contributed to acidification potential was electricity, followed by vetiver fiber production.

For the total eutrophication potential (EP), the main contributions in this impact category were nitrous oxide (N₂O), phosphate (PO₄), nitrate (NO₃), nitrogen dioxide (NO₂) and chemical oxygen demand (COD) associated with nutrient enrichment such as fertilizer and with pesticide production. In comparison of total EP between formulations 1 and formulation 2, the impact of the EP of formulation 2 (1.23E-02kg PO₄ eq.) was approximately the same as formulation 1 (1.22E-02 kg PO₄ eq.). The most important process contributing to eutrophication potential was cassava starch production, followed by electricity.

The total ozone depletion potential (ODP) was calculated using the contribution of trichlorofluoromethane (CFC-11), chlorofluorocarbons and other volatile organic compounds. The comparison of ODP between formulation 1 and formulation 2 revealed that the ODP of formulation 2 (7.65E-07 kg CFC-11 eq.) was higher than formulation 1 (3.83E-07 kg CFC-11 eq.). The most important process contributing to ozone depletion potential was vetiver fiber production, followed by cassava starch production.

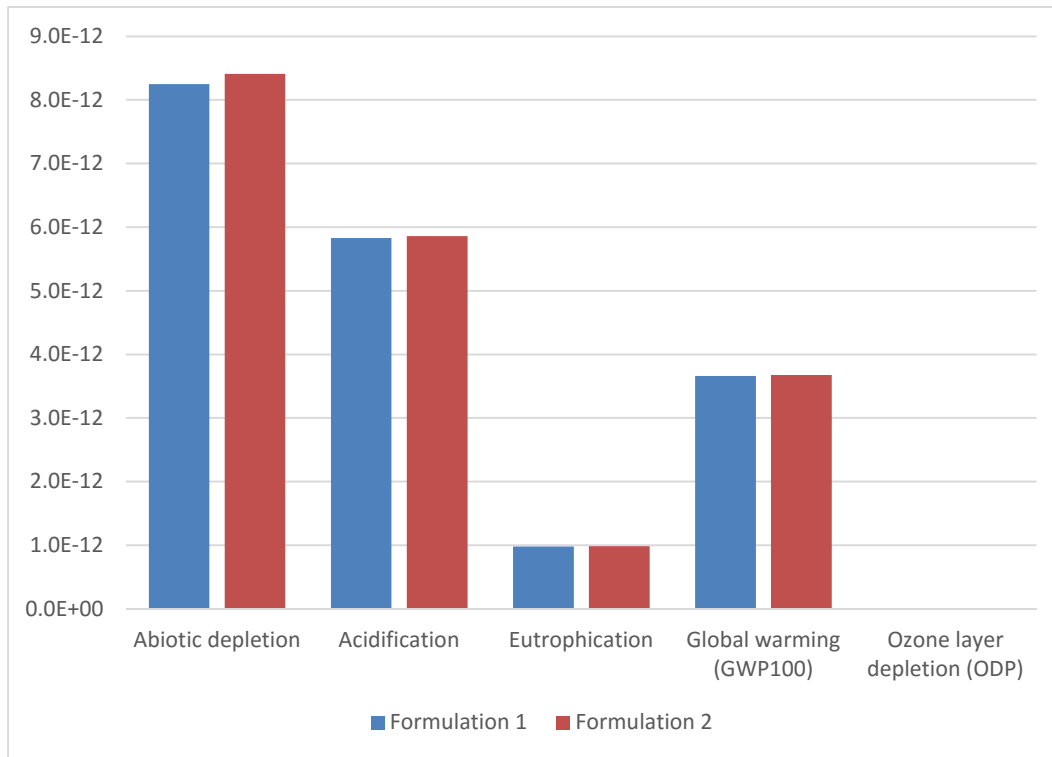
5.9.2 Normalization

The normalization value from the characterization step allows the impact category results to be compared relative to a reference baseline. After normalization, all impact indicators obtain the same unit. This study used CML 2 baseline 2000 V2.04 with World 1995 [94,99], which is a commonly used as a normalization reference system. This means the total annual emissions or resources use in the world for the given year 1995 are selected as the reference value [100].

The environmental impact results for the two formulations of TPCS biocomposite pellets are illustrated in Table 5.8 and Figure 5.7. Figure 5.7 shows a graphical view of the normalized impact assessment results. There were no significant differences in the normalized results for these biocomposite pellets. There were slight differences in most categories but not enough to be significant.

Table 5.8 Normalized LCIA profiles for formulation 1 and formulation 2 of TPCS biocomposite pellets

Impact category	Formulation 1	Formulation 2
Abiotic depletion	8.25E-12	8.41E-12
Acidification	5.83E-12	5.86E-12
Eutrophication	9.79E-13	9.84E-13
Global warming (GWP100)	3.66E-12	3.67E-12
Ozone layer depletion (ODP)	6.87E-15	11.40E-15



Method: CML 2 baseline 2000 V2.05 / World, 1995 / Normalization

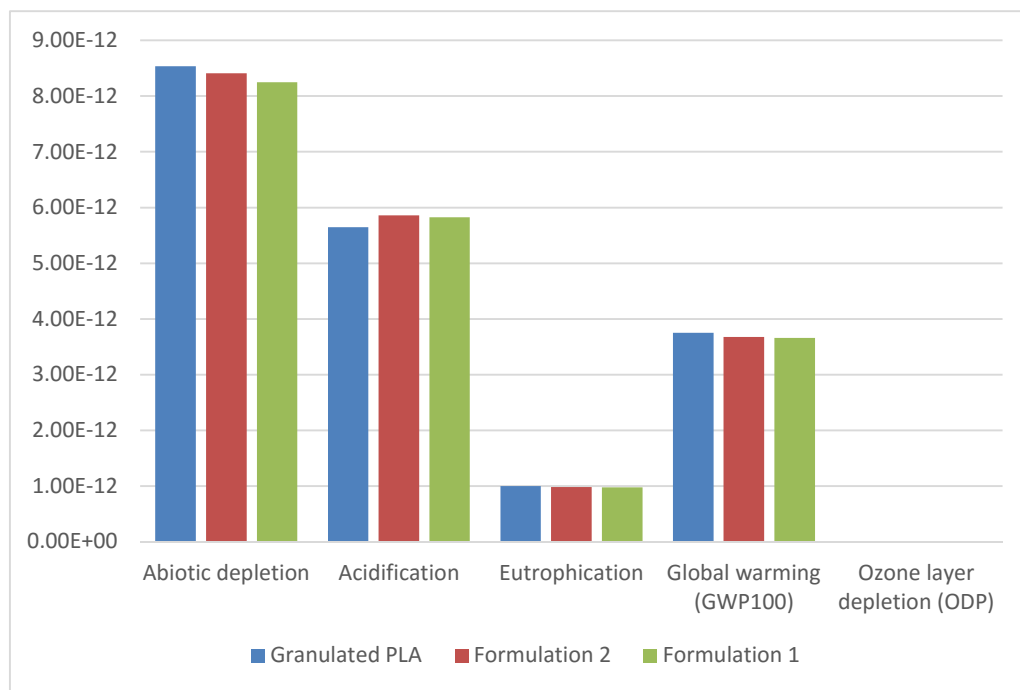
Figure 5.7 Normalized LCIA profiles for formulation 1 and formulation 2 of TPCS biocomposite pellets

5.9.3 Comparative LCIA of the two biocomposite formulations against granulated polylactide (PLA)

The life cycle impact assessments of the biocomposite pellets were compared with a commercial biopolymer, granulated polylactide (PLA) from NatureWorks, for which data are available in the ecoinvent database. A comparison of normalized values for the two formulations of the biocomposites against granulated polylactide (PLA) biopolymer are presented in Table 5.9 and Figure 5.8. The two biocomposite formulations performed slightly better than granulated polylactide in all the environmental impact categories except acidification potential and ozone layer depletion potential, but not enough to be significant.

Table 5.9 Environmental impacts of the two formulations and PLA (production value per functional unit)

Impact category	Granulated PLA	Formulation 2	Formulation 1
Abiotic depletion	8.54E-12	8.41E-12	8.25E-12
Acidification	5.65E-12	5.86E-12	5.83E-12
Eutrophication	10.00E-13	9.84E-13	9.79E-13
Global warming (GWP100)	3.75E-12	3.67E-12	3.66E-12
Ozone layer depletion (ODP)	2.64E-15	11.40E-15	6.87E-15



CML 2 baseline 2000 V2.05 / World, 1995

Figure 5.8 Environmental impacts of the two formulations and PLA based on normalization

5.10 Sensitivity analysis

The sensitivity analysis examines changes resulting from assumptions that may affect the results of the study. It aims to assess the reliability of the results. In this study, cassava starch production has byproducts, which are cassava peel, cassava root, cassava pulp and sand, as shown in Table 5.10. The main product in cassava starch production is to obtain cassava starch, which is more expensive than co-products. Therefore, economic allocation was used as the default approach. In the case of mass allocation, the environmental impact will be apportioned among the main products and co-products based on their relative mass flow. Mass allocation was used as an alternative approach.

In Table 5.10, the economic value of the main product and co-products from the Office of Agricultural Economics of Thailand and the Thai Tapioca Starch Association (TTSA) showed that the cassava starch price is equal to 0.42 USD/kg. Cassava peel, cassava pulp, root of cassava and sand are equal to 0.01 USD, 0.02 USD, 0.01 USD and 0.01 USD/kg, respectively (Office of Agricultural Economics of Thailand, 2008). The mass allocation can be seen in Table 5.10 based on the quantity of the product and co-products.

Table 5.10 Quantity and average price of allocation for the production of cassava starch

Products	Quantity, (kg)	Average price, (USD/kg)	Price (USD)	Economic Allocate (%)	Mass Allocation (%)
cassava starch	1000.00	0.42	421.33	94.31	41.15
cassava peel	146.27	0.01	0.75	0.17	6.02
root of cassava	40.72	0.01	0.09	0.02	1.68
cassava pulp	1222.84	0.02	24.33	5.45	50.32
sand	20.33	0.01	0.24	0.05	0.84
Total	2430.17		446.74	100	100

In this study, only formulation 1 was examined to analyze the influence of allocation methods. It can be observed in Figure 5.9 that all the impact categories have different degrees of response to the change of allocation method. Some of the impact categories such as abiotic depletion potential, acidification potential and global warming potential had little difference, while other impact categories such as eutrophication potential and ozone layer depletion had dramatic differences. Overall, this means that the model is sensitive to the allocation method change as shown by the differing results.

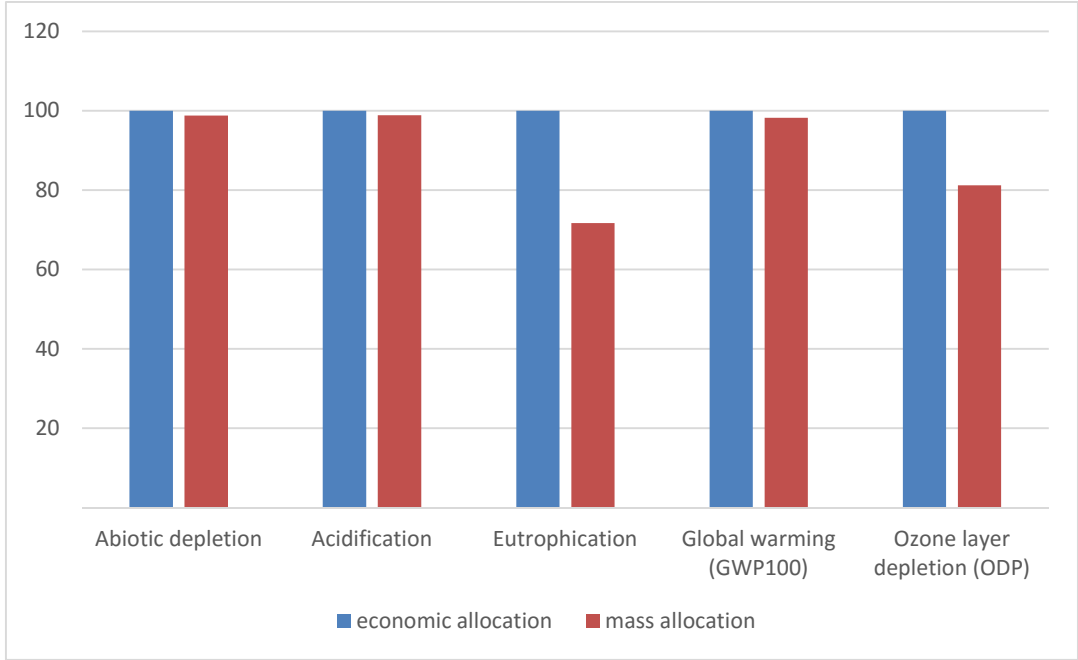
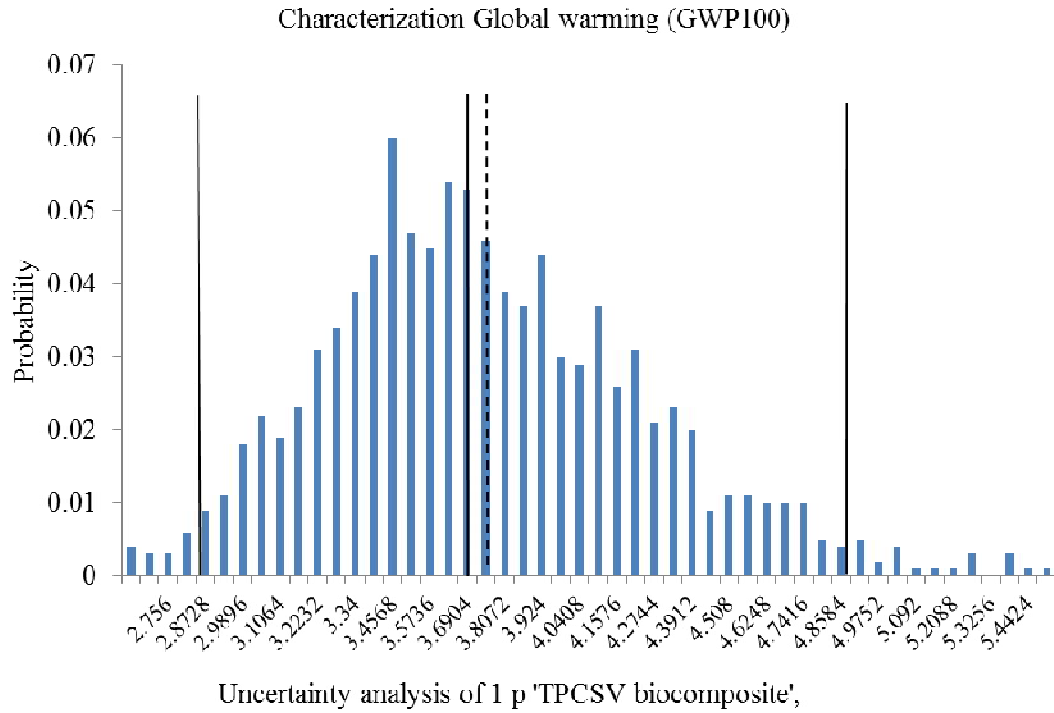


Figure 5.9 Environmental impact comparison per kg of formulation 1 of TPCSV biocomposite pellet for economic and mass allocation

5.11 Uncertainty analysis of LCIA

The effect of uncertainty in the LCA of thermoplastic cassava starch reinforced by vetiver fiber was evaluated using Monte Carlo simulation, based on the variety of data sources and assumptions causing variations in the study. The calculation was performed by Monte Carlo simulation programmed in Simapro 7.3.3 software with the CML 2 Baseline 2000 v2.05 method for global warming with running 1000 iterations and the input values were based on average and standard deviation of each value in the unit process, which was assessed by a pedigree matrix shown in Table B.6. The results are presented in the histograms of Figure 5.10 and Figure 5.11.



Method: CML 2 baseline 2000 V2.05 / World, 1995, CI: 95 %

Figure 5.10 Probability distribution of characterization of GWP100 for TPCSV biocomposite pellet

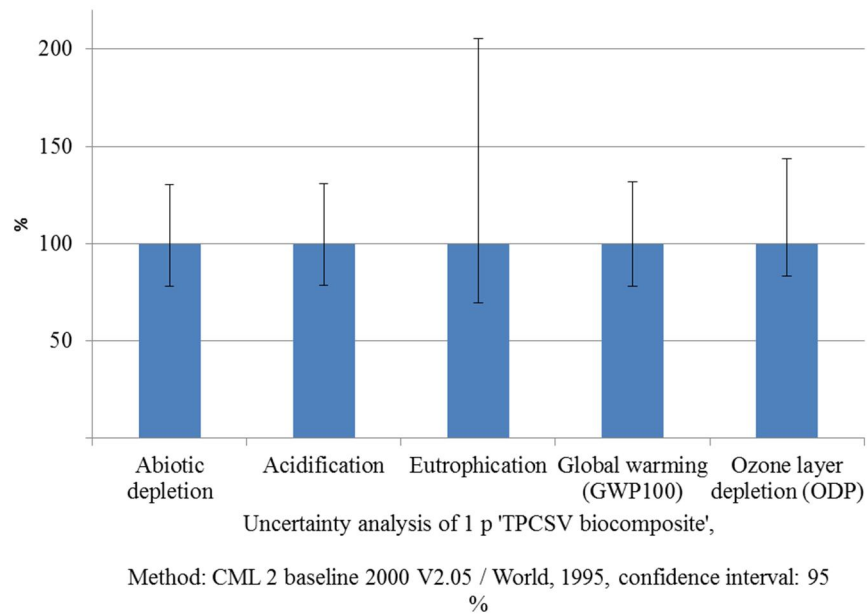


Figure 5.11 Uncertainty of characterization of TPCSV biocomposite

As shown in Figure 5.10 and 5.11, the error bars show the uncertainty ranges at the 2.5th and 97.5th percentile to mean value and the value results showed in Table 5.11.

Table 5.11 Uncertainty analysis for TPCSV biocomposite

Impact category	Mean	Median	SD	CV	2.50%	97.50%	Std.err. of mean
ADP, (kg Sb eq)	0.0279	0.0275	0.00368	13.20%	0.0215	0.0359	0.00417
AD, (kg SO ₂ eq)	0.0202	0.0199	0.00263	13.00%	0.0156	0.026	0.00412
EP, (kg PO ₄ ⁻³ eq)	0.0169	0.0154	0.00575	34%	0.0108	0.0316	0.0108
GWP100, (kg CO ₂ eq)	3.75	3.69	0.498	13.30%	2.89	4.86	0.0042
ODP, (kg CFC-11 eq)	.31E-07	8.98E-07	1.42E-07	15.20%	7.50E-07	1.29E-06	0.00481

At 97.5%, confidence interval indicating that by repeating, 95% of the cases the characterization results would fall in this interval. In these cases, the larger degree of uncertainty was introduced in eutrophication due to the large uncertainty in cultivation stages and the major drivers are fertilizer and fuels. On the other hand, abiotic depletion, acidification, global warming and ozone layer depletion of thermoplastic cassava starch reinforced by vetiver fiber showed lower variance.

5.12 Conclusions

The aim of this research was to study the environmental impacts of 1 kg of pellets of thermoplastic cassava starch reinforced by vetiver fiber and compare it with a conventional biopolymer, granulated polylactide resin. The environmental impacts of the two formulations were not dramatically different as shown in Table 5.2. The total energy consumption for laboratory scale manufacturing of the TPCSV pellets was about 75 MJ. About 56.1 MJ was for compounding. In terms of environmental impact categories, abiotic depletion, acidification and global warming potentials of the two formulations showed slightly higher impact value due to the electricity from

polymer production. Cassava starch production was the main contributor to the eutrophication potential. Vetiver fiber production was the main contributor to the ozone layer depletion potential.

On the other hand, when comparing the major environmental impacts associated with the granulated polylactide resin and thermoplastic cassava starch reinforced by vetiver fiber (TPCSV) pellet, the abiotic depletion, eutrophication and global warming (GWP100) of the TPCSV resin were slightly lower than that of granulated polylactide, which acidification and ozone layer depletion (ODP) were slightly higher than the granulated polylactide. These results are based on TPCSV pellet products fabricated on a laboratory scale. The environmental impacts may go down with large-scale manufacturing due to reduced energy use and more efficiency [157]. This could make these products have lower environmental impacts, when compared to the products fabricated on a laboratory scale.

Chapter 6

Conclusion and Future Study

6.1 Conclusions

The production of thermoplastic cassava starch reinforced by vetiver fiber has been examined with three different studies: First, in polymer processing, the samples were prepared on a laboratory scale manufacture using an internal mixer, compression molding and the experimental design methodology. Second, DMR methodology was used as an evaluation method for testing the biodegradability of the biocomposites. Third, life cycle analysis was used to evaluate the potential environmental impacts of these materials. These studies were designed to help to increase the utilization of the natural fiber biocomposites.

Mixture design of experiments was utilized to develop response surface models that could be used to characterize and optimize the tensile and flexural properties of thermoplastic cassava starch composites reinforced by natural fibers. The amounts of starch and glycerol have great influence on processability. A high proportion of starch resulted in decreasing the mobility of the starch chain, giving more brittleness, while glycerol increased the mobility of the starch chains. The optimum strength was observed at the weight fraction of 60 wt% of cassava starch, 21 wt% of glycerol with 13 wt% of vetiver fiber. This study showed that the mechanical properties of TPCS were improved by mixing with vetiver fiber. Scanning electron microscopy showed that vetiver fiber was well attached within the matrix but not well dispersed and aligned within the matrix. Thermal stability was improved due to the cellulose from the vetiver fiber in the matrix.

Biodegradability testing of the thermoplastic cassava starch biocomposites was examined by a direct measurement respirometric (DMR) approach in accordance with ASTM 5338 and ISO 14855 standards. The test was performed by measuring the CO₂ evolution and results converted to

percent of mineralization. The results showed that all of the thermoplastic cassava starch biocomposites can be considered as biodegradable polymers since they can reach or exceed 70 % mineralization in accordance with the ISO 14855 standards. The rates of degradation in the study varied depending on not only the properties of the compost such as moisture content, temperature, pH and microbial types and quantities but also the properties of the test substances such as water solubility, and the test duration. Modeling of biodegradability correlating the response as a function of component proportion in weight percentage was achieved. The ANOVA test showed that the model was reliable to be used to design the composites

The LCA methodology used in this study was conducted according to the International Organization for Standardization (ISO), which were defined in ISO 14040 series framework [139]. The aim of this study was to gain preliminary results for environmental impacts of two formulations of 1 kg of pellets of thermoplastic cassava starch reinforced by vetiver fiber and a conventional biopolymer, granulated polylactide (PLA). The results showed that the environmental performance of the two formulations were not dramatically different. The major energy consumption for laboratory scale manufacturing of the TPCSV pellets was the compounding process, which is from the electricity. In terms of environmental impact categories, granulated polylactide had slightly higher impact values than the TPCSV pellets in abiotic depletion, eutrophication and global warming potentials. Cassava starch production was the main contributor to the eutrophication potential. Vetiver fiber production was the main contributor to the ozone layer depletion potential. When comparing the environmental impacts between the granulated polylactide resin and thermoplastic cassava starch reinforced by vetiver fiber (TPCSV) pellets, the abiotic depletion, eutrophication and global warming (GWP100) of the TPCSV resin were slightly lower than that of the granulated polylactide. Acidification and ozone layer depletion (ODP) were slightly higher than the environment impact of the granulated polylactide. Therefore,

based on the study parameters, the environmental performances of thermoplastic cassava starch biocomposites is not significantly different from the granulated polylactide. It should be noted that, however, that this is based on laboratory scale production.

6.2 Future study

Based on the studies of TPCSV biocomposite, suggestions for future study include:

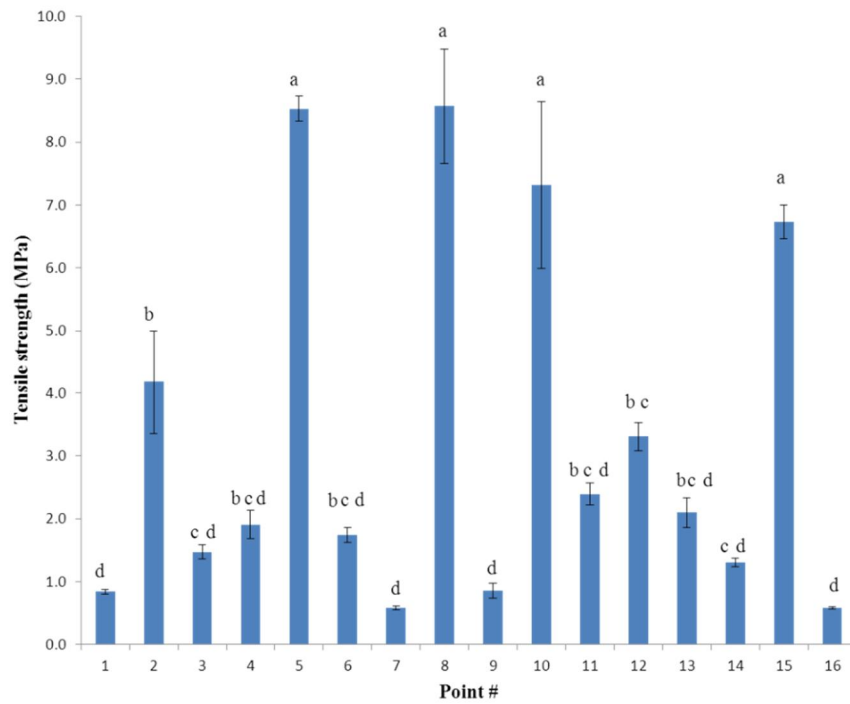
- Performing product design using TPCSV biocomposite with real applications. Also, considering other factors to study such as water resistance and thermal stability etc.
- Different matrices from other starches or different natural fibers should be studied using a similar approach as in this study. Moreover, blending with commercial biopolymers may achieve desired properties.
- Due to the space limitation in the chamber for biodegradation testing, the results from the TPCSV samples may not be able to be compared properly. Simultaneous testing should be performed for biodegradation testing.
- Investigation of the effect of the main components in this biodegradability test by a mixing design approach could show the influence of components related to the properties. However, other experimental design should be considered by using similar techniques.
- Modifying and/or reducing the electricity in polymer processing can improve the environmental performance of the thermoplastic cassava starch composite production.
- Reducing of fuel, fertilizer, pesticides and herbicides connected to cassava and vetiver cultivation can improve the environmental impacts such as eutrophication, acidification potentials, etc.

- Transportation, end-of-life and land use should be incorporated in further studies in order to examine the effects on the overall results and to identify improvement opportunities.

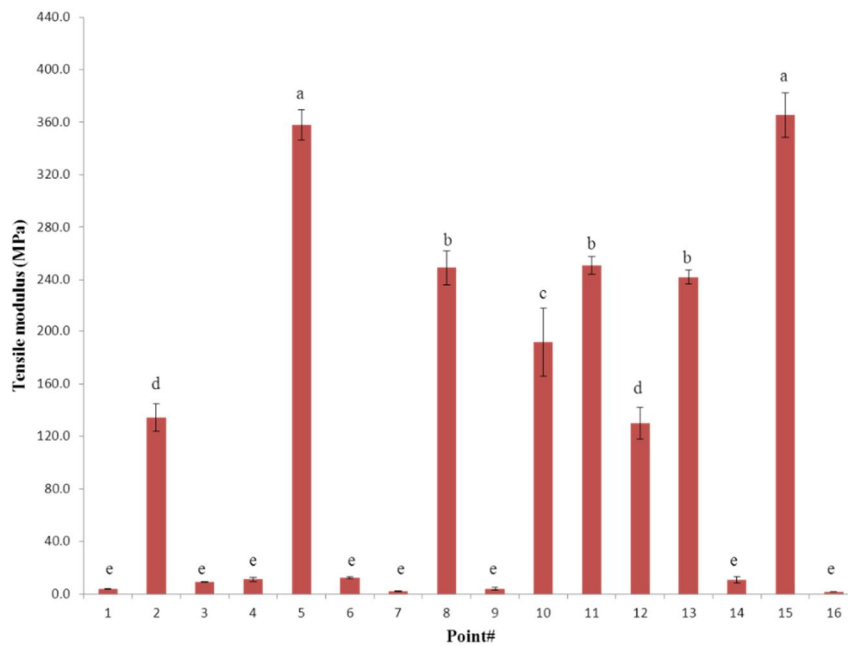
APPENDICES

APPENDIX A

THE FOLLOWING FIGURES DEAL WITH CHAPTER 3

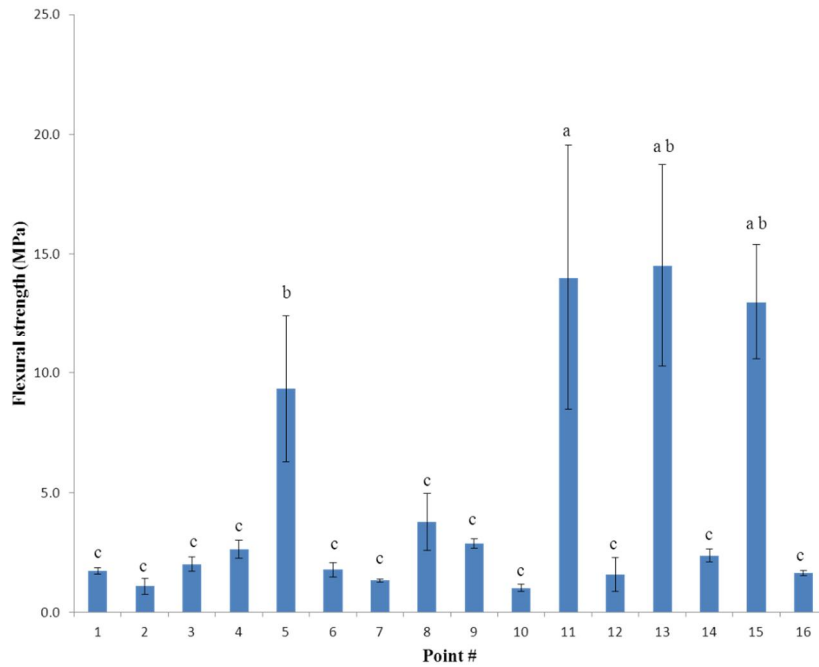


(a)

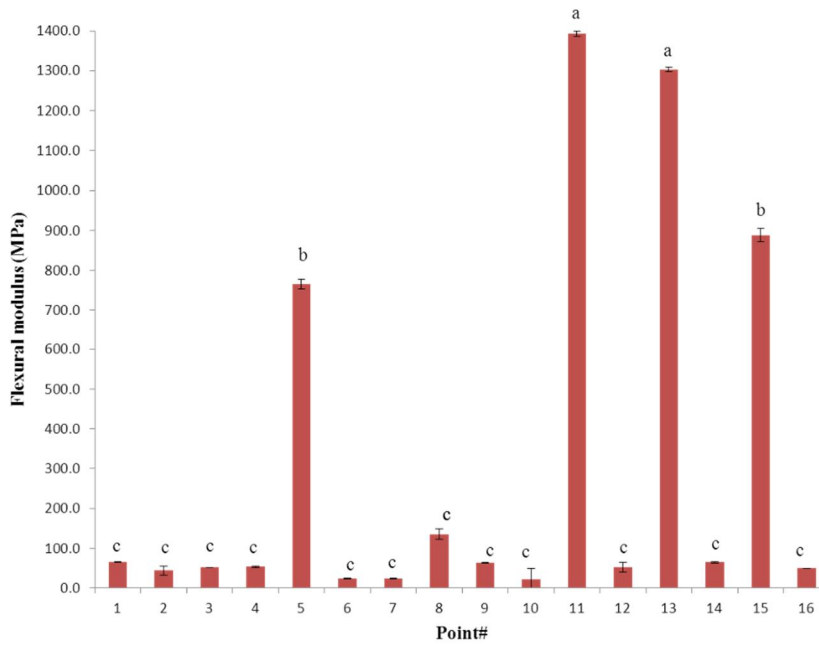


(b)

Figure A.1 The investigation of significance difference of measured tensile strength (a) and tensile modulus (b) of thermoplastic cassava starch composites reinforced by paper fiber

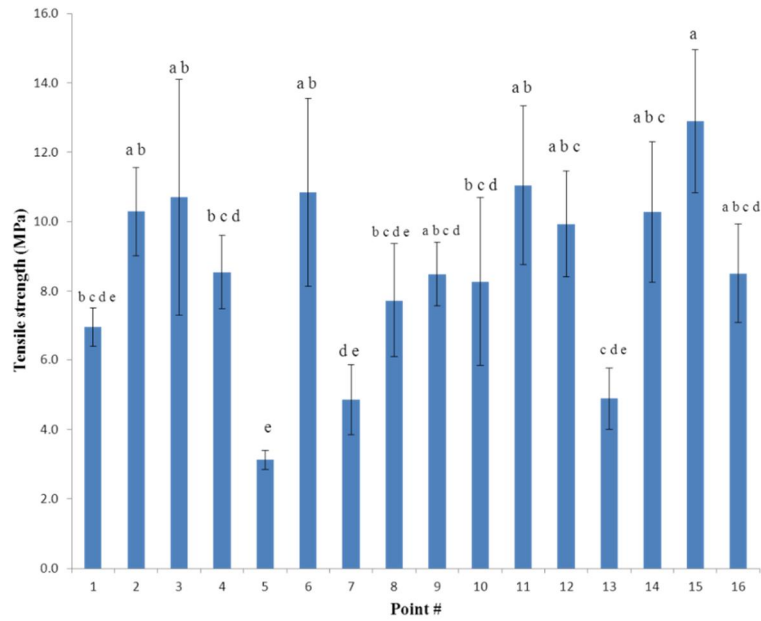


(a)

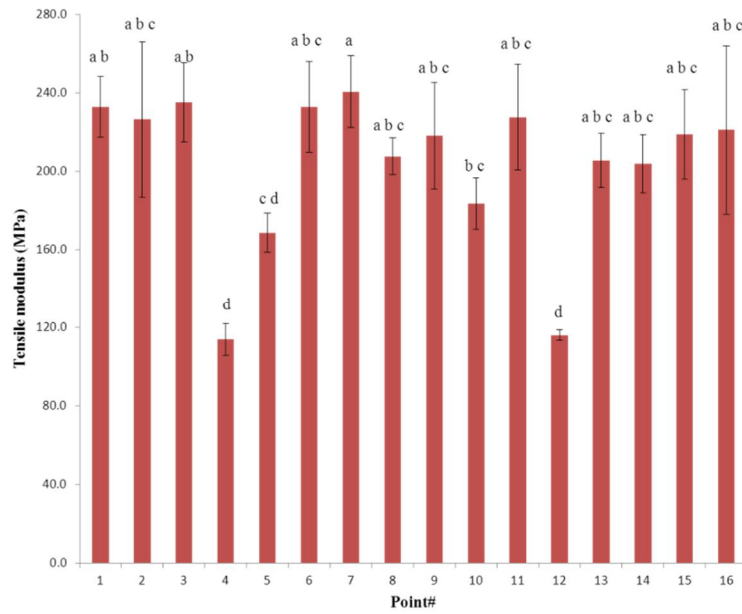


(b)

Figure A.2 The investigation of significance difference of measured flexural strength (a) and flexural modulus (b) of thermoplastic cassava starch composites reinforced by paper fiber

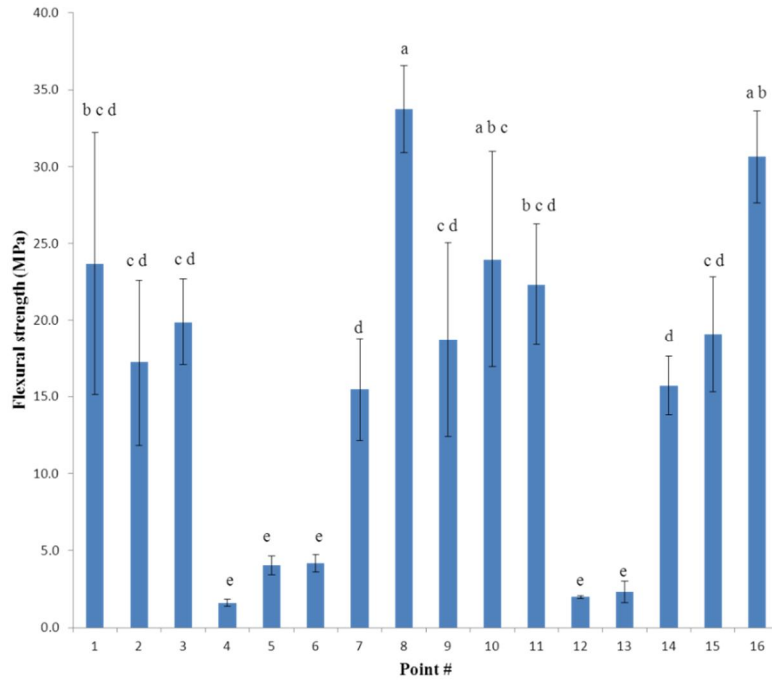


(a)

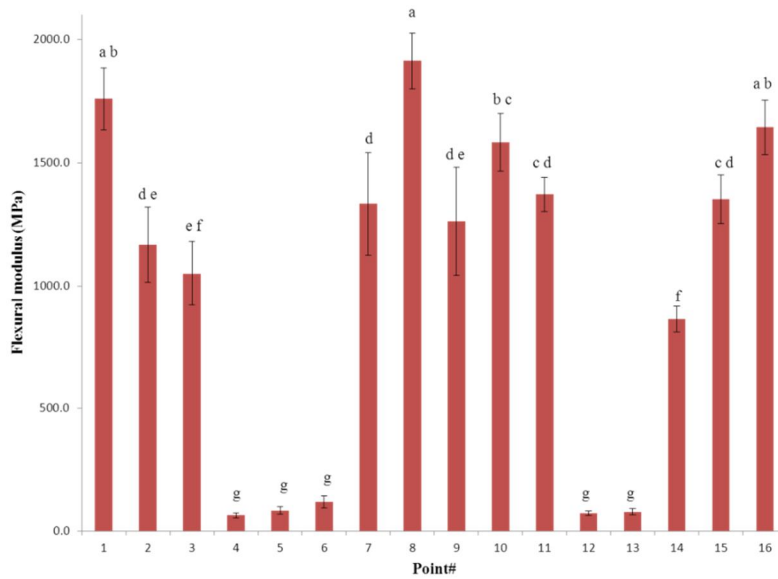


(b)

Figure A.3 The investigation of significance difference of measured tensile strength (a) and tensile modulus (b) of thermoplastic cassava starch composites reinforced by vetiver fiber.

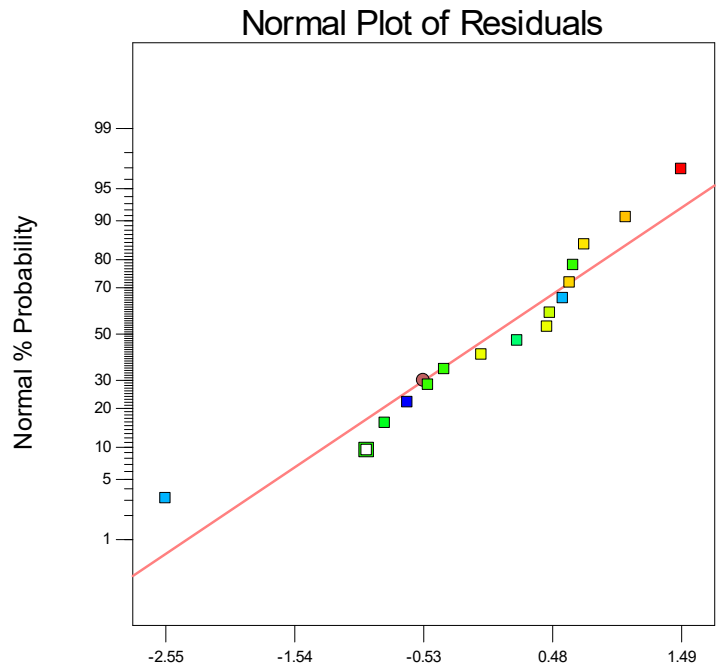


(a)



(b)

Figure A.4 The investigation of significance difference of measured flexural strength (a) and flexural modulus (b) of thermoplastic cassava starch composites reinforced by vetiver fiber



Internally Studentized Residuals

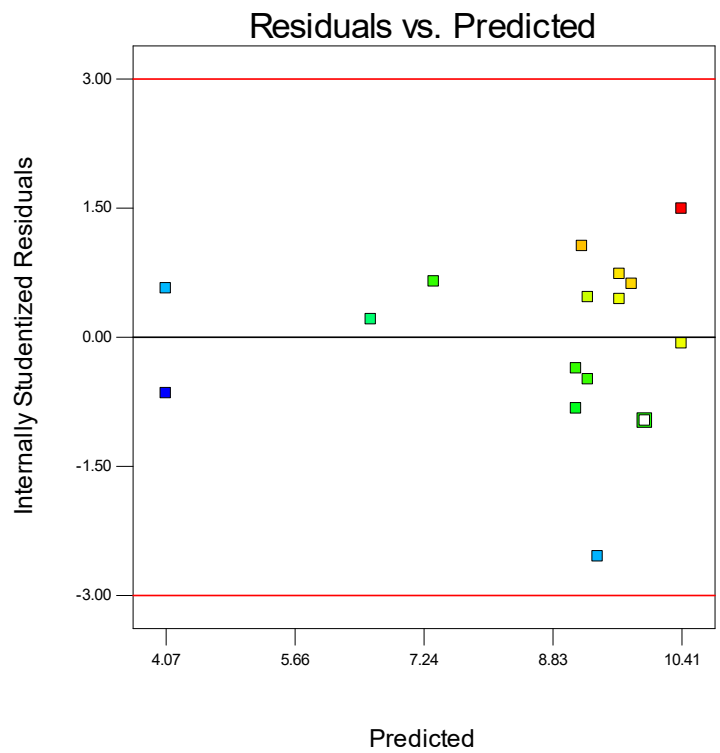


Figure A.5 The plots of diagnostic case statistics for tensile strength model of TPCS with vetiver fiber

Figure A.5 (cont'd)

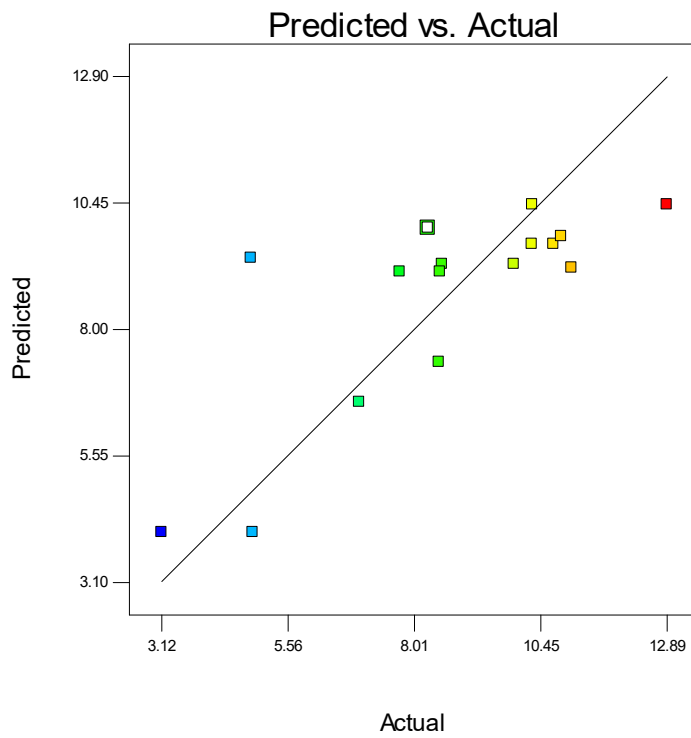
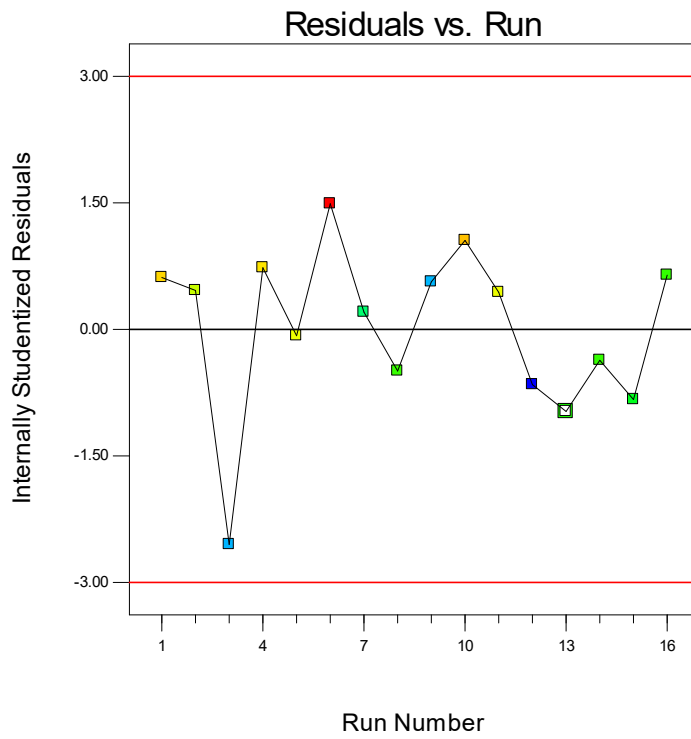


Figure A.5 (cont'd)

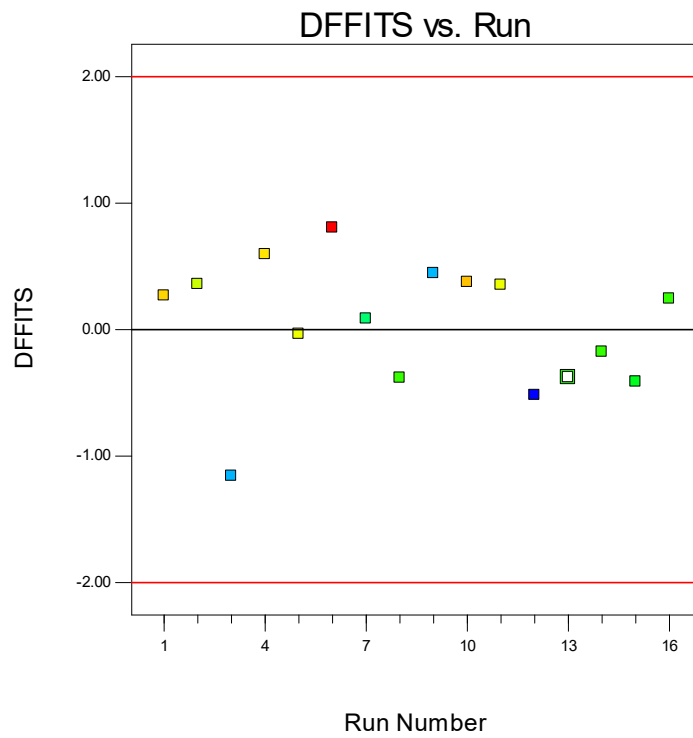
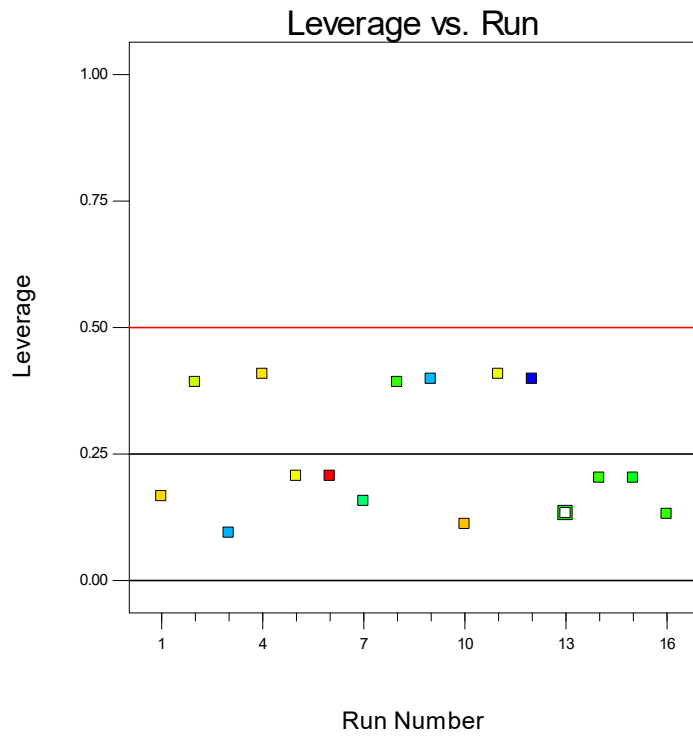
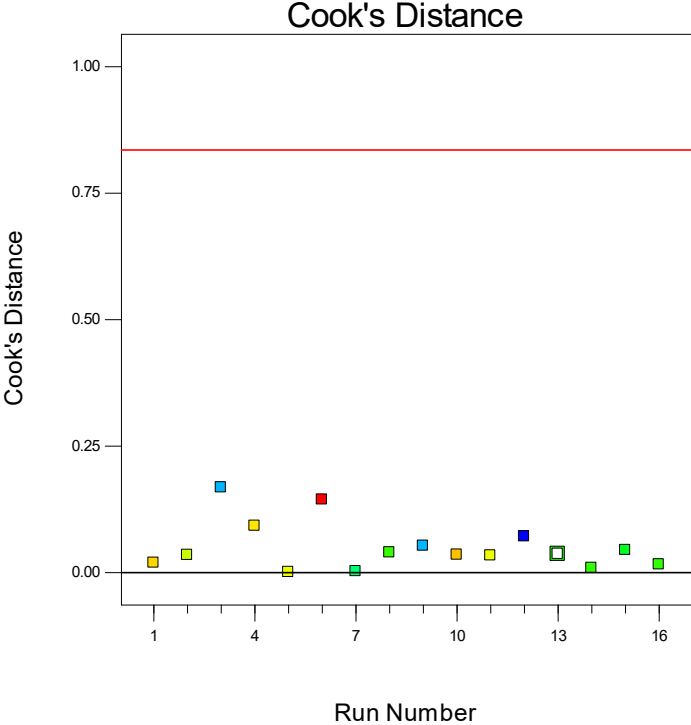


Figure A.5 (cont'd)



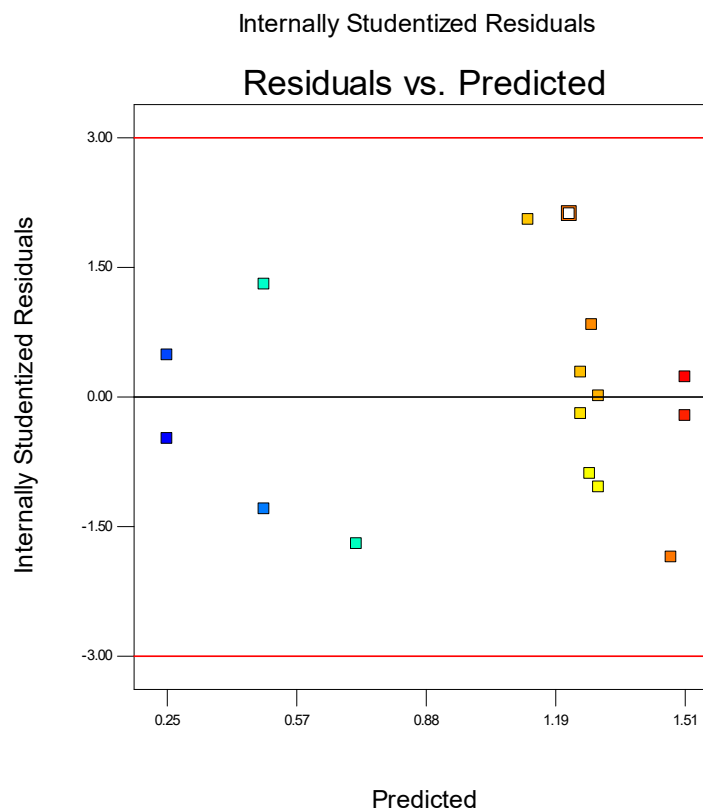
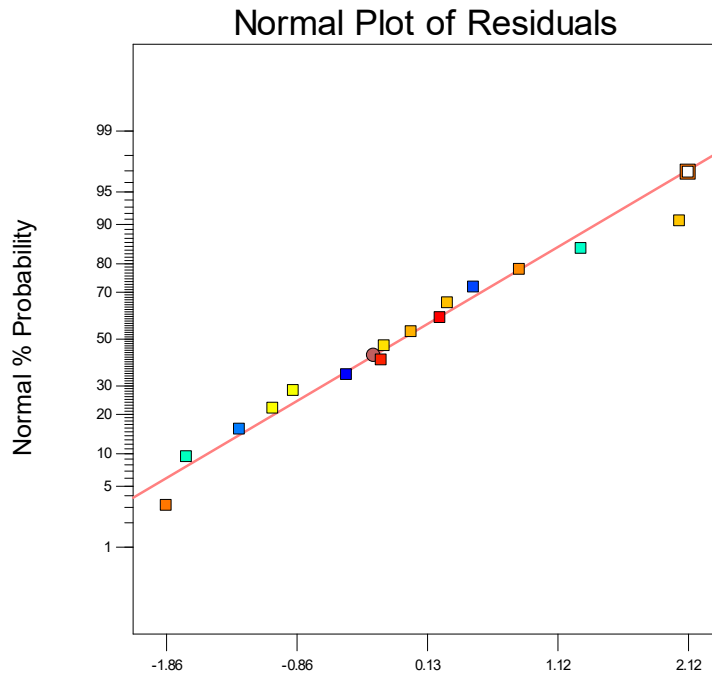


Figure A.6 The plots of diagnostic case statistics for flexural strength model of TPCS with vetiver fiber

Figure A.6 (cont'd)

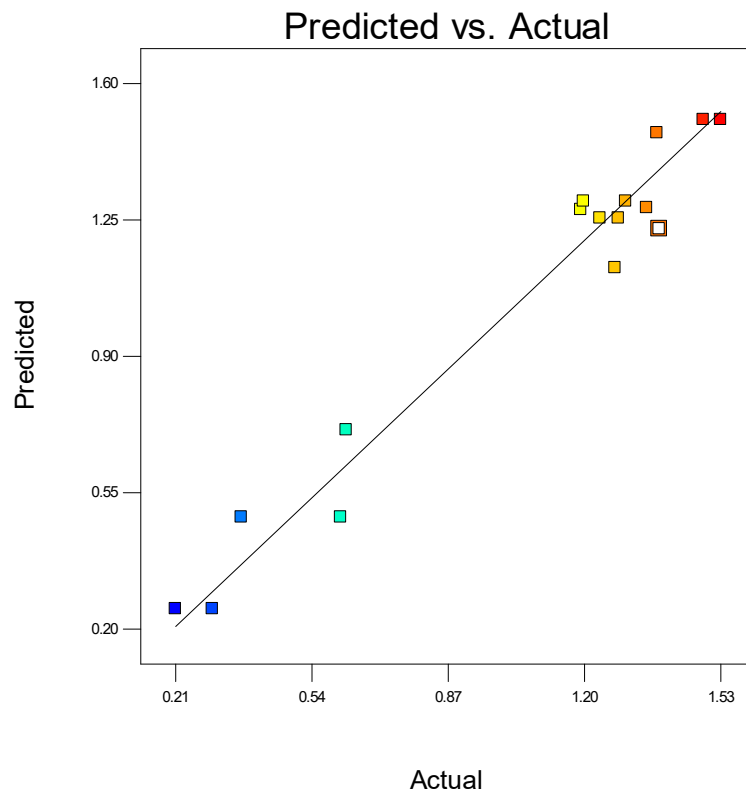
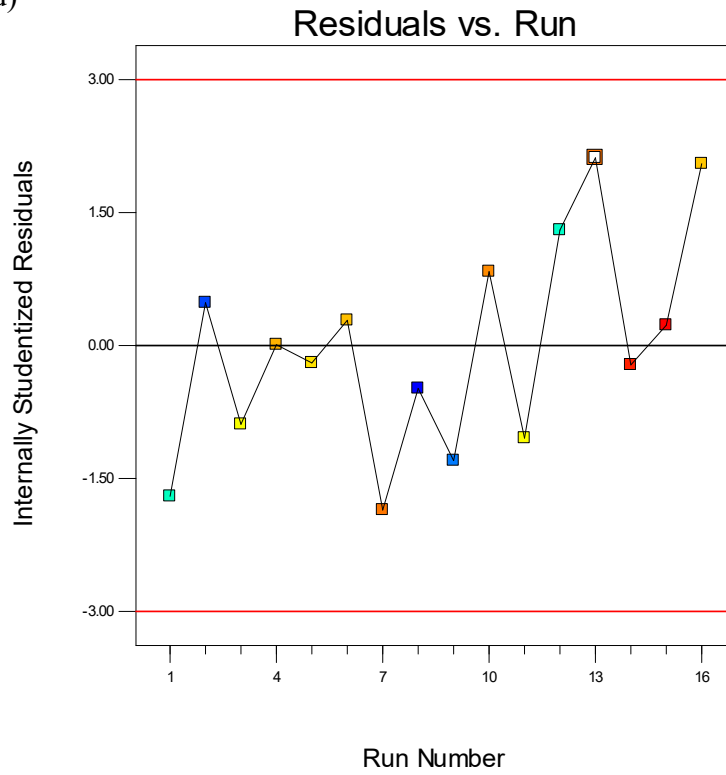


Figure A.6 (cont'd)

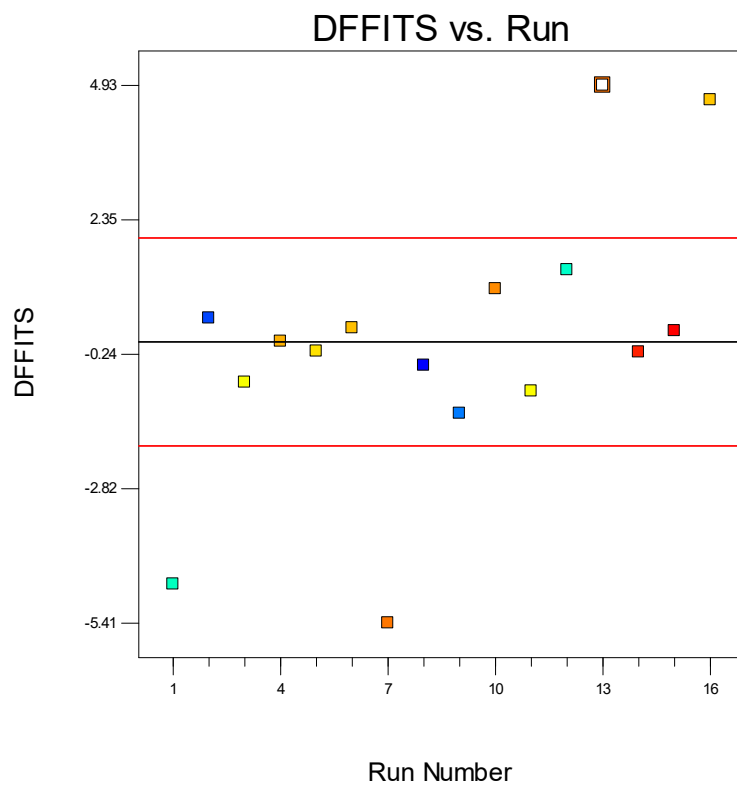
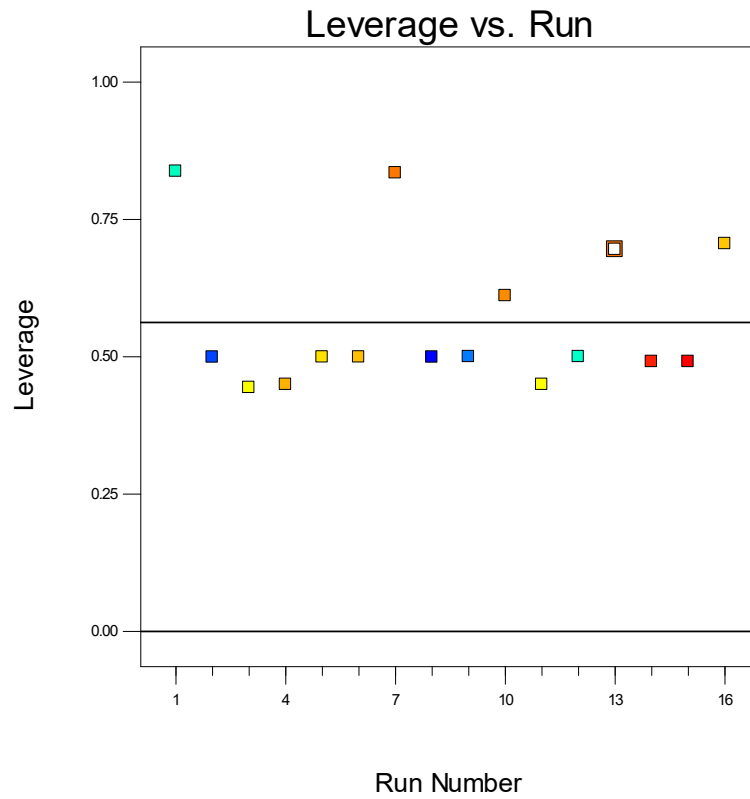
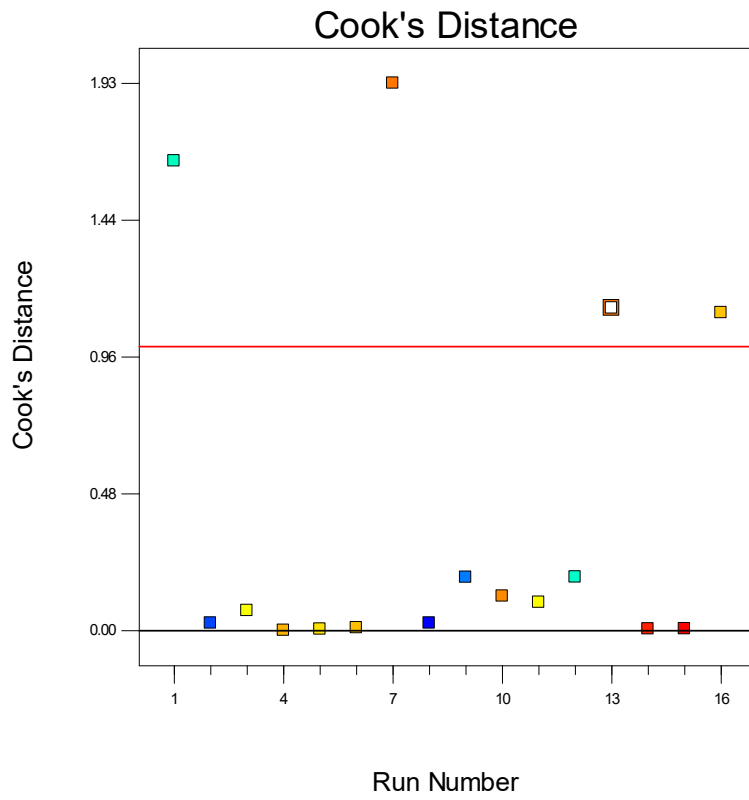


Figure A.6 (cont'd)



APPENDIX B

THE FOLLOWING TABLES DEAL WITH CHAPTER 5

Table B.1 Classification and Characterization factors

Classification Factors for Abiotic Depletion potential [103]

Substance	ADP (in kg Sb eq)
Antimony (Sb)	1
Arsenic (As)	0.00917
Boron (B)	0.00467
Bromine (Br)	0.00667
Chlorine (Cl)	4.86E-08
Chromium (Cr)	0.000858
Crude oil	0.0201
Natural gas	0.0187
Hard coal	0.0134
Soft coal	0.00671
Fossil energy	0.000481

Calculation of ADP in LCIA:

Amount of emission (kg) from LCI \times ADP classification factor

Classification Factors for Acidification Potential (AP)[103]

Substance	AP (in kg SO ₂ eq)
SO ₂	1
NH ₃	1.88
NO _x	0.7
HCl	0.88
HF	1.6

Calculation of AP in LCIA:

Amount of emission (kg) from LCI \times AP classification factor

Table B.1 (cont'd)

Classification Factors for Eutrophication Potential (EP) [103]

Substance	EP (in kg PO ₄ ³⁻ eq)
Phosphates	1
Ammonia	0.35
Ammonium	0.33
Nitrates	0.42
Nitrogen Oxides	0.13

Calculation of EP in LCIA:

Amount of emission (kg) from LCI × EP classification factor

Classification Factors for Global Warming Potential (GWP₁₀₀) [103]

Substance	GWP ₁₀₀ (in kg CO ₂ eq)
CO ₂	1
CH ₄	21
N ₂ O	310
NO _x	296
CFC-11	4000
CFC-113	5000
CFC-114	9300
CFC-115	9300
CFC-12	8500
CFC-13	11700

Calculation of GWP in LCIA:

Amount of emission (kg) from LCI × GWP classification factor

Table B.1 (cont'd)

Classification Factors for Ozone Depletion Potential (ODP) [103]

Substance	ODP (in kg CFC-11 eq)
Trichlorofluoromethane (CFC11)	1
Chlorinated hydrocarbons	0.5
Chlorofluorocarbons	0.4
Other volatile organic compounds	0.005

Calculation of ODP in LCIA:

Amount of emission (kg) from LCI \times ODP classification factor

Table B.2 Life cycle inventory of cassava cultivation for 1 ton of cassava starch production
[145–149], [158–160]

Input	Unit	Quantity per 1 ton
Materials		
Fresh stems	stems	269.67
Cassava peel	kg	1.01
Fertilizer		
Nitrogen Fertilizer, N	kg	3.28
Phosphorous Fertilizer, P2O5	kg	2.61
Potassium Fertilizer, K2	kg	3.14
manure	kg	217.86
Herbicide		
Paraquat	kg	0.21
Glyphosate	kg	0.31
Zinc,	kg	0.42
Alaclor	kg	0.15
Fuel		
Diesel	kg	8.23
Output	Unit	Quantity per 1 ton
Products		
Cassava yield	ton	1
Plant waste	kg	491.29
cassava stem		723.92
Air emissions		
Carbon dioxide	kg	8.60
Nitrogen oxide	kg	0.18
sulfur dioxide	kg	0.01
Nitrous oxide	kg	0.04
Ammonium	kg	0.24
VOC	kg	0.04

Table B.3 Life cycle inventory for the production of 1 ton cassava starch [148, 160–162]

Input	Unit	Quantity per 1 ton
Materials		
Cassava root	kg	4350.00
Sulfur dioxide	kg	1.01
Water	kg	15893.60
Fuel		
Bunker oil	kg	33.58
Electricity	KWh	173.34
fuel oil (drying)	kg	13.26
diesel	L	1.64
biogas	kg	51.22
Output	Unit	Quantity per 1 ton
Products		
Cassava starch	kg	1000
Co-products		
Cassava peel	kg	146.27
Rootstock	kg	40.72
Fibrous residue	kg	1222.84
Sand	kg	20.33
Soild Waste		
Starch residual waste	kg	106.36
Air emissions		
Cabon dioxide	kg	143.80
Carbon monoxide	kg	145.48
Nitrogen oxide Nox	kg	1.64
Sulfur dioxide SO2	kg	0.60
Steam	kg	269.44
Water emissions		
Waste water	kg	13763.50
Biochemical Oxygen Demand, BOD	kg	105.08
Chemical Oxygen Demand, COD	kg	215.02
Nitrogen	kg	6.50
Phosphorous	kg	0.40
Suspended Load	kg	90.05

Table B.4 Life cycle inventory of vetiver cultivation for 1 ton of vetiver fiber production [151]

Input	Unit	Quantity per 1 ton
Materials		
slips	plants	315
Nitrogen Fertilizer	kg	8.379
Phosphorous Fertilizer	kg	1.673
Potassium Fertilizer	kg	7.21
fungicide	L	38.5
manure	kg	210
Fuel		
Diesel	L	2.1
Output	Unit	Quantity per 1 ton
Products		
Vetiver grass	ton	1

Table B.5 Life cycle inventory for the production of 1 ton vetiver fiber

Input	Unit	Quantity per 1 ton
Materials		
Vetver grass	kg	3140
NaOH	kg	503
Water	kg	223600
Fuel		
Natural gas,	kg	580
Electricity	KWh	375
Output	Unit	Quantity per 1 ton
Products		
Vetiver fiber	kg	1000
Water emissions		
Waste water	kg	173600

Table B.6 Pedigree matrix

The pedigree matrix [163] for this study was based on the literature as shown in Table, which was used to assess the quality of data by finding the standard deviation of each data. The value of the standard deviation (SD) was calculated according to the following equation:

$$SD = \exp\sqrt{[\ln(U1)^2 + \ln(U2)^2 + \ln(U3)^2 + \ln(U4)^2 + \ln(U5)^2 + \ln(U6)^2]}$$

where

U1 = The corresponding score of reliability.

U2 = The corresponding score of completeness.

U3 = The corresponding score of temporal correlation.

U4 = The corresponding score of geographical correlation.

U5 = The corresponding score of technological correlation.

U6 = The corresponding score of sample size.

Table B.6 (cont'd)

Indicator	1	2	3	4	5
Reliability	Verified data based on measurement	Verified data partly based on assumptions or non-verified data based on measure	Non-verified data partly based on assumptions	Qualified Estimate (e.g. by industrial expert)	Non-qualified estimate
U1	1.00	1.05	1.10	1.20	1.50
Completeness	Representative data from a sufficient sample of sites over an adequate period to even out normal fluctuations	Representative data from a smaller number of sites but for adequate periods	Representative data from adequate number of sites but from shorter periods	Representative data but from a smaller number of sites and shorter periods or incomplete data from an adequate number of sites and periods	Representativeness unknown or incomplete data from a smaller number of sites and/or from shorter periods
U2	1.00	1.02	1.05	1.10	1.20
Temporal correlation	< 3 years difference to year of study	< 6 years difference to year of study	< 10 years difference to year of study	< 15 years difference to year of study	Age of data unknown or > 15 years difference to year of study
U3	1.00	1.03	1.10	1.20	1.50
Geographical correlation	Data from area under study	Average data from larger area in which the area under study is included	Data from area with similar production conditions	Data from area with slightly similar production conditions	Data from unknown area or area with very different production conditions
U4	1.00	1.01	1.02	NA	1.10

Table B.6 (cont'd)

Indicator	1	2	3	4	5
Technology correlation	Data from enterprises, processes, and materials under study	Data for processes and materials under study but from different enterprises	Data from processes and materials under study but from different technology	Data from related processes or materials but same technology	Data on related processes or materials but different technology
U5	1.00	NA	1.02	1.50	2.00
Sample size	> 100, continuous measurement, balance of purchased products	> 20	> 10	> = 3	unknown
U6	1.00	1.02	1.05	1.10	1.20

Table B.6 (cont'd)

Group	Process	Input	U1	U2	U3	U4	U5	U6	SD
	Materials								
Cassava cultivation	Fertilizer	Nitrogen	1.2	1.1	1.03	1.02	1.2	1.05	1.082
		Phosphorous	1.2	1.1	1.03	1.02	1.2	1.05	1.082
		Potassium manure	1.2	1.1	1.03	1.02	1.2	1.05	1.082
	Herbicide	Paraquat	1.2	1.1	1.03	1.02	1.2	1.05	1.082
		Glyphosate	1.2	1.1	1.03	1.02	1.2	1.05	1.082
		Zinc	1.2	1.1	1.03	1.02	1.2	1.05	1.082
		Alaclor	1.2	1.1	1.03	1.02	1.2	1.05	1.082
	Pesticide	Pesticide	1.2	1.1	1.03	1.02	1.2	1.1	1.090
	Fuel	Diesel	1.2	1.1	1.03	1.02	1.2	1.1	1.090
Cassava starch production	Materials	Sulfur dioxide	1.2	1.1	1.03	1.02	1.2	1.1	1.090
		Water	1.2	1.1	1.03	1.02	1.2	1.1	1.090
	Fuel	Bunker oil	1.2	1.1	1.03	1.02	1.2	1.1	1.090
		Electricity	1.2	1.1	1.03	1.02	1.2	1.1	1.090
		Fuel oil	1.2	1.1	1.03	1.02	1.2	1.1	1.090
		Diesel	1.2	1.1	1.03	1.02	1.2	1.1	1.090
		Biogas	1.2	1.1	1.03	1.02	1.2	1.1	1.090
		Coal	1.2	1.1	1.03	1.02	1.2	1.1	1.090
Vetiver cultivation	Materials								
	Fertilizer	Nitrogen	1.2	1.2	1.2	1.02	1.2	1.1	1.153
		Phosphorous	1.2	1.2	1.2	1.02	1.2	1.1	1.153
		Potassium manure	1.2	1.2	1.2	1.02	1.2	1.1	1.153
	Fuel	Diesel	1.2	1.2	1.2	1.02	1.2	1.1	1.153
	Vetiver production	Materials	NaOH	1.2	1.1	1.03	1.02	1.5	1.1
		Water	1.2	1.1	1.03	1.02	1.5	1.1	1.242
Fuel		Natural gas	1.2	1.1	1.03	1.02	1.5	1.1	1.242
		Electricity	1.2	1.1	1.03	1.02	1.5	1.1	1.242

REFERENCES

REFERENCES

- [1] T. U. States, “Facts and Figures 2009,” *Environ. Prot.*, 2009.
- [2] R. J. Roberts and M. Chen, “Waste incineration--how big is the health risk? A quantitative method to allow comparison with other health risks.,” *J. Public Health (Oxf)*., vol. 28, no. 3, pp. 261–6, Sep. 2006.
- [3] United States Environmental Protection Agency, “Municipal Solid Waste Generation , Recycling , and Disposal in the United States: Facts and Figures for 2012,” pp. 1–14, 2012.
- [4] S. Chuayjuljit, S. Hosililak, and A. Athisart, “Thermoplastic Cassava Starch / Sorbitol-Modified Montmorillonite Nanocomposites Blended with Low Density Polyethylene : Properties and Biodegradability Study,” vol. 19, no. 1, pp. 59–65, 2009.
- [5] S. Taj, M. A. Munawar, and S. Khan, “NATURAL FIBER-REINFORCED POLYMER COMPOSITES,” *Carbon N. Y.*, vol. 44, no. 2, pp. 129–144, 2007.
- [6] A. A. S. Curvelo, A. J. F. De Carvalho, and J. A. M. Agnelli, “Thermoplastic starch ± cellulosic ® bers composites : preliminary results,” vol. 45, 2001.
- [7] M. P. Islam, K. H. Bhuiyan, and M. Z. Hossain, “Vetiver Grass as a Potential Resource for Rural Development in,” vol. X, no. 5, pp. 1–18.
- [8] N. Teramoto, T. Motoyama, R. Yosomiya, and M. Shibata, “Synthesis, thermal properties, and biodegradability of propyl-etherified starch,” *Eur. Polym. J.*, vol. 39, no. 2, pp. 255–261, Feb. 2003.
- [9] D. J. Thomas and A. A. William, *Starches*. St. Paul, Minn: Eagan Press, 1999.
- [10] S. H. Imam, D. F. Wood, B.-S. C. Mohamed A. Abdelwahab, T. G. Williams, G. M. Glenn, and William J. Orts, “Starch Chemistry, Microstructure, Processing, and Enzymatic Degradation,” in *Starch-Based Polymeric Materials and Nanocomposites Chemistry, Processing, and Applications*, J. Ahme, B. K. T. Wa, S. H. I. Mam, and M. A. . Rao, Eds. 2012, pp. 5–25.
- [11] L. Yu and L. Chen, “Polymeric Materials from Renewable Resources,” pp. 1–15, 2009.
- [12] S. Pérez, P. M. Baldwin, and D. J. Gallant, *Starch Granules I*, Third Edit. Elsevier Inc., 2009.
- [13] R. F. Tester, J. Karkalas, and X. Qi, “Starch—composition, fine structure and architecture,” *J. Cereal Sci.*, vol. 39, no. 2, pp. 151–165, Mar. 2004.

- [14] S. M. Narayana, "Physicochemical and Functional Properties of Tropical Tuber Starches : A Review," *Starch - Stärke*, vol. 54, pp. 559–592, 2002.
- [15] G. N. G. Amani, F. A. Tetchi, and P. Colonna, "Molecular and physicochemical characterisation of starches from yam , cocoyam , cassava , sweet potato and ginger produced in the Ivory Coast," vol. 1916, no. December 2006, pp. 1906–1916, 2007.
- [16] M. A. Hanna and Y. Xu, "Starch – Fiber Composites," pp. 349–366, 2009.
- [17] H. F. Zobel, "Molecules to Granules: A Comprehensive Starch Review," *Starch - Stärke*, vol. 40, no. 2, pp. 44–50, 1988.
- [18] A. J. F. Carvalho, *7 Starch : Major Sources , Properties and Applications as Thermoplastic Materials*, no. 2008. Elsevier, 2013.
- [19] W. F. Breuninger, K. Piyachomkwan, and K. Sriroth, "Tapioca / Cassava Starch : Production and Use," in *STARCH: CHEMISTRY AND TECHNOLOGY*, Third Edit., J. BeMiller and R. Whistler, Eds. Elsevier Inc., 2009, pp. 541–568.
- [20] H. S. Ellis and S. G. Ring, "A Study of Some Factors Influencing Amylose Gelation," vol. 5, no. June 1984, pp. 201–213, 1985.
- [21] V. M. Leloup, P. Colonna, and a. Buleon, "Influence of amylose-amylopectin ratio on gel properties," *J. Cereal Sci.*, vol. 13, no. 1, pp. 1–13, Jan. 1991.
- [22] A. A. Karim, M. H. Norziah, and C. C. Seow, "Methods for the study of starch retrogradation," vol. 71, 2000.
- [23] P. D. Orford, R. Parker, S. G. Ring, and a C. Smith, "Effect of water as a diluent on the glass transition behaviour of malto-oligosaccharides, amylose and amylopectin.," *Int. J. Biol. Macromol.*, vol. 11, no. 2, pp. 91–6, Apr. 1989.
- [24] T. W. Schenz, "Glass transitions and product stability—an overview," *Food Hydrocoll.*, vol. 9, no. 4, pp. 307–315, Dec. 1995.
- [25] C. G. Biliaderis, C. M. Page, T. J. Maurice, and B. O. Juliano, "Thermal characterization of rice starches: a polymeric approach to phase transitions of granular starch," *J. Agric. Food Chem.*, vol. 34, no. 1, pp. 6–14, Jan. 1986.
- [26] A. C. Bertolini, *Starches: characterization, properties, and applications*. Boca Raton: Taylor & Francis, 2010.
- [27] M. Mitrus, "TPS and Its Nature," in *Thermoplastic Starch: A Green Material for Various Industries*, L. P. B. M. Janssen and L. Moscicki, Eds. Wiley-VCH Verlag GmbH & Co. KGaA, 2009, pp. 77–104.

- [28] J. Yu, J. Gao, and T. Lin, "Biodegradable thermoplastic starch," *Appl. Polym. Sci.*, vol. 62, no. 9, pp. 1491–1494, Nov. 1996.
- [29] K. J. Zeleznak and R. C. Hosenev, "The glass transition in starch.pdf," *Cereal Chem*, no. 64, pp. 121–124, 1987.
- [30] D. Lourdin, L. Coignard, H. Bizot, and P. Colonna, "Influence of equilibrium relative humidity and plasticizer concentration on the water content and glass transition of starch materials," *Polymer (Guildf)*, vol. 38, no. 21, pp. 5401–5406, Oct. 1997.
- [31] O. Vilpoux and L. Averous, "Starch-based plastics," in *Technology, use and potentialities of Latin American starchy tubers*, 2004, pp. 521–553.
- [32] S. H. I. Swanson, C L, R. L. Shogren, G. F. Fanta, "Starch-Plastic Materials--Preparation, Physical Properties, and Biodegradability (A Review of Recent USDA Research)," *Environ. Polym. Degrad.*, vol. 1, no. 2, pp. 155–166, 1993.
- [33] O. O. Fabunmi, L. G. T. Jr, S. Panigrahi, and P. R. Chang, "Developing Biodegradable Plastics from starch," vol. 0300, no. xxxx, pp. 1–12, 2007.
- [34] A. Vazquez and V. A. Alvarez, "Starch – Cellulose Fiber Composites," in *Biodegradable Polymer Blends and Composites from Renewable Resources.*, L. Yu, Ed. Hoboken, New Jersey: John Wiley & Sons, Inc., 2009, p. 245.
- [35] M. Huang, J. Yu, and X. Ma, "Ethanolamine as a novel plasticiser for thermoplastic starch," *Polym. Degrad. Stab.*, vol. 90, no. 3, pp. 501–507, Dec. 2005.
- [36] W. Jiang, X. Qiao, and K. Sun, "Mechanical and thermal properties of thermoplastic acetylated starch/poly(ethylene-co-vinyl alcohol) blends," *Carbohydr. Polym.*, vol. 65, no. 2, pp. 139–143, Jul. 2006.
- [37] E. M. Teixeira, A. L. Da Róz, A. J. F. Carvalho, and A. A. S. Curvelo, "The effect of glycerol/sugar/water and sugar/water mixtures on the plasticization of thermoplastic cassava starch," *Carbohydr. Polym.*, vol. 69, no. 4, pp. 619–624, Jul. 2007.
- [38] A. J. F. Carvalho, M. D. Zambon, A. A. S. Curvelo, and A. Gandini, "Size exclusion chromatography characterization of thermoplastic starch composites 1. Influence of plasticizer and fibre content," *Polym. Degrad. Stab.*, vol. 79, no. 1, pp. 133–138, 2003.
- [39] A. L. Vilpoux O, *NATURAL POLYMER BLENDS Starch – Cellulose Blends*. Sao Paolo, Brazil: Collection Latin American Starchy Tubers, 2004.
- [40] J. J. G. van Soest, K. Benes, D. de Wit, and J. F. G. Vliegthart, "The influence of starch molecular mass on the properties of extruded thermoplastic starch," *Polymer (Guildf)*, vol. 37, no. 16, pp. 3543–3552, Aug. 1996.

- [41] Scott Beckwith, "Natural Fiber Reinforcement Materials," *Composites Fabrication*, pp. 12–16, 2003.
- [42] M. John and S. Thomas, "Biofibres and biocomposites," *Carbohydr. Polym.*, vol. 71, no. 3, pp. 343–364, 2008.
- [43] a. K. Mohanty, M. Misra, and G. Hinrichsen, "Biofibres, biodegradable polymers and biocomposites: An overview," *Macromol. Mater. Eng.*, vol. 276–277, no. 1, pp. 1–24, Mar. 2000.
- [44] K. G. Satyanarayana, G. G. C. Arizaga, and F. Wypych, "Biodegradable composites based on lignocellulosic fibers—An overview," *Prog. Polym. Sci.*, vol. 34, no. 9, pp. 982–1021, Sep. 2009.
- [45] M. Pervaiz and M. M. Sain, "Carbon storage potential in natural fiber composites," *Resour. Conserv. Recycl.*, vol. 39, no. 4, pp. 325–340, Nov. 2003.
- [46] R. M. Rowell and U. F. Service, "A NEW GENERATION OF COMPOSITE MATERIALS FROM AGRO-BASED FIBER POTENTIAL COMPOSITES FROM AGRO-RESOURCES," pp. 659–665, 1995.
- [47] A. K. Bledzki, V. E. Sperber, and O. Faruk, "Natural and Wood Fibre Reinforcement in Polymers," *Macromolecules*, vol. 13, no. 8, 2002.
- [48] E. Zini and M. Scandola, "Green Composites : An Overview," 2011.
- [49] R. Malkapuram, V. Kumar, and N. Yuvraj Singh, "Recent Development in Natural Fiber Reinforced Polypropylene Composites," *J. Reinf. Plast. Compos.*, vol. 28, no. 10, pp. 1169–1189, 2008.
- [50] A. K. Bledzki, S. Reihmane, and J. Gassan, "Properties and modification methods for vegetable fibers for natural fiber composites," *J. Appl. Polym. Sci.*, vol. 59, no. 8, pp. 1329–1336, Feb. 1996.
- [51] P. Chandranupap and P. Chandranupap, "Pulping Of Vetiver Grass With NH₄ OH-KOH-AQ Mixtures," *AJCHE*, vol. 11, no. 2, pp. 37–44, 2011.
- [52] S. B. Leschine, "Cellulose degradation in anaerobic environments.," *Annu. Rev. Microbiol.*, vol. 49, pp. 399–426, Jan. 1995.
- [53] C. J. Biermann, *Handbook of Pulping and Papermaking*, Second. London: Academic Press Limited, 1996.
- [54] A. K. Bledzki and J. Gassan, "Composites reinforced with cellulose based fibres," *Polym. Sci.*, vol. 24, pp. 221–274, 1999.

- [55] B. Madsen, "Properties of Plant Fibre Yarn Polymer Composites An Experimental Study," 2004.
- [56] H. Lilholt and J. M. Lawther, "Natural organic fibres," in *Comprehensive Composite Materials*, A. Kelly and C. Zweben, Eds. Elsevier, 2000, pp. 303–325.
- [57] A. Bismarck, S. Mishra, and T. Lampke, *Plant Fibers as Reinforcement for Green Composites*, vol. 6. CRC Press, 2005.
- [58] J. Ren and R. Sun, *Hemicelluloses*, 1st ed. Elsevier.
- [59] D. E. Akin, "What Are Natural Fibres? Chemistry of Plant Fibres," in *Industrial Applications of Natural Fibres: Structure, Properties and Technical Applications*, Jörg Müssig, Ed. John Wiley & Sons Ltd., 2010.
- [60] P. Fratzl, I. Burgert, and H. S. Gupta, "On the role of interface polymers for the mechanics of natural polymeric composites," *Phys. Chem. Chem. Phys.*, vol. 6, no. 24, pp. 5575–5579, 2004.
- [61] M. Eder and I. Burgert, "Natural Fibres – Function in Nature," in *Industrial Applications of Natural Fibres*, J. MUSSIG, Ed. John Wiley & Sons, Ltd, 2010, pp. 23–40.
- [62] T. R. Manual, P. Truong, T. Tan, and V. A. N. E. Pinners, "VETIVER SYSTEM APPLICATIONS," vol. 501, no. 3.
- [63] P. Truong, T. T. Van, and E. Pinners, "THE VETIVER SYSTEM FOR AGRICULTURE," 2008.
- [64] F. G. Torres, O. H. Arroyo, and C. Gomez, "Processing and Mechanical Properties of Natural Fiber Reinforced Thermoplastic Starch Biocomposites," *J. Thermoplast. Compos. Mater.*, vol. 20, no. 2, pp. 207–223, Mar. 2007.
- [65] X. Ma, J. Yu, and J. F. Kennedy, "Studies on the properties of natural fibers-reinforced thermoplastic starch composites," *Carbohydr. Polym.*, vol. 62, no. 1, pp. 19–24, Oct. 2005.
- [66] Z. A. Norshahida Sarifuddin, Hanafi Ismail, "EFFECT OF FIBER LOADING ON PROPERTIES OF THERMOPLASTIC SAGO STARCH / KENAF CORE FIBER," *Bioresour. Technol.*, vol. 7, pp. 4294–4306, 2012.
- [67] J. Gironès, J. P. López, P. Mutjé, a. J. F. Carvalho, a. a. S. Curvelo, and F. Vilaseca, "Natural fiber-reinforced thermoplastic starch composites obtained by melt processing," *Compos. Sci. Technol.*, vol. 72, no. 7, pp. 858–863, Apr. 2012.

- [68] A. B. Dias, C. M. O. Müller, F. D. S. Larotonda, and J. B. Laurindo, “Mechanical and barrier properties of composite films based on rice flour and cellulose fibers,” *LWT - Food Sci. Technol.*, vol. 44, no. 2, pp. 535–542, 2011.
- [69] A. A. S. Curvelo, A. J. F. de Carvalho, and J. A. M. Agnelli, “Thermoplastic starch–cellulosic fibers composites: preliminary results,” *Carbohydr. Polym.*, vol. 45, no. 2, pp. 183–188, 2001.
- [70] H. Ibrahim, M. Farag, H. Megahed, and S. Mehanny, “Characteristics of starch-based biodegradable composites reinforced with date palm and flax fibers.,” *Carbohydr. Polym.*, vol. 101, pp. 11–9, Jan. 2014.
- [71] H. F. Giles, J. R. Wagner, and E. M. Mount, *Extrusion - The Definitive Processing Guide and Handbook*. William Andrew Publishing/Plastics Design Library, 2005.
- [72] Z. R. Lazic, *Design of Experiments in Chemical Engineering*. Wiley, 2004.
- [73] D. C. Montgomery, R. H. Myers, and C. M. Anderson-Cook, *Response surface methodology: Process and Product Optimization Using Designed Experiments*, 3rd ed. John Wiley and Sons, Inc., 2009.
- [74] J. A. Cornell, *A primer on experiments with mixtures*. N.J: John Wiley & Sons, Inc, 2011.
- [75] D. C. Montgomery, *Design and Analysis of Experiments*, 5th ed. 2001.
- [76] J. A. Cornell, *Experiments with mixtures: Designs, models, and the analysis of mixture data*. New York: Wiley, 1981.
- [77] R. B. Srivastava and T. Vishnoi, *Biodegradable Polymers and Polymeric Composites*, 1st ed. UK: Smithers Rapra Technology Ltd, 2012.
- [78] C. Booth, “The mechanical degradation of polymers,” *Polymer (Guildf.)*, vol. 4, no. 1, pp. 471–478, Jan. 1963.
- [79] J. Scanlan and W. F. Watson, “Statistical Treatments of Rubber Structure,” *Rubber Chem. Technol.*, vol. 33, no. 5, pp. 1201–1217, 1960.
- [80] H. Roper and H. Koch, “The Role of Starch in Biodegradable Thermo- plastic Materials *,” vol. 42, no. 4, 1990.
- [81] A. A. Shah, F. Hasan, A. Hameed, and S. Ahmed, “Biological degradation of plastics: a comprehensive review.,” *Biotechnol. Adv.*, vol. 26, no. 3, pp. 246–65, 2008.
- [82] Smatsumura, “Mechanism of biodegradation,” in *Biodegradable polymers for industrial applications*, R. Smith, Ed. Woodhead Publishing Limited, 2005, p. 372.

- [83] E. C. Aguirre, “Design and Construction of a Medium-Scale Automated Direct Measurement Respirometric System to Assess Aerobic Biodegradation of Polymers,” Michigan State University, 2013.
- [84] M. van der Zee, “Biodegradability of Polymers – Mechanisms and Evaluation Methods,” in *Handbook of Biodegradable Polymers*, C. Bastioli, Ed. Shawbury: Rapra Technology Limited, 2005, pp. 1–31.
- [85] K. Leja and G. Lewandowicz, “Polymer Biodegradation and Biodegradable Polymers – a Review,” vol. 19, no. 2, pp. 255–266, 2010.
- [86] B. SCHWARZWALDE, R. ESTERMANN, and L. MARINI, “The Role Of Life-Cycle-Assessment For Biodegradable Products: Bags And Loose Fills,” in *BIORELATED POLYMERS Sustainable Polymer Science and Technology*, M. van der Z. Emo Chiellini, Helena Gil, Gerhart Braunegg, Johanna Buchert, Paul Gatenholm, Ed. New York: Kluwer Academic/ Plenum Publishers, 2001, pp. 371–382.
- [87] I. Kyrikou and D. Briassoulis, “Biodegradation of Agricultural Plastic Films: A Critical Review,” *J. Polym. Environ.*, vol. 15, no. 2, pp. 125–150, Apr. 2007.
- [88] T. Kijchavengkul, R. Auras, M. Rubino, M. Ngouajio, and R. Thomas Fernandez, “Development of an automatic laboratory-scale respirometric system to measure polymer biodegradability,” *Polym. Test.*, vol. 25, no. 8, pp. 1006–1016, Dec. 2006.
- [89] H. . Abd El-Rehim, E.-S. a Hegazy, a. . Ali, and a. . Rabie, “Synergistic effect of combining UV-sunlight–soil burial treatment on the biodegradation rate of LDPE/starch blends,” *J. Photochem. Photobiol. A Chem.*, vol. 163, no. 3, pp. 547–556, May 2004.
- [90] M. Vikman, M. Itävaara, and K. Poutanen, “Measurement of the biodegradation of starch-based materials by enzymatic methods and composting,” *J. Environ. Polym. Degrad.*, vol. 3, no. 1, pp. 23–29, Jan. 1995.
- [91] R. Gattin, A. Copinet, C. Bertrand, and Y. Couturier, “Biodegradation study of a starch and poly(lactic acid) co-extruded material in liquid, composting and inert mineral media,” *Int. Biodeterior. Biodegradation*, vol. 50, no. 1, pp. 25–31, Jul. 2002.
- [92] G. Li, P. Sarazin, W. J. Orts, S. H. Imam, and B. D. Favis, “Biodegradation of Thermoplastic Starch and its Blends with Poly(lactic acid) and Polyethylene: Influence of Morphology,” *Macromol. Chem. Phys.*, vol. 212, no. 11, pp. 1147–1154, Jun. 2011.
- [93] M.-M. Pang, M.-Y. Pun, and Z. A. M. Ishak, “Degradation studies during water absorption, aerobic biodegradation, and soil burial of biobased thermoplastic starch from agricultural waste/polypropylene blends,” *J. Appl. Polym. Sci.*, vol. 129, no. 6, pp. 3656–3664, Sep. 2013.

- [94] Y.-L. Du, Y. Cao, F. Lu, F. Li, Y. Cao, X.-L. Wang, and Y.-Z. Wang, "Biodegradation behaviors of thermoplastic starch (TPS) and thermoplastic dialdehyde starch (TPDAS) under controlled composting conditions," *Polym. Test.*, vol. 27, no. 8, pp. 924–930, Dec. 2008.
- [95] L. Shen and M. K. Patel, "Life Cycle Assessment of Polysaccharide Materials: A Review," *J. Polym. Environ.*, vol. 16, no. 2, pp. 154–167, May 2008.
- [96] G. Rebitzer, T. Ekvall, R. Frischknecht, D. Hunkeler, G. Norris, T. Rydberg, W.-P. Schmidt, S. Suh, B. P. Weidema, and D. W. Pennington, "Life cycle assessment part 1: framework, goal and scope definition, inventory analysis, and applications.," *Environ. Int.*, vol. 30, no. 5, pp. 701–20, Jul. 2004.
- [97] J. Widheden and E. Ringström, "Life Cycle Assessment," in *Handbook for Cleaning/Decontamination of Surfaces*, I. Johansson and P. Somasundaran, Eds. Elsevier B.V., 2007, pp. 695–720.
- [98] D. W. Pennington, J. Potting, G. Finnveden, E. Lindeijer, O. Jolliet, T. Rydberg, and G. Rebitzer, "Life cycle assessment part 2: current impact assessment practice.," *Environ. Int.*, vol. 30, no. 5, pp. 721–39, Jul. 2004.
- [99] ISO 14044, "Environmental Management-Life cycle assessment-Requirements and guidelines." International Organization for Standardization, 2006.
- [100] M. Guo, "Life Cycle Assessment (LCA) of Light-Weight Eco-composites," Imperial College London, 2012.
- [101] E. Rudnik, "Environmental impact of compostable polymer materials," in *Compostable Polymer Materials*, First edit., Oxford: Elsevier Ltd., 2008, pp. 183–199.
- [102] M. Patel, "13. Environmental Life Cycle Comparisons of Biodegradable Plastics," in *Handbook of Biodegradable Polymers*, First., C. Bastioli, Ed. Shawbury: Rapra Technology Limited, 2005, pp. 431–484.
- [103] Arnold Tukker, *Handbook on Life Cycle Assessment*, vol. 7. New York: Kluwer Academic Publishers, 2004.
- [104] A. P. Acero, C. Rodríguez, and A. Cirola, "LCIA methods: Impact assessment methods in Life Cycle Assessment and their impact categories," Berlin, GERMANY, 2014.
- [105] M. E. A. Goedkoop, "SimaPro Database Manual Methods library," Netherlands, 2010.
- [106] M. Goedkoop, R. Heijungs, M. Huijbregts, A. De Schryver, J. Struijs, and R. Van Zelm, "A life cycle impact assessment method which comprises harmonised category indicators at the midpoint and the endpoint level," 2009.

- [107] T. a. Hottle, M. M. Bilec, and A. E. Landis, “Sustainability assessments of bio-based polymers,” *Polym. Degrad. Stab.*, vol. 98, no. 9, pp. 1898–1907, Sep. 2013.
- [108] T. Qiang, D. Yu, A. Zhang, H. Gao, Z. Li, Z. Liu, W. Chen, and Z. Han, “Life cycle assessment on polylactide-based wood plastic composites toughened with polyhydroxyalkanoates,” *J. Clean. Prod.*, vol. 66, pp. 139–145, Dec. 2013.
- [109] S. Madival, R. Auras, S. P. Singh, and R. Narayan, “Assessment of the environmental profile of PLA, PET and PS clamshell containers using LCA methodology,” *J. Clean. Prod.*, vol. 17, no. 13, pp. 1183–1194, Sep. 2009.
- [110] G. M. Bohlmann, “Biodegradable packaging life-cycle assessment,” *Environ. Prog.*, vol. 23, no. 4, pp. 342–346, Dec. 2004.
- [111] S. . Joshi, L. . Drzal, a. . Mohanty, and S. Arora, “Are natural fiber composites environmentally superior to glass fiber reinforced composites?,” *Compos. Part A Appl. Sci. Manuf.*, vol. 35, no. 3, pp. 371–376, Mar. 2004.
- [112] L. M. Matuana and J. Kim, “Fusion Characteristics of Rigid PVC / Wood-Flour Composites by Torque Rheometry,” *J. Vinyl Addit. Technol.*, no. 13, pp. 7–13, 2007.
- [113] ASTM D638-10, “Standard Test Method for Tensile Properties of Plastics.” 2010.
- [114] ASTM D790-10, “Standard Test Methods for Flexural Properties of Unreinforced and Reinforced Plastics and Electrical Insulating Materials.” 2010.
- [115] ASTM D3418-08, “Standard Test Method for Transition Temperatures and Enthalpies of Fusion and Crystallization of Polymers by Differential Scanning.” ASTM Committee D20, pp. 1–7, 2012.
- [116] C. A. . Collins, “Manufacture and Properties of Thermoplastic Starch Biocomposites,” West Virginia University, 2012.
- [117] R. Fatoni, “Product Design of Wheat Straw Polypropylene Composite by,” 2012.
- [118] L. Avérous and E. Pollet, “Environmental Silicate Nano-Biocomposites,” *Green Energy Technol.*, vol. 50, pp. 13–39, 2012.
- [119] J. F. Mano, D. Koniarova, and R. L. Reis, “Thermal properties of thermoplastic starch/synthetic polymer blends with potential biomedical applicability.,” *J. Mater. Sci. Mater. Med.*, vol. 14, no. 2, pp. 127–35, Feb. 2003.
- [120] N. OTHMAN, N. A. AZAHARI, and H. ISMAIL, “Thermal Properties of Polyvinyl Alcohol (PVOH)/Corn Starch Blend Film,” *Malaysian Polym. J.*, vol. 6, no. 6, pp. 147–154, 2011.

- [121] A. Wattanakornsiri, K. Pachana, S. Kaewpirom, P. Sawangwong, and C. Migliaresi, “Green composites of thermoplastic corn starch and recycled paper cellulose fibers,” *Songklanakarinn J. Sci. Technol.*, vol. 33, no. 4, pp. 461–467, 2011.
- [122] United States Environmental Protection Agency, “Municipal Solid Waste Generation , Recycling , and Disposal in the United States: Facts and Figures for 2013,” pp. 1–16, 2013.
- [123] United States Environmental Protection Agency, “Municipal Solid Waste Generation , Recycling , and Disposal in the United States : Facts and Figures for 2010,” pp. 1–12, 2010.
- [124] D. Crowley, “Health and Environmental Effects of Landfilling and Incineration of Waste - A Literature Review,” 2003.
- [125] ISO 14855-1, “Determination of the ultimate aerobic biodegradability and disintegration of plastic materials under controlled composting conditions. Part 1 : method by analysis of evolved carbon dioxide.” International Organization for Standardization, Geneva, 2005.
- [126] ISO 14855-2, “Determination of the ultimate aerobic biodegradability of plastic materials under controlled composting - Method by analysis of evolved carbon dioxide. Part 2: Gravimetric measurement of carbon dioxide evolved in a laboratory scale test,” vol. 2006. International Organization for Standardization, Geneva, 2006.
- [127] ASTM D5338-98, “Standard Test Method for Determining Aerobic Biodegradation of Plastic Materials Under Controlled Composting Conditions.” 2003.
- [128] E. C. Aguirre, “Design and Construction of a Medium-Scale Automated Direct Measurement Respirometric System to Assess Aerobic Biodegradation of Polymers,” Michigan State University, 2013.
- [129] ASTM D6400, “Standard Specification for Labeling of Plastics Designed to be Aerobically Composted in Municipal or Industrial Facilities.” ASTM International, 2012.
- [130] T. Kijchavengkul, R. Auras, M. Rubino, S. Selke, M. Ngouajio, and R. T. Fernandez, “Biodegradation and hydrolysis rate of aliphatic aromatic polyester,” *Polym. Degrad. Stab.*, vol. 95, no. 12, pp. 2641–2647, Dec. 2010.
- [131] R. a. Gross, J. Gu, D. Eberiel, and S. P. McCarthy, “Laboratory-Scale Composting Test Methods to Determine Polymer Biodegradability: Model Studies on Cellulose Acetate,” *J. Macromol. Sci. Part A*, vol. 32, no. 4, pp. 613–628, Apr. 1995.
- [132] K. S. Y. Kuzyakova, J.K. Friedelb, “Review of mechanisms and quantification of priming effects (Review).,” *Soil Biol. Biochem.*, vol. 32, p. 1485±1498, 2000.

- [133] R. Chandra and R. Rustgi, "Biodegradable polymers," *prog. polyme. sci*, vol. 23, no. 97, pp. 1273–1335, 1998.
- [134] C. Way, D. Y. Wu, K. Dean, and E. Palombo, "Design considerations for high-temperature respirometric biodegradation of polymers in compost," *Polym. Test.*, vol. 29, no. 1, pp. 147–157, 2010.
- [135] G. Kale, T. Kijchavengkul, R. Auras, M. Rubino, S. E. Selke, and S. P. Singh, "Compostability of bioplastic packaging materials: an overview.," *Macromol. Biosci.*, vol. 7, no. 3, pp. 255–77, Mar. 2007.
- [136] M. J. Anderson and P. J. Whitcomb, *RSM Simplified: Optimizing Processes Using Response Surface Methods for Design of Experiments*. Boca Raton, FL: CRC Press, Taylor & Francis Group, LLC, 2005.
- [137] "Plastics Business Magazine | Demand for Biodegradable Plastics Increasing." [Online]. Available: <http://www.plasticsbusinessmag.com/e-news/stories/050713/biodegradable.shtml#.VbBZv6RViko>. [Accessed: 23-Jul-2015].
- [138] D. K. Platt and R. T. Limited, *Biodegradable Polymers: Market Report*. Rapra Technology, 2006.
- [139] ISO 14040, "Environmental management-Life cycle assessment-Principle and framework." International Organization for Standardization, U.S., 2006.
- [140] M. P. Islam, K. H. Bhuiyan, and M. Z. Hossain, "Vetiver Grass as a Potential Resource for Rural Development in Bangladesh," *CIGR J.*, vol. X, no. 5, pp. 1–18, 2008.
- [141] L. A. Simpson, "A Manual of Soil Conservation and Slope Cultivation," 2009.
- [142] D. Keomany, "Compare Life Cycle Assessment of Cassava Starch Production Between Thailand and Lao PDR," King Mongkut's University of Technology Thonburi, 2010.
- [143] P. Keeratiurai, "Carbon Footprint of Tapioca Starch Production using Life Cycle Assessment in Thailand," *Eur. J. Sci. Res.*, vol. 77, no. 2, pp. 293–302, 2012.
- [144] S. Khongsiri, "Life Cycle Assessment of Cassava Root and Cassava Starch," Kasetsart University, 2009.
- [145] W. J. Van Zeist, M. Marinussen, R. Broekema, E. Groen, A. Kool, M. Dolman, and H. Blonk, "LCI data for the calculation tool Feedprint for greenhouse gas emissions of feed production and utilization Dry Milling Industry," Gouda, 2012.
- [146] B. O. Awerije, "EXPLORING THE POTENTIAL OF CASSAVA FOR AGRICULTURAL GROWTH AND ECONOMIC DEVELOPMENT IN NIGERIA," University of Plymouth, 2014.

- [147] D. Pimentel, “Energy inputs in food crop production in developing and developed nations,” *Energies*, vol. 2, no. 1, pp. 1–24, 2009.
- [148] Y. Moriizumi, P. Suksri, H. Hondo, and Y. Wake, “Effect of biogas utilization and plant co-location on life-cycle greenhouse gas emissions of cassava ethanol production,” *J. Clean. Prod.*, vol. 37, pp. 326–334, 2012.
- [149] J. B. Agudelo, H. C. Peláez, and C. N. Merino, “Life Cycle Assessment for bioethanol produced from cassava in Colombia,” *Evaluación del ciclo vida del bioetanol Prod. a partir la yuca en Colomb.*, vol. 6, no. 2, pp. 69–77, 2011.
- [150] T. L. T. Nguyen, S. H. Gheewala, and S. Garivait, “Energy balance and GHG-abatement cost of cassava utilization for fuel ethanol in Thailand,” *Energy Policy*, vol. 35, no. 9, pp. 4585–4596, 2007.
- [151] S. H. R., “Economics of Production and Value Addition to vetiver in costal Karnataka,” *Agricultural Sciences*, 2010.
- [152] R. J. Joy, “‘SUNSHINE’ VETIVERGRASS,” Hoolehua, Hawaii, 1998.
- [153] S. C. Jimba and A. A. Adedeji, “Effect of Plant Spacing in the Nursery on the Production of Planting Materials for Field Establishment of Vetiver Grass,” *TROPICULTURA*, vol. 21, no. 4, pp. 199–203, 2003.
- [154] N. Tipsotnaiyana, T. Tongsumrith, and S. Netpradit, “Development of Mixed Paper Pulp from Weeds for Corrugating Medium,” in *Asian-Pacific Regional Conference on Practical Environmental Technologies*, 2007, p. 71.
- [155] A. Juangthaworn, “Life Cycle Assessment for Environmental Performance Comparison of Cassava-Based and Polystyrene Foam Packages,” KU, 2008.
- [156] O. Chavalparit and M. Ongwandee, “Clean technology for the tapioca starch industry in Thailand,” *J. Clean. Prod.*, vol. 17, no. 2, pp. 105–110, 2009.
- [157] L. Mahalle, A. Alemdar, M. Mihai, and N. Legros, “A cradle-to-gate life cycle assessment of wood fibre-reinforced polylactic acid (PLA) and polylactic acid/thermoplastic starch (PLA/TPS) biocomposites,” *Int. J. Life Cycle Assess.*, vol. 19, no. 6, pp. 1305–1315, 2014.
- [158] D. Dai, Z. Hu, G. Pu, H. Li, and C. Wang, “Energy efficiency and potentials of cassava fuel ethanol in Guangxi region of China,” *Energy Convers. Manag.*, vol. 47, no. 13–14, pp. 1686–1699, 2006.
- [159] T. L. T. Nguyen, S. H. Gheewala, and S. Garivait, “Full chain energy analysis of fuel ethanol from cane molasses in Thailand,” *Appl. Energy*, vol. 85, no. 8, pp. 722–734, 2008.

- [160] K. Suthee, "Life Cycle Assessment of Cassava Root and Cassava Starch," Kasetsart University, 2009.
- [161] J. Akadate, "Life Cycle Assessment for Environmental Performance Comparison of Cassava-Based and Polystyrene Foam Packages," Kasetsart University, 2008.
- [162] O. Chavalparit and M. Ongwandee, "Clean technology for the tapioca starch industry in Thailand," *J. Clean. Prod.*, vol. 17, no. 2, pp. 105–110, Jan. 2009.
- [163] B. P. Weidema and M. S. Wesnæs, "Data quality management for life cycle inventories—an example of using data quality indicators," *J. Clean. Prod.*, vol. 4, no. 3–4, pp. 167–174, 1996.